Satellite remote sensing of lake temperatures for climate research.

The Remote Sensing of Lake Surface Temperatures and their Use in Climate Research

Simon John Brown

Thesis submitted in fulfilment of the requirements for the degree of Doctor of Philosophy

Mullard Space Science Laboratory
Department of Space and Climate Physics
University College London

September 1994

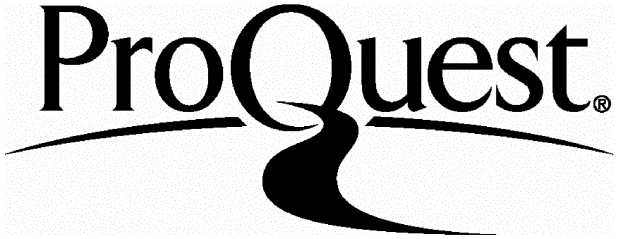

Abstract

This thesis is concerned with the satellite remote sensing of lake surface temperatures for use in climate research. The link between weather and lake temperature is investigated, particularly how the annual pattern of weather determines the annual pattern of lake temperature. Studies are made of how changes in climate might affect this link and how surface temperature measurement might serve as a proxy monitor or indicator of climate change. A thermal lake model is developed and used to investigate the effects of changing the individual meteorological components. This research leads to a new understanding the way in which how lakes respond to climate. The feasibility of using satellite remote sensing to monitor lake temperatures is assessed and the results of two case studies are presented. The first case study is a field validation campaign on a tropical lake (Lake Malawi) which represents a detailed investigation of the issues involved in accurate measurement of lake surface temperatures from space. The second study is an investigation of the accuracy to which the annual cycle of surface temperature, for a northern temperate lake (Lough Neagh, N. Ireland), can be determined.

Contents

Figures

Chapter 1.

Chapter 2.

Chapter 4.

Chapter 5.

Tables

Acknowledgements

There are many people who deserve thanks for helping me not only in the research for my PhD but also in the preparation of this thesis. Dr. Ian Mason in particular has been influential in guiding my work and keeping my eyes focused on the real issues. For this I would like to thank him and in particular for his comments on this manuscript. I would like to thank Chris Rapley for being so enthusiastic and creating the Remote Sensing Group at MSSL which is such a stimulating environment to work in. I would like to thank all the RSG for making MSSL such a warm place to work. I would particularly like to thank Andy Harris for always being ready to bounce ideas off, and the unsung heroes of all scientific research, the computer system managers, David Palmer and Colin Johnson.

There have been many contributions from people outside MSSL whom I would like to thank.

I gratefully acknowledge Albin Zavody of DRAL as the original author of the atmospheric transmission model which is used extensively in this work, and also for his suggestions and help.

I am most grateful to the Malawian government for allowing the field work in Malawi to be undertaken. I would like to thank the Natural Resources Institute of the ODA for providing the financial and logistical support for this campaign and Chris Sear for organising it and collecting the satellite images. I am also grateful to Andy Menz for allowing me to use the facilities at Senga bay and providing me with lodgings on site, and to Graeme Patterson for logistical support and assistance during the cruise.

Thanks are due to Dr. C. E. Gibson and Dr. R. V. Smith of the Freshwater Biological Development Unit, Department of Agriculture for Northern Ireland, for providing the in situ data for Lough Neagh, and to the University of Dundee Satellite Station for providing many many AVHRR images, and to DRAL for providing many many ATSR images.

Final thanks go to SERC for providing the funding for my PhD.

"The heavens declare the glory of God;
The skies proclaim the work of his hands."

Psalm 19: v1-2

Chapter 1.

The Satellite Remote Sensing of Lake Surface Temperatures for Climate Research.

1.1 Introduction

In the last few decades there has been an increasing concern as to whether the climate is changing. This concern arises not only from historical records which show that the climate can change, but also that man's activities could be influencing the climate, (Houghton et al. 1990). This potential influence stems from the fact that the atmosphere has a warming influence on the surface of the earth, the so called "greenhouse effect". The gases which achieve this are known as the "greenhouse gases" and man, mainly through the burning of fossil fuels, is increasing the atmospheric concentration of some of these gases. To determine the validity of this concern climatic indicators, whether direct or indirect, need to be identified and monitored. Indirect indicators, sometimes referred to as proxy indicators, are geophysical entities which would respond and change with a change in climate and which could be monitored by some measurable parameter. Direct indicators are what generally would be considered "components" of the climate system such as air temperature or rain fall.

Lake temperatures, particularly lake surface temperatures, are a potential candidate for being proxy climatic indicators. One can see this from general observations of lakes and their temperatures. Lakes in tropical Africa are warmer than lakes in northern Europe. It is unlikely that lakes in Mexico will freeze in the winter months yet the further north one goes the more likely the lakes are to freeze and to be frozen for longer periods until in northern Canada all lakes freeze for considerable portions of the year. It is from these general observations that one can understand that the temperature of a lake is strongly determined by its position on the earth and hence the climate that it is subjected to. Furthermore even a rudimentary look at the possible energy exchange methods that a lake can undergo indicates that the water temperature is intimately linked to the meteorological conditions and hence the climate. There are three possible paths through which energy can be exchanged with a lake, through the bedrock, through inflows and outflows and through the surface. For many lakes the first two are found to be small, (Ragotzkie 1987) leaving the surface energy exchanges to determine the water temperature. Since these heat exchanges are controlled by the meteorological conditions

a lake's temperature is therefore linked to the climate of the region it is in. The potential of lakes as proxy indicators is enhanced by the fact that lakes are well distributed over much of the globe and therefore could provide regional monitoring of climate. Therefore, this thesis in part tries to assess the usefulness of lake surface temperatures as proxy climate indicators. It reviews the physical mechanisms determining the lake temperature and from this determines how a lake might respond to a change in climate.

The most appropriate means of obtaining these temperatures is by remote sensing, particularly if a global sample is required for regional monitoring. The reasons for this are two fold, firstly satellites can provide regular synoptic global sampling and secondly such satellite systems are already in operation. Satellite radiometers suitable for this application have been in operation since 1978 with NOAA 7 of the TIROS-N/NOAA satellite series. Data from these satellites have been regularly archived and therefore there may already be a lengthy data record which has yet to be exploited. Continued coverage by appropriate radiometers are also planned for several years to come thereby extending the records further. Therefore, the second half of this thesis addresses the problems of retrieving the surface temperatures of lakes with regard to the application of using them as proxy climate indicators.

To summarise, this thesis sets out to investigate the usefulness of lake surface temperatures as proxy climate indicators and the potential of remote sensing for the measurement of these temperatures. This chapter will set out some of the background for this study followed by a discussion of the problem to be tackled resulting in a dividing of the problem into areas of research and ending with an overview of the thesis structure.

1.2 Characteristics of Climate

Reviews of the climate system have been published previously, for example Houghton (1984) & Harries (1990). It is not considered appropriate in this thesis to give a detailed description of the climate and if a more in depth discussion is sought then the reader is directed to the two previous references. It is beneficial, however, to discuss in general terms the nature of the climate and the climate system to put into context the use of lake temperatures for climate research. The climate is generally accepted to be in some sense the average weather, its fluctuations and its influence on the earth's surface (Leith, 1984) where "weather" in this sense includes components such as the cryosphere, oceanic state and not exclusively the atmosphere. However, this description is insufficient to form the basis for scientific research and needs developing. The characteristics of the climate of a region need careful definition, especially if one is looking for climate change, to ensure

that comparable measures are being used and that one is detecting climate change and not a difference in selection technique or definitions etc. (Folland et al. 1990). Weather is the state of the atmosphere at a particular place at a given moment in time whereas climate is a measure of the expected weather with some idea of the variability which might be encountered. This expected weather therefore necessitates the assumption of a time frame where the weather has been measured, from which the climate can then be derived. The choice of the length of the time frame used influences the resulting climate measured as there is a natural variability on many different time scales. The choice of time scales has caused much confusion in the detection of current climate change. Obviously the longer one looks back in the weather record a greater variability will be detected (Folland et al. 1990). This approach might not be a particularly helpful way to proceed. The inclusions of the weather of the ice age in our "expected weather" is obviously inappropriate as there could be significant changes in more recent weather which would be small compared to the differences between glacial and inter-glacial periods and yet have a significant effect on humanity.

Expected weather is still not a useful parameter as it is a complicated concept and involves many processes. To simplify this for climate research, one is generally forced to break down the "expected weather" into its component parts which can then be measured and monitored and for which statistics can be calculated. Typically these can be meteorological variables like air temperature, rain fall, wind, humidity etc. or non atmospheric parameters such as sea surface temperature and sea ice extent. Annual averages are commonly used even though the annual cycle is an integral part of the climate of a region. Perhaps more accurate or complete are the seasonal or monthly averages which give us an indication of the weather to be expected throughout the year and will detect subtler changes that the annual averages might miss. Climate change can also take the form of a change in the statistics and types of weather systems which are encountered in a region. Obviously there is a strong link between the meteorological variables and the weather systems and often a change in a meteorological parameter can be explained by a change in the weather systems.

Variability is a significant characteristic of the climate for a region and should not be ignored. Even if the average values of particular parameters were not to change, an increase in the variability would be a significant change especially as most natural disasters are caused by extreme events.

Global climate change is not a new thing for the earth. There have been many changes in the past varying from the large scale changes such as the Ice Ages to smaller ones such as

the "little Ice Age" which occurred between ~ 1400-1800 AD. Since changes in the climate are a natural part of the earth system it is important to note why there is such an interest in current change, particularly as there has been criticism of the climate research community based on this fact. The concern stems from two factors, the first is that the cause of the potential change is man's own activities. The emission of radiatively active gases (CO_2, CFC, methane etc.) will change the radiative behaviour of the atmosphere and this could change the earth's climate significantly. The second reason is that the time scale for this change to occur is unprecedented in history. There has been a general cooling of the earth in the past 2 million years yet current climate models indicate that this could be reversed in just 100 years, (Budyko et al. 1988). These factors have precipitated a rapidly growing concern over the climate system and has led to an increased level of climatic research. This has principally resulted in the international World Climate Research Programme (WCRP) which evolved out of the Global Atmospheric Research Programme (GARP) and together are jointly sponsored by the International Council of Scientific Unions (ICSU) and the World Meteorological Organisation (WMO). WCRP has singled out two main questions to answer - firstly to what extent can the climate be predicted and secondly, what is the extent of man's influence on climate. Part of this programme has spawned the World Weather Watch (WWW) which has been developed to measure more accurately and comprehensively the world's weather from which a baseline climate can be derived. Further to this development in research programmes is the growing need for geophysical parameters which would indicate climate change, these are called indicators which are either direct or proxy. An example of such an indicator is the retreat of glaciers in Europe which has been taken to be an indication of climate warming, (Folland et al. 1990). Another has been investigated by Mason et al. (1994) who have shown how closed lake volumes (those without surface outlet) can provide a measure of the aridity of a region (high aridity being a characteristic of low precipitation and high evaporation). It is the need for independent climatic indicators of this kind to confirm or not the presence of climatic change which has spawned the work described in this thesis.

1.3 Lakes in climate studies

Lakes are quite abundant over the earth's surface as can be seen from Fig 1.1 which is a global plot of lakes larger than 100 km^2 compiled by Birkett (1994). With current satellite radiometers, which provide global synoptic coverage, it will not be possible to measure lakes smaller than ~ 16 km^2 as the radiometer pixel size is approximately 1 km^2. The number of lakes which satisfy this criteria can be estimated from Fig. 1.2. This is a plot of lake area against frequency of occurrence for the entire globe which has been

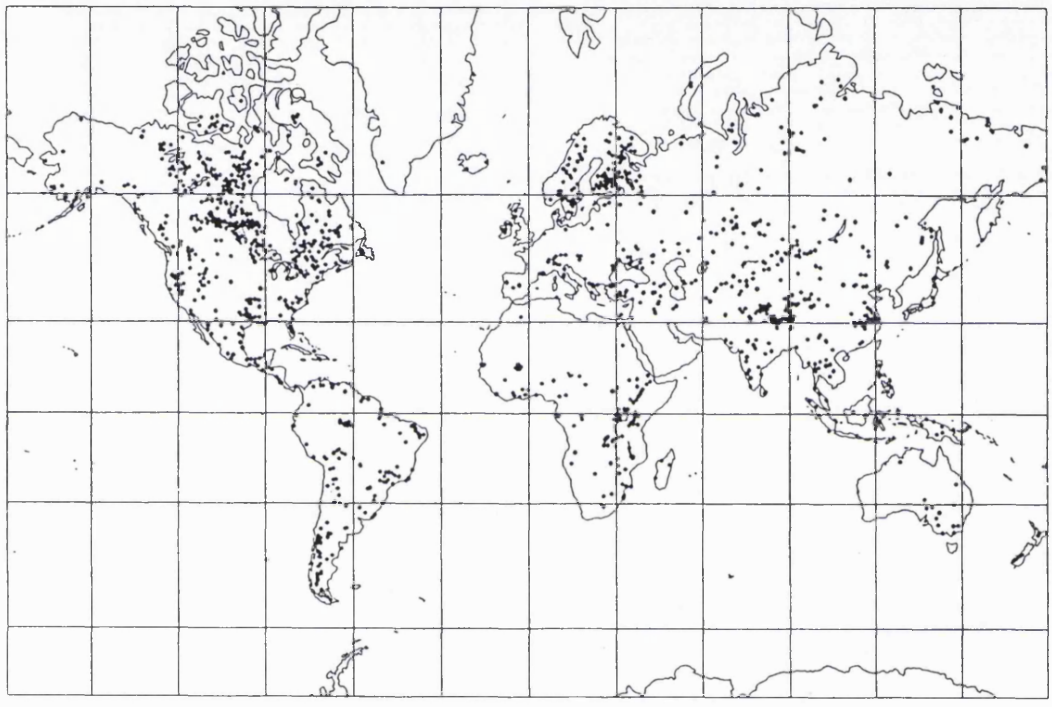

Figure 1.1 Global distribution of lakes over 100 km2 in extent, taken from Birkett (1994).

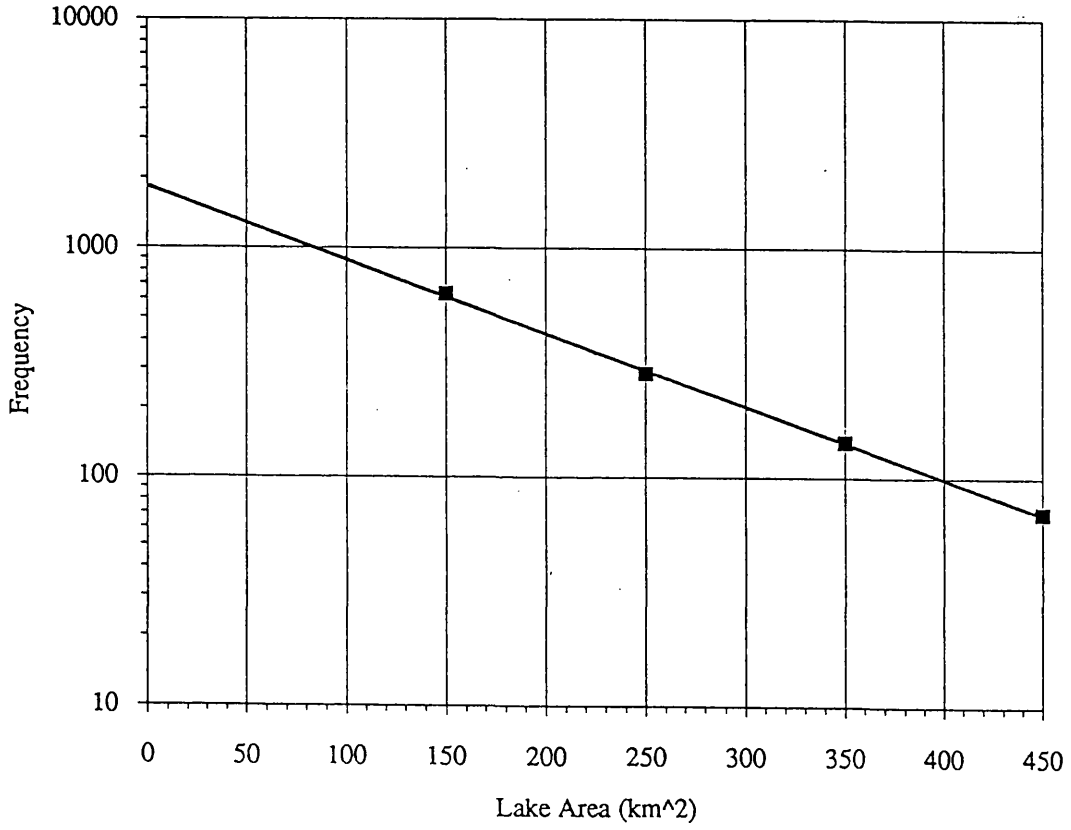

Figure 1.2 Size distribution of lakes globally, from Birkett (1994), indicating that there are thousands of lakes from which surface temperatures can be measured using AVHRR or ATSR

derived from Birkett (1994). From this plot one can estimate that there are more than a thousand lakes greater than this minimum size which is encouraging for their use as global climate monitors. This is especially so when compared to the number of glaciers and their distribution from which such strong implications about global warming have been inferred from their retreat, (Folland et al. 1990).

The majority of work which has been published concerning lakes and climate change can roughly be divided into two categories. The first has been concerned with the effect climate change will have on the freeze/thaw dates of lakes which freeze. The second has focused on the effect climate change will have on water quality, where the temperature of the water has an important role. This is understandable for countries such as Canada and the USA where lakes are considered a natural resource which are an important component of the tourist industry. Chapter 3 contains a detailed review of the published work in these areas, however it is appropriate to give an overview of this work without detailed references here.

Concerning the relationship of lake freeze and thaw dates with changes in climate, most of this work has been empirical correlations with historical records. It is found that the dates that a lake freezes and thaws is well correlated with a measure of the mean air temperature preceding the phase change date. This has prompted some authors to speculate that monitoring these dates could provide an indicator of climate change. It has also been suggested that, as the ice records were often started before reliable air temperature records, this correlation could provide a way of determining air temperatures for these earlier periods. Unfortunately little has been said on the noise or the natural variability of the freeze/thaw dates and therefore it is difficult to determine how useful these parameters would be in detecting climate change. Furthermore investigations into the physical basis for these correlations are few.

The amount of published work on lake temperatures and climate change is less than that on freeze and thaw dates. This is a little surprising as the lake temperature could provide information throughout the year rather than just the early winter and spring. The studies which have been published, with regard to the temperature of lakes, can be roughly divided into those which determine the effect of changing the meteorology (generally produced from a global circulation model) on thermal lake models, and those which make empirical correlations using historical records. Results from the modelling studies have indicated that there could be significant changes in the thermal structure and absolute temperature of lakes due to climatic change. From the historical studies it has been found that water temperatures can show periodicities which cannot be seen in air

temperatures. Again there has been little work on the detailed interaction between climate and lake temperatures. The general thrust of the temperature work has been to determine what will happen to the water temperature from a change in climate and not what a detected change in water temperature could imply for the climate. How lake temperatures might be used and what information about climate change they might provide has yet to be determined and which is in part what this thesis attempts to address through a physical understanding of the lake/climate link.

1.4 The Remote Sensing of lake temperatures

Remote sensing offers a number of advantages for the measurement of lake temperatures. The remote sensing of sea surface temperature (SST) is already a well developed field and has been used for a number of years to produce SST maps, and therefore it might be a suitable method for the measurement of lake surface temperatures. The first and probably the most important feature provided by remote sensing is the nature of its sampling. It is possible with satellite borne radiometers to cover the majority of the earth's surface in a very short time. The NOAA AVHRR series of satellites do this approximately every 6 hours and with ATSR this is done approximately every 1.5 days. Obviously this coverage can be disrupted by cloud and therefore in reality it will take longer. Even so satellites are the only method which comes near to providing synoptic coverage on a global scale. The alternative method for obtaining regular global lake temperatures would be through a network of ground based sampling programs which would need a very large amount of new resources and manpower and international co-operation. Furthermore such a programme would introduce a new factor, namely the problem of inter-calibration and standardising of sampling procedures. With remote sensing far less new resources would be needed as these satellites are already in operation and the inter-calibration and sampling problem would be much reduced.

1.5 The research task

This section will discuss how the research task, as defined by the earlier stated questions, was approached. These questions were "Can lake surface temperatures be used as proxy climatic indicators?" and "Can remote sensing monitor lake surface temperatures for this purpose?" Answering both these questions would initially involve assessing what the literature can tell us of what is already understood, highlighting what new understanding is required and establishing the research necessary to obtain this understanding.

As stated earlier the techniques involved in the remote sensing of SST's would hopefully provide a starting point for the remote sensing of lake surface temperatures. The transferral of these techniques to the remote sensing of lake temperatures needs to be investigated to ensure that it is appropriate and feasible and that any assumptions made for the sea surface retrieval are valid for use over lakes. Therefore this chapter is followed by a literature review of the remote sensing of surface water temperatures and it's relevant techniques. The accuracy of the retrieved temperatures needs to be determined as this has implications on the size of signal that can be detected in the lake as a proxy climatic indicator. This is not restricted to a single measurement but to measurements throughout the year. As cloud can obscure the surface, coverage and cloud statistics also need to be investigated to ensure that a regular measurement of the surface temperature can be obtained. The criteria needed to define regular will depend in some respects on how the lake temperature is related to the weather and how the lake responds to changes.

With regard to lake temperatures and their relation to climate, a literature review was performed on relevant topics. This started with a review of the thermal characteristics of lakes and their general response through the annual cycle. It was found that considerable effort has gone into parameterising of the surface heat exchange equations and these are well developed and detailed. These studies have resulted in quite comprehensive thermal models which can predict, from meteorological parameters, the lake temperature with considerable accuracy. Published work which has shown temperature changes using GCM output and these thermal lake models need to be reviewed to see if there were any indications as to how the lake's response can be interpreted with regard to climate. Their findings could then be taken into account when interpreting the results of this study. The work using historical data also needed to be scrutinised for causal links which could throw light onto the link between lakes and climate.

It was decided that this work was a good starting point for the proposed research and a lake temperature model was developed, from the surface energy flux parameterisations, for use as a tool to help investigate the lakes response to climate. It was proposed to model the lake signal (temperature change) from climatological data which has been produced form the Hadly Centre's GCM for selected sites around Europe. This would have indicated the temperature accuracy requirement needed for climate monitoring. Unfortunately, however, there have been delays in the distribution of this data and therefore it has been impossible to include this study in this thesis. Instead the importance and effect of changes in the individual meteorological variables was investigated. The model was also used to investigate the time response of a lake to

changes in meteorology to investigate how closely coupled the lake's surface temperature is to the daily weather.

To investigate the remote sensing of lake temperatures two case studies were undertaken. The first was to determine how accurately the surface temperature could be retrieved from a single measurement. This involved measuring the radiative temperature of the surface and hence the use of an in situ radiometer. To determine whether the atmospheric correction techniques developed for SST retrieval are appropriate the atmospheric profiles of water content and temperature were measured by radiosondes. From these radiosondes correction coefficients were also derived. Measurements of the skin effect (see chapter 2 for explanation of this) were also taken to provide an understanding of range and value that it can take and if possible its parameterisation from meteorological parameters. This work was undertaken through a two week field expedition to Lake Malawi. This lake was chosen for two reasons firstly due to the logistical and financial support of the Natural Resources Institute who have an ongoing field campaign on this lake, and secondly, due to the lake being in a continental situation, which should provide the most dissimilar atmospheric conditions to those found over the oceans.

Due to the lack of funds and time, the above expedition had a limited time span. However, as the goal is to measure the annual temperature cycles it would be valuable to have a validation of such a cycle. Therefore the second case study was performed which consisted of determining the temperature of Lough Neagh in Northern Ireland over a period of approximately one year. Satellite retrieved temperatures were compared with weekly in situ water temperatures which were provided by the Freshwater Biological Investigation Unit, Belfast. The validation utilised both AVHRR and ATSR but for separate years. This study was therefore an indication as to how accurately the annual temperature cycle of this particular lake can be monitored and also provides information on the cloud/coverage problem for this area. This study helps in establishing the feasibility of the regular monitoring of lake temperatures and highlights the procedures required and the likely problems that might be encountered.

1.6 Thesis overview

This section is an overview of the work presented in this thesis. This is to provide a framework for the reader which it is hoped will facilitate their understanding of how the different sections are linked together. The following chapters of this thesis, in order, are as follows:

Chapter 1. This introduction.

Chapter 2. A review of the principles of remote sensing surface water temperatures. This includes background on thermal radiation, a description of the instruments used both satellite and ground based radiometry, calibration of satellite data, atmospheric correction, and the skin effect.

Chapter 3. A review of the thermal characteristics of lakes and the physics of the heat exchange processes through the surface. A review of published work on the correlations found between meteorological parameters and lake temperatures or freeze/thaw events. A review of the results found from modelling lake temperatures from GCM output.

Chapter 4. Development of a mixed layer lake temperature model from the surface heat flux parameterisations in chapter 3 and validation using meteorological and water temperature data for Lough Neagh.

Chapter 5. Application of model developed in chapter 4 to facilitate the understanding of the link between lake temperature and climate change.

Chapter 6. Case study of the remote sensing of lake temperatures, using results from a field expedition to Lake Malawi.

Chapter 7. Case study of the monitoring of the annual temperature cycle of a lake from satellite, using data for Lough Neagh, Northern Ireland.

Chapter 8. Conclusions and recommendations for further work.

Chapter 2.

Remote Sensing Techniques for the retrieval of surface temperatures.

2.1 Overview

This chapter reviews the techniques of infrared remote sensing for the derivation of surface temperatures particularly water bodies although many of the subjects discussed here are applicable to land or ice surface temperature retrieval. The chapter starts with the fundamental physics of thermal radiation. Instrument characteristics and operation are then discussed for both satellite radiometers and ground based radiometers. This is followed by an overview of radiation transfer for the atmosphere which leads to techniques of atmospheric correction. The chapter ends with a description and discussion of the "skin effect" and the influence this has on the retrieval of surface water temperatures.

2.1 Thermal radiation

All objects whose temperatures are not at absolute zero emit radiation. The strength of this emission and its spectral distribution is described by the Planck function and the measure to which the object behaves as a perfect radiator, or black body. The Planck function has the form;

$$B_\lambda(T) = \frac{2hc^2}{\lambda^5} \frac{1}{e^{(hc/\lambda kT)} - 1}$$

where λ is the wavelength
T is the temperature of the body (2.1)
h is Planck's constant
c is the speed of light
k is the Boltzmann constant.

A body which is a perfect radiator is often called a black body (BB) due to the fact that a perfect radiator has a zero reflectance and therefore appears black. Such a body has an emissivity of unity and emits according to the Planck function. The definition of the spectral emissivity, ε_λ is:

$$\varepsilon_\lambda = \frac{R_\lambda(T)}{B_{\lambda(black-body)}(T)} \tag{2.2}$$

where $R_\lambda(T)$ is the radiance emitted by the body at wave length λ and for temperature T.

The spectral emissivity tends to be a weak function of temperature but can vary significantly with wavelength (Robinson 1985). For many materials $\varepsilon\lambda$ varies strongly with incidence (or exitance) angle and water is one of these materials.

The net radiation emitted from a black body per square metre is found by integrating the Planck function which results in the Stefan-Boltzmann equation;

$$M = \sigma T^4 \tag{2.3}$$

where σ is the Stefan-Boltzmann constant, of value 5.67 x 10^{-8} $Wm^{-2}K^{-4}$

The peak in radiance can be found by setting the derivative of the Planck function with respect to wavelength to zero to produce the Wien displacement law;

$$\lambda_{max} = l/T \tag{2.4}$$

where l is a constant of value 2898 μmK.

Using equation (2.4) and using the approximate temperatures of the earth and sun (300K and 6000K respectively) we find that the peak in the solar radiation is at ~0.5μm and the peak for the earth is ~10μm. Furthermore if the spectral distribution of radiation for each temperature is determined, accounting for the reduction in radiance due to the sun earth distance, one finds that the radiation from each body occupies almost completely different parts of the spectrum (Fig 2.1), with the only region of overlap being in the 3-4 μm region. This being the case, it is possible to develop sensors which will only detect radiation whose source is either the sun or which is thermally emitted from the earth. Instruments operating in the 3-4 μm region will during the day will have contributions from both the sun and the earth but during the night only the earth will contribute.

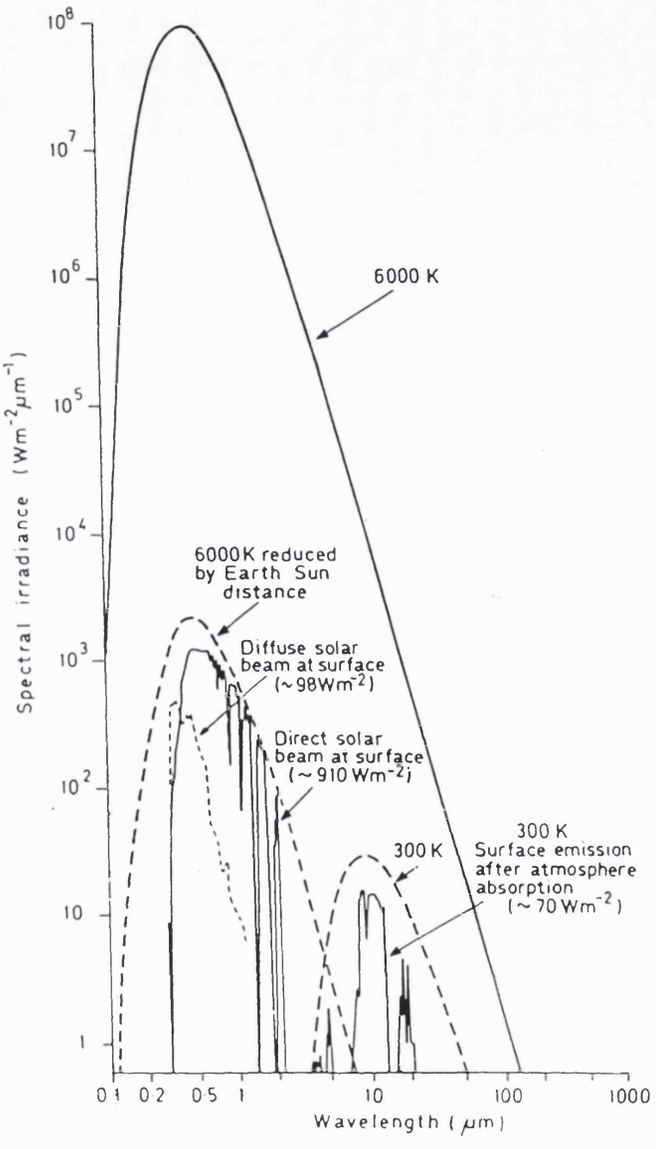

Figure 2.1 Spectral irradiance curves for the sun (6000K), the solar flux (i.e. accounting for the distance between the sun and the earth) and for the earth (300K). Effects of atmospheric absorption are also shown for both sources. From Schott and Henderson-Sellers (1984)

2.2 Infrared Radiometers

The following sections will concentrate on two satellite instruments, the Advanced Very High Resolution Radiometer (AVHRR/2) and the Along Track Scanning Radiometer (ATSR). This section will describe their design, operation and calibration and their relative merits and will end with a section describing a ground based radiometer designed and built by CSIRO Australia which has been used for validations studies with these satellites, one such validation exercise is presented later in this thesis.

2.2.1 AVHRR

The Advanced Very High Resolution Radiometer was first flown in 1978 on the TIROS-N/NOAA series of satellites which are an operational meteorological satellite series in a polar, sun-synchronous orbit at an altitude ~850km with an orbit inclination of ~99° giving an orbit period of ~100min and full earth coverage twice every 24 hours. There are two such satellites in orbit at the same time separated by ~90° in longitude and hence ~6 hours in time, providing a total of at least four passes of any given area in 24 hours (approximately 01:30, 08:30, 13:30 & 20:30 local time). A summary of the instrument characteristics is given in Table 2.1. Due to the very large swath width, it is possible to get more overflights at high latitudes although the drawback of such a wide swath is that the projected instantaneous field of view (IFOV) increases dramatically from 1.1×1.1km at nadir to approximately 4×2km at the edge, together with considerable image distortion. The first AVHRR included only 4 channels and it was with AVHRR/2 that a fifth was introduced. Due to budget restrictions, flight spares of AVHRR were launched after the development of AVHRR/2 resulting in one of each generally in orbit. This is unfortunate as the 4 channel instrument is restricted in the atmospheric correction methods that can be used as will be seen in a later section.

The AVHRR/2 instrument, in essence, is a Cassegrain telescope with a detector assembly at the principle focus. In front of the telescope is a rotating planar mirror which provides the scanning movement across track. The satellite path through the orbit produces the along track displacement with the speed of the scan mirror set so that the mirror will have completed a complete revolution in the time it has taken the satellite travel 1.1km along the ground and so a continuous image can be built up of successive scans. A disadvantage of this design is that the system is only focused on a particular portion of the earth for a very short period (~25 μsec) and so only a small amount of energy can be gathered to produce a signal. This requires the detectors to be cooled in order to limit the noise in the measurement of the signal.

	Channel	AVHRR	AVHRR/2
Wavebands (μm)	1	0.58† – 0.68	0.58 – 0.68
	2	0.725 – 1.10	0.725 – 1.10
	3	3.55 – 3.93	3.55 – 3.93
	4	10.5 – 11.5	10.3 – 11.3
	5	channel 4 repeat	11.5 – 12.5
† 0.55 μm on TIROS-N			
Sensitivity of thermal IR channels (3, 4, 5)		NEΔT	0.12 deg K at 300 K
No. of digitisation levels			1024
Angular field of view			1.3 ± 0.1 mrads
Ground IFOV at nadir		approx.	1.1 X 1.1 km (4 X 4 km in low resolution mode)
Cross-track scan			± 55.4°
Swath width			2580 km

Table 2.1. Characteristics of the Advanced Very High Resolution Radiometer (AVHRR). From Robinson (1985).

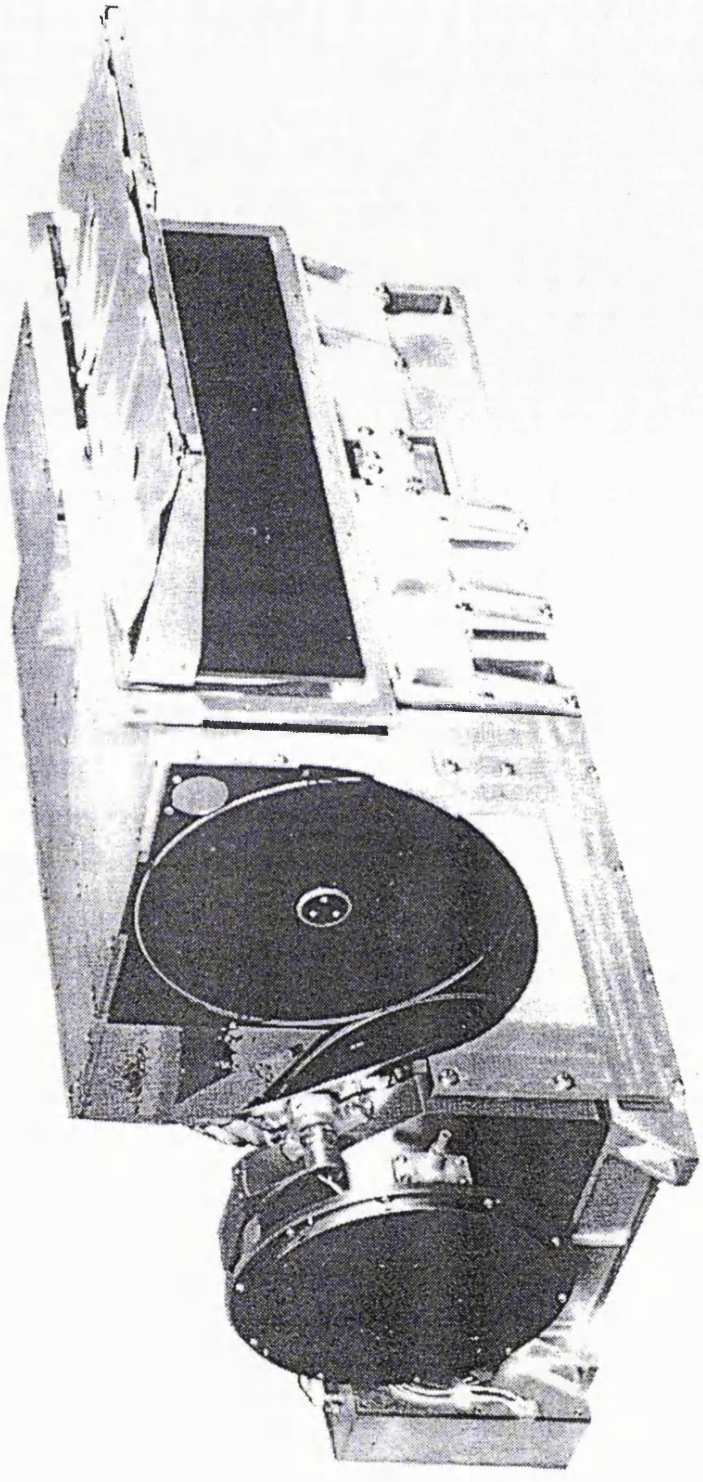

Figure 2.2 Image of AVHRR. The mirror motor housing can be seen at the left hand end with the passive radiant cooler on the right with its sun shield. From ITT (1989)

The cooling apparatus for AVHRR/2 can be seen in Fig 2.2, a photo of the instrument, as the large dark rectangular area with a silvered sun shield above. This is a passive cooling system where the detectors are effectively allowed to radiate out to cold space, which is very close to absolute zero. With this mechanism the AVHRR/2 detectors are cooled to ~105K (ITT 1989). The advantage of the passive cooling system is that there are few moving parts and there is no energy requirement to drive the system. Disadvantages are that there is a practical limit in the temperature to which the detectors can be cooled, and that they need shielding from radiation sources such as the sun.

The maximum possible resolution of the instrument is determined by the diameter of the telescope aperture and the wavelength of the radiation and can be calculated by the Rayleigh criterion ($\alpha = 1.22\lambda/d$), so for AVHRR/2, (aperture 20cm, wavelength 12μm) the resolution is ~0.07 milliradians. In fact the field stops are set at 1.4 milliradians and therefore this is the effective resolution of the instrument. These field stops determine the IFOV of the instrument which when projected to the ground at nadir produce 1.1×1.1 km pixels.

The infrared measurements are calibrated via a two point calibration method. The calibration targets are a view of space and a region of the detector housing where there is an enhancement of the surface emissivity and where 4 platinum resistance thermometers have been placed. The temperature of space is taken to be zero and the on board calibration target is ~ 285K although this can change by up to 5K through an orbit, (Brown et al. 1985). The radiance is calculated for both and a linear counts to radiance relationship determined. Unfortunately the detectors have a non-linear response to radiance and therefore additional corrections need to be applied, (NOAA 1986). As can be seen from Fig. 2.3 these corrections can be quite large, furthermore there will be a different value of correction with scene temperature and with different calibration target temperature (Brown et al. 1985) and so a series of correction values is provided from which the appropriate correction can be interpolated for a given scene and calibration target temperature combination. An alternative non-linear correction method has been proposed by Steyn-Ross and Steyn-Ross (1992) where the correction is performed in radiance space before the radiances are converted into temperatures and it is this method which is employed in later studies using AVHRR/2. Further difficulties in the accurate calibration of AVHRR/2 are due to the on board calibration target. The thermal cycling throughout an orbit is such that the temperature difference between the 4 PRT detectors within the target can be as large as 2K, (Brown et al. 1985), thereby introducing uncertainty as to the real effective temperature of the calibration target.

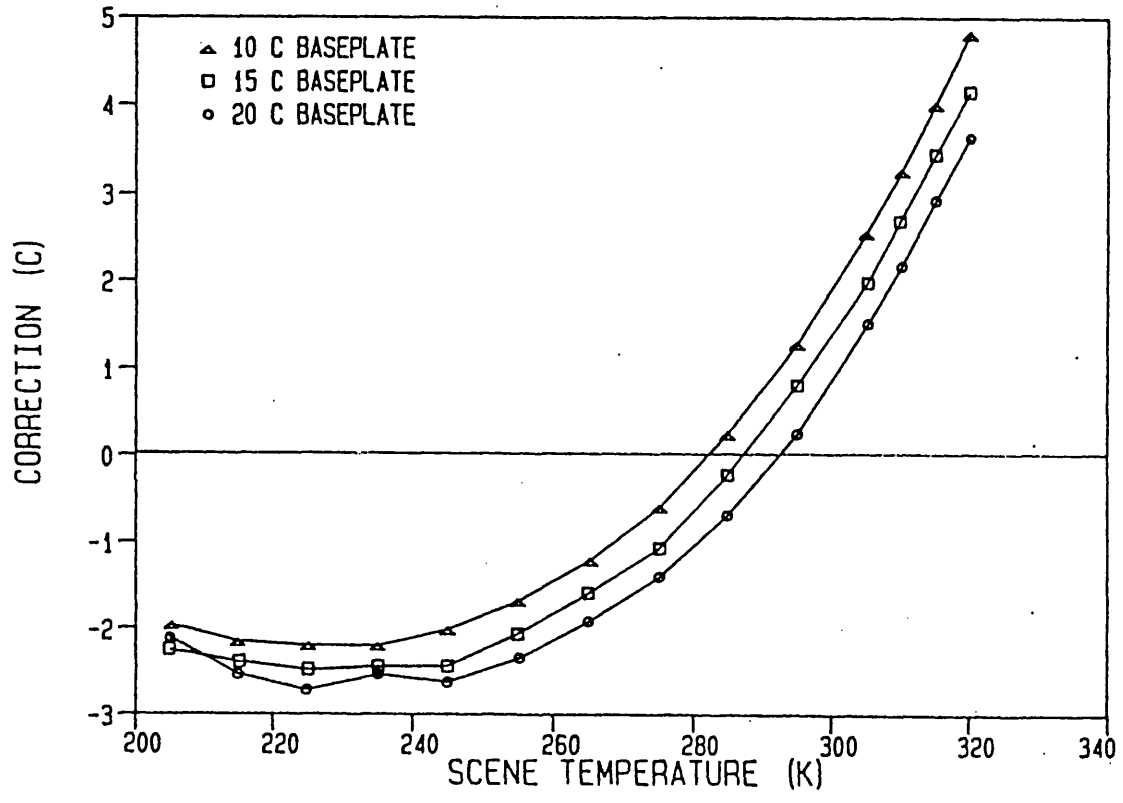

Figure 2.3 Non-linear correction for channel 4 (11μm) of NOAA11 for different scene temperatures and different calibration target temperature. From Weinreb et al. (1990).

The absolute accuracy of AVHRR/2 was carefully investigated by Brown et al. (1985) where it was found that the combination of the detector noise (~0.12K) with the uncertainty in the calibration resulted in an uncertainty in the brightness temperatures of 0.2K. The use of such an optimistic estimate of error was cautioned by Weinreb et al. (1990), particularly as the temperature of reference calibration target, against which the satellite was calibrated pre-launch, was not known to better than ± 0.35K. In spite of this the general indication from validation exercises is that a figure of 0.3K is a reasonable estimate, (Robinson 1985).

2.2.2 ATSR

The Along Track Scanning Radiometer (Fig. 2.4) launched on July 1st 1991 as part of the instrument payload of ERS-1. ATSR was developed to address the increasing accuracy being required in sea surface temperatures for climate research. For example it is now recognised that sea surface temperature anomalies, such as the El Niño southern oscillation, play an important role in climate processes. To monitor these requires accuracies to a few tenths of a degree, (Folland et al. 1990).

ERS-1 is in a polar orbit of inclination of 81.45° and altitude of ~785 km. The orbits are arranged so that the satellite is either in an exact 3 or 35 day repeat but within the 35 day orbit there is a 3 day sub-cycle. This means that for a particular position there will be similar passes every three days but a full 35 days will have to elapse before the exact pass re-occurs. ATSR has similar channels to AVHRR/2 in the infrared, namely 3.7, 11 & 12 μm. It also has one near-infrared channel at 1.6 μm which is included to facilitate cloud identification. Furthermore, the 1.6 μm channel can also discriminate between clouds and ice or snow. Data from this channel is interleaved with data from the 3.7 μm channel with the 1.6μm being transmitted during the day and the 3.7 μm during the night. Table 2.2 is a summary of the main specifications of ATSR. Considerable effort has been spent in ground processing of the raw data to provide users with calibrated geolocated products. Various products are generated from the ATSR data, a full description of which can be found in Závody et al. (1994).

ATSR was designed to provide a new level of accuracy in satellite remote sensing of sea surface temperature drawing on the experience of the AVHRR/2 programme. One of the areas where improved accuracy is desirable is in the atmospheric correction. Atmospheric correction of infrared images relies on the differential absorption of radiation of the atmosphere for at least two channels of the instrument. This differential absorption can be due to the use of different wavelengths or from different path lengths through the atmosphere. ATSR incorporates this second method in addition to the first. It achieves

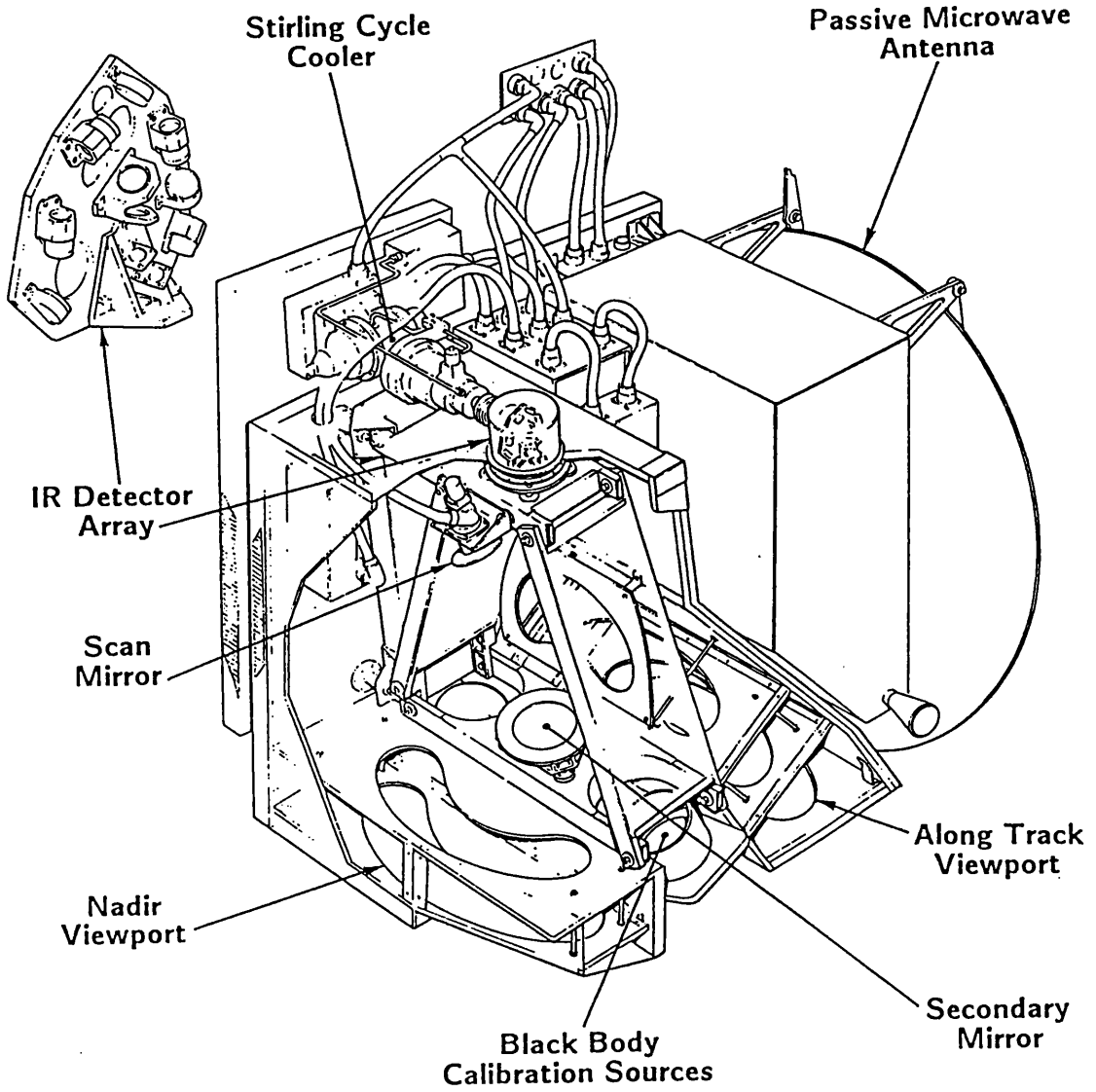

Figure 2.4 Diagram of the ATSR instrument showing the main novel features, in particular the forward look viewport, the Stirling cycle cooler and the two calibration targets. Diagram courtesy of DRAL.

Channel	Wavelength (μm)	NEΔT K (target @ 298K)	Digitisation K per count
1a	1.6 (day only)		
1b	3.7 (night only)	0.025	0.020
2	10.9	0.028	0.021
3	11.9	0.025	0.044
FOV centre of nadir image		~ 2.0 x 1.0 km @ 5% response	
FOV centre of forward image		~ 3.0 x 2.5 km @ 5% response	
Swath width		512 km	

Table 2.2. Characteristics of the Along Track Scanning Radiometer, ATSR.

this by adopting a conical scan where the cone is angled so that one edge of the cone is perpendicular to the earth's surface (the nadir image) and the other edge points forward along the satellite direction and intersects the earth at an angle of ~55° (the forward image). The atmospheric path length for the forward image is approximately 1.75 times that of the nadir image and is viewed two minutes before the nadir image. This arrangement assumes that the atmosphere and the surface have not altered between the two images. A schematic diagram of ATSR's scanning geometry is given in Fig 2.5. This scanning arrangement effectively doubles the number of parameters that one can use in determining the atmospheric correction. This is expected to improve the uncertainty in the sea surface temperature retrieval from ± 0.6K in the case of AVHRR/2 (McClain et al. 1985) to an accuracy goal of less than 0.25K for ATSR's $^1/_2°$x$^1/_2°$ in latitude and longitude spatially averaged product Delderfield et al. (1986).

A further improvement over AVHRR/2 is the reduction of detector noise. This is due, in part, to a novel active cooling mechanism based on the Stirling cycle, which cools the detector assembly to ~85K. The other factor which contributes to the reduction in detector noise is the increase in the time the detector is focused on one pixel for 75μsec which provides a larger signal. This helps to achieve detector noise values of 0.03-0.02K NEΔT, despite a smaller primary mirror of 15cm aperture to that of AVHRR/2's 20cm. Unfortunately, due to telemetry restrictions, the 12μm channel data is compressed by transmitting the difference between the 11μm and the 12μm counts which has resulted in an increase in the noise to 0.04K. However due to an interference with the cooling motor the noise increases to 0.08K. This could, in theory, be removed through processing and modelling the interference.

The calibration of the ATSR signal is the other major area where improvement was desired over that of AVHRR/2. For ATSR, a two point calibration system is still employed but instead of one calibration target temperatures being at 0K and the other at the ambient satellite temperature, the hot and cold target temperatures correspond to the maximum and minimum expected in scene temperature, that is to say for the sea ~0° - 30° C. This minimises the effect of the non-linearity of the detectors. Furthermore, the non-linear nature of the detectors has been determined pre-launch and is removed in processing.

The design of the ATSR calibration targets (hereafter called black bodies or BB) is also considerably different to that for AVHRR/2. The design specification for the black bodies stated that the absolute error in the retrieved sea surface temperature due to the calibration scheme should be less than 0.1K. This requirement stems from the overall

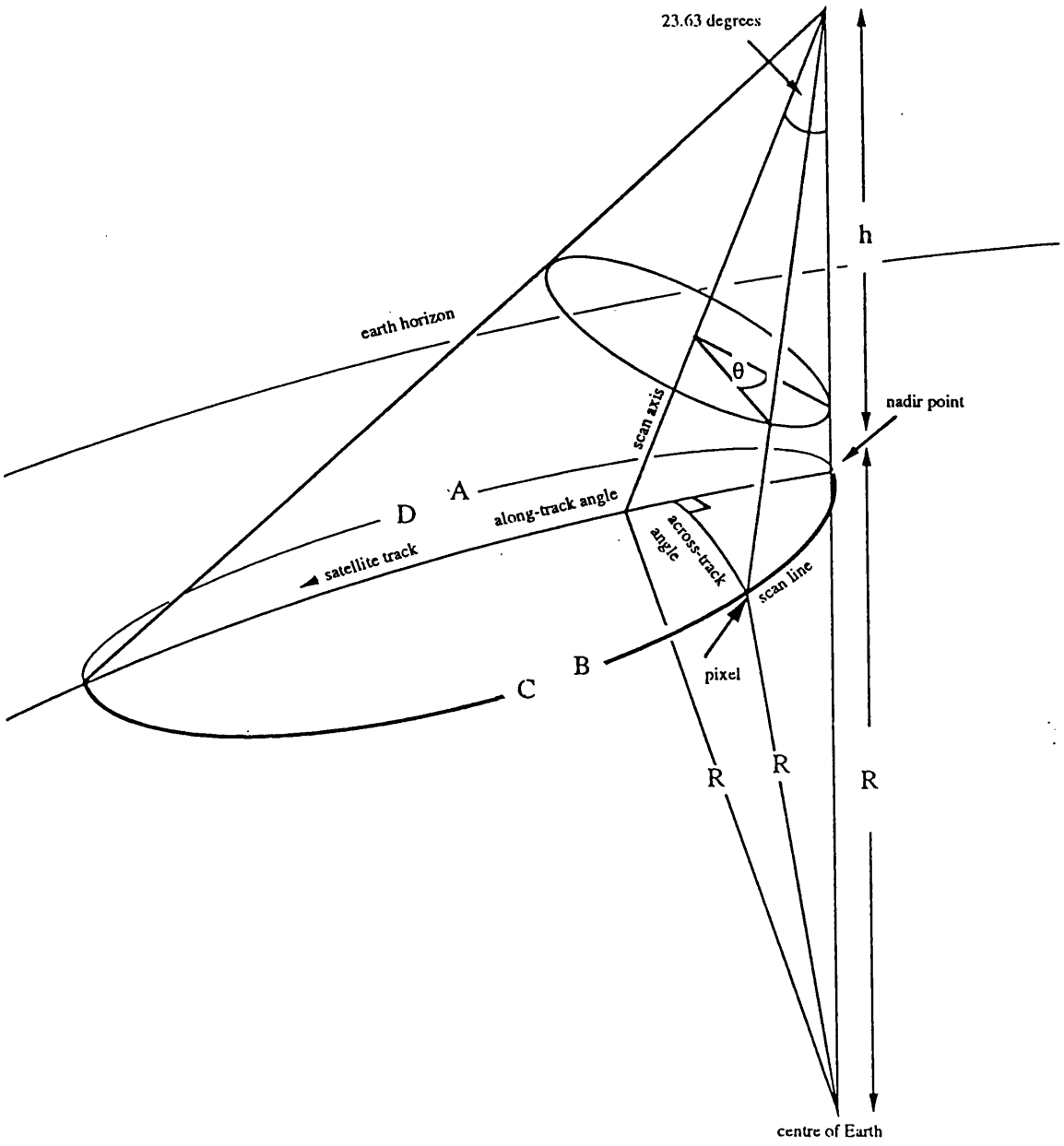

Figure 2.5 Diagram illustrating the ATSR scanning arrangement. The IR detectors view the Earth's surface via a rotating mirror, inclined at 23.45°to the vertical, which transcribes an elliptical swath ABCD every 150 ms as the satellite travels along the sub-satellite track. The earth measurements are interrupted between BC and DA to enable the detectors to view the hot and cold black bodies on-board the spacecraft. From Závody et al. (1994)

requirement that the sea surface temperature should be determined to ± 0.25K, (Delderfield et al. 1986). The implications of this 0.1K requirement for the calibration translates into three main specifications for the black body design, (Mason et al. 1990):

- A high and uniform emissivity of > 0.998
- Thermal uniformity within the black body, gradients < 30mK on viewed surface
- Accurate temperature monitoring of the black bodies throughout the mission to better than ± 30 mK accuracy

As can be seen from Fig 2.4 the black bodies are situated between the forward and nadir view apertures and therefore are viewed once each for a complete revolution of the scan mirror providing continuous calibration. At the time of writing ATSR is still performing well, although the 3.7 μm channel detector failed in May 1992. It has provided considerable quantities of quality data and looks set to provide the accuracy initially envisaged.

2.2.3 CSIRO Radiometer

The previous two sections have described satellite borne radiometers. This section describes a radiometer which has been developed for use on the ground specifically for the validation of ATSR. The radiometer was designed and built by CSIRO Australia and consists of a detector pod which includes the detectors, two calibration targets and preamplifiers. This pod is connected to the main control electronics via an umbilical cable. The radiometer is a two channel radiometer with the channels centred at 11 & 12 μm, similar to the channels of ATSR. The output is in the form of analogue volts which can then be recorded via a logger.

A system to cool the detectors to below 100K would be too large and expensive and so the radiometer employs a different technique from that used on satellites to measure the radiance. The method used involves constantly swapping into the field of view of the detector the target and a reference source. The detector is a device which produces a voltage dependant on the difference in radiance falling on the detector and that leaving the detector. If the detector is allowed to equilibrate with the incoming radiation the voltage falls to zero. Therefore by constantly chopping the scene against a reference radiance a suitable signal can be generated.

The radiometer contains two calibration targets (apart from the reference target) which can be moved into the detectors field of view. One of these targets is at ambient temperature and the other contains a regulated heater which is held at ~10K above the ambient target. The temperatures of the bodies are monitored via a semiconducting device which outputs a voltage proportional to its temperature. To reduce detector noise

the signal can be integrated over 1, 3 or 10 seconds. The radiometer can be run in two separate modes. The first is manual where the calibration targets or the external view are selected on the control box. The second is an automatic calibration cycling where a 90 second view of each calibration target is interspersed with 90 seconds of the external view, i.e. cold - external - hot - external - cold etc.

To supplement this internal calibration method a further calibration can be performed with what is termed a "stirred bucket" as described in Schluessel et al. (1990). This consists of a container where water is continually forced up from the bottom of the container to upwell on the surface. The water temperature is monitored very accurately and the radiometer pointed at the breaking surface to perform the calibration. It is necessary to have the surface continually broken so that the temperature of the emitting surface is at the same temperature as that measured by the thermometer, otherwise a temperature gradient or "skin effect" would form (see later section). The calibration is made by calculating the brightness temperature of the water surface from the radiance measured by the radiometer using the radiometers internal calibration. This is then compared with the temperature measured by the thermometer in the bucket and the radiometer brightness temperature corrected to that of the bucket thermometer. This calibration correction (the difference between the radiometer brightness temperature and the temperature measured in the bucket) can then be applied to brightness temperatures measured for the object of interest.

This calibration method accounts for several factors which would otherwise hinder the accurate retrieval of water temperatures and therefore makes it very advantageous:

- As the emissivity of water is not unity one can only produce brightness temperatures. If the bucket is viewed at the same angle as the target of interest the precise emissivity for that angle does not need to be known and allows the conversion of brightness temperature to physical temperature.
- Furthermore as the emissivity is not unity there will be downwelling radiation from the sky reflected into the radiometer. Again if the bucket is viewed at the appropriate angle this component of the detected radiation can effectively be removed as the correction is to the physical temperature measured in the bucket.
- If there is any error in the internal calibration the use of the bucket facilitates the removal of these errors as well so long as the temperature in the bucket is close to the target temperature.

A numerical description of the bucket calibration is as follows (in radiance units)

$$\text{Radiance\_detected} = \varepsilon . B_{(T)} + (1-\varepsilon) I_{\downarrow} + \text{calibration\_error}$$

$$\text{Radiance\_correction} = \text{Radiance\_detected}_{\text{Bucket}} - B_{(T\_Bucket)} \qquad (2.5)$$

giving

$$\text{Corrected\_radiance} = \text{Radiance\_detected}_{\text{Water}} - \text{Radiance\_correction}$$

where:

$B_{(T)}$ is the Planck radiation

$I_{\downarrow}$ is the downwelling sky radiance

ε is the emissivity of water

Such a "stirred bucket" was constructed from two plastic washing up bowls with one smaller to fit in the larger, a schematic diagram of which is depicted in Fig 2.6. The smaller was fixed into the larger so that the water pumped into the smaller could overflow and thereby be collected and drained away. The water was pumped into the inner bucket via a pipe passing through the bottom of the outer bucket. The section of pipe inside the smaller bucket contained small holes angled so as to direct the pumped water towards the water surface in the bucket. The bucket was fed by a pump with the water intake situated so that the water was near the same temperature as the target of interest. This reduced the extrapolation needed for the bucket calibration. The flow of water was adjusted so that the surface was constantly being broken. The temperature of the bucket was monitored by a platinum resistance thermometer for which special support electronics were designed and constructed at MSSL to minimise the effects of temperature on the connecting wires and the electronics to an extent that under all expected temperature scenarios, the temperature of the water in the bucket can be monitored to 20 mK. A dexion frame was constructed so that the bucket could be slid into and out of the radiometers view without moving the radiometer. The resultant accuracy of this method was found to be $\pm$ 0.1K for surface water temperatures.

2.3 Atmospheric absorption

As the radiation passes through the atmosphere some proportion will be absorbed. Furthermore, the atmosphere itself also emits some radiation which will contribute to the radiation reaching the detector. Therefore, if this is to be accounted for, the absorption process needs to be understood. The absorption is due to atoms and molecules of the atmosphere having excitational state intervals with the same energy as the photons of the solar radiation or of the terrestrial radiation. Absorption of the solar radiation is mainly due to O_2 and O_3 molecules and for the terrestrial radiation it is primarily CO_2 and H_2O.

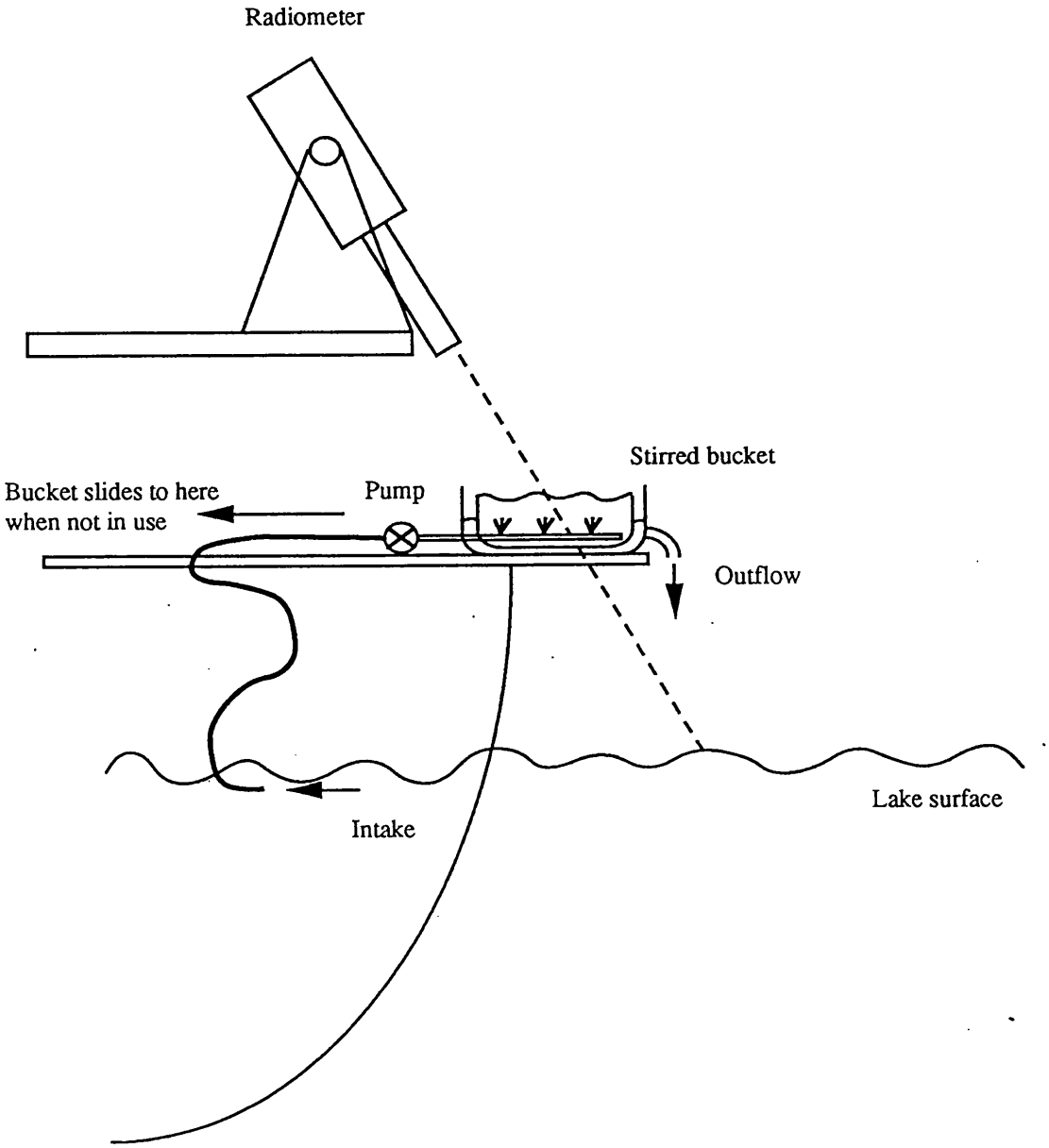

Figure 2.6 Schematic diagram of the "stirred bucket" constructed to calibrate the CSIRO Radiometer and to correct for reflected sky radiation. The apparatus was arranged so that the bucket could be slid into view of the radiometer without moving the radiometer.

A detailed discussion of spectral line absorption is considered inappropriate for this thesis and therefore will only be discussed in general terms. It is suffice to say that the absorption of radiation by the atmosphere is complicated with several factors contributing to its complexity, the major ones being, from Harris (1991):

- The mixing ratios of the absorbers, particularly that of water vapour as it is not constant with space or time
- The temperature and pressure varies through the atmospheric column
- Line shapes are collision broadened by different amounts
- Doppler broadening can occur at high altitudes
- Absorption lines can overlap particularly at low altitudes

A further factor which needs to be accounted for is what is termed the "continuum absorption". The exact nature of this absorption is still to be determined although it is generally considered to be due to water vapour dimers. These dimers have very large numbers of vibrational and rotational states and together with the low amount of energy needed to dissociate them their absorption spectra is effectively continuous. As this absorption is due to dimers the strength of absorption depends on the partial pressure of water vapour as individual water vapour molecules are more likely to pair up the greater the density of molecules. It has been found that the absorption is inversely related to temperature which follows the dimer hypothesis as at higher temperatures the molecules are more likely to dissociate. As stated earlier the nature of the absorption is still not fully understood and it has recently been suggested that the level of absorption could be in error by as much as 30% (Kilsby et al. 1992).

2.4 Radiative Transfer

The development of an equation to describe the atmospheric effect on the detected signal is complicated by the fact that the problem is not just one of absorption. As the atmosphere is not at absolute zero it will also emit radiation into the detector. In fact for some parts of the atmosphere the temperature difference between the atmosphere and the emitting surface is such that the emitted radiation equals that absorbed. On the whole the mean temperature of the atmosphere is lower than the surface and therefore there is a net decrease in the radiance detected at the satellite compared to that emitted at the surface. The level of absorption is determined to the first order by the quantity of absorbing medium whereas the level of emission is not only determined by the quantity of the emitting material but also its temperature, which in the case of the atmosphere is closely related to its altitude.

To formulate an equation for the passage of radiation through the atmosphere it is useful to consider a plane-parallel atmosphere which is assumed to be uniform in the horizontal. It is also assumed that the atmosphere is in thermodynamic equilibrium so that the only vertical transport of energy is by emission and absorption. These assumptions stipulate that the net horizontal transfer of energy is zero and so only the vertical components need to be considered. Following Harris' (1991) treatment of Houghton (1987), and using Fig. 2.7, the absorption dI by an elemental slab (thickness dz) of an incident radiance I is proportional to the mass of the absorber ρdz where ρ is the density of the absorber and with an absorption coefficient of k, giving:

$$dI = -Ik\rho dz \tag{2.6}$$

The elemental slab will also be emitting radiation and as it is assumed that it is in thermodynamic equilibrium. The earth's atmosphere is obviously not in thermodynamic equilibrium as there is convection and forced vertical movements of air. However one can assume at a given point and time there is a condition of local thermodynamic equilibrium and so Kirchoff's law can be applied and the emissivity of the slab can be taken to be equal to the absorbtivity. Thus the net radiation leaving the top of the slab is:

$$dI = -Ik\rho dz + B(T(z))k\rho dz \tag{2.7}$$

where T(z) is the temperature of the atmosphere at height z. The optical path, $\chi(z)$, is defined as $\int_z^{\infty} k\rho dz$ and therefore (2.7) can be written as:

$$dI = Id\chi - B(T(z))d\chi \tag{2.8}$$

and integrating from ground to space gives:

$$\begin{aligned} I &= \int_{\chi(z_0)}^{0} Ie^{-\chi}d\chi - \int_{\chi(z_0)}^{0} B(T(z))e^{-\chi}d\chi \\ &= I_0\tau(z_0,z_1) + \int_{\tau(z_0,z_1)}^{1} B(T(z))d\tau(z,z_1) \end{aligned} \tag{2.9}$$

where I_0 is the upwelling radiance at ground level and τ, the fractional transmission is given by:

$$\tau = e^{-\chi} = e^{-\int_z^{\infty} k\rho dz} \tag{2.10}$$

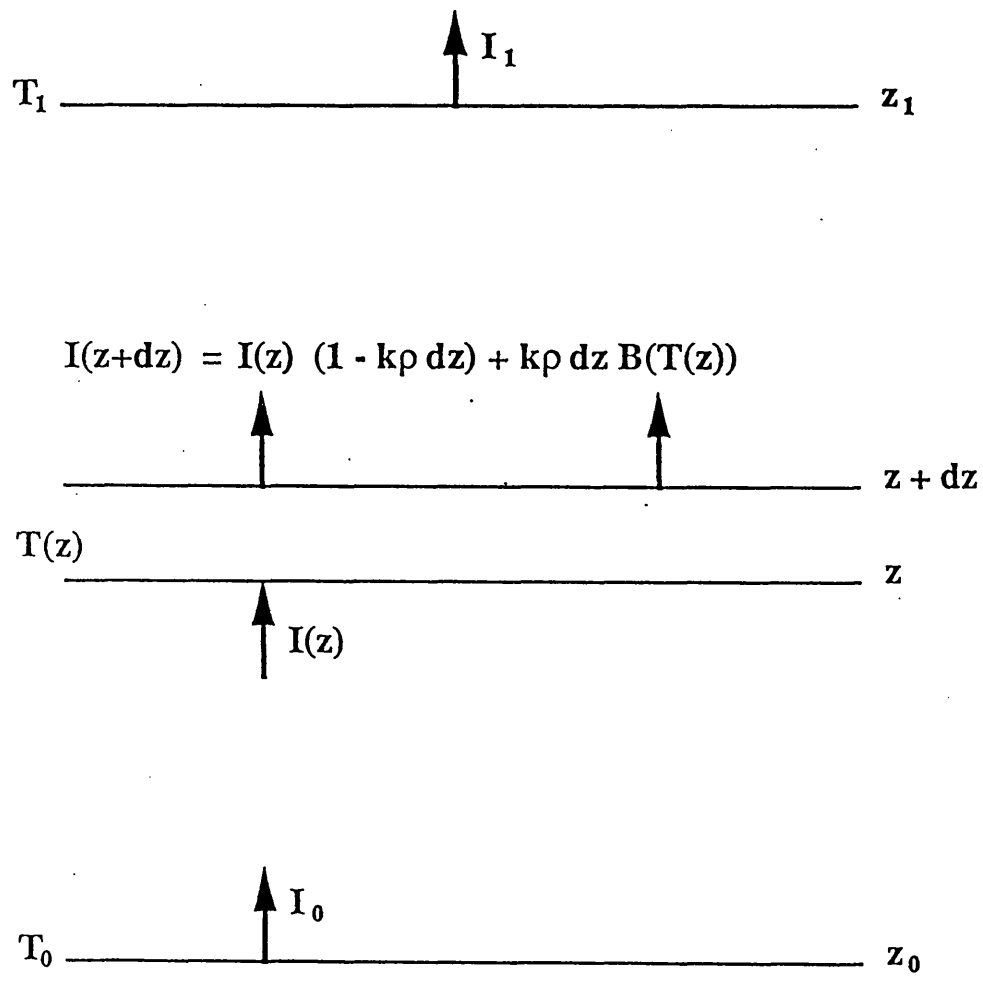

Figure 2.7 Schematic illustrating contribution of elemental slab at height z, thickness dz, to the upwelling radiance observed at $z = z_1$. From Harris (1991).

The value of I_0 would be the Planck radiation at the surface temperature if the surface had an emissivity of one. However this is not the case with ocean which has an emissivity of ~0.98. One cannot simply multiply the Planck radiation by the emissivity as there will be reflection as well at the surface towards the satellite. The contribution to I_0 will be the reflectivity multiplied by the downwelling radiation from the sky. This can be calculated in a similar way to the atmospheric emission in eq. (2.9) and integrating from space to the ground, gives:

$$I_0 = \varepsilon B(T_0) - (1-\varepsilon) \int_1^{\tau(z_1,z_0)} B(T(z)) d\tau(z,z_0) \tag{2.11}$$

which now can be inserted into (2.9). All the above equations have ignored the wavelength dependence of these processes and it should be borne in mind that all these calculations are specific to a particular wavelength. Often it is useful to consider the radiative transfer in terms of the variable pressure as the atmospheric parameters are often measured by balloon at various pressure levels, and so including the wavelength dependence and setting the limits to be p_0 at ground level and 0 at the top of the atmosphere, we get:

$$I_\lambda = I_{0\lambda} t_\lambda(0,p_0) - \int_1^{t_\lambda(0,p_0)} B_\lambda(T(p)) dt_\lambda(0,p) \tag{2.12}$$

2.5 Atmospheric Correction

Measurements of surface radiance from space are taken at wavelengths which are situated in regions of the spectrum called "windows" where the atmospheric effects are at a minimum. The main windows are at 3-4μm, 8.5-9.5μm and 10-14μm. However, as can be seen in Fig 2.8, even in these regions there is some absorption. This absorption can result in up to a 10K deficit in the brightness temperatures recorded by the satellite (Barton 1983). The main absorbers of interest for SST retrievals in these windows are H_2O and CO_2. Unfortunately, the quantity and vertical distribution of H_2O is very variable in the troposphere and the effects that it has on the radiation detected from the surface is consequently very varied and needs specific correction, at least as an average correction for each scene and at best for each pixel.

There are in general three main approaches in the correction of remotely sensed surface radiances for atmospheric effects. The most direct, although probably the least practicable, is the modelling of the atmospheric effects, on a scene by scene basis, from

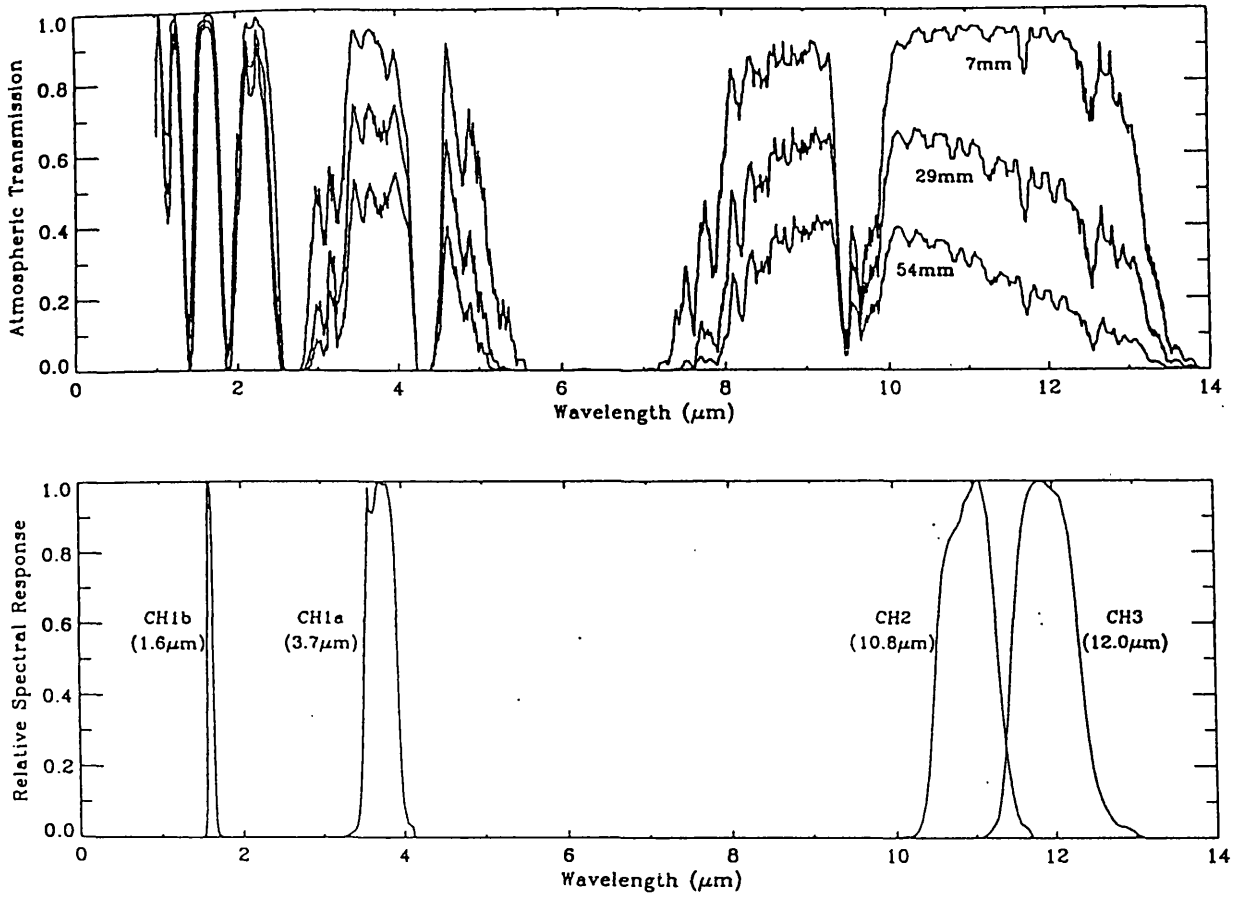

Figure 2.8 Atmospheric transmission for three different amounts of precipitable water, 7mm, 29mm and 54mm corresponding to polar, temperate and tropical respectively. The corresponding ATSR channels are also shown. From Mason (1991).

direct measurements of the atmospheric profiles of temperature and water vapour. These are provided by coincident launches of radiosondes at or near the time and position of the satellite image. This method obviously relies on the radiosondes and therefore is restricted to regions where the infrastructure for regular radiosonde launches is available. Routine surface temperatures of the Great Lakes are produced with this method as part of the "Coast Watch" programme in Canada. There are drawbacks with this method, in particular there will be variations in the water/temperature profiles across the image which will not be represented by the single radiosonde and therefore the correction applied to these areas will not be as appropriate.

It would be far more useful if the atmospheric correction could be determined from measurements made by the satellite. This would eliminate the problem of availability of simultaneous ancillary data such as radiosondes. Such measurements have been available for some years now and are based on measuring the radiance from the surface so that there is a difference in levels of absorption and emission from the atmosphere for each of the measurements. This difference in absorption and emission can be due to using different wavelengths where the atmosphere has different absorption properties or through different path lengths of the atmosphere at the same target. Deschamps and Phulpin (1980) and McMillin (1975) are examples of the first approach from which the "Split Window" correction method is derived and Saunders (1967a) is an example of the second and from this concept ATSR was developed (Závody 1982). A further advantage of this method of differential absorption is that the atmospheric correction can be determined for each pixel of the scene.

To date the use of different wavelengths has been the main method of atmospheric correction mainly due to the availability of instruments to do so, and consequently there is more published material on this method. The correction principle from multispectral measurements can be derived from the radiative transfer equation and following Deschamps and Phulpin (1980) and Harris (1991) we consider the radiance deficit, ΔI_λ, caused by the absorption and re-emission of the atmosphere. From eq. (2.12) we can write:

$$\begin{aligned} \Delta I_\lambda &= B_\lambda(T_0) - I_\lambda \\ &= -\int_1^{t_\lambda(0,p_0)} \left(B_\lambda(T_0) - B_\lambda(T(p))\right) dt_\lambda(0,p) \end{aligned} \tag{2.13}$$

The radiance deficit can also be expressed as a temperature deficit such that:

$$\Delta T_\lambda = T_0 - T_\lambda$$

where

$$B_\lambda(T_\lambda) = I_\lambda$$

We can link these two deficits together as the Planck function has near-linear behaviour at the temperatures of interest and therefore we assume, for small $\Delta T\lambda$:

$$\Delta T_\lambda = \frac{\Delta I_\lambda}{\left(\frac{dB_\lambda}{dT}\right)_{T_0}} \tag{2.14}$$

We also assume that $B_\lambda(T(p))$ can be expanded about the surface temperature T_0 by using a first order Taylor approximation:

$$B_\lambda(T(p)) = B_\lambda(T_0) + \left(\frac{dB_\lambda}{dT}\right)_{T_0}(T(p) - T_0) \tag{2.15}$$

and so substituting (2.14) and (2.15) into (2.13) we get:

$$\Delta T_\lambda = -\int_0^{p_0}(T_0 - T(p))dt_\lambda(0,p) \tag{2.16}$$

One final assumption is now needed and that is the differential change in transmittance can be written:

$$dt_\lambda(0,p) = -k_\lambda dU(p) \tag{2.17}$$

where $k\lambda$ is the absorption coefficient and $U(p)$ the content of the absorbing gas. This assumption is saying that the exponential absorption which actually occurs in the atmosphere can be approximated by linear absorption and so the absorption is proportional to the total content of absorber. This approximation is realistic if the total quantity of absorber is quite small and so is often referred to as the "thin atmosphere" approximation. Substituting (2.17) into (2.16) we get:

$$\Delta T_\lambda = -k_\lambda \int_0^{p_0}(T_0 - T(p))dU(p) \tag{2.18}$$

We can now see that the integral is independent of wavelength as it depends only on the atmospheric temperature and absorber structure and so we can write:

$$\Delta T_\lambda = k_\lambda f(T(p), U(p)) \tag{2.19}$$

and so if the temperature deficit is observed in two different wavelengths, we have:

$$\frac{T_0 - T_{\lambda 1}}{k_{\lambda 1}} = \frac{T_0 - T_{\lambda 2}}{k_{\lambda 2}} \tag{2.20}$$

which re-arranging for T_0, gives:

$$T_0 = T_{\lambda 1} \cdot \left(\frac{k_{\lambda 2}}{k_{\lambda 2} - k_{\lambda 1}} \right) + T_{\lambda 2} \cdot \left(\frac{-k_{\lambda 1}}{k_{\lambda 2} - k_{\lambda 1}} \right) \tag{2.21}$$

or

$$T_0 = a_1 T_{\lambda 1} + a_2 T_{\lambda 2}$$

This is only for two wavelengths and can be expanded to include more, but this demonstrates that if the above assumptions are valid the surface temperature can be derived from a linear combination of radiometric temperatures at different wavelengths. In practice, a constant term is needed to take into account the non-unit emissivity of the surface and the effects of other gases such as CO_2 which are well-mixed and therefore can be treated as a constant effect.

Equation (2.21) is a simplification of reality and it is prudent to consider the reasons for this method to fail or to start to break down. The first is that for some regions of the earth the atmosphere is not thin. This is particularly so for the tropics which can have vertical transmittances as low as 20% for the 12μm channel of ATSR (Harris and Mason 1992). This is reflected in the modelled retrieval accuracies by Llewellyn-Jones et al. (1984) where the RMS uncertainty calculated for the tropics is six times greater than for the North Atlantic. Secondly the absorption coefficient, $k\lambda$ actually depends on temperature and pressure and so it is not particularly realistic to bring it out side the integral in equation (2.18) although if $k\lambda(T)$ is similar in form for both 11 & 12μm this will not matter. Finally, in the 3.7μm region of the spectrum the Planck function is decidedly non-linear with the dependence of the emitted radiation following $\sim T^{13}$.

It is often useful to consider the atmospheric correction to be applied to one channel as a function of the brightness temperature difference of two channels. We can therefore re-write equation (2.21) as:

$$T_0 = a_0' + a_1' T_{\lambda 1} + a_2' \left(T_{\lambda 1} - T_{\lambda 2} \right) \tag{2.22}$$

This allows graphical representation of the atmospheric correction, such as in Fig. 2.9. where we can see that the atmospheric correction to be applied to the 11μm brightness

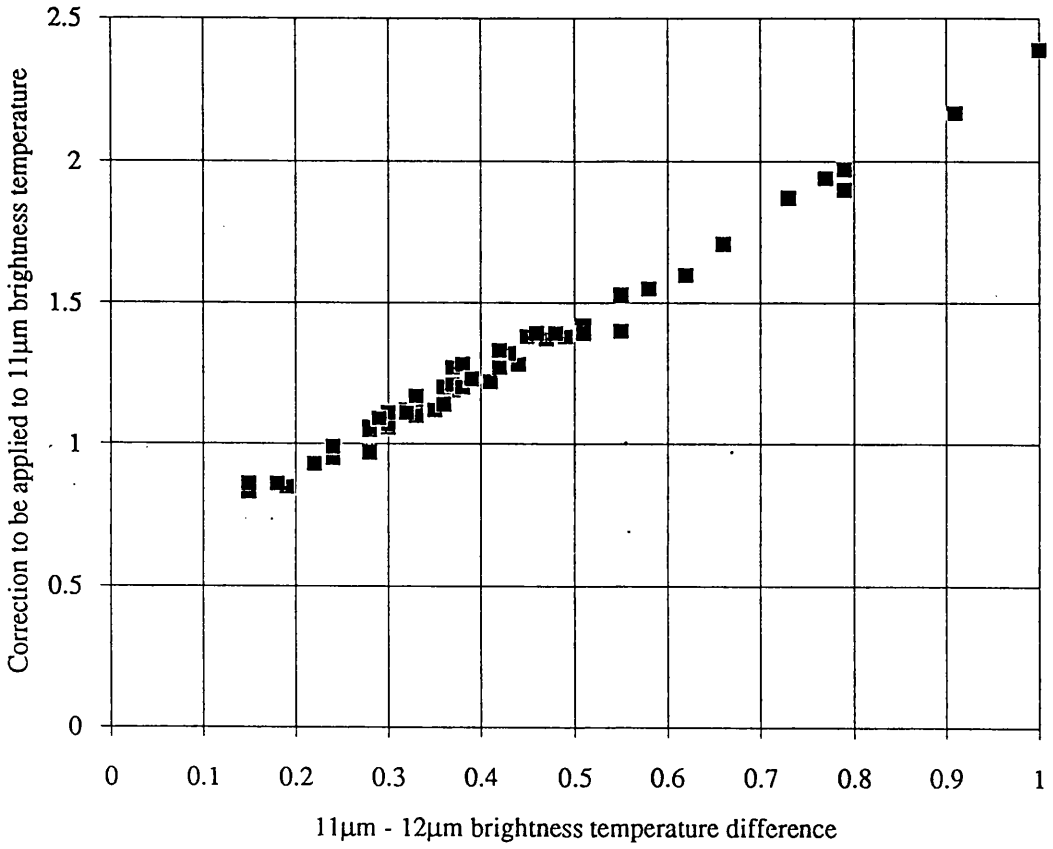

Figure 2.9 The relationship between the correction required for the 11 μm channel and the difference between the 11 & 12 μm brightness temperature. Brightness temperatures were generated using the line-by-line atmospheric transmission model described in the main text and 60 North Atlantic radiosonde profiles. A line regressed through these points would represent the conventional 'split-window' algorithm.

temperature is proportional to the brightness temperature difference between the 11μm & 12μm channels.

The brightness temperatures in Fig. 2.9 and throughout this thesis were generated using an atmospheric transmission programme developed specifically for the development of atmospheric correction of the thermal infrared, by Albin Zavody at the Rutherford Appleton Laboratory. A full description of this programme is shortly to be published (Závody et al. 1994).

There are currently two main methods for producing the coefficients in equation (2.22). The first has already been mentioned in passing where coefficients are calculated from a representative sample of the atmospheres by the radiative transfer model. The model requires as input the temperature and water vapour profiles through the atmosphere, which are a representative sample of the atmospheres that might be encountered, and from which brightness temperatures are calculated. These brightness temperatures are then regressed against the surface temperatures which are taken to be, in the ocean case, the temperature of the bottom layer of each atmosphere. This is a reasonable assumption since in general the atmosphere has had sufficient time to equilibrate with the sea surface. Such coefficients will produce the temperature of the emitting surface which is, in the case of water, within the top few tens of microns. This is termed the skin temperature, and can be several tenths of a degree different from the temperature a few centimetres below the surface often termed the bulk temperature (further discussion of this phenomenon follows in a later section). It is found that even if the bottom of the atmosphere is at a different temperature from the surface there is little effect on the coefficients with the predominant effect being to move the calculated brightness temperatures up and down the regression line in Fig. 2.9.

Water has an emissivity which is near to but less than unity and which varies with angle. Masuda et al. (1988) is the most comprehensive study to date on the emissivity of water for the thermal atmospheric windows for both fresh and salt water. Spectral emissivities are tabulated for wavelengths 3.5μm - 4.1μm and 8.0μm - 13.0μm for incidence angles from 0° to 85°. Furthermore Masuda et al. (1988) calculate the effect that wind speed has on the average emissivity for a surface. This is due to the wind roughening the surface and thereby introducing different incidence angles to the nominal incidence angle. As can be seen from Fig. 2.10 the emissivity of a plane water surface is fairly high and constant at small incidence angles but beyond 50° starts to fall rapidly. It is this non-linearity that causes the change in emissivity. The lower emissivity introduced with the larger angles dominates and therefore the emissivity drops. The higher

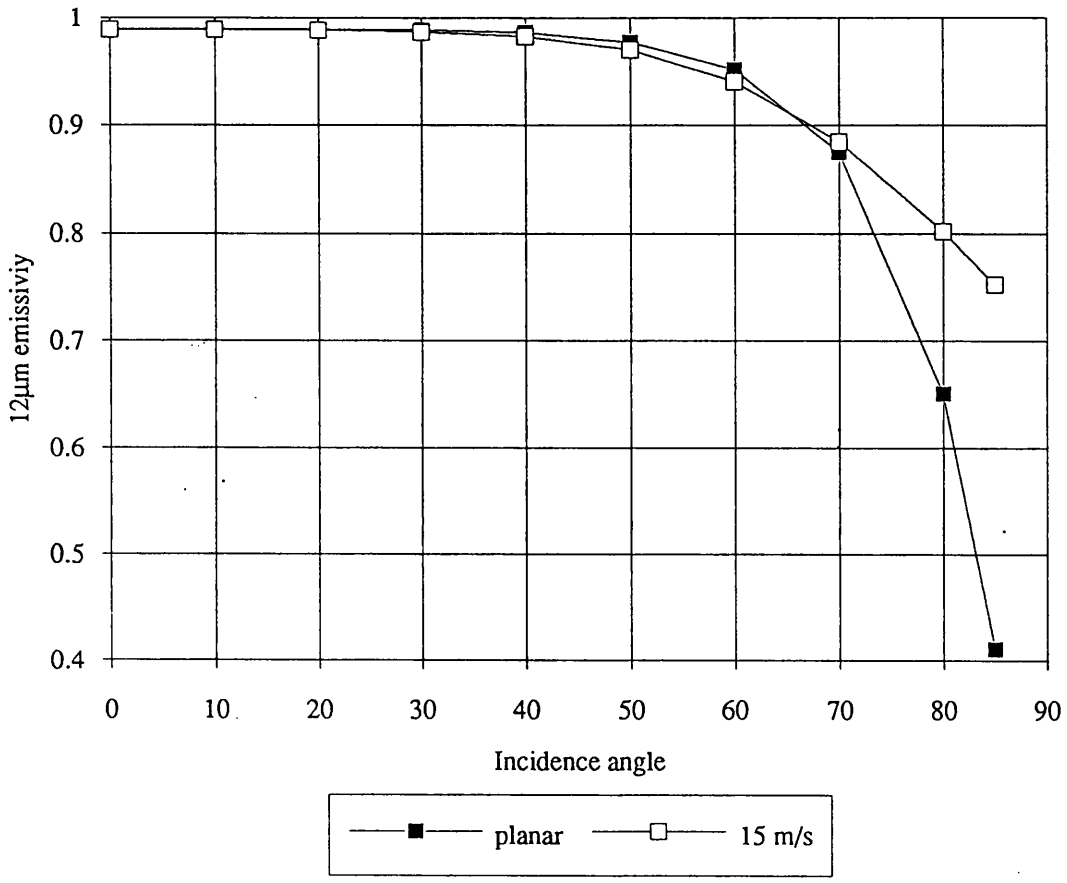

Figure 2.10 Water emissivity at 12µm for various incidence angles. Emissivity is plotted for both planar and a roughened surface corresponding to 15 m/s wind. Data from Masuda et al. (1988).

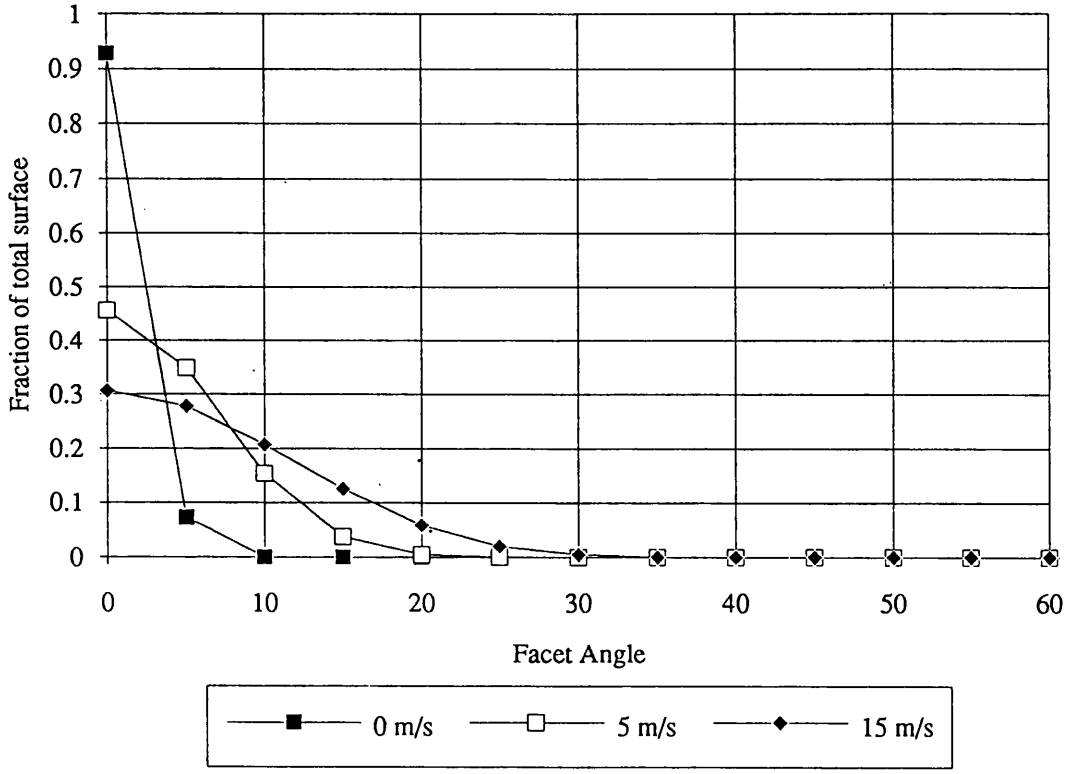

Figure 2.11 Angular distribution of surface facets with respect to the vertical due to wind roughening of the surface for 0, 5 and 15 m/s wind, after Cox and Munk (1955).

the wind the greater the angles introduced (Fig. 2.11) and therefore the larger the drop in emissivity (Fig. 2.10). Masuda used a wind roughening model developed from sunglint studies by Cox and Munk (1955). As can be seen from Fig 2.10 the effect of wind on emissivity is small at small incidence angles but in the region of 40° the effect starts to become noticeable.

The second method of determining the coefficients is to regress the measured brightness temperatures with in situ measured water temperatures. This method is used in the NOAA MCSST sea surface temperature product which is an operational product derived from AVHRR/2. For this product AVHRR/2 brightness temperatures are regressed against an extensive set of coincident buoy temperatures to produce the coefficients. These coefficients are not producing the temperature of the emitting layer in the ocean but that of the sub-surface or "bulk" temperature, where the buoy temperature is measured. Difficulties with this method include the need for extensive buoy data and the necessary spatial and temporal coincidence with the satellite data which, due to clouds, can be difficult to acquire. Furthermore the relationship between the temperature of the emitting surface and the bulk temperature is complicated and quite variable and therefore the accuracy of the retrieved temperature can never be better than the variability of this skin-bulk difference and in fact will be worse as there will be some atmospheric correction error. This skin-bulk difference or "skin effect" is dealt with in more detail in the following section.

Many authors have reported results of using both these methods with varying degrees of success, e.g. Barton (1983), Harris (1991), Llewellyn-Jones et al. (1984), McClain et al. (1983), McClain (1989), Minnett (1991), Brown et al. (1991). As AVHRR has only two thermal channels, one of which is sensitive to solar radiation, atmospheric correction can only be performed at night. However, the 3.7μm channel has severe interference and so little work has been performed using this instrument. Minnett (1991) gives an overview of some of these results and describes an error budget for AVHRR/2 which is reproduced in Table 2.3 which shows that the best one can expect to do with AVHRR/2 is ±0.35K. However Minnett (1991) finds that the general consensus of the above authors is that the mean biases are found to be ~±0.5K and with standard deviations of ~0.4 to 1K when comparing with bulk temperatures. Minnett (1991) attributes some of this increased error to temporal and spatial differences between the in situ and the satellite data. Better agreement might be possible if in situ radiometric temperatures were used but such measurements have been found to be difficult to make with high accuracy and are beset with cloud problems. Such problems have plagued the validation of ATSR sea surface temperature retrievals although validation exercises are starting to be published

Source of Uncertainty	Uncertainty, K	Comments and References
Brightness Temperature Measurements at Channels 4 and 5		
Prelaunch		
Black body target	up to ±0.35	*Weinreb et al.* [1990]
Calibration transfer	±0.1	*Weinreb et al.* [1990]
Inflight		
Residual nonlinearity correction	±0.1	*Weinreb et al.* [1990]
Detector noise/digitizer	±0.05	*Dudhia* [1989]; could be reduced by pixel averaging
Total	±0.2 to ±0.4	
SST Retrievals Using a Split-Window Algorithm		
Brightness temperatures		
Channel 4	±0.2 to ± 0.4	likely to be correlated between channels and
Channel 5	±0.2 to ± 0.4	not be amplified by algorithm
Atmospheric effect		
Residual	±0.2 to ±0.6	not correlated with brightness temperature errors
Total	±0.35 to ±1.0	

Table 2.3 Error budget for sea surface temperature retrieval by AVHRR. From Minnett (1991).

e.g. Mutlow et al. (1994) and indicate that ATSR has a significant contribution to make to the subject of sea surface temperature measurement.

2.6 Skin Effect

The skin effect is the temperature difference between the very surface of the water (termed the skin temperature) and the temperature of the water a few centimetres below the surface. Emitted radiation comes from this skin layer and so it is the skin temperature that radiometers measure. The thickness of this layer depends on the wavelength used but is generally less than 0.1mm (Robinson 1985), and therefore it is particularly difficult to measure directly which makes direct calibration of radiometers difficult. This can be solved by deliberately destroying the skin effect with equipment such as the stirred bucket described earlier.

The skin effect has been known for many years, one of the earliest references cited by Eifler (1993) is 1940 yet it was not until the mid 1960s that there was specific research into the phenomena. It is important to clarify that the skin effect should be distinguished from the diurnal thermocline or deck layer temperature variations. The diurnal layer's depth depends mainly on the level of wind induced mixing and is approximately 1m deep and ~ 1.5-0.15°C warmer than the water below this layer. Such a layer is due to solar insolation heating this region and should not be confused with the skin effect layer which is due to an entirely different mechanism and is in the region of 10^{-3}m rather than 1m in thickness as in the deck layer.

The skin effect arises due to two physical processes. Under normal situations there will be a heat flux either into or out of the water surface. Little solar radiation is absorbed in the first few cm of water and so for this thin layer the net flux is determined by evaporation, conduction and longwave radiation. For most weather conditions it is found that the net flux is generally out of the water for this layer. Secondly, away from the air-water interface (1cm to ~1m) there is sufficient turbulent mixing to remove any temperature inhomogeneity. However, as the air-water interface is approached turbulent mixing is impeded until at the boundary a laminar sub layer is established. In this region the only mechanism available for heat transfer is molecular conduction and therefore if there is a heat flux through this layer there must be a temperature gradient. Robinson et al. (1984) provides an extensive review of the literature on this subject and much of the following material is taken from this work.

The general characteristics of the skin effect are that the sign is determined by the sign of the heat flux. A net heat flux out of the surface will produce a skin temperature which is lower than that under the surface layer and vice versa. Unfortunately there is no consensus in the terminology for what constitutes a positive skin effect. In general the heat flux is out of the surface and therefore skin cooler than bulk. From this a general terminology has formed that this situation is quoted as a positive skin effect. However, this terminology leads to confusion when there is a flux into the surface and the skin is hotter than bulk resulting in a skin effect which is negative which for many is counter intuitive. Therefore in this thesis I have taken a negative skin effect to mean that the skin temperature is less than the temperature just below the surface. The largest range in skin effect measured in the field are reported by Schluessel et al. (1990) of -1.0 to 1.0K but these were under extreme conditions. A typical value would range between -0.5 and -0.1K for most clear sky conditions (Hepplewhite 1989). Another feature of the skin effect is that it can form very quickly. Robinson et al. (1984) report the findings of Ewing and McAlister (1960) where they observed the re-formation of a -0.6K skin effect in 10 seconds after vigorous stirring to destroy the skin had stopped.

The most widely used approach in parameterising the skin effect is that proposed by Saunders (1967b) where the air-water interface is taken as a solid wall/fluid boundary. The general situation with the fluxes and physical processes is depicted schematically in Fig. 2.12 and a magnified region of the actual interface in Fig 2.13. The net heat flux through the surface at night is composed of the thermal radiation emitted from the surface, Q_S, the thermal radiation from the sky, Q_a, the sensible heat flux, Q_C and the evaporative heat flux, Q_e, to give:

$$Q_N = Q_s + Q_a + Q_c + Q_e \tag{2.23}$$

From Fig. 2.13 one can see that there are two regions separated by a transition region. In the molecular layer the temperature gradient is linear, in the transition region it is non-linear and in the turbulent region there is no temperature gradient. Saunders (1967b) simplified this to a single linear region with no transition where the temperature gradient was given by the net heat flux out of the water, Q_N (+ve flux in the upward direction) and the conductivity of the molecular layer, k, in the relation:

$$Q_N = -k\frac{\partial T}{\partial z} = -k\frac{\Delta T}{\delta} \tag{2.24}$$

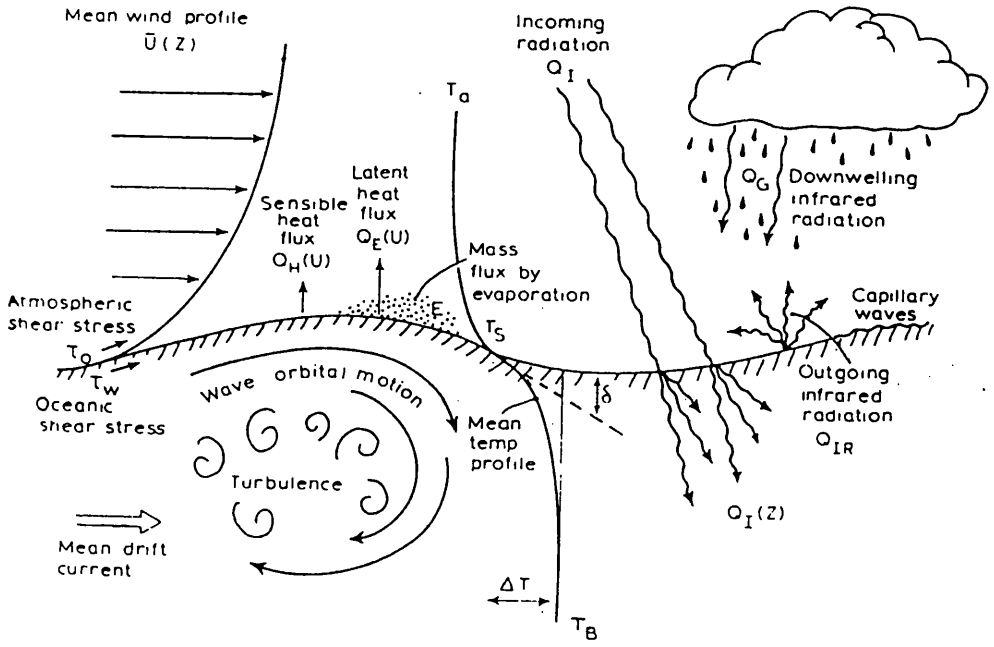

Figure 2.12 A schematic diagram of the physical processes occurring at the air/water interface of the ocean which contribute to the temperature drop across the aqueous boundary layer (Katsarros 1980 reproduced in Robinson 1985).

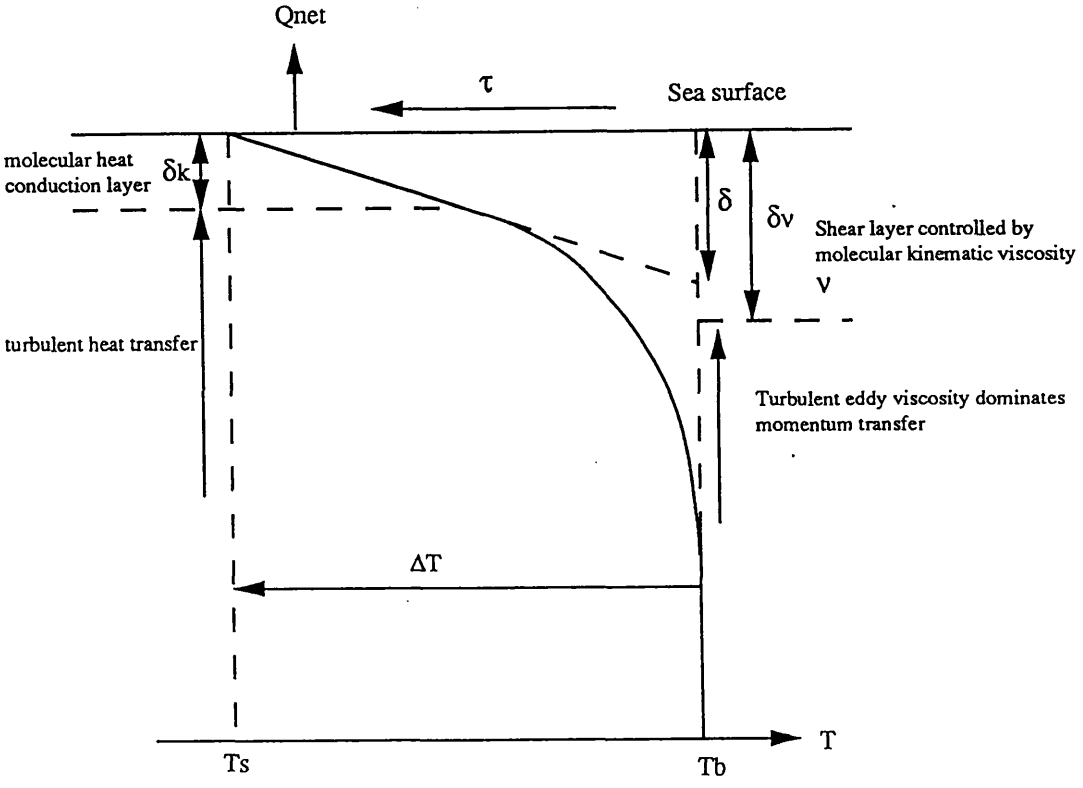

Figure 2.13 Detail of the air/water interface with definitions of the different layers near the surface as described in the text. A molecular heat conduction layer at the very surface has a linear temperature gradient for a heat fluxes passing through it. This layer is separated from the fully turbulent region by a transition layer which has a smaller non-linear temperature gradient.

and through dimensional considerations, the shear layer depth δ_ν is given by:

$$\delta_\nu \approx \frac{\nu}{U^*} \tag{2.25}$$

and is taken to be the thickness of the layer, δ, where the linear temperature gradient can be applied, to give:

$$\Delta T = \frac{\lambda Q_N \nu}{k U^*} \tag{2.26}$$

where λ is a dimensionless constant and U^* the wind friction velocity.

At zero wind stress (2.26) is singular but under these conditions there is no turbulent transfer and the above formulation is not appropriate. During the day there will be solar insolation and equation (2.23) should be modified to account for the solar flux. However as the layer of interest is so thin it has been found that the solar component has very little effect (Paulson and Simpson 1981). Contrary to this Schluessel et al. (1990) found it necessary to include a solar term in their empirical formulation of the day-time skin effect, although this is probably due to their bulk temperature being measured at 2m. Water at this depth is probably below the diurnal thermocline and therefore does not include information of the solar heating which water higher up would.

Much of the literature concerning the skin effect which uses the Saunders (1967b) formulation has been focused on the empirical determination of λ. Measurements are made directly of ΔT and the other parameters in (2.26) and a regression is formed to produce λ. The values found are summarised in Robinson et al. (1984) where the ranges reported are 2.2 to 15. Robinson et al. (1984) report that Saunders himself cautioned the initial success of his formulation (Saunders 1973), as the theory has to be a simplification of reality as the water surface is a free boundary. This will tend to reduce the thickness of the boundary layer and also suggests that λ will in fact be a coefficient dependent on the surface conditions, and hence wind, which has been found to be the case by many authors. One might also expect λ -> 0 as U^* -> 0 to stop (2.26) behaving in a non-physical way. Similarly there will be an upper limit but this in fact occurs due to a break down in the physical model when the wind is so strong that the molecular layer is broken with the formation of breaking waves.

Recently there has been a new approach to the formulation of the skin effect (Eifler 1992). In this work Eifler attempts a more realistic formulation of the fluid dynamics of

the fluid/fluid interface. A detailed explanation of the formulation is not considered necessary for this thesis. It is suffice to say that islands of laminar flow form at the surface or interface and grow in length. At a critical size they break down and this is characterised by a relatively violent ejection of fluid from the interface, which is in turn followed by a flow of less turbulent fluid towards the interface. These processes are called "burst" and "sweep" events. Waves on the surface fix the occurrence of these "burst" and "sweep" events to the ascending portion of the water wave, and it is at these events where momentum, and hence mass and heat, are transferred between the air and water. During the descending part of the wave, momentum, mass and heat are transferred within the fluids providing the transport mechanism for heat between the interface and the bulk. From this model it is possible to analytically determine the λ coefficient in eq. (2.26) which is found to depend on, amongst other things, the wind speed and the depth where the subsurface water temperatures are measured. Eiffler points out that the deeper the surface temperature is taken the more that temperature will be de-coupled from the processes determining the skin effect and the skin and bulk temperatures become less correlated. This is probably the cause of the differences in the value of λ found by many authors as the depth which the bulk temperature is taken is not standardised but determined by the measurement set-up. Eifler (1992) finds considerable agreement with the λ values found in the field by Grassl (1976) and Paulson and Simpson (1981) which have bulk temperatures taken at quite shallow depths, 5cm and 1m respectively.

There have been other attempts to derive an expression for the skin effect by empirical means. One such attempt is that of Schluessel et al. (1990). An extensive data set was acquired off the Spanish coast and North Africa which samples a wide range of meteorological conditions with a corresponding range of skin effect. Results validating the Saunders approach were disappointing and therefore a multiple regression was performed on the individual heat fluxes in equation (2.23) against the skin effect. A regression was performed for day and night fluxes which provided estimates of the skin effect to ± 0.17K and ± 0.1K respectively compared with ± 0.13K for the Saunders formulation. As stated earlier a potential problem with this data set is that the majority of the bulk temperatures were taken at a depth of 2 m which for calm conditions could be below the diurnal thermocline and above during rougher periods. This could explain the large positive skin effects that were occasionally recorded. Therefore the application of Schluessel's formulae to other situations should be made with caution and cannot be seen as a replacement for the Saunders equations.

2.7 Summary

This chapter has attempted to overview and summarise the different physical processes which are present or involved with the remote sensing of surface water temperatures. These have included the nature of emitted thermal radiation, the processes that the surface radiation undergoes as it passes through the atmosphere and the correction of this absorption by the atmosphere and the atmosphere's emission. There are also descriptions of two satellite-borne radiometers and one ground based which include discussion of their accuracies and calibration schemes. The chapter concludes with a description of the skin effect and its importance when interpreting surface and space-borne radiometer-derived temperatures. Work published on the parameterizing and modelling of the skin effect is reviewed and caution is recommended when applying empirical skin effect models.

Chapter 3.

Review of the Thermal Characteristics of Lakes and previous work on their climate response.

3.1. Introduction

The temperature structure and thermal behaviour of a lake through the year is dominated by three things; the climate that it is exposed to, the physical characteristics of the lake and the density/temperature relationship of water. Broadly speaking, the climate determines the energy fluxes into and out of the lake if we assume that the heat exchanges only occur through the surface. The physical dimensions of the lake e.g. area, fetch, depth and volume, can generally be considered as determining how a particular lake will respond to a climate regime, and the density/temperature relationship of water determines the internal temperature structure of a lake.

This chapter comprises a review of the current state of knowledge on the thermal characteristics of lakes, with particular emphasis on their relationship to climate. It begins with a discussion of the thermal behaviour of lakes through an annual cycle, and then discusses the heat exchange processes. It then addresses the factors specifically affecting lake temperature, before moving onto previous thermal modelling of lakes and finally discussing how the thermal characteristics of lakes have been used for climate research to date.

3.2 Thermal behaviour of lakes round the annual cycle

The thermal behaviour of lakes is well known in general terms. To explain this behaviour it is instructive to describe the progress of an idealised temperate latitude lake through an annual cycle. I will use a format similar to that of Ragotzkie (1987). Figure 3.1 is a schematic diagram of the variation of temperature with depth, of a lake for the twelve months of the year and should be consulted for the following discussion.

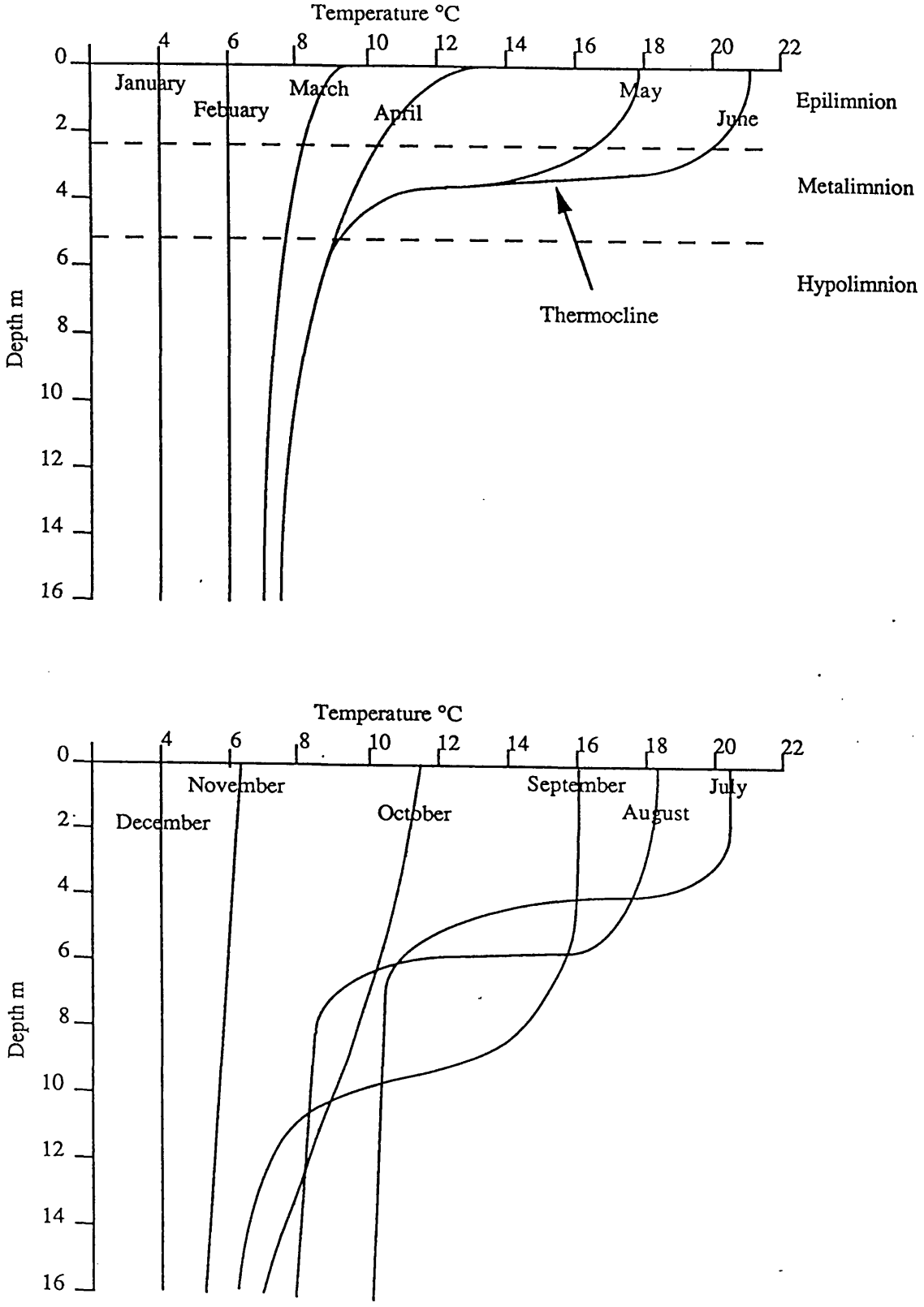

Figure. 3.1 Schematic diagram of the evolution of the temperature profile for a N. hemisphere mid latitude lake through the annual cycle.

Starting in late winter when the ice, if there was any, has broken up and melted, the lake will be isothermal in the temperature range of 1 - 5 °C. As spring progresses, heating will take place mainly by solar radiation penetrating into the upper layers of the lake. This energy is mixed uniformly throughout the lake and the lake temperature will begin to rise. As spring runs into early summer the rate of heating of the upper layers of the lake increases to a degree which is higher than the rate of mixing to the lower levels. This effect is aided by the exponential decrease in the solar insolation with depth. Therefore the temperature of the upper layers becomes hotter relative to those below. As this continues, a temperature-induced convective stability develops due to the hotter surface water having a lower density. This further restricts the downwards transport of heat by wind mixing. The resulting vertical temperature structure in mid-summer is an upper isothermal layer well mixed due to wind mixing; a bottom layer cooler by several degrees; and a layer between these two where there is a large temperature gradient with an inherent density stability preventing the vertical mixing of water between the top and the bottom layer. An example of this is Fig. 3.2 which shows summer temperature profiles for Linsley Pond, Connecticut. The upper layer is called the epilimnion, the lower layer the hypolimnion and the transition region is called the metalimnion. The thermocline is defined as the plane of maximum temperature gradient with depth in the metalimnion layer i.e. the plane connecting the points of inflection in the temperature profiles for all points on the lake (Hutchinson 1975).

It is not always the case that a lake will stratify even if there is a lake at a similar latitude which does. This can be due to higher levels of wind, such as the differences between a continental and a maritime climate. Fig. 3.3 demonstrates this with two lakes, Evangervatn in western Norway and Holsfjord in eastern Norway, which receive the same energy flux but have strikingly different summer temperature profiles. The very weak thermocline for Evangervatn is due to the generally higher wind speeds which do not allow a buoyantly stable epilimnion to form. Many lakes in the British Isles do not form or rarely form marked thermoclines due to the maritime climate of the UK and the associated higher winds and cooler summer air temperatures (Hutchinson 1975).

Through the summer this stratification persists if formed, and the temperature of the epilimnion increases with very little heat being transferred to the hypolimnion. At the end of summer and the beginning of autumn there will come a time when the lake changes from having a net gain in energy to a net loss. This is due to the level of solar radiation decreasing, the rate of evaporation increasing and the conduction component swapping from into to out of the lake (see section 3.3 for detailed discussion of these energy exchanges). Cooling occurs at the surface of the lake and as this cool surface

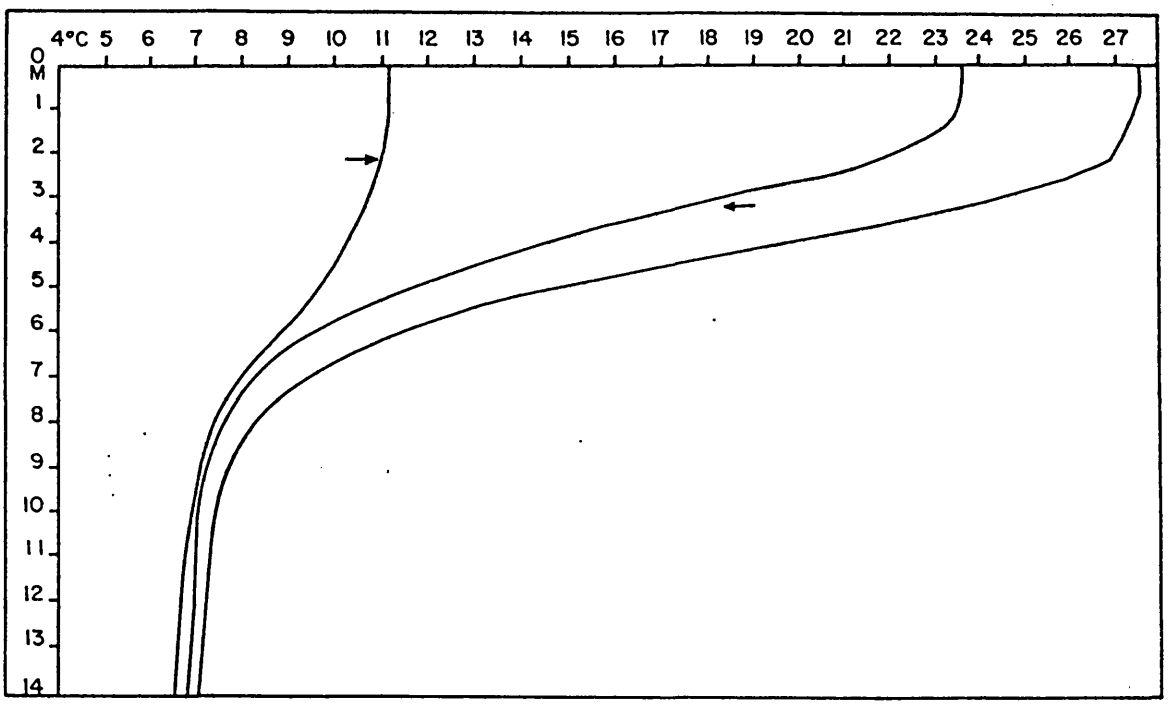

Figure 3.2 Temperature profile for Linsley Pond, Connecticut for August 3-17 showing a distinct thermocline. Reproduced from Hutchinson (1975)

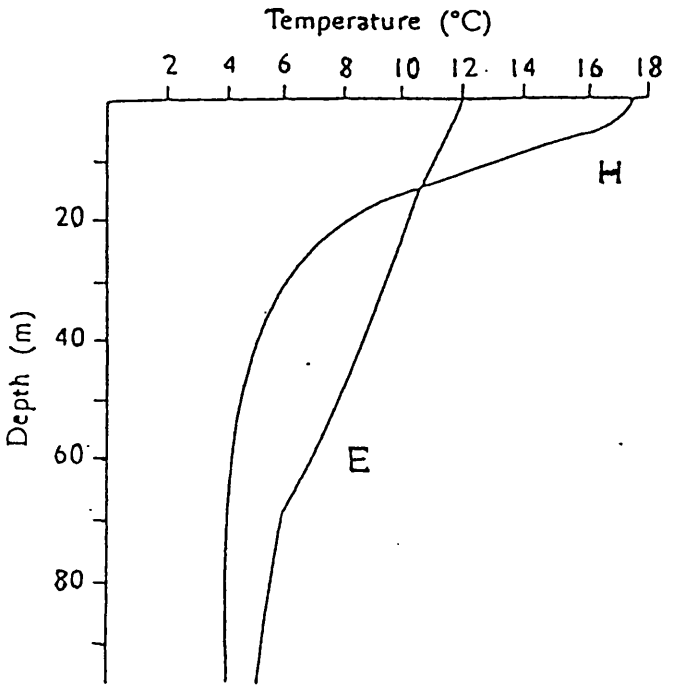

Figure 3.3 Temperature profiles for Evangervatn in western Norway and Holsfjord in eastern Norway showing the effect of continental (Holsfjord) vs. maritime (Evangervatn) climate on the formation of thermoclines. Reproduced from George (1989)

water becomes denser relative to the water immediately below, it sinks. Thus the epilimnion continues to be isothermal as it cools and the temperature difference producing the thermocline is slowly eroded. There is also, however, an increase in the level of wind which is generally associated with the autumn. The depth of the thermocline deepens due to the combined effect of this increased wind and the reduction in the temperature-induced stability. Eventually the thermocline is small enough that the increased wind mixing destroys it completely and again the lake is isothermal but at a higher temperature than when it became stratified in the spring. Cooling continues through the autumn and early winter. If the water temperature falls below 4°C, the temperature of maximum density, one might expect there to be a inverse thermocline (surface cooler than below) but the small change in density below 4°C means that the wind can easily destroy any inverse thermocline which may develop.

If the lake is to freeze then the surface water needs to be at 0° C and this generally occurs on clear, still nights when there can be a rapid loss of heat from the surface to the atmosphere, primarily by radiation, without any wind mixing with the warmer deeper layers. Since the whole lake surface experiences this condition at the same time, the lake can completely freeze over in a very short period, often in a single night (Ragotzkie 1987).

Once the lake freezes the only heat losses that can occur are conduction and radiation from the surface of the ice. Heat gains are from solar radiation penetrating the ice and heating the water. Heat is also released from the sediments generally resulting in a net gain in heat for the water. Once the ice is covered with snow the rate of heat exchange through the ice falls dramatically. Snow insulates the ice against conduction to the atmosphere and the high albedo of snow reduces the amount of solar radiation reaching the water. It is, however, still found that the water continues to experience a very small net gain in heat with snow cover (Ragotzkie 1987). The net thermal energy content of the water and ice, however, falls due to the energy needed to melt the ice.

Underneath the ice thermal gradients can exist since there is now no wind mixing. After freezing there will be an inverse thermocline with the water near the ice near 0° C. It is also possible, however, to get quite large positive thermoclines just below the ice due to melted water from a temporary thaw being very low in dissolved solutes and therefore of lower density. Solar radiation penetrating the ice can heat this dilute layer to several degrees above 4° C without producing instability (Hutchinson 1975).

Ice break-up is preceded by the disappearance of the overlying snow, melted by the warmer air of spring. The melted snow can then evaporate, freeze or drain away. Once the snow is gone there is strong solar heating, through the ice, of the water underneath due to the drop in albedo, and the ice is melted from the bottom up. At a given thickness the ice becomes structurally unsound and a strong wind can break up the ice sheet in less than a day. Once the ice is broken it rapidly melts with the energy coming from the heat stored in the lake and the mixing which can now take place due to the exposed water surface to the wind.

This brings us back to the spring situation of general circulation. Lakes which follow this thermal cycle, that is of two periods in the year where the lake is isothermal in autumn and spring and being completely mixed by the wind, usually termed general circulation, are called dimictic. Warm monomictic lakes are those which experience one period of general circulation and whose minimum temperature exceeds 277K. Cold monomictic are those with again one period of general circulation but whose maximum temperature does not exceed 277K. Oligomictic lakes are those which are rarely in general circulation, polymictic those which are often in circulation, and meromictic lakes those which remain unmixed due to stability from density gradients caused by dissolved salts (Hutchinson 1975).

3.3 Heat exchange processes

For most lakes, the majority of the heat transfer occurs at the surface of the water. There are lakes which have significant energy exchanges, due to geothermal activity, with the bedrock and sediments on which they lie but these are a small minority and most lakes have a small energy exchange with the bottom sediments. Inflows and outflows are for many lakes generally small compared with the surface fluxes with the exception of small lakes which are part of a fast flowing river system (Ragotzkie 1987). To understand the thermal behaviour of lakes it is therefore important to understand the physical processes which make up the surface energy flux. These components are radiation (both short and long wave), water evaporation and condensation, and surface conduction which combine to form the surface heat flux equation;

$$\Phi_{Net} = \Phi_{Sol} + \Phi_{Long\_in} - \Phi_{Long\_out} - \Phi_{Evap} - \Phi_{Cond} \qquad (3.1)$$

A more detailed account of how these fluxes are determined can be found in the following chapter, but here is presented a qualitative overview of these processes.

Shortwave Radiation Φ_{Sol}

The majority of the shortwave radiation incident on the surface is direct radiation from the sun, although there is a smaller component of scattered sunlight from the rest of the sky. The level of direct and scattered shortwave radiation depends on the absorption and scattering along the atmospheric path and on the level and type of cloud if present. Atmospheric scattering and absorption is due to atmospheric molecules as well as aerosols. The explicit calculation of the atmospheric attenuation is generally not feasible as this involves detailed information of atmospheric constituents, which are usually not available, and requires considerable computing effort. Therefore the atmospheric attenuation is usually empirically approximated, which is acceptable due to its relatively low variability, or it can be derived with a solar radiometer. Sunshine duration has been traditionally measured with the Campbell-Stoakes sunshine recorder which relies on focused sunlight burning a track across a piece of card. This gives a good measure of strong direct sunlight but there is a threshold level of solar flux needed to cause a burn. Therefore low flux levels associated with translucent thin cirrus will not be represented in the recorder, and neither will scattered radiation. It has been noted (Henderson-Sellers 1984) that this deficiency can be a source of significant error. The level of indirect solar radiation is also dependent on the level and type of cloud cover. Obviously thick blanket cloud will produce low fluxes but thin cirrus and broken cloud can produce high levels of scattered light.

The albedo of the lake varies with the angle of incidence and level of surface roughness but is generally very low except at large incidence angles, typically in the region of 0.06 (Henderson-Sellers 1984). Following Beer's law, this radiation penetrating the surface will be absorbed in an exponential fashion however this is not found experimentally. Henderson-Sellers (1984) reports that a certain fraction, β of the incident sunlight is found to be absorbed in a surface layer z_n, which is approximately 0.6m, after which exponential absorption takes place. Thus the rate of energy absorption with depth has the form,

$$\Phi(z) = (1-\beta)\Phi_0 e^{-\eta(z-z_n)}$$

where

Φ_0 is the rate of solar radiant energy absorption at the surface

η is the extinction coefficient.

The extinction coefficient can have a large variation in value (0.1 -10 m^{-1}) depending on the suspended sediment load and the photosynthetic activity of the lake as shown in Fig. 3.4. For example Lough Neagh in Northern Ireland, the subject of a case study and

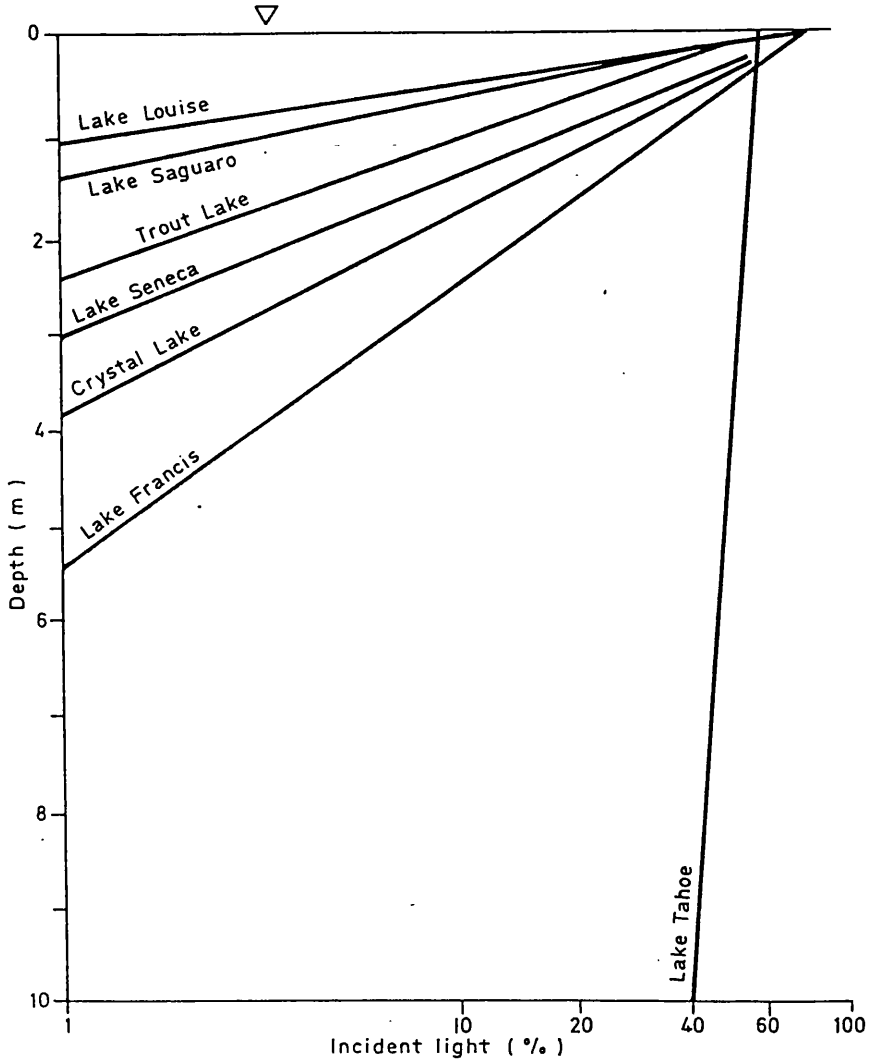

Figure 3.4 Variation of light intensities with depth for several lakes world-wide. Reproduced from Henderson-Sellers (1984).

modelling in later chapters, has a measured unity optical depth of 0.4m (Gibson 1990). If there is any surface floating material like algal blooms then z_n becomes very small and β becomes very large as most of the incident sunlight is absorbed by the bloom and little passes into the lower layers.

Longwave Radiation Φ_{Long_out} and Φ_{Long_in}

The longwave radiation budget of a lake has two components. The first is the radiation emitted from the lake (Φ_{Long_out}) and is a straight forward calculation from the Stefan-Boltzman law. The emissivity of the lake, ε_W, is generally very high and can be taken to be ≈ 0.97 (Henderson-Sellers 1984), but can change considerably if there are any surface slicks or algal blooms (Robinson 1985). The second longwave component is the thermal emission from clouds and the atmosphere into the lake (Φ_{Long_in}). This can also be calculated from the Stefan-Boltzman equation, however the evaluation of the emissivity and the temperature of the atmosphere is quite difficult. Various layers in the atmosphere (including clouds) contribute to the down-welling radiation, each of which will be at different temperatures and have different emissivities. It is only possible to explicitly calculate the down-welling flux of the atmosphere if one has knowledge of the atmospheric temperature and constituent profiles and the cloud field from which a solution to the radiation transfer equation can be numerically found. If an attempt to calculate the down welling radiation is to be made, and a solution to the full radiation transfer equation is not possible in the circumstances, then some mean atmosphere temperature needs to be determined with an average emissivity which is dependent on the level of cloudiness and atmospheric water content. A common approach to the problem is to take the atmospheric temperature and humidity to be that of ground level as this is what is routinely and easily measured, and use an empirical relation for the emissivity to compensate for the overestimation of the actual emitting temperature of the atmosphere. Increased cloud cover will increase the downwelling radiation due to its higher temperature relative to the air above it and can be empirically accounted for in the estimate of emissivity or added in as a separate term independent of the air temperature.

Evaporation Φ_{Evap}

Evaporation is a major energy loss in the heat budget of a lake, and occurs in the top layer of water molecules. The physical principles of this were established by Dalton in 1802. It depends directly on the vapour pressure gradient across the air/water boundary and is thus affected by the temperatures of the air and water, the stability of the atmosphere above the water, the atmospheric water content and the level of wind. As water is evaporated, the water vapour pressure in the atmosphere increases and if there is no form of water vapour removal, the air will eventually saturate preventing further

evaporation. Convection and wind provide mechanisms for this removal, however, it is very difficult to quantify these processes. As they are difficult to parameterise through explicit physical processes, empirical relations have been developed. These however have difficulty in representing all the different meteorological conditions found over lakes, e.g. from calm conditions to high winds and unstable to stable atmospheres. Evaporative energy loss can be broken down into two components. The first is the energy associated with the phase change from water to a vapour and is parameterised in the latent heat of vaporisation. The second component is the heat loss associated with the physical removal of mass at the temperature of the water and is parameterised by the specific heat of water. This second component is far smaller than the first and can be neglected (Henderson-Sellers 1986). If the water vapour pressure in the air is greater than that of the water then the lake can gain water molecules or if the air saturates condensation can take place.

Conduction. Φ_{Cond}

This also occurs at the water surface but is a smaller energy exchange process compared with those previously mentioned. It depends on the temperature gradients in the water and the atmosphere in the boundary layer. The extent of this boundary layer is of the order of 0.1cm and 0.4cm for the water and air respectively. Outside this layer turbulent energy transfer mechanisms dominate (Ragotzkie 1987). Conduction is often referred to as the sensible heat transfer.

In limnological studies it has been found convenient to relate the evaporative heat flux and the conductive heat flux via the Bowen ratio. As discussed by Henderson-Sellers (1986), this is the ratio of the conductive to the evaporative heat flux and assumes that the turbulent diffusivities for water vapour and sensible heat are the same. Thus only one of the two fluxes needs to be determined and the other can be derived from the Bowen ratio. It can be derived from semi-empirical equations for the evaporative and conductive energy fluxes,

$$\Phi_e = -\rho L_v K_v \frac{\partial q}{\partial z}$$

$$\Phi_c = -\rho c_p K_h \frac{\partial T}{\partial z}$$

where

Φ_{Evap}, Φ_{Cond} are the evaporative and conductive heat fluxes respectivly,
L_v is the latent heat of vaporisation,
q is the specific humidity,
c_p is the specific heat at constant pressure,
K_v, K_h are the turbulent diffusivities for water vapour and sensible heat.

K_V and K_h are functions of atmospheric stability, height from the surface and friction velocity. The Bowen ratio can then be deduced by using the approximation

$$q = 0.622.e/p$$

where e is the vapour pressure and p the atmospheric pressure giving the Bowen ratio the from Henderson-Sellers (1986)

$$B = \frac{\Phi_c}{\Phi_e} = \frac{c_p K_h p}{L_v K_v 0.622} \cdot \frac{\partial T}{\partial e}$$

Parameterisation of the conduction heat flux is complicated by similar factors to the evaporative flux.

Minor energy exchange processes

There are other energy fluxes in the energy budgets of lakes which are generally very small compared to those mentioned above. The sediments and bedrock (excluding geothermal activity) tend to store up heat during the summer months and release it during the winter. This has a stabilising effect by being out of phase with the majority of the heating processes. It has been found to be a very small contribution to the energy budget during the summer months but if the lake becomes frozen then the release of heat from the sediments during the winter are a significant heat source. Other sources are precipitation, inflow and outflow; all of these will be ignored in further discussions as precipitation is a small contribution to the energy budget and studies in this thesis will be limited to lakes where the inflow and outflow are small.

3.4 Limnological Factors affecting lake temperature

As well as climate related parameters (air temperature, humidity etc.) there are a number of limnological factors which influence the lake temperature. The temperature dependence of the density of water has a very important role in determining the temperature structure and behaviour of a lake through the annual cycle. This dependence

is depicted in Fig. 3.5. One can see that the maximum density occurs at ≈ 4°C but more important, in regard to lake temperatures, is the low magnitude of the gradient of the curve around this maximum density. At higher temperatures it is much larger and this is fundamental to the thermal behaviour of lakes. A lake with a vertical temperature gradient of 4 to 10°C will have the same stability against convective mixing as a lake with a temperature gradient of 26 to 27°C (Ragotzkie 1987). As stated in an earlier section, in early spring, when if there was any ice it has melted, the lake is in the region of 4°C it will have very little density induced stability to resist wind mixing. Therefore the whole lake can be isothermal as there is enough energy in the wind to mix the whole lake. However as the lake heats up as a whole the gradient of the density/temperature increases sharply and an increasing amount of energy is needed to overcome the stability caused by a given temperature difference. Due to the increasing solar flux levels of spring and the time lag for mixing to the bottom the surface/bottom water temperature difference can eventually become large enough that there is not sufficient energy in the wind mixing to overcome the temperature induced stability. As mentioned earlier there are regions where the wind is strong enough to prevent this happening. A similar situation occurs during the autumn where the epilimnion is losing energy until the top/bottom temperature difference is small enough that the wind can overcome the lakes stability and complete mixing is possible. Many lakes in the temperate latitudes will pass from this area of low stability to the regions of higher stability and back again through the annual cycle and this is reflected in the thermal structure of the lake.

The fetch of a lake can have a considerable influence on a lakes temperature characteristics. Fetch has been defined as the length of open water over which the wind has blown (Hutchinson 1975) and is therefore dependent on the direction of the wind for lakes which are not circular. It has also been defined as the square root of the surface area of the lake (Gorham and Boyce 1989). This latter definition is not dependent on lake/wind orientation but can clearly be an over-simplification for long thin lakes. The depth of the summer thermocline has been shown to be related to fetch by many people, such as Ragotzkie (1987), Gorham and Boyce (1989) and Henderson-Sellers (1984). Empirical relationships have been established for restricted areas, for example several lakes in central Canada and Wisconsin have been shown to follow a very simple relationship relating unobscured fetch with the depth of the summer thermocline, of:

$$D = 4 \,.\, \sqrt{F}$$

where D is the depth of the thermocline in metres and F the fetch in Km (Ragotzkie 1987). The reason for this relation is that the larger the fetch the larger the mixing effect

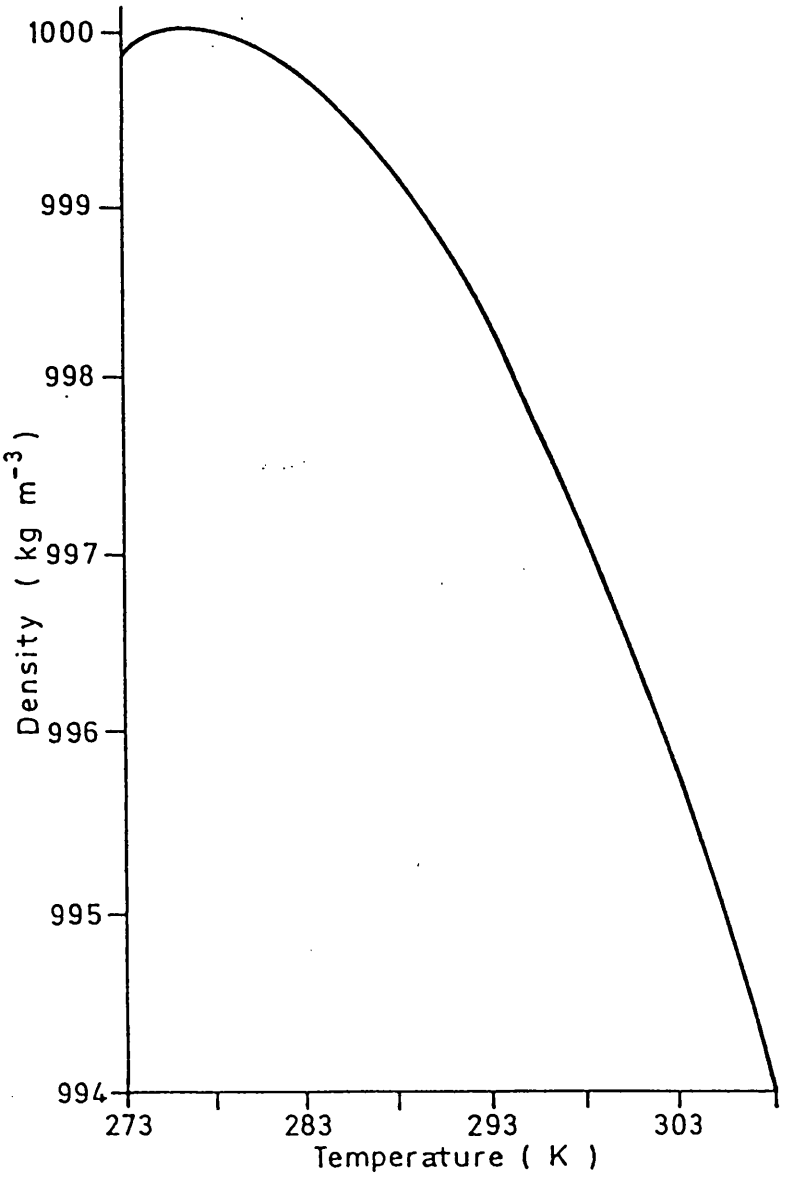

Figure 3.5 Density of water as a function of temperature at a pressure of 1 atmosphere. Maximum density occurs at ~277K. Reproduced from Henderson-Sellers (1984).

for a given wind speed and the heat absorbed in the top layers will be mixed further down. A more physical approach is taken by Gorham and Boyce (1989) taking into account lake depth. The best estimates of the thermocline depth are models which take account of the fluid dynamics within the lake and the relevant meteorological forcing, but a review of these is considered to be outside the bounds of this thesis.

Fetch has also been shown to be correlated to the temperature at which a lake freezes (Ragotzkie 1987). Fig. 3.6 shows this relation. This effect can be explained by the fact that to freeze the lake water needs to be at 0°C. Although water at this temperature is less dense than hotter water, the temperature induced stability is very weak. The larger the fetch the stronger the mixing force for a given level of wind. Therefore lakes with a large fetch are more likely to experience a wind which will destroy the inverse thermocline and thus prevent freezing. Thus these lakes need to cool to a lower temperature to have a stronger inverse thermocline to resist the wind mixing. Also at these lower temperatures less heat needs to be lost so freezing can take place in a shorter time for a given rate of heat loss. Further more, the longer the lake takes to cool down, the cooler the general weather, so the rate of heat loss increases, which in turn increases the probability of the lake freezing.

Altitude has a similar effect to that of latitude away from equatorial regions, see Fig. 3.7, which diagrammatically shows the relation between latitude and altitude for various types of lake. Hutchinson (1975) reports the findings of Halbfass (1923) for Loch Hope and Laoghal on the west coast of Scotland. These Lochs are of comparable area and depth but lie at altitudes of 3.8 and 113m respectively. Halbfass (1923) reports Loch Hope to be warmer than Loch Laoghal by 0.8-2.8 °C at all depths and attributes this difference to the altitude differences of the Lochs, though without offering any detailed mechanism. It is interesting to note that the temperature change of air due to adiabatic expansion for this altitude difference would only be ≈ 0.6 °C. This indicates that lake temperatures are more sensitive to altitude than the adiabatic cooling of air warrants, a possible explanation for this is suggested in Chapter 5.

The depth of a lake has an important role in determining its thermal characteristics mainly through determining the heat capacity of the lake. Shallow lakes do not stratify in summer due to the expected thermocline depth being larger than the lake depth. For a given surface area a shallow lake has less heat capacity and therefore can cool faster and this is reflected in earlier freezing dates for shallow lakes compared with deep lakes. The smaller heat capacity also allows the temperature of shallow lakes at the time of ice

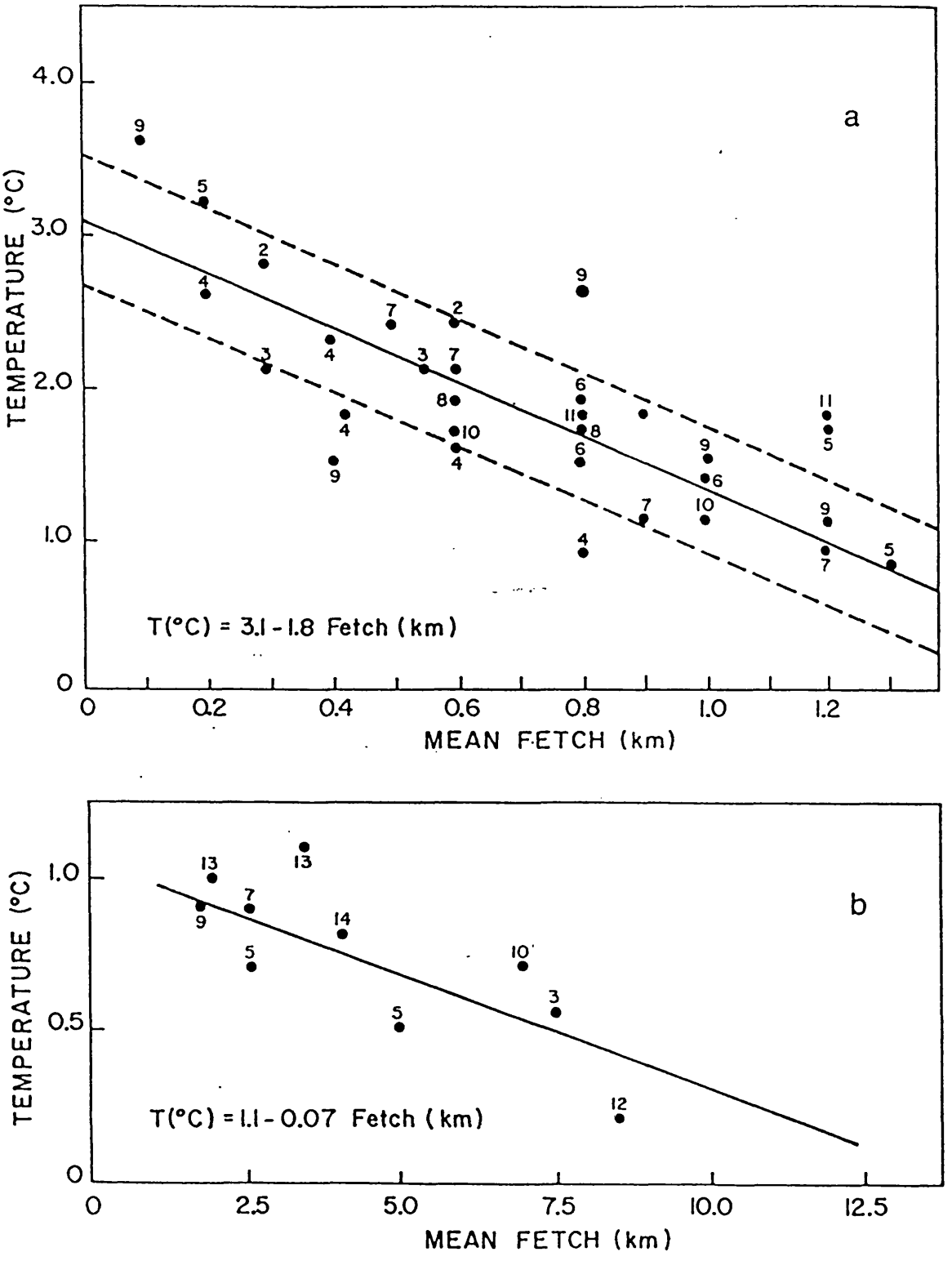

Figure 3.6 Relationship between water temperature at the time of freeze-up and fetch for Wisconsin lakes. Numbers above points are mean depth in metres. Reproduced from Ragotzkie (1987).

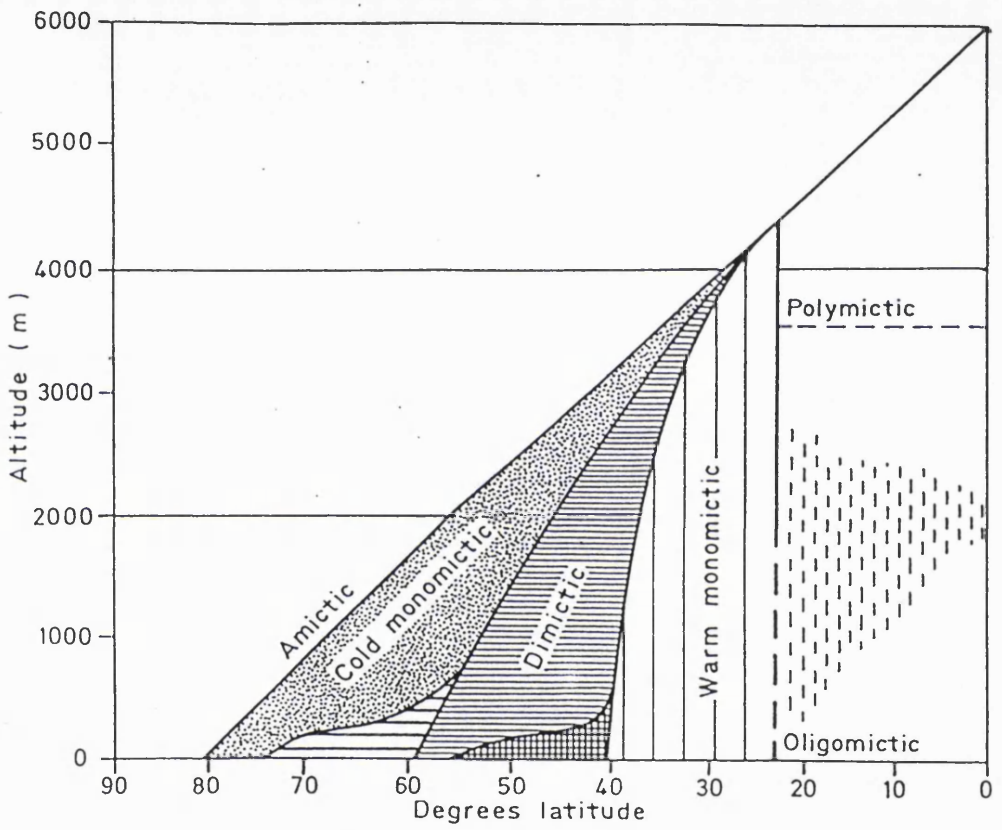

Figure 3.7 Schematic diagram showing the relationship between lake type, latitude and altitude. The hatched region is where there is a transition between Warm Monomictic and Dimictic and similarly for the widely spaced horizontal bars between Dimictic and Cold Monomictic. Reproduced from Henderson-Sellers (1984).

break-up to be higher than deep lakes, because of the small level of net heat flux into the lake during ice cover.

Very large and deep lakes, such as the Great Lakes, which have gently sloping sides can experience a peculiar thermal situation called a thermal bar. This is when the water in the shallower water near the shore heats up rapidly relative to the deeper central water. Due to the size of the lake the warm water is not mixed into the rest of the lake before it has reached a temperature several degrees higher than the central waters. Therefore there is a horizontal temperature gradient and hence density and pressure gradients as well, with resulting pressure induced currents. As the current begins to flow due to these pressure gradients, the Coriolis force comes into effect and, if the lake is large enough, the water flow becomes geostrophic with an anticyclonic circulation near-shore and weak cyclonic flow offshore with the convergence at the thermal bar, the point of highest density, at 4°C. Fig. 3.8 shows the results of a model predicting the currents associated with a thermal bar.

Large horizontal surface temperature gradients can also occur in summer if there is a sustained strong wind in a constant direction. This can push the epilimnion downwind and expose the cooler hypolimnion.

3.5 Previous work on the thermal modelling of lakes

Traditionally lake thermal models have been deterministic, and constructed for specific lakes or small regions. Models generally start out with a physical representation of the heat transfer components based on well known physical laws and principles. However for many conditions an exact physical description is unknown, so an empirical function or constant is added to the physical reasoning to model the observed effect. This has generally involved obtaining large amounts of in situ data from which the coefficients or empirical functions of the model can be determined and the model 'tuned'. There are basically two types of model which use meteorological data to calculate the water temperature. The simplest are the surface energy budget models and have had considerable success (Sraskraba 1980). These assume that all the major heat exchanges occur through the surface of the lake and that the water which is affected by the heat fluxes is well mixed. That is to say for a lake which is in general circulation the water affected is the entire lake, but for a stratified lake only the water above the thermocline takes part in the energy exchange processes (Ragotzkie 1987). The other type of models are dynamic models which try and represent the hydrodynamics of the lake. These are

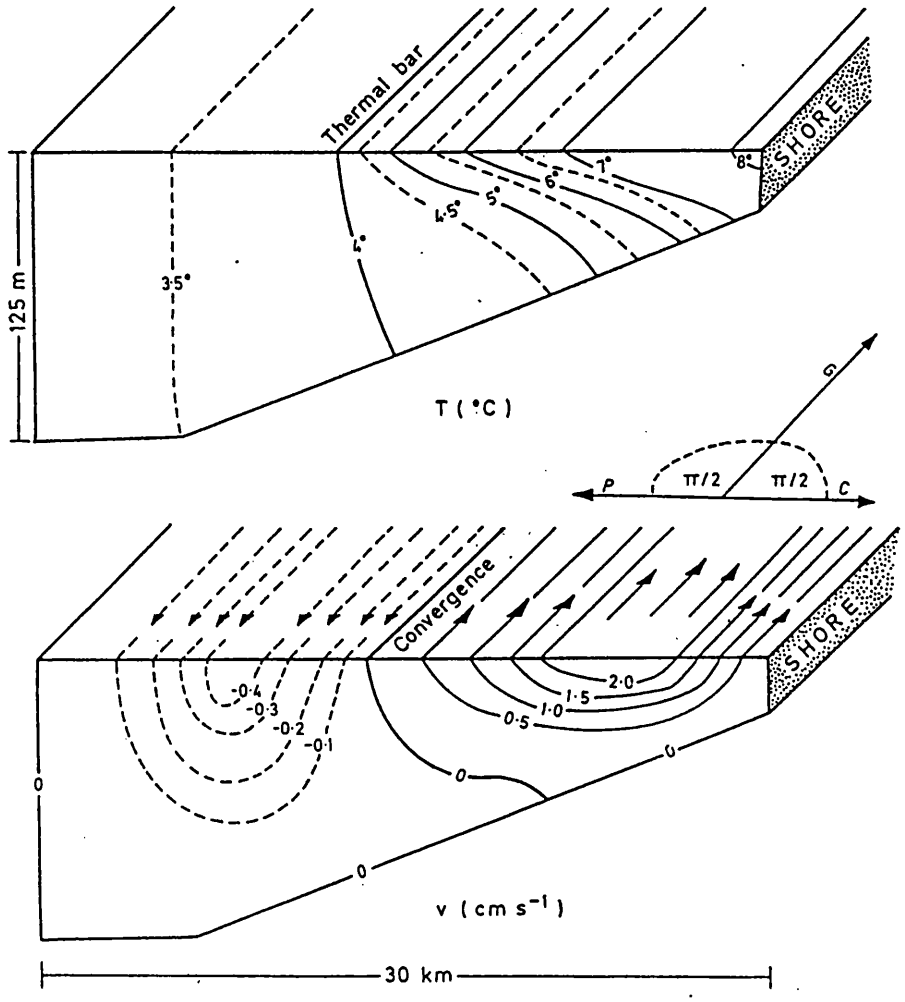

Figure 3.8 Section through a model of a thermal bar showing temperature and resulting current distribution. Horizontal temperature gradients produce density gradients and hence currents. Geostrophic balance is established resulting in the currents shown. Reproduced from Henderson-Sellers (1984)

useful if the internal temperature structure of a lake is of interest, but have the disadvantage of being computationally intensive.

The problems associated with models which need "tuning" to a particular lake are that one needs historical records of the lake's thermal behaviour and meteorological conditions, both of which might not be available and are difficult and expensive to collect. Secondly the set of coefficients derived by these records, or the form of the model developed, is generally not universal and so generally cannot be applied to other lakes in a different climates or situations with any confidence. For example some models developed for the United States cannot accommodate periods of ice cover in their simulations and therefore are unsuited to much of the northern latitudes (Henderson-Sellers 1984). Hence such models are difficult to generalise as a way of monitoring climate change, for example, from a temperature series of a number of lakes distributed over the globe.

There has been an attempt at global modelling of lake temperature by Sraskraba (1980). The rationale behind this model is that the sinusoidal nature of the solar radiation flux reaching the ground for clear skies, which is a function of day number and latitude, will be in some way followed by annual lake temperature cycles. In the development of this model Straskraba finds from a study of approximately fifty lakes between 26°S and 74°N that an equation for the surface water temperature has the form

$$T(t,f) = A_0 + A_1 \mathrm{Sin}\big(p(t+f)/180\big)$$

with the coefficients A_0, A_1 and ϕ derived from least squares fitting to the fifty lake temperature records. It was found that this equation can describe 85-95% of the thermal variation of lakes in this latitude region. Figure 3.9 is the surface temperature cycle predicted by this model for selected latitudes. Testing this equation on ten other lakes not included in the regression indicates the model's success is high, Fig. 3.10. Deviation from the model for particular lakes has been suggested to be due to variations in continental, topographic and cloud climatology (George 1989). For northern lakes which freeze this model is also inadequate as the heat transfer processes change completely with ice cover.

Figure 3.11 depicts Straskraba's findings for the latitudinal variation of A_0 and A_1. Mean lake temperature (A0) decreases with increasing latitude due to lower net annual solar insolation at higher latitudes. The semi amplitude shows a more complex variation with latitude with the maximum at $\approx 50°$ and dropping off sharply at the polar regions to zero

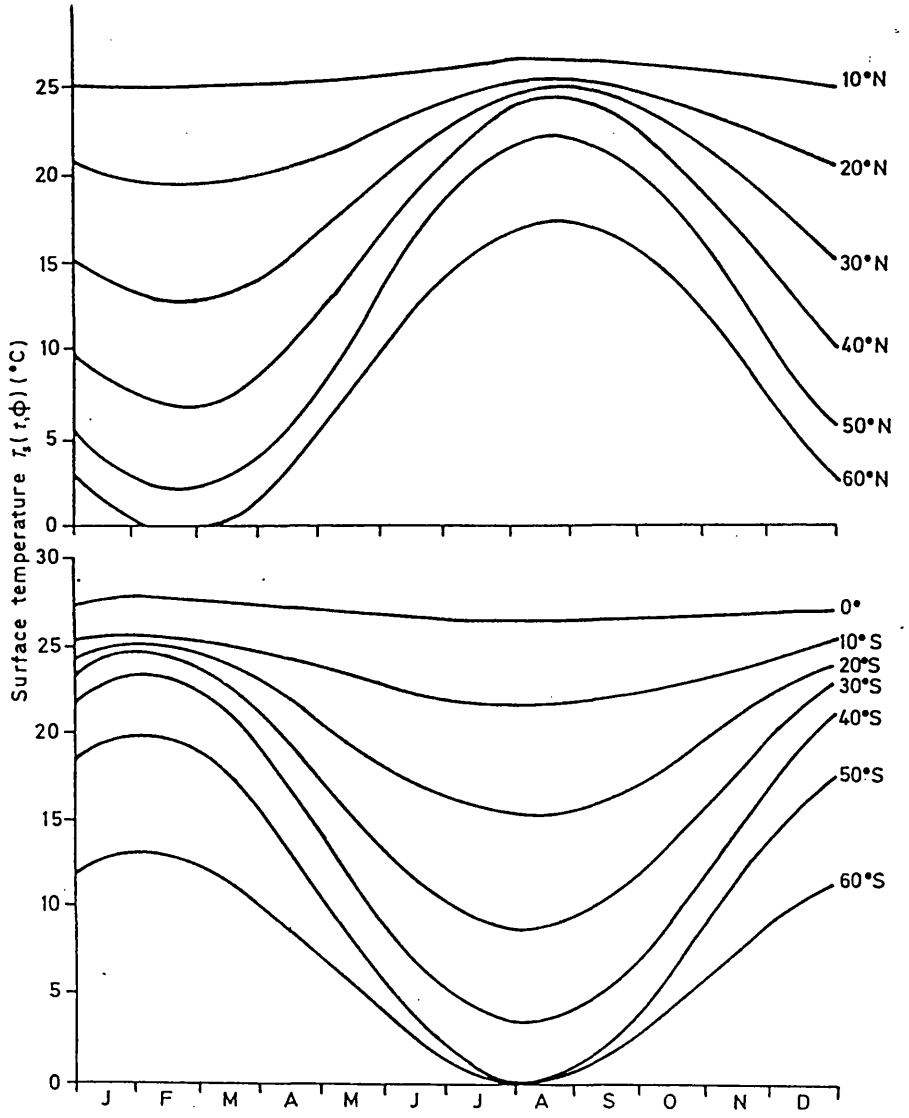

Figure 3.9 Annual surface temperature for selected latitudes modelled by Sraskraba (1980), for northern and southern hemispheres.

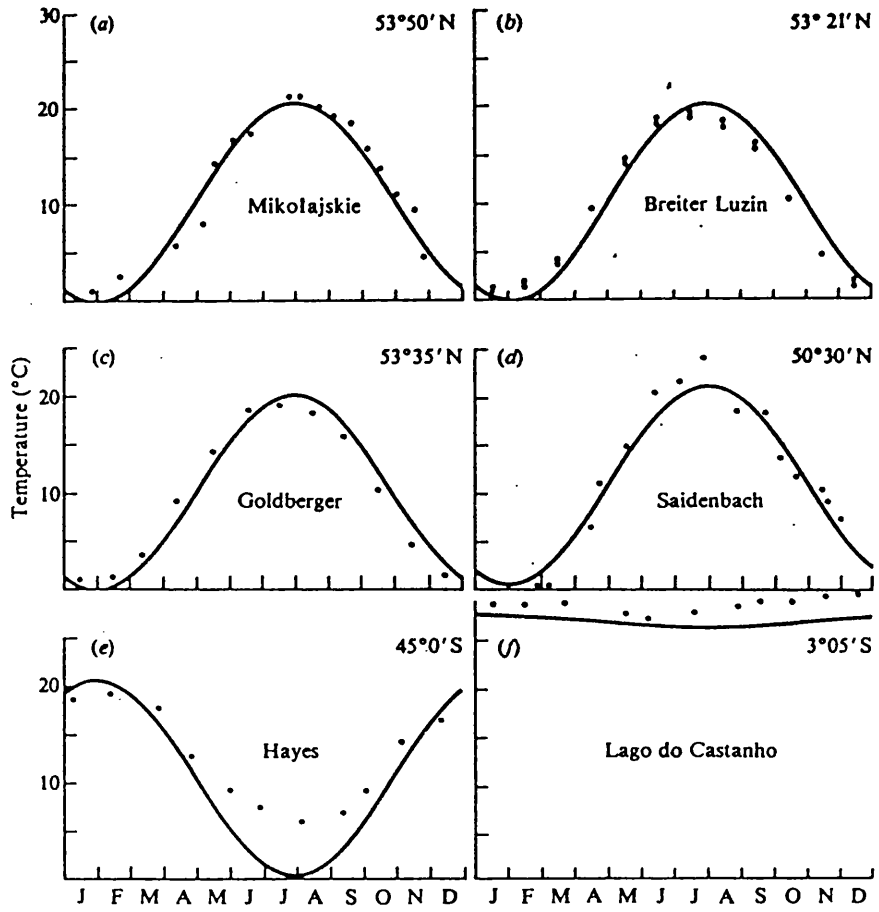

Figure 3.10 Modelled (line) and measured (points) surface temperature for six lakes not used in the regression to determine Straskraba's model. Reproduced from Sraskraba (1980).

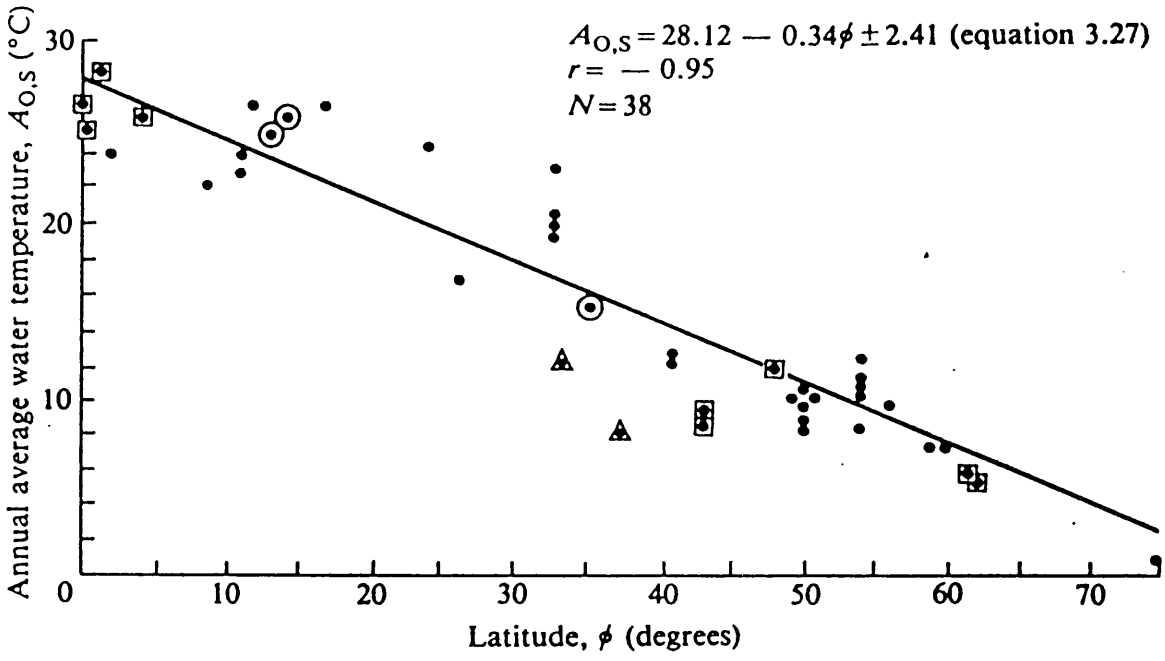

a)

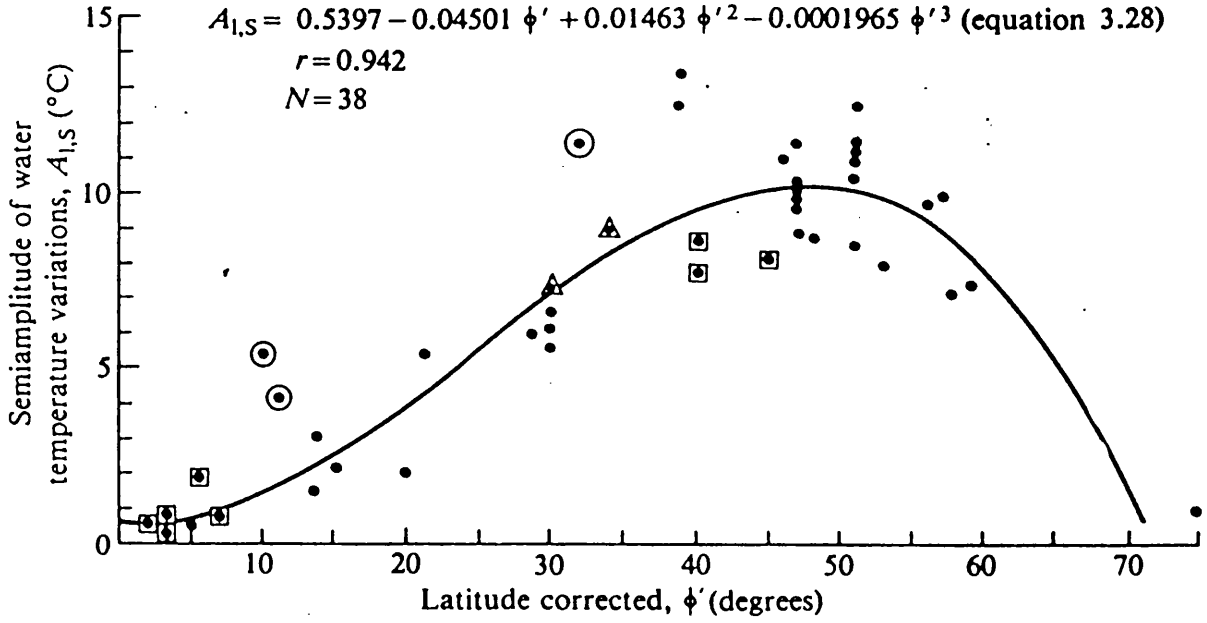

b)

Figure 3.11 a) Mean annual surface temperature (A_0) for lakes against latitude with linear approximation for medium size lakes at altitudes less than 2000m, b) Semi-amplitude of the annual surface temperature (A_1) for the same lakes in a) with a polynomial approximation for medium size lakes at altitudes less than 2000m, Squares - large lakes , circles - shallow lakes, triangles - lakes above 2000m. Reproduced from Sraskraba (1980).

where lakes are permanently frozen. At the equator the mean annual insolation is high but the annual variation is low. At mid latitudes there is a moderate mean annual insolation but large annual variation and at high latitudes the mean is low and the annual variation high. Straskraba points out that these results reflect the annual mean and the annual variation in the solar insolation, with latitude for the latitudes 0° - 40°, Fig. 3.12. The deviation between the modelled mean lake temperature and the average solar isolation at higher latitudes Straskraba ascribes to lakes at these latitudes having the potential to freeze in the winter. Interestingly Straskraba points out that this transition point (± 40° latitude) is the same latitude where it has been found that the bottom temperatures of lakes reach 4°C , the temperature of maximum density. Hence the lakes can inversely stratify and freeze.

A different approach to understanding the temperature that a particular lake has is to consider the temperature that the lake would eventually attain if the meteorological conditions were constant. That is to say the temperature at which there would be no net heat exchange through the surface of the lake. This was first introduced by Edinger et al. (1968) where the heat exchange equations were simplified enabling the surface heat flux to be expressed as a first order linear equation,

$$\Phi_{net} = -K(T_e - T_w)$$

K is the heat exchange coefficient (3.2)

T_e is the equilibrium temperature.

Both K and Te are a function of the meteorology over the lake and the form of the heat exchange equation and therefore will vary with weather, seasons and location.

From this equation one can easily see that if the water temperature is below the equilibrium temperature then the lake will gain heat and similarly if it is hotter it will lose heat. However neither K nor Te is constant with time so the magnitude and the sign of the heat flux going into the lake will change with time. The heat exchange coefficient was generally found by Edinger et al. (1968) to vary between 12 & 50 $Jm^{-2}sec^{-1}K^{-1}$. Edinger et al. (1968) also looked at the specific case of constant K and sinusoid Te which varied with time:

$$T_e(t) = T_m + T_a \sin(2\pi\omega t + \phi)$$

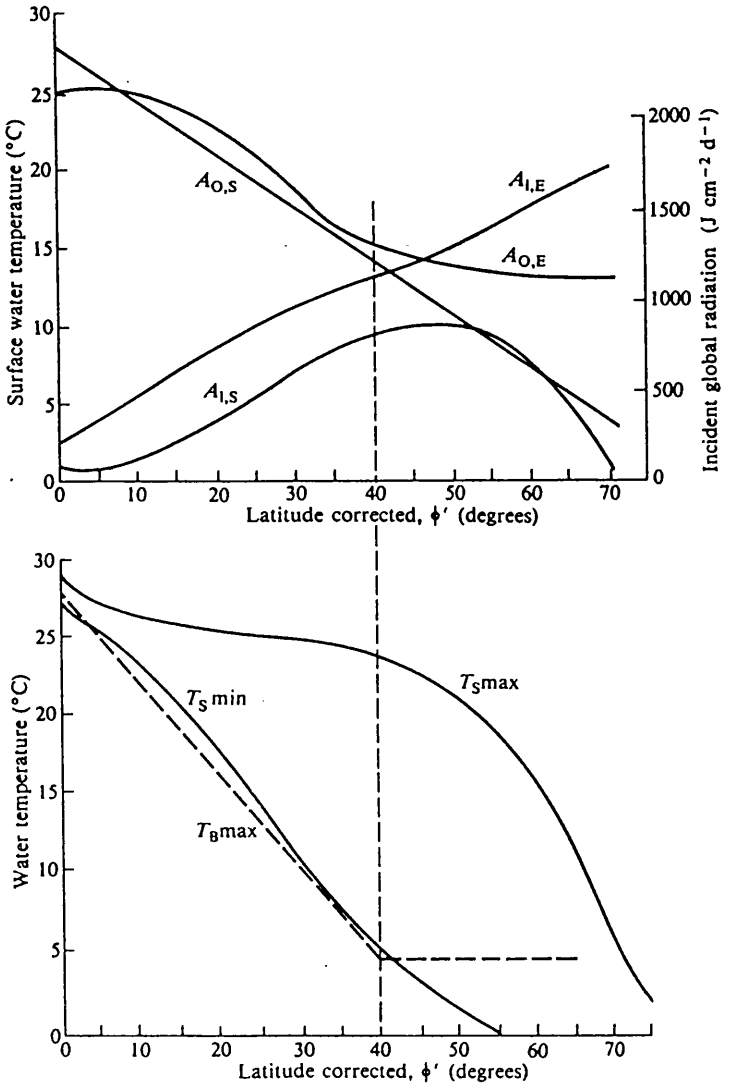

Figure 3.12 Comparison of the latitudinal trends of water temperature with incident solar radiation. Upper panel the mean ($A_{0,s}$) and semi-amplitude ($A_{1,s}$) of water temperature compared with that found for the incident global radiation, $A_{0,e}$ and $A_{1,e}$ respectively. Lower panel maximum and minimum surface water temperatures, $T_s$max and $T_s$min and maximum bottom temperatures $T_b$max vs. latitude. Dashed line represents the latitude where trends for water temperature start to deflect from those for radiation.

Solutions for Tw are,

$$T_w(t) = T_m + T'_a \sin(2\pi\omega t + \phi - \alpha) + e^{-kt/h} F(0)$$

$$T'_a = \frac{T_a}{\sqrt{1+\left(\frac{2\pi\omega h}{k}\right)^2}}$$

$$\alpha = \tan^{-1}\left(\frac{2\pi\omega h}{k}\right), \quad 0 < \alpha < \pi/2$$

where

h is the depth of the lake

k is a constant containing the heat exchange coefficient

ω is the period of T_e

From these solutions one can see that as the period of the oscillation approaches that of a year the ratio between the water temperature to the equilibrium temperature approaches unity and the maximum and minimum temperatures achieved by the water are not far off those of the equilibrium temperature. There will be a time lag between the maximum Te and water temperature and this takes the form,

$$\tau = \frac{\alpha\zeta}{2\pi}$$

ζ is the period of interest

Which for the annual cycle (ζ=365 days) will be of the order of a few days. Conversely fluctuations of Te on a very short time scale will not be significantly represented by the water temperature.

3.6 Previous work on the use of lake thermal behaviour in climate research

This section will review published work in relation to the use of lake thermal properties in climate research. The vast majority of this published work has concerned itself with the freezing and thawing of lakes. Much of the work has been purely empirical with several authors having shown a correlation between the dates of freezing and thaw break-up, and a measure of the mean air temperature (Robertson et al. 1992), (Anderson 1987), (Palecki and Barry 1986), (Ruosteenoja 1986), (Skinner 1986), (Tramoni et al. 1985).

The findings of McFadden (1965) as reported in Ragotzkie (1987) are that the freeze dates of lakes in North America are correlated to the running mean of the air temperature. Small lakes were found to freeze when the 3 day running mean of the air temperature

reaches 0°C and for large lakes when the 40 day running mean reaches 0°C. For the break-up date, small lakes thawed when the 3 day running mean reached +5°C and for large lakes the 40 day running mean reaching +5°C, Fig. 3.13. Palecki and Barry (1986) studied freeze/thaw dates for Finland and found that a change in the mean November air temperatures of 1.1°C related to a change of 5 days in the freeze up date and a 1.0°C change in the mean April air temperature related to a 5 day change in the thaw date. Similarly Tramoni et al. (1985) found that a 5 day delay in the freeze date corresponded to a -1°C change in the air temperature of the preceding 30 days from the freeze date.

Ruosteenoja (1986) took a more physical approach and developed a thermodynamic model to predict the thaw date, with considerable success, from winter air temperatures. Robertson et al. (1992) attempted all three of these approaches, statistical regression, running means of air temperature and a heat transfer model. From a very long time series of freeze/thaw dates and air temperature for lake Mendota they found a 5 day delay in the freeze date corresponded to a 0.9°C increase in the November/December mean air temperature, and an earlier thaw date of 6 days relates to a warming of the January to March air temperatures by 1.0°C. They also note that if there is a general warming of 1° then this would produce a change of 11 days in the number of ice covered days for the lakes and that this should be a sensitive indicator of climate change. They use historical ice freeze/break-up records to determine, independently of air temperatures, changes in climate since 1855. They highlight the advantages of ice records as having undergone less changes in measurement methodology, extending in the case of lake Mendota 30 years prior to reliable air temperature records and potentially being more sensitive to climatic changes as a 1°C change in air temperature is predicted to change the ice cover period by more than 10 days.

Little attention has been given in these studies to error analysis with at most the errors being quoted with no discussion and at worst no error quoted at all. Robertson (1992) determined the standard deviation on the regression between freeze date and mean November/December temperature to be approximately ± 6 days and a similar value for the thaw date. This indicates a signal to noise value less than one. This has important consequences with regard to the use of lake freeze/thaw dates for monitoring climate change. For example if we assume that there is a 0.3°C per decade warming in air temperatures (Houghton et al. 1990), this will correspond to a 0.15 days/year change in the freezing date. If the freeze date was monitored yearly it would take more than ten years before the signal would become discernible from the noise by one sigma and 36 years for a 3 sigma result.

a)

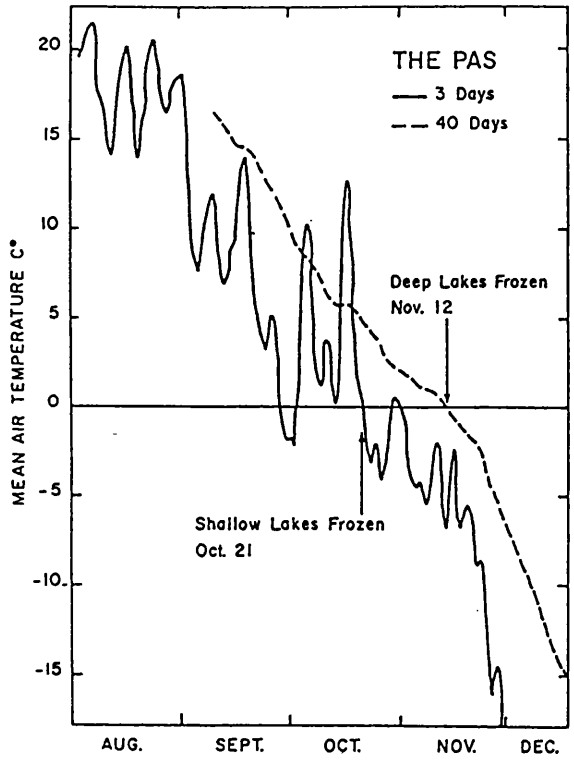

b)

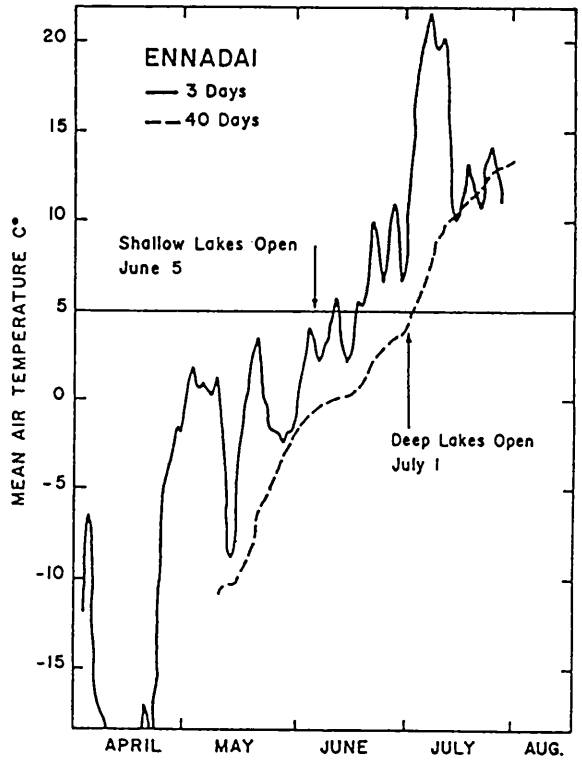

Figure 3.13 a) Comparison of lake freezing dates for the Pas, Manitoba, and b) ice break-up dates for Ennadi, N.W.T., with 3 day and 40 day running mean air temperatures. Reproduced from Ragotzkie (1987).

It is not clear why so little work has been published using lake temperatures in climate research. One reason could be the difficulty of obtaining data sets which are comprehensive enough to allow an in depth study. Ice records are generally more extensive and this has fostered more freeze/thaw work using this data relative to temperature work. Also as mentioned earlier traditionally work concerned with lake temperature has been specific to a particular lake and trying to achieve the best possible description of the lakes temperature regime. Ragotzkie (1987) outlined a crude procedure to estimate a lake's annual heat budget (defined as the difference between the maximum and minimum heat content of the lake in an annual cycle) without detailed in situ data, and that this could be used as a "climatic indicator" yet does not discuss in detail how a lake's annual heat budget can be related to climate.

Robertson (1989) attempted to determine how a lake's temperature responds to changes in mean air temperatures. His approach was to establish how Lake Mendota's temperature has responded in the past to changes in air temperature. He developed two models, one a statistically determined empirical correlation and the second a dynamic one dimensional model which predicts temperature and salinity profiles. With these he tries to establish the relationship between air temperature and the epilimnion temperature, hypolimnion temperature and the thermocline depth. He found that the dynamic model predicted that the epilimnion temperature reflected 40-65% of the change in air temperature, hypolimnion temperature 25-45% and there was no statistically significant change in the thermocline depth. The statistical regression model predicted 50-100%, 20-60% correspondingly and small yet complicated changes in the thermocline depth. These results are shown in Figs. 3.14a) & 3.14b). All these results were derived from changing only the air temperature and keeping the other meteorological parameters constant.

McCormic (1990) has similarly investigated the change in lake temperature structure through dynamic modelling of Lake Michigan. McCormic, however, used the output from Global Circulation Models with predicted anthropogenic greenhouse gas changes, to provide estimates of the changes in all meteorological parameters, not just the air temperature, and so potentially may provide a more realistic prediction of the changes that could be expected for lake temperatures. However, he emphasises that the results are not a prediction of the temperature change to come but that they are a sensitivity study, and that they indicate that considerable changes could occur under global warming. Fig 3.15 shows the change in temperatures for all depths throughout the year from 3 different

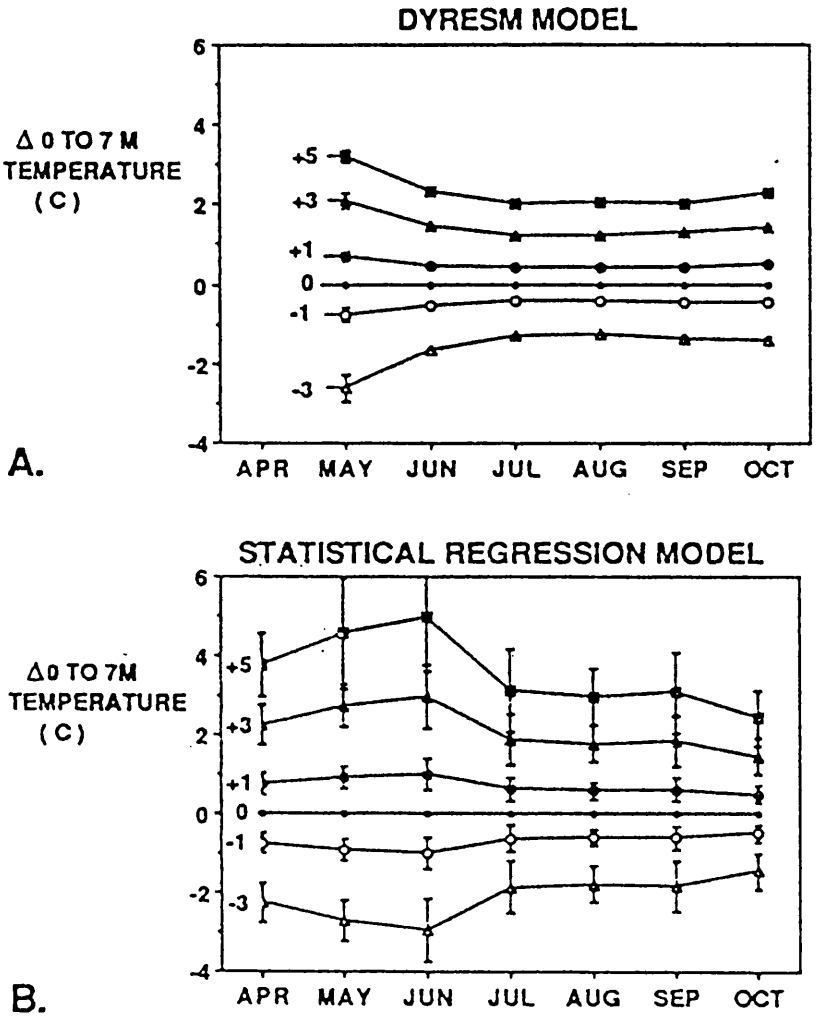

Figure 3.14a),b) Estimated changes in mean epilimnion temperature in response to changes in air temperature. a) is results from thermal modelling and b) from a statistical regression based on past meteorological data. For both plots the air temperature has been changed by -3, -1, 0, +1, +3, +5 °C. From Robertson (1989)

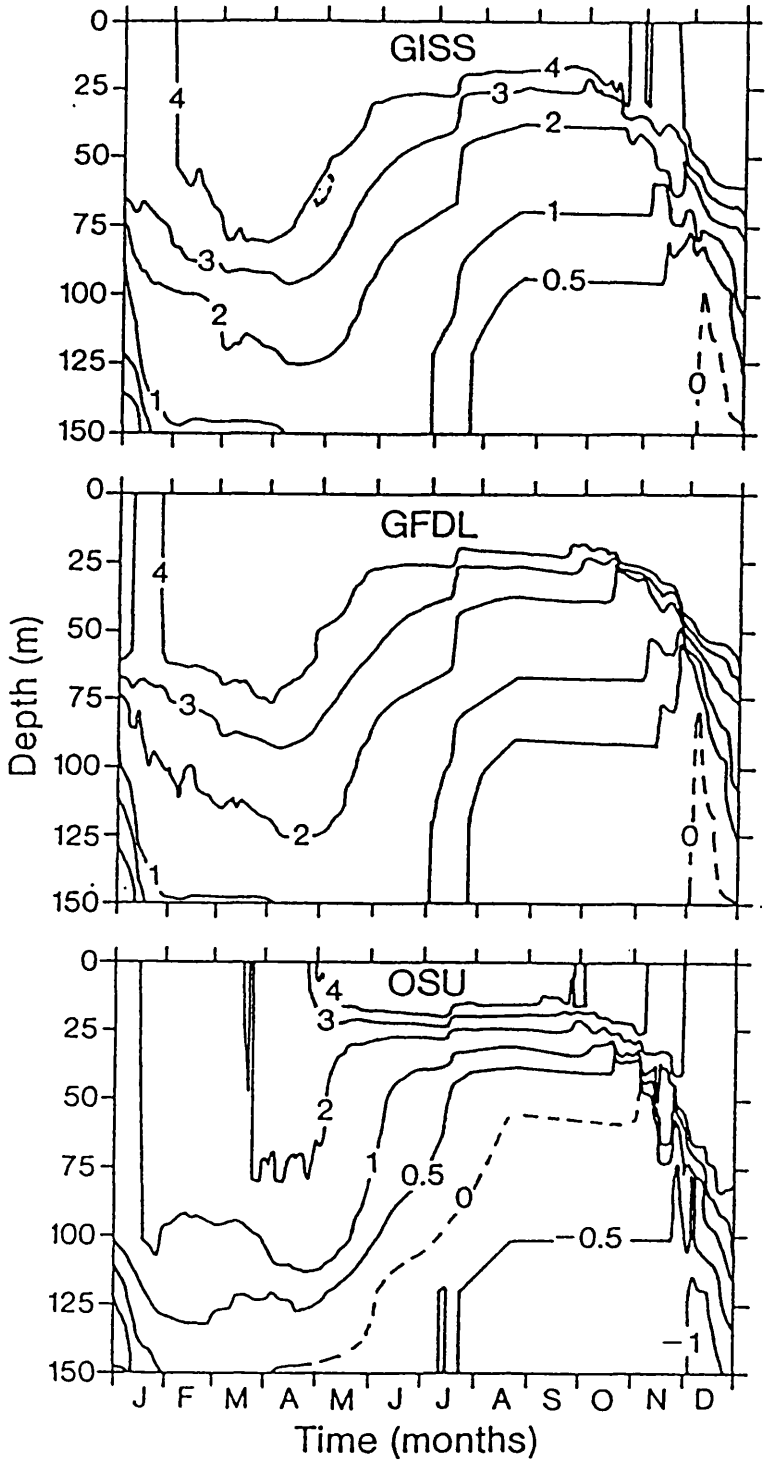

Figure 3.15 Modelled annual temperature profile difference in Lake Michigan. Graphs are of differences in modelled lake temperature using past meteorological records and the GCM modelled meteorology at 2xCO2 levels. The three GCMs used are the Goddard Institute for Space Studies (GISS), the Geophysical Fluid Dynamics Laboratory (GFDL) and the Oregon State University (OSU). Reproduced from McCormic (1990).

GCMs. His main conclusions are: a) surface water temperatures would be higher throughout the year: b) The heat content of the water column would be higher: c) The epilimnion would be shallower with stronger temperature gradients in the metalimnion: d) The duration of the summer thermocline would increase and that there is the potential that the lake would not undergo general circulation in autumn.

George (1989) has presented results which could indicate the potential of lake temperatures for detecting and monitoring climate change. He found that from a 40 year time series of water temperature for lake Windermere that he could detect a 10 year periodicity in the mean June surface water temperatures which was not detectable in the corresponding mean June air temperatures, (Fig 3.16). George (1989) mentions that a similar cycle has been detected in the Celtic Sea and is thought to reflect the combined influence of the solar insolation and the relative strength of the trade and westerly winds.

A more comprehensive look at the effect of global warming might have on lakes has been performed by Schindler et al. (1990) where a 2°C warming has been observed in air and lake temperatures over the last 20 years for the north-western region of Ontario. The combination of the reduction and this temperature increase has caused considerable change in the chemical balance of the lake which has significantly changed the concentration of phytoplankton. The clarity of the lakes has however increased due to the lower levels of dissolved organic carbon entering the lake producing deeper thermoclines with higher wind speeds. The temperature increase in water temperatures is sufficient to remove some temperature intolerant species from some of these lakes.

3.7 Conclusions

In this chapter I have reviewed the current state of knowledge on the thermal regime of lakes and the ways in which a lake exchanges energy with the environment. This has taken the form of an overview of a typical lakes annual temperature cycle, a description of the heat exchange processes, factors which affect lake temperature, models of lake temperature and finally the findings of other researchers which relate to the response of lakes to climate.

It is clear from the work which has been reviewed that lake temperature cycles and freeze/thaw events respond to climate with sometimes apparently greater detectability or higher signal to noise than air temperatures. The processes of heat exchange between a lake and the environment are well understood and have been used successfully to forward model lake temperatures. Lake thermal features, e.g. freeze/thaw dates and June water

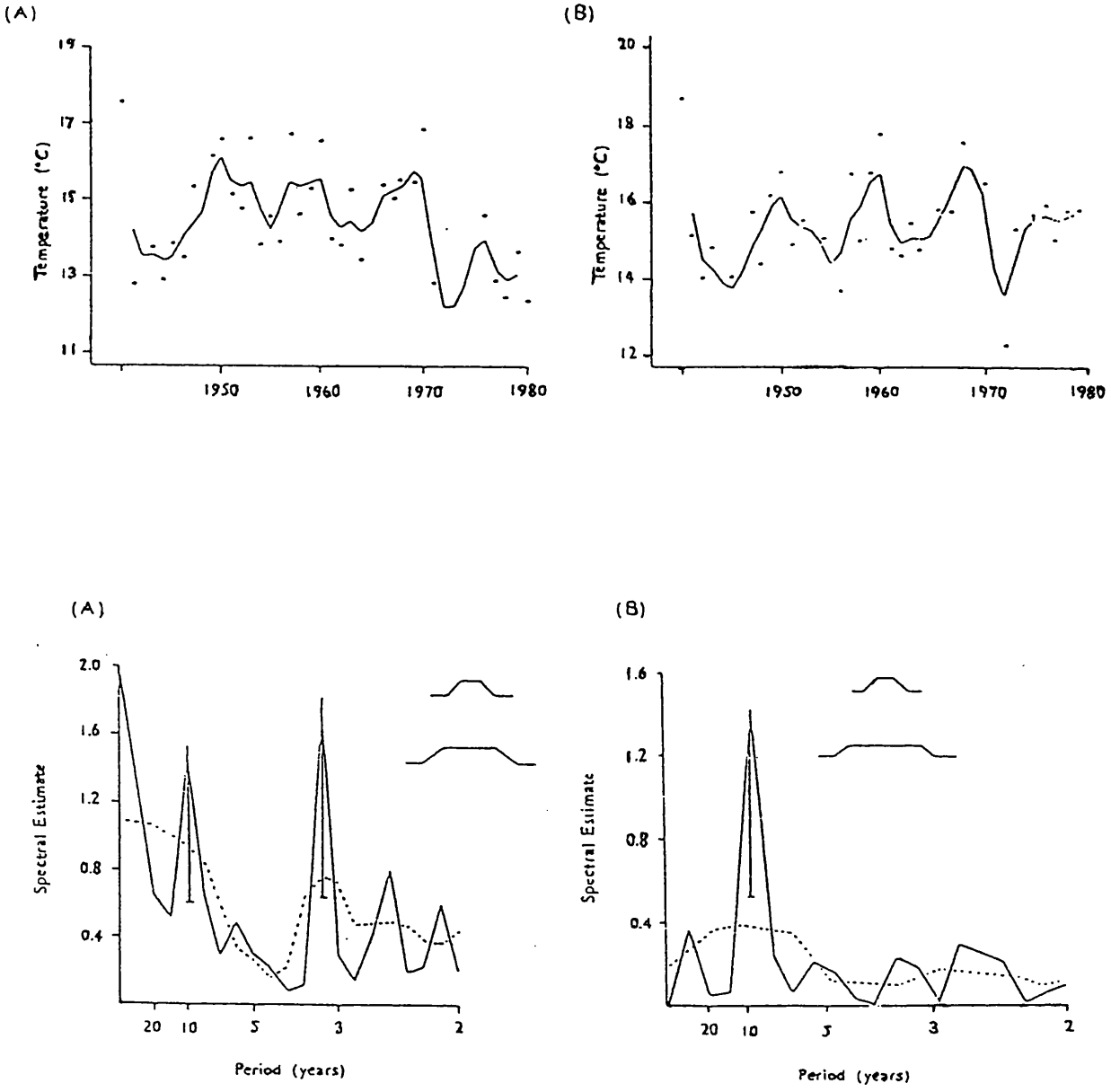

Figure 3.16 A 40 year record of mean June temperatures at Windermere for a) air temperatures and b) surface water temperatures. Line is smoothed data with a running mean weighted by 0.25, 0.5, 0.25. Below is the corresponding frequency spectra, solid line high-resolution, dashed low-resolution. Note the single spike in the water temperature spectra. Reproduced from George (1989).

temperatures, through to the annual cycle have been suggested as potentially useful proxy monitors of climate. However there are gaps in our understanding of the causal link between a change in the lake's thermal behaviour and a change in climate. This has arisen from the direct linking of climatic parameters with lake parameters which are in fact indirectly linked and are thus correlations. This situation has developed due to the nature of previous studies being empirical correlations rather than physical models of the relevant processes. Therefore with the current level of understanding of the link between lakes and climate the proposal for the global use of lake surface temperatures as proxy climatic indicators is premature.

To address this situation, and to establish the potential for lakes as climatic indicators, the following research is required: firstly, a general understanding of how lakes are linked to climate. This can be determined from models which are developed from understood physical processes occurring in and on the lake. Secondly the selection/development of measurable geophysical parameters which are linked to climate and where the link is understood. Finally the estimation of the potential climatic signal and the noise characteristics of the measured parameter. The research presented in the following chapters of this thesis are directed towards addressing these questions.

Lake model selection

There are many lake models reported in the literature, many of which are reviewed by Imberger and Patterson (1990), which are of varying complexity and success in predicting lake temperatures. The simplest of these are purely energy exchange models where the distribution of the energy through the water column is ignored and assumed to be uniform or well mixed. Each of the energy exchange processes is individually calculated and the net heat gain or loss of the water body is then calculated. Temperatures can then be calculated for the relevant volume of water form the specific heat of water. The more complex models, once the energy exchanges with the environment are calculated, are concerned with the subsequent distribution of the energy through the water column and the lake. The simplest of these models determines this redistribution of energy through molecular diffusion in one dimension whereas the most complex which tries to account for all turbulent processes in three dimensions.

The choice of lake model which is appropriate for this climatic study obviously depends on the objectives of the work and to some degree the availability of suitable in situ data. As was discussed at the end of the previous chapter there is a need to establish the potential for lakes as climatic indicators and how they are linked to climate. For this to be achieved a general or first order understanding of the link between lake temperatures and climate should be determined. We need to establish the generic behaviour of lakes with respect to climatic parameters irrespective of any individual lake's physical characteristics or location. Once this is understood and the potential of lake temperatures as good climatic indicators has been established a more detailed investigation of lake thermal behaviour will be warranted. Another factor which will influence the choice of lake model is the proposed method of temperature measurement. As this is remote sensing the temperature that will be measured will be that of the very surface of the lake. The model should, therefore, be capable of determining the temperature of this layer whereas its ability to calculate the temperature of lower layers is of secondary importance. Models which require site specific data or whose results are strongly influenced by such data will inherently be less useful in achieving a generic understanding of lakes' response to climate.

For the mixed layer models, the choice is between different parameterisations of the heat exchange processes (solar absorption, longwave absorption and emission, evaporation and conduction). A review of published parameterisations of these fluxes has been performed by Henderson-Sellers (1986).

The more sophisticated models which describe the distribution of energy through the water column are often referred to as one dimensional models. The major differences in published models of this type are in the representations of how the surface fluxes (via such equations as discussed by Henderson-Sellers (1986)) are distributed down the water column. The first models approached this problem by characterising all turbulent

transport processes by a single parameter, the eddy diffusivity. An example of such a model is the University of Salford Eddy Diffusion Model (USED) described by Henderson-Sellers (1984). The disadvantage with these types of model is the need for calibration for each lake with extensive data sets of both meteorological and temperature profile data to determine the eddy diffusion coefficient. Such tuning to a particular lake is not desirable for the work proposed in this thesis in trying to establish the generic behaviour of lakes.

A different approach has been taken by many investigators by attempting to model the principal turbulent fluxes individually. The more sophisticated the model the more the individual turbulent fluxes are represented. All these models determine the distribution of heat through the interaction of turbulent kinetic energy opposing the density-induced vertical stability. This approach has been widely used with many models being published which are based on these ideas, e.g. CE-QUAL-R1 (Laboratory 1982), DYRESM (Imberger and Patterson 1981), UFILS1 (Rice et al. 1989). These models have been very successful and widely used, however, they still rely on empirically derived coefficients for various hydrodynamic and thermodynamic processes and are therefore not universally applicable, (Gosink 1987). These models also require more parameters to describe the lake, such as extinction coefficient and salinity, to be able to accurately model the temperature structure. Such detailed in situ data is not readily available and is again very lake specific and so does not lend it self to determining general lake behaviour.

There are three dimensional models which attempt to represent the complete motion of the lake water, however, these require a detailed knowledge of the lake basin and are therefore very lake specific. This precludes such models from this study.

The type of model chosen for use in this thesis was a mixed layer with the surface fluxes determined by the parameterisations of the individual processes recommended by Henderson-Sellers (1986). The parameterisations presented by Henderson-Sellers (1986) were not modified. The choice of this model satisfies the requirement of being very general and not specific to a particular lake and does not require calibration with in situ data. Such a model requires the least information on the characteristics of the lake, in fact only the depth of the mixed layer. The simple relation between the energy fluxes and the lake temperature also allows, as demonstrated in a later section, the time response of the lake to be simply determined. This model is also the least computationally demanding. The disadvantages of this model are that it is quite a simplification of reality and therefore will have deficiencies and might not represent some lakes. However, this is thought to be acceptable for this type of study, that of an initial preliminary investigation of the generic thermal behaviour of lakes to changes in climate.

Chapter 4.

The development of a lake temperature model.

4.1 Introduction

This chapter describes the development of a general lake temperature model based on the energy fluxes through the surface of the lake. The equations for the energy fluxes are those reported by Henderson-Sellers (1986) . The model calculates the temperature of the water which is thermally coupled to the boundary layer, that is to say that if the lake is stratified the temperature calculated will be that of the epilimnion; if the lake is in general circulation it will be the temperature of the whole lake. The model is validated with a comprehensive in situ data set. The rationale behind the development was to try and construct a model which did not contain equations with coefficients which had been tuned to a data set from a particular lake. This would then allow the model to be used to investigate general climate/lake temperature behaviour and not be limited to a particular lake. It would also allow future investigations using different climate data without the need for in situ water temperature data. It is used in Chapter 5 to help investigate the general response of lake surface temperature to climate change.

4.2 Model development

This model, to be referred to as the HS model, is a development of a surface heat budget model described by Henderson-Sellers (1986), where Henderson-Sellers has performed a general literature review of the heat exchange equations for lakes. The equations used are those which Henderson-Sellers has suggested as being the most appropriate. Most of these equations are based on physical principles but where these are lacking or insufficiently understood an empirical approximation has been introduced.

The heat flux through the surface of a lake can be represented by the equation:

$$\Phi_{Net} = \Phi_{Sol} + \Phi_{Long\_in} - \Phi_{Long\_out} - \Phi_{Evap} - \Phi_{Cond} \qquad (4.1)$$

where

Φ_{net} is the net heat flux into the lake,

Φ_{Sol} is the solar flux,

Φ_{Long_in} is the down welling longwave flux,
Φ_{Long_out} is the up welling longwave flux,
Φ_{Evap} is the evaporation flux,
Φ_{Cond} is the conduction flux.

For each of these components, the equations for their fluxes are:

4.2.1 Solar flux equation

$$\Phi_{Sol} = \sum_{\alpha>0}(A_s.\Phi_s(\alpha)) \tag{4.2}$$

and

$$\Phi_s(\alpha) = (\Phi_{sd} + \Phi_{ss})[1-(1-k)C_1] \tag{4.3}$$

$$\Phi_{sd} = S\sin(\alpha)\tau^m \tag{4.4}$$

$$\Phi_{ss} = 0.38(S-\Phi_{sd})\sin(\alpha) \tag{4.5}$$

$$A_S = \frac{a_0}{a_0+\sin\alpha}$$

$$a_0 = 0.02+0.01(0.5-C_1)\{1-\sin[\pi(I-81/183)]\}$$

Φ_{sd} is the direct solar component
Φ_{ss} is the scattered solar component
α is the solar altitude.
A_s is the shortwave albedo
τ is the atmospheric transmission
m is the optical air mass
S is the solar constant
I is the Julian date
k is a constant dependent on latitude
C_1 is the cloud cover where
$C_1 = 1-n/D$
n is the number of sunshine hours
D the maximum possible value of n

4.2.2 Long wave flux equations

For the down welling flux:

$$\Phi_{Long\_in} = \varepsilon_w \varepsilon_a \sigma T_a^4 \tag{4.6}$$

$$\varepsilon_a = 0.84 - \frac{n}{D}\left(0.1 - 9.973\times10^{-6} e_a\right) + 3.491\times10^{-5} e_a \text{ for } \frac{n}{D} \geq 0.4$$

$$\varepsilon_a = 0.87 - \frac{n}{D}\left(0.175 - 29.92\times10^{-6} e_a\right) + 2.693\times10^{-5} e_a \text{ for } \frac{n}{D} \leq 0.4$$

where

ε_a is the emissivity of air

ε_w is the emissivity of water

σ is the Stefan - Boltzmann constant

T_a is the air temperature

e_a is the vapour pressure of the air

For the up welling flux:

$$\Phi_{Long\_out} = \varepsilon_w \sigma T_w^4 \tag{4.7}$$

T_w is the temperature of the water surface

4.2.3 Evaporation and Conduction flux equations

For the evaporation flux:

$$\Phi_{Evap} = \left[\lambda\left(T_{wv} - T_{av}\right)^{1/3} + 0.0627 u_2\right]\left(e_{sw} - e_a\right) \tag{4.8}$$

where

$\lambda = 0.027$ for $T_{wv} \geq T_{av}$

$\lambda = 0.0$ for $T_{wv} \leq T_{av}$

$$T_{nv} = \frac{T_n}{1 - \left(\frac{0.378 e_n}{p}\right)}$$

e_{sw} is the saturated water vapour pressure at the water temperature

p is the atmospheric pressure

T_n is either T_w for T_{wv} or T_a for T_{av}

For the conduction flux:

$$\Phi_{Cond} = \Phi_{Evap} 0.61 \times 10^{-3} p \frac{(T_w - T_a)}{(e_{sw} - e_a)} \tag{4.9}$$

The equation used for calculating the vapour pressure, e_v is:

$$e_v = RH.2.1718 \times 10^{10} e^{\frac{-4157}{(T-33.19)}}$$

where

T is the temperature

RH is the relative humidity

All flux equations have units of Wm^{-2}.

The model takes as input variables:

Latitude for the lake,
Atmospheric pressure,
Mixed depth,
Atmospheric transmission for broad band solar radiation,
Mean daily air temperatures at 2m,
Mean daily relative humidity at 2m,
Mean daily cloud cover at 2m,
Mean daily wind speed at 2m,

and outputs daily average mixed depth water temperatures. The optical depth is not required as the model assumes that the majority of the solar radiation is absorbed in the mixed layer. Fetch is not required as it is assumed that the wind speed will be constant over the lake and the effect of fetch will only affect the mixed depth which is an input variable.

The mechanics of the model are that the net flux for the next day is calculated from the next day's meteorology and the current day's water temperature. This is then applied to the current heat content of the lake determined from the temperature of the lake and its depth. From the new heat content the next day's temperature is calculated. Certain parameters; the mixed depth, the atmospheric pressure and the atmospheric transmission, were taken as being constant for the purposes of this study and the effect of these will be discussed in a later section.

The individual flux equations warrant a brief discussion on their formulation. For the solar flux there are two components, the direct solar radiation and the scattered radiation. The scattered radiation is taken to be a fraction of the difference between the direct flux and the solar constant and is a function of solar altitude. The direct flux depends on the solar constant and is a function of the atmospheric transmission and the optical path. These two fluxes are then combined with a term to account for the effect of clouds. Generally clouds will reduce the amount of solar flux entering into a lake by obscuring the sun, however there are cases when the maximum solar flux occurs not during clear skies but during broken cumulus when the solar disc is not obscured. This is because the cumulus increases the level of scattered radiation. When averaged over a day however cloud will generally cause a net reduction in solar flux. The portion of the incident solar flux entering the lake is governed by the short-wave albedo of fresh water. In this model this is taken to be a function of the solar angle and cloud. The inclusion of cloud into the albedo is a surprising concept, as the reflectivity of the surface is entirely defined by the refractive index of the water and the air immediately above. The inclusion of cloud is therefore presumably to account for the reflected radiation being scattered back into the lake. This however is describing a phenomena which is not the albedo and should perhaps be considered as a multiple reflection term. The solar flux is calculated for every hour the sun is above the horizon and averaged for the 24 hour period.

The long wave flux out of the lake is straightforward but the flux into the lake is more complicated. Since it is unlikely that sufficient knowledge is available about the state of the atmosphere to model the radiative transfer for the whole atmosphere, simplifications are needed so that the down welling flux can be calculated from parameters which are easily and routinely measured, such as air temperature, humidity and cloud. The emissivity of air is determined in part by the water vapour content, but will increase with cloud cover due to cloud having a very high emissivity and a temperature which is higher than the air above its base. Unfortunately this is very difficult to model, which has led to the two empirical equations for different cloud amounts. Fig. 4.1 shows the variation of the sky emissivity for data from Lough Neagh described later in this chapter. We can see that there is little variation through the year and this is probably due to the relatively constant level of cloud and humidity in this case. This also tells us that if the mean value is near reality then any error in the annual variation will be small.

The evaporation and conduction heat terms are particularly difficult to model. They rely on estimating the rate of removal of heat and water vapour from the surface. This is carried out by wind and convection, wind being the major factor. In the past models have not tried to estimate the convection contribution explicitly but have used regression to

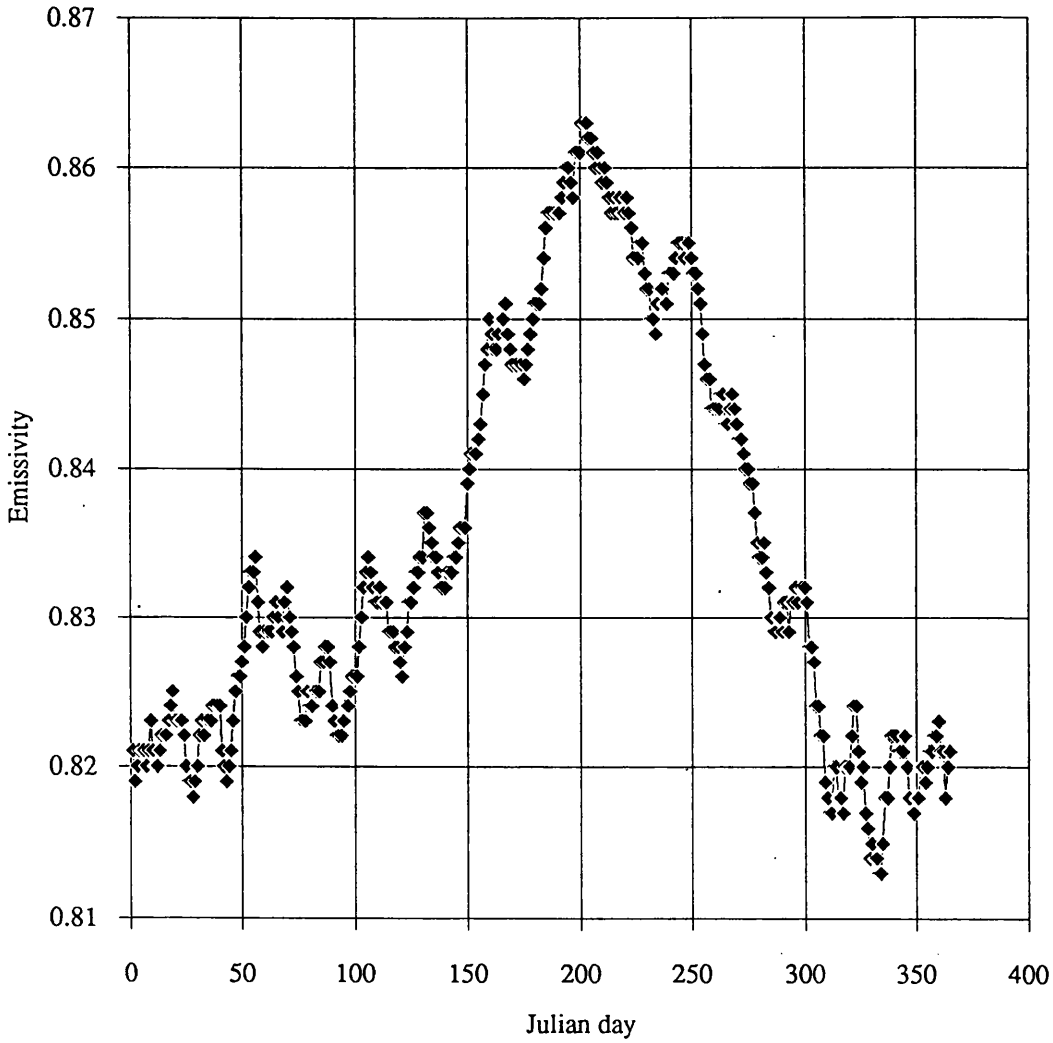

Figure 4.1 Atmospheric emissivity calculated from meteorological data for Lough Neagh by the HS model.

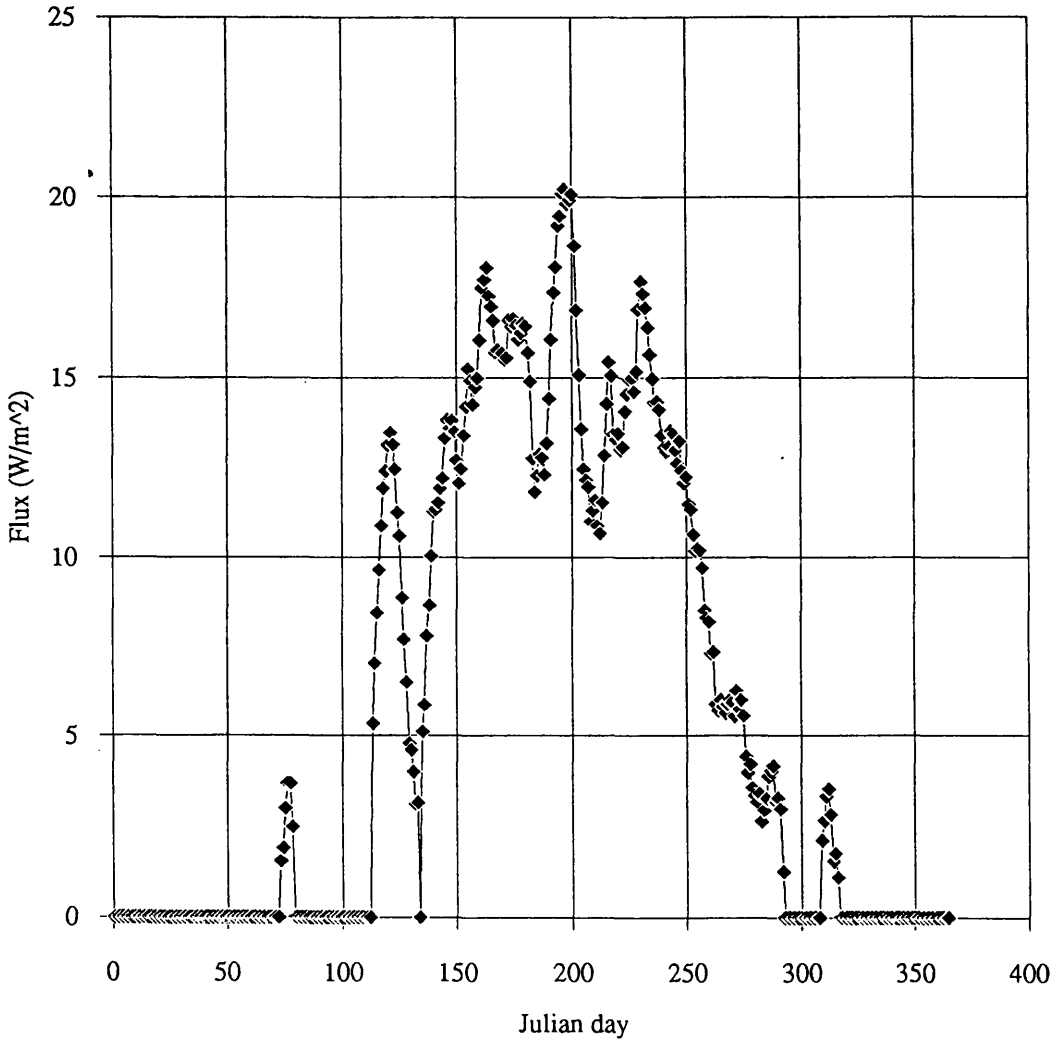

Figure 4.2 Heat flux out of the lake due to evaporative convection calculated from meteorological data for Lough Neagh by the HS model.

account for the convection within the wind term or as a constant. The formulation used in the HS model, however, does attempt to calculate the convection independently and the results of this, for evaporation, are shown in Fig. 4.2, which are derived from Lough Neagh data. The peak flux due to convection is approximately 10% of the total peak evaporation flux.

4.3 Validation

Two meteorological data sets have been used with this model although only one has in situ surface water temperatures which can be used for validation. The data without water temperatures was compiled by Henderson-Sellers (1986) to describe the climate of the UK. The second was provided by Chris Gibson of The Freshwater Biological Investigation Unit, Belfast. This consists of a 7 year daily time series (1974-1980) of max/min day/night air temperatures, relative humidity, solar flux and wind speed taken from Aldergrove, a site near the north-east shore of Lough Neagh. The in situ data were recorded 500m off Ardmore Point daily at approximately 12:00. The first data set will be referred to as the UK data and the second the LN data. Due to Lough Neagh's mean depth being quite shallow at 8.9m and the high level of wind the lake is generally well mixed (Stewart and Gibson 1987), and therefore the depth used in the model is 8.9m and is the same when comparisons are made with the UK data results. Both runs took the lakes to be at 55° latitude and with an atmospheric pressure of 101100 Pa and an atmospheric transmission of 0.75.

Graphical representations of these climatologies are in Figs. 4.3a) - 4.3c). The LN data are the daily means for the seven years which have had a ten day running mean filter passed over them to remove some of the higher frequencies. One can see that the UK air temperature is considerably cooler than the LN data for the winter and the summer but quite similar for the autumn. The relative humidities are similar as well with little annual variation. The cloud cover is higher in the LN data with little annual variation unlike the UK data. The largest difference between the two data sets is in the wind speed where the LN wind is at least twice as large as the UK data and generally larger.

The model takes average air temperatures and therefore the day/night max/mins needed to be combined to produce this. Several combinations were tried to see which was appropriate and produced the most realistic temperatures. This was found to be the average of the daily maximum and the night maximum. Averages of all four of the day max and night min, which one might think would be the best representation of the mean air temperature, produced temperatures which are too low. Assuming that the model is

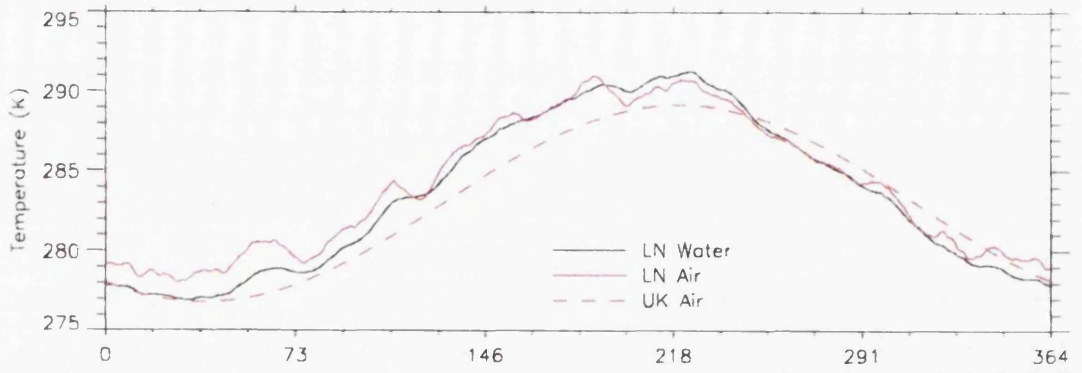

a)

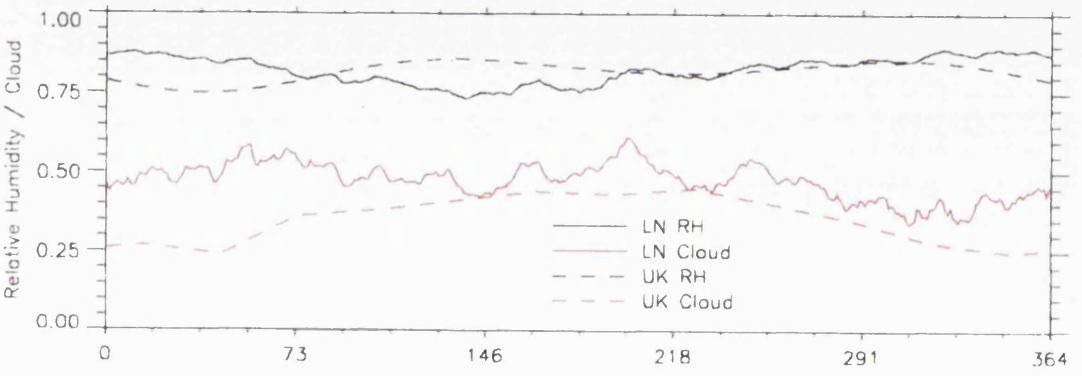

b)

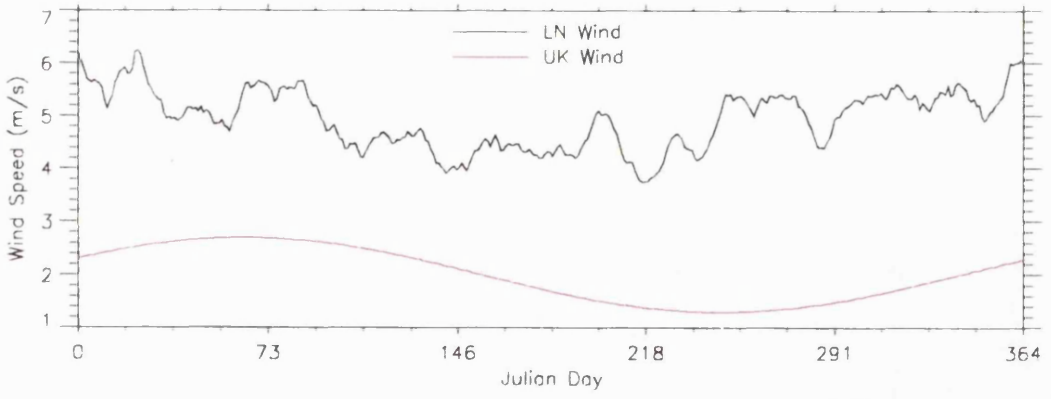

c)

Figure 4.3a) Daily air and water temperatures for Lough Neagh calculated as the mean of 7 years of daily data smoothed with a 10 day running mean. This is compared with a representation of the UK meteorology produced by Henderson-Sellers (1986).

b) As for Fig. 3.4a) but for relative humidity and cloud. Relative humidity is measured from 0.0 - 1.0 and the cloud is measured as the fraction of the number of sun obscured hours over the maximum possible number of sun hours.

c) As for Fig. 3.4a) but for wind speed.

correct this would suggest that the diurnal cycle of the air temperature is not symmetric and does not follow a simple sine function but rather there are brief periods of cold temperatures separated with warmer periods of relatively constant temperatures. This could however indicate an error in the formulation of the model which requires a bias in the air temperatures yet this is unlikely as the model produces consistently accurate results. The accuracy of the formulation used for the mean daily air temperature could be assessed from a high temporal resolution air temperature data set.

Since the LN data consisted of solar fluxes instead of cloud amounts a measure of the cloud cover needed to be estimated from these fluxes. This was done by using the solar flux equations (4.2-4.5) and rearranging for the cloud amount, calculating the flux for cloud free conditions and using the measured flux, e.g.

$$C_1 = \left(\frac{1}{1-k}\right)\left(1 - \frac{\Phi_{Measured}}{\Phi_{Cloud\_free}}\right)$$

It was also found that the coefficient for the wind term in the evaporation flux needed to be increased by a factor of 2 to produce temperatures which were realistic when compared to the measured temperatures. The reasons for this are unclear, but one possible explanation is that as the wind speed is taken over the land it might be lower than that found over the lake. However it is unlikely that this would account for such a difference especially as this would mean that the mean wind speeds over the lake were unrealistically high. Changing this parameter is also contrary to the original philosophy of trying to develop a model which had no coefficients "tuned" to a particular lake. To see if this change is needed specifically for Lough Neagh or if it is a more general "improvement" needed by the model needs further work with an independent data set for a different area, which due to a lack of suitable data has not yet been performed.

The result of the HS model for the 7 year data set is shown in Fig. 4.4, and a detailed plot of years 77-78 in Fig. 4.5. Agreement between the measured and modelled temperature is very good with excursions from the seasonal trend being well represented. There are short periods where the modelled temperature is a degree or more different to the measured temperature but these do not persist and occur infrequently. A histogram of the daily differences (modelled-measured) for the whole seven years is plotted in Fig. 4.6, and indicates that the distribution of the differences is close to gaussian with a mean difference of 0.37±0.02°C and a standard deviation of 0.96°C. This compares favourably with other models, -0.5±0.1°C (Stewart and Gibson 1987), which have used the same

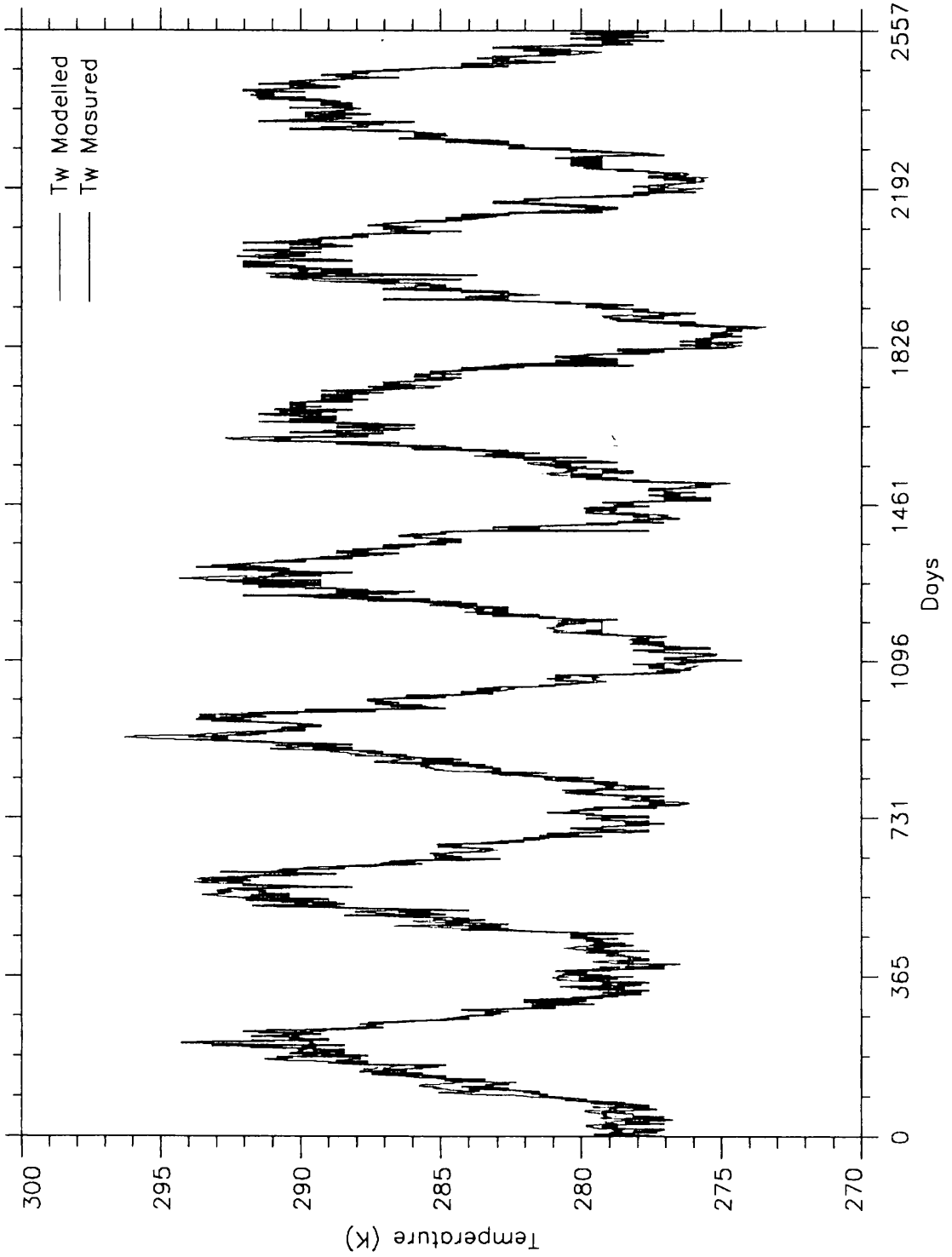

Figure 4.4 Predicted temperatures from the HS model compared with the measured surface water temperatures for Lough Neagh, for the years 1974 - 1980.

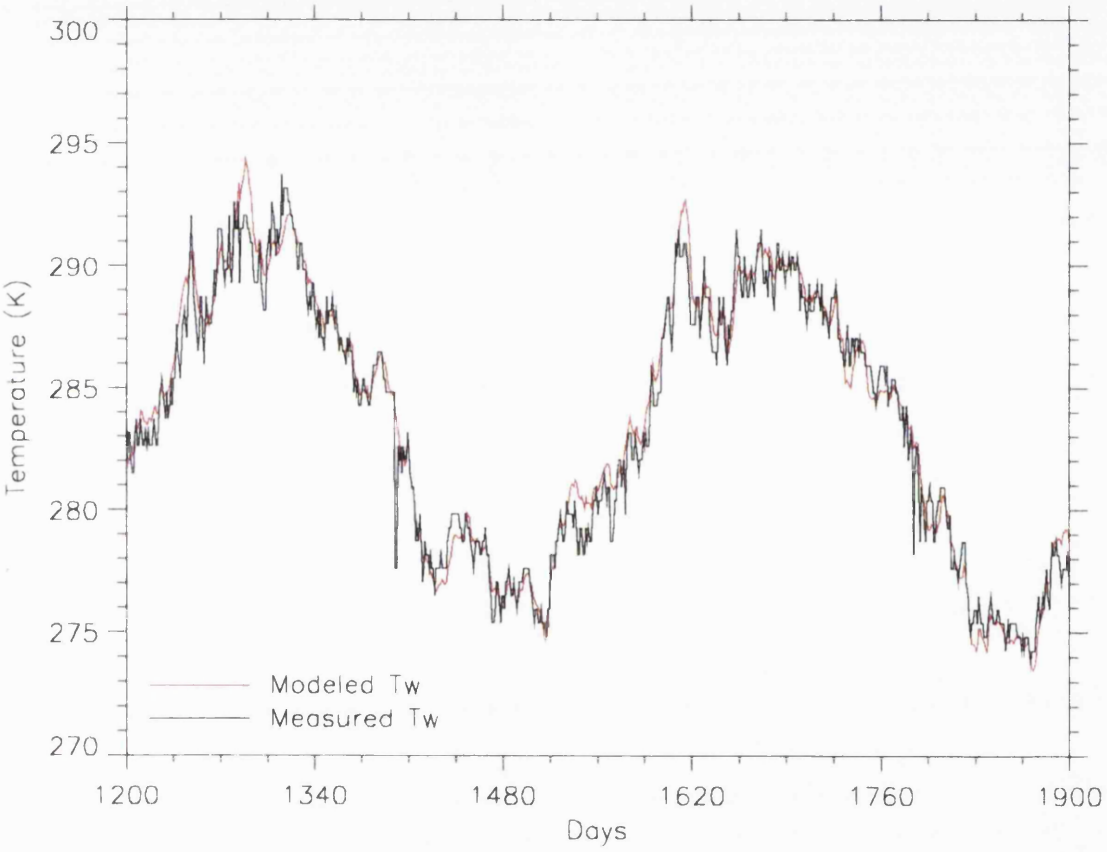

Figure. 4.5 Detail of Fig. 4.4 for the years 1979 and 1980. Note good agreement between modelled and measured temperatures even for short period fluctuations.

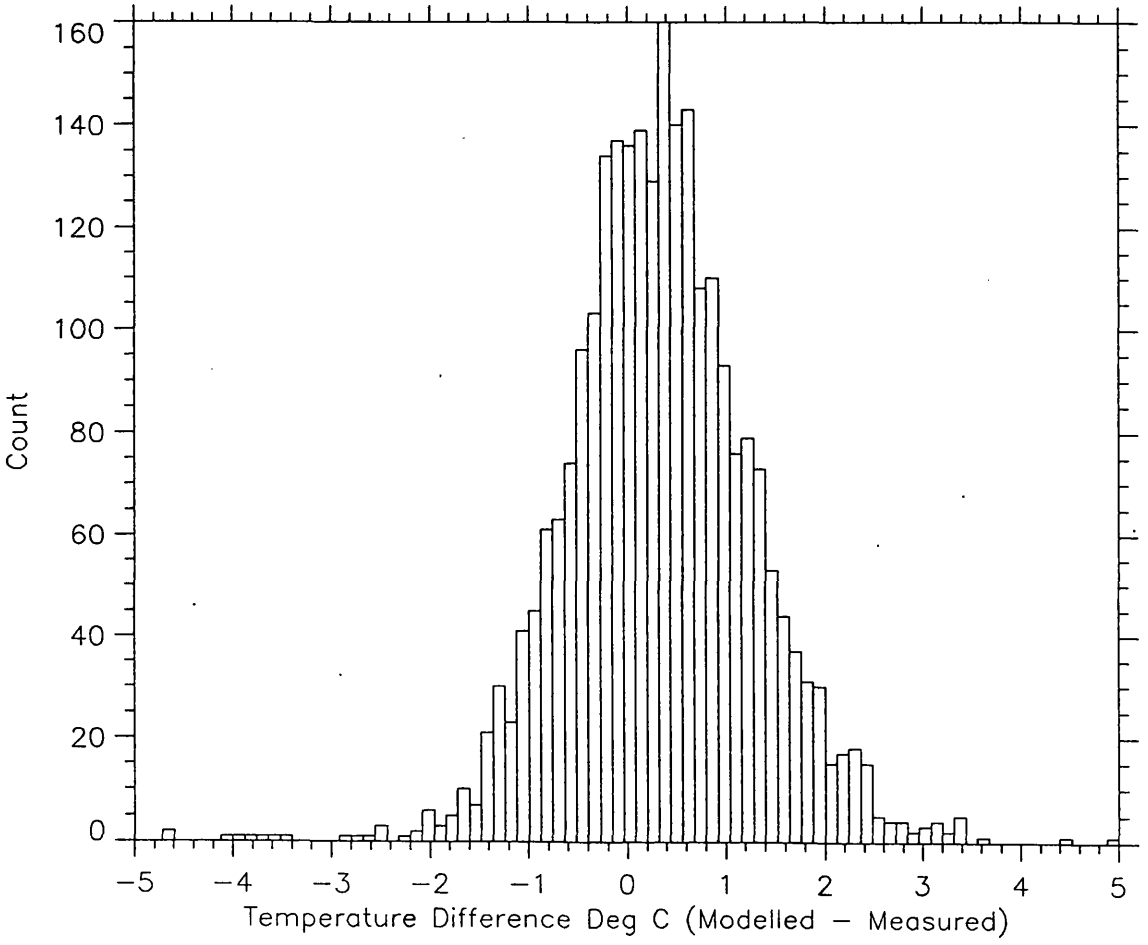

Figure 4.6 Histogram of differences (modelled - measured) for the seven year Lough Neagh data set. The distribution follows a gaussian form, with a mean offset of 0.37°C and a standard deviation of 0.96°C.

meteorological data but have performed optimisation routines for the flux coefficients to achieve the greatest agreement between the measured and modelled temperatures.

4.5 Comparison of UK and LN meteorology.

The different temperatures that the LN and UK meteorologies produce are shown in Fig. 4.7, the LN temperature derived from the seven year average meteorology. The major difference is that the UK data produces cooler winters and hotter summers and autumns. The net fluxes for the two meteorologies are shown in Fig. 4.8, and the breakdown of these net fluxes in Fig. 4.9. It can be seen that as regard to seasonal trends, the temperature is in effect the derivative of the net flux with the peak of the net flux corresponding to the maximum rate of heating of the lake. The temperature differences are reflected in the net flux differences with the spring flux being generally smaller for Lough Neagh and the winter flux being less negative. The breakdown of the net flux into its constituent components is quite illuminating. Although the LN air temperature is generally higher than that for the UK, reflected in a larger long wave flux and a larger conduction flux into the lake, the actual lough has a higher evaporative loss than the "UK lake". The solar flux is smaller for the actual lough due to the greater cloud cover.

The model can be used to investigate the effects of keeping certain parameters constant which in reality are variable and so investigate their influence. The atmospheric pressure will change as different weather systems cross the lake and as the type and frequency of these has some annual dependency there will be an effect on the annual water temperature cycle. However the magnitude of the effect of pressure on the resultant water temperature is very small as can be seen in Fig. 4.10 . This shows the effect of varying the atmospheric pressure from one atmosphere by ±10%. The error in keeping the pressure constant is therefore considered to be negligible. The effect of keeping the atmospheric transmission constant is however much larger as can be seen in Fig. 4.11 where the transmission is changed by ±0.05 from 0.75. Unfortunately this parameter is difficult to measure and there are limited records in which it has been monitored, none of which have been found for the relevant period over Lough Neagh. This has necessitated this parameter being kept constant. This is an area where further work is needed to assess the nature of the variability in the transmission and how it might change in the future.

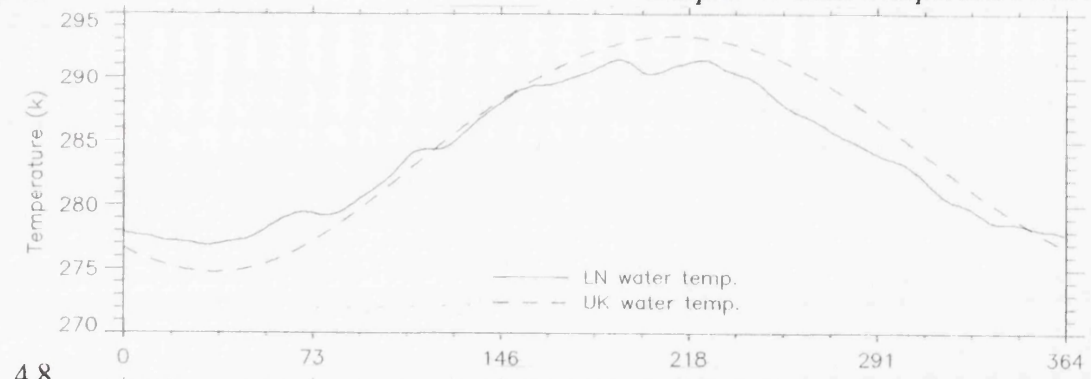

Fig. 4.8

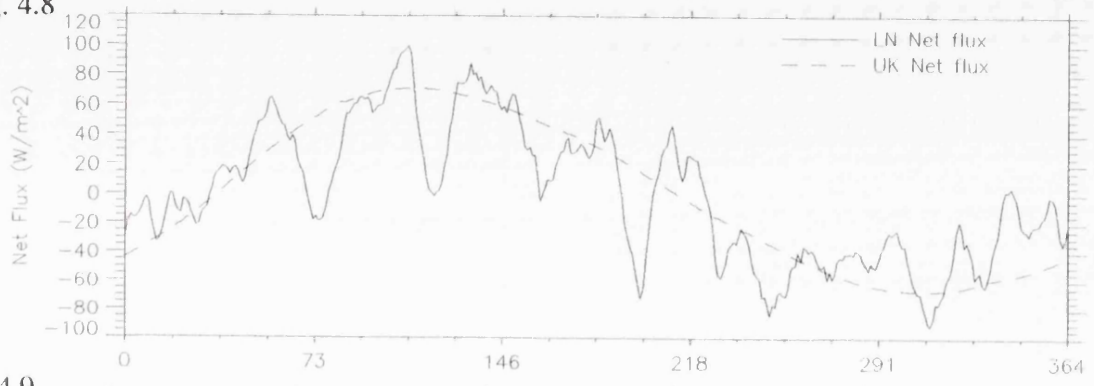

Fig. 4.9

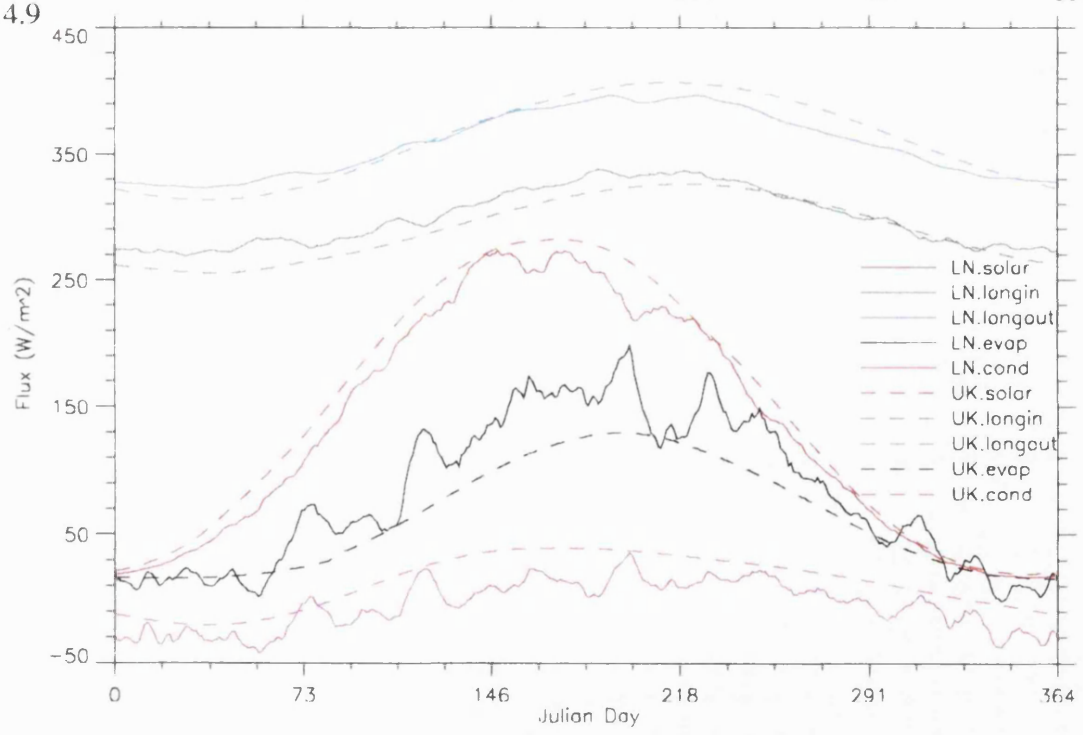

Figure 4.7 Modelled temperature from the HS model comparing temperatures produced from Lough Neagh data and UK data. Note the UK data produces warmer summer temperatures although the air temperature for Lough Neagh is warmer in summer.

Figure 4.8 Comparison of the net fluxes for the UK data and the LN data.

Figure 4.9 Constituents of the net flux for the UK data and the LN data. Solar and longin are heat gains to the lake and longout, evap and cond are losses.

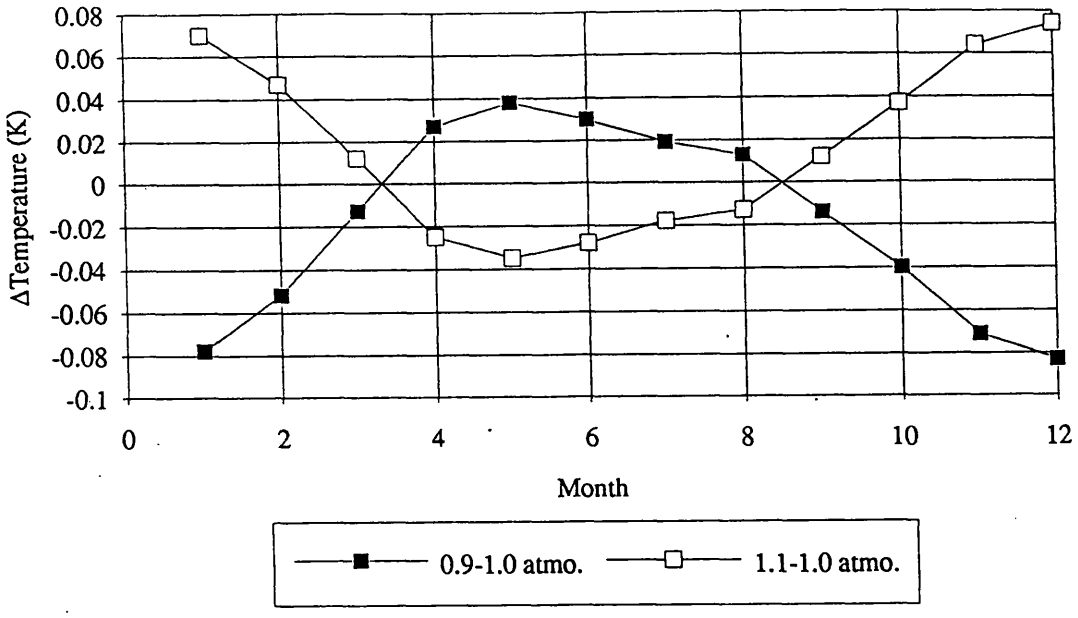

Fig. 4.10

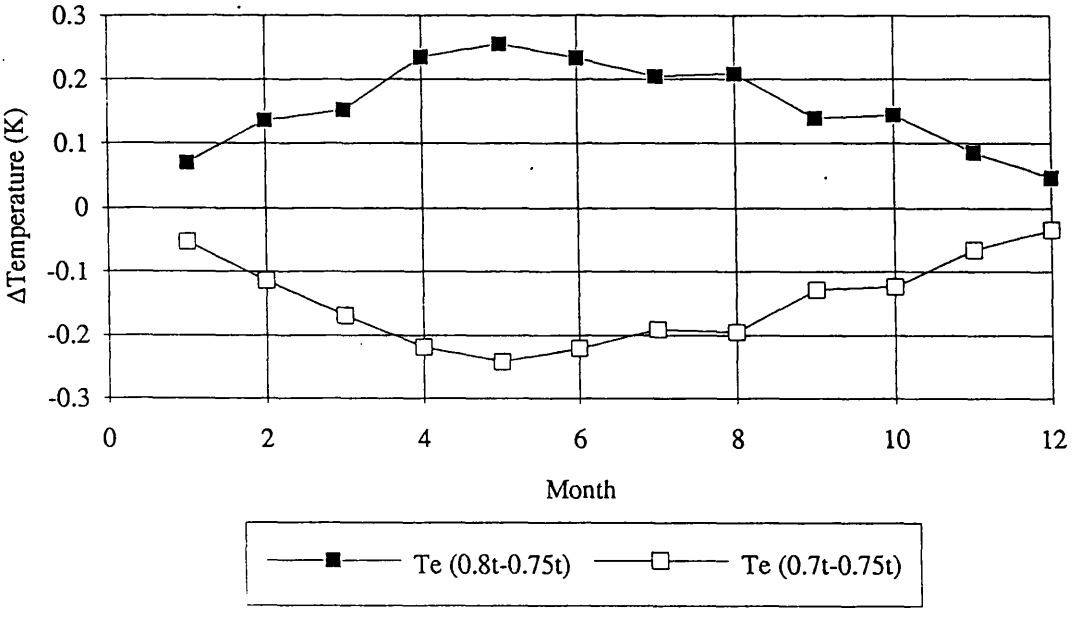

Fig. 4.11

Figure 4.10 Effect of increasing and decreasing the atmospheric pressure by 0.1 atmospheres on the modelled temperature.
Figure 4.11 Effect of increasing and decreasing the atmospheric transmission by 0.05 on the modelled temperature.

4.5 Conclusion

In this chapter a lake temperature model based on the heat flux though the surface of the lake has been developed and validated. Good agreement has been achieved between the model and the surface temperature of Lough Neagh in Northern Ireland with mean differences for a 7 year daily record of 0.37±0.02°C and standard deviation of 0.96°C. The model has been developed so that the effect of climatic change on lake temperatures can be investigated and is therefore is designed as a general tool rather than specifically to determine a particular lake temperature as accurately as possible. Although some modifications were needed to get good agreement with the validation data set the model is taken to be a good description of the physics of energy exchanges through lake surfaces in general. Therefore it is thought that the HS model is a valid tool to investigate the changes in the fluxes and hence the temperature effects that climatic change might cause.

Chapter 5.

Lake temperatures as climatic indicators.

5.1. Introduction

In Chapter 3 it was discussed that lakes could potentially become useful proxy indicators of climatic change. This has been indicated by previous research which has investigated the physical basis for heat transfer between the lake and the environment, and also by research into correlations between certain lake phenomena and meteorological parameters. Since these have been focused on correlations, the causal link with climate change has not been fully investigated and therefore is not well understood. To address this lack of knowledge research is needed to establish the physical basis which links lake temperature variations to climate changes and should be based on the physical processes which determine the energy exchanges between lakes and the environment. Therefore the primary question which this chapter addresses is, how can lakes be used as proxy monitors of climate? Such a question can be put in many forms, such as how do lake temperatures respond to climatic change, or what is the climate signal provided by lake temperatures? The great potential of lakes are that they are distributed over the global land surface relatively uniformly and that they could be monitored by remote sensing techniques with their inherent synoptic, uniform and self-consistent sampling characteristics. Furthermore as they are determined by a combination of meteorological parameters, lake temperatures could turn out to indicate climatic change in a similar way that the retreat of glaciers are indicating a change which is not yet discernible in the air temperature records.

This chapter begins with a critical discussion of some of the climate related work on lakes described in previous chapters, making use of results from the HS model described in chapter 4. The principle result of this is the establishment of air temperature as an important parameter for the annual temperature cycle of a lake. There then follows the development of the concept of an equilibrium temperature being the climatic signal that the lakes are subjected to. How lakes respond to this signal is then discussed and their filtering characteristics investigated together with how lakes of different physical characteristics would respond to the same climate. The natural conclusion to the chapter would have been to estimate the expected climatic signal and the lake signal from simulations of climatic change. It was proposed to do this using the results from the

Hadley Centre for Climate Research's Global Circulation Model. However, due to delays in the distribution of this data this has not been possible. Instead the effects of the individual components of the climate system, which affect lake temperatures, are investigated and the net effect of specific scenarios of climate change discussed.

5.2 The role of solar insolation and air temperature on the annual lake temperature cycle

As described in chapter 3, it was found by Sraskraba (1980) that 85-95% of an annual temperature cycle for a lake can be modelled by a simple sinusoidal function superimposed onto an annual mean, and that the mean and amplitude of the sinusoid depends on latitude. Sraskraba (1980) implied that this can be attributed to a similar sinusoid behaviour of the net solar radiation reaching the ground, which is also a function of latitude. Deviations from this sinusoid pattern are suggested to be due to altitude, continental vs. maritime climate and localised phenomena. George (1989) develops this idea and suggests that cloud is the major factor which determines the difference between the predicted (from the sinusoid model) and the actual radiation reaching the ground, and can therefore explain the deviations of the lake temperatures from Straskraba's lake model. This concept of a lake temperature being primarily determined by the level of solar radiation has interesting consequences in trying to understand how lakes will respond to climate change. Assuming that the solar constant and the atmospheric transmission will not change, then the only parameter which can affect lake temperatures in Straskraba's model is cloud cover. Not only is this difficult to accept conceptually, it does not seem to be borne out by other work. For example, Robertson (1989) found a strong relationship between air temperature change and water temperature change. Furthermore if one looks at the annual water temperature cycle predicted by Straskraba's model together with the modelled water temperature from the HS model for LN and UK meteorologies, Fig 5.1, there are some interesting features. Note that the Straskraba temperature is lower for the winter temperatures for LN meteorology and lower throughout the year for the UK meteorology. There is good agreement during the summer and early autumn for Lough Neagh. Note also that the latitudes are similar for both the LN and the UK data. The winter difference cannot be attributed to cloud cover as the cloud cover for Lough Neagh is quite constant throughout the year, (Fig. 4.3b). Also, as will be shown in a later section, changing the cloud cover during the winter has little effect on the water temperature. Therefore it is reasonable to assume that there are other factors which are causing the difference between the water temperatures predicted by Straskraba's model and that for Lough Neagh.

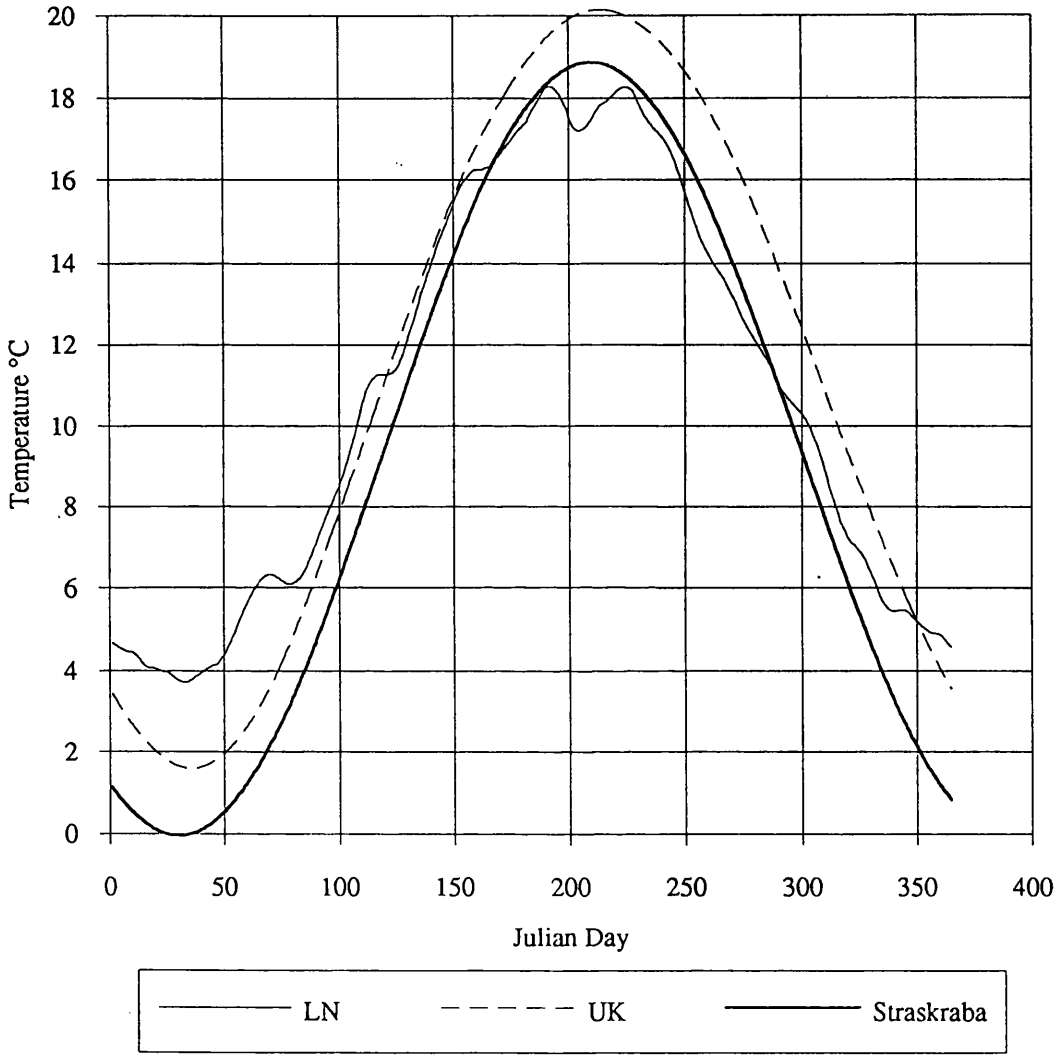

Figure 5.1 Modelled surface lake temperature from Straskraba's model for latitude 55° and from the HS model using LN and UK meteorology (see chapter 4.)

Sraskraba (1980) also states that altitudinal and latitudinal effects are inter-convertible, i.e. an increase in altitude leads to a decrease in temperature similar to the effect of increasing latitude. This is directly contrary to the previous supposition that lake temperatures are determined by level of solar radiation. If this is the case then one would expect higher lakes to be hotter due to less atmospheric absorption not cooler as an increase in latitude would produce. A hypothesis that annual lake temperature cycles are directly determined by the solar flux is a simplification of reality, and where a correlation has been interpreted as direct cause and effect. In fact, all the meteorological parameters will play their part in modifying the heat fluxes which in turn will determine the lake temperature. The general correlation between lake temperatures and solar flux then arises because the seasonal cycle and its variation with latitude obviously have a strong effect on the annual pattern of most meteorological parameters.

It was found by Robertson (1989) that air temperature had a very important role in determining the temperature of Lake Madison in the U.S.A. Fig. 4.3a) shows for Lough Neagh that this too is the case with the water temperature closely following the air temperature. This strong dependence of the water temperature with air temperature is not surprising when we look at the heat exchange equations in the previous chapter where the air temperature occurs in three of the five heat fluxes. It is easy to understand this link conceptually. A sudden step decrease in air temperature, for example, would dramatically increase the evaporation and conduction fluxes out of the lake, whilst decreasing the longwave fluxes into the lake. Thus the lake would experience a strong cooling effect reducing the water temperature. A comparable but opposite effect would occur for an increase in air temperature. Hence it is the nature of the lake to follow changes in the air temperature. This is not in discord with Straskraba's findings as the air temperature has similar sinusoidal annual cycles and latitudinal dependencies, as shown by Henderson-Sellers (1986) who found that sinusoids sufficiently described the seasonal air temperatures for South Africa and the UK. To establish further the importance of air temperature over solar flux, the HS model of chapter 4 was run using the daily mean meteorology for Lough Neagh, but with the solar flux fixed at the 1st January level throughout the year. The result is shown in Fig. 5.2a). This experiment was repeated but with the air temperature now fixed at the 1st January level, Fig. 5.2b). This simulation shows that a large part of the annual cycle is determined by the air temperature. The *difference* between the modelled lake temperature with constant solar flux, and the measured temperature has the same form as the solar flux cycle i.e. the solar flux is responsible, in part, for the temperature *deficit* between this modelled and measured lake temperature for constant cloud from early spring to mid summer.

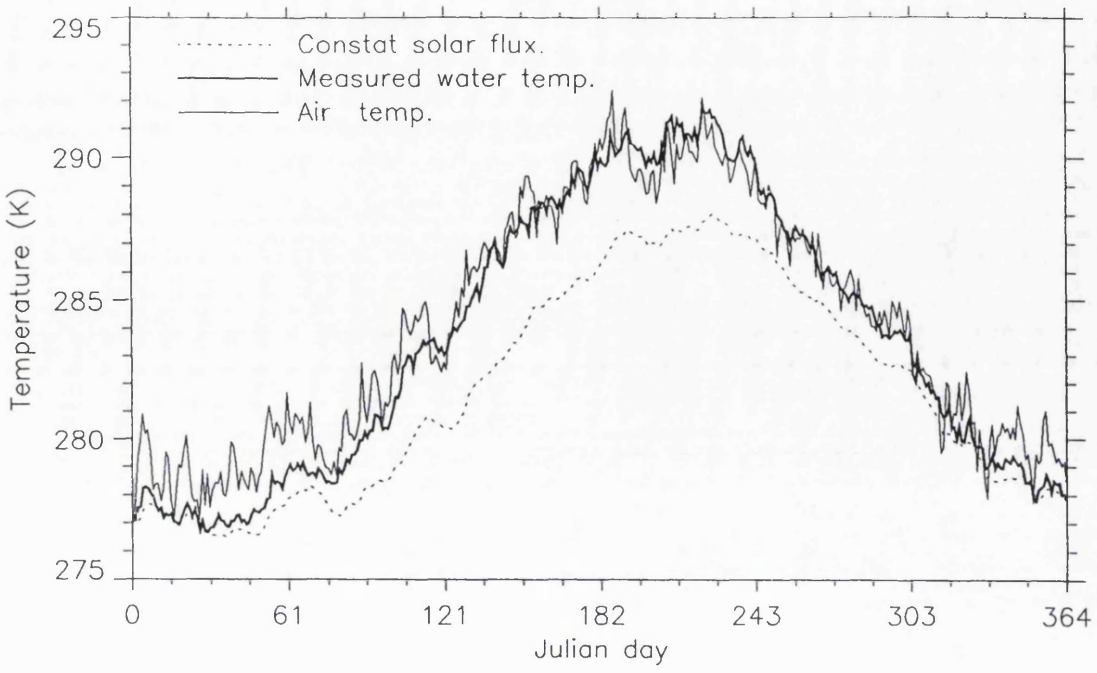

a)

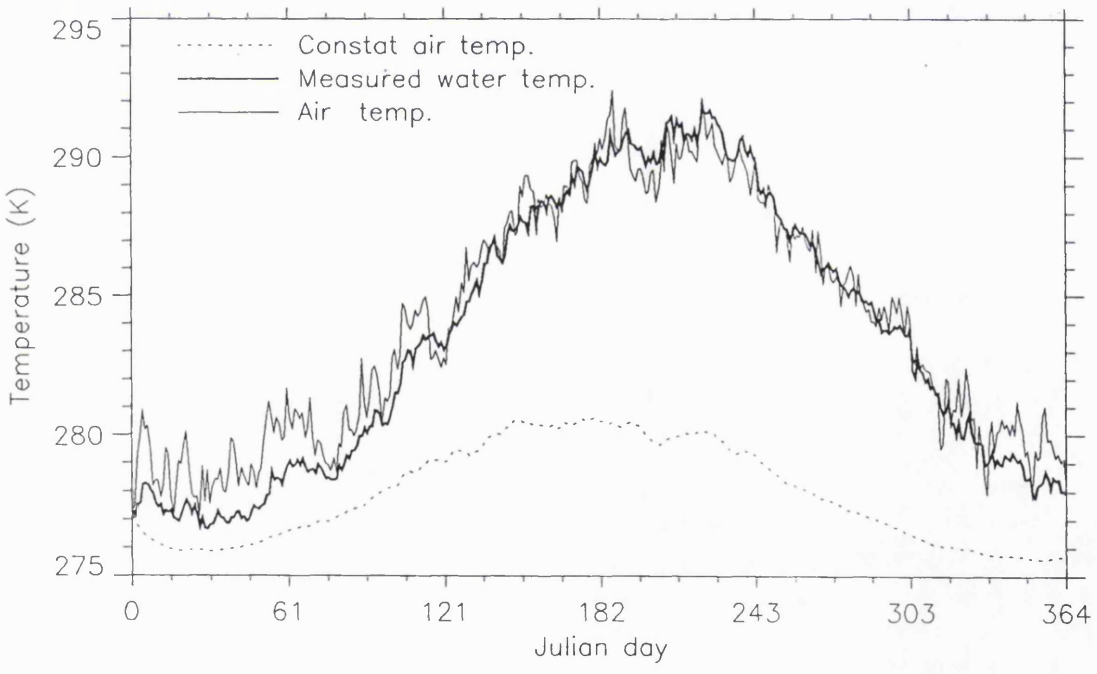

b)

Figure 5.2a) Modelled Lough Neagh water temperature with solar flux fixed at 1st January level compared with the mean air temperature and measured water temperature. Indicating the importance of air temperature in determining the water temperature.

b) As for a) but with air temperature fixed at 1st January level

Sraskraba (1980) also reports that the mean annual lake surface temperature follows the same latitudinal trend as mean annual global incident radiation, for latitudes 0 to 40°, Fig. 3.12. Deviation above 40° is attributed to the fact that for latitudes greater than 40°, maximum lake bottom temperatures reach 4°C so that it is now possible for the lake to inversely stratify and to freeze. Although it is not fully explained why this is the cause of the difference, perhaps a more acceptable explanation would be that since the lake temperature has only been correlated with the surface solar flux this correlation breaks down above 40°. In other words the correlation between the process which determines the lake temperature and the solar flux is valid only for the latitudes 0 - 40°. For example it would have been interesting for Straskraba to have plotted similar parameters for the air temperature with latitude. Unfortunately a source for these data has not yet been found to make this comparison.

This dependence on air temperature and the form of the heat exchange equation explains the observed sensitivity of a lake to altitude. As discussed in chapter 3, two lochs in Scotland which were in the same region were found to have water temperatures which differed by 0.8-2.8°C and this was attributed to their altitude difference of 110m. Although the adiabatic lapse rate of air would only produce a change in air temperature of 0.6°C the heat exchange equation (eq. (4.1) & (4.6)) indicates a mechanism which would produce a larger effect. The thermal emission of the atmosphere is biased towards the lower regions of the atmosphere. This is firstly because the lower regions are warmer and therefore will emit more energy than the higher layers, and secondly because they are generally contain more moisture which increases the emissivity of the air and its opacity. Thus these lower layers will emit more and "obscure" the higher atmosphere. Therefore, by removing some of this lower layer, the effect of increasing the altitude will have a larger effect on reducing the emitting sky temperature than one would expect due to the lapse rate alone.

In summary, the general seasonal pattern in lake temperatures is suggested to be primarily determined by the air temperature annual cycle. The other meteorological parameters do have an important influence on the water temperature cycle but in the main these effects are perturbations on the pattern determined by the air temperature.

5.3 Inter-annual variations in lake annual temperature cycles

Although the majority of the seasonal cycle in lake water temperatures is determined by the air temperature cycle, when considering the differences from year to year the other meteorological parameters can become significant as the magnitude of the inter-annual

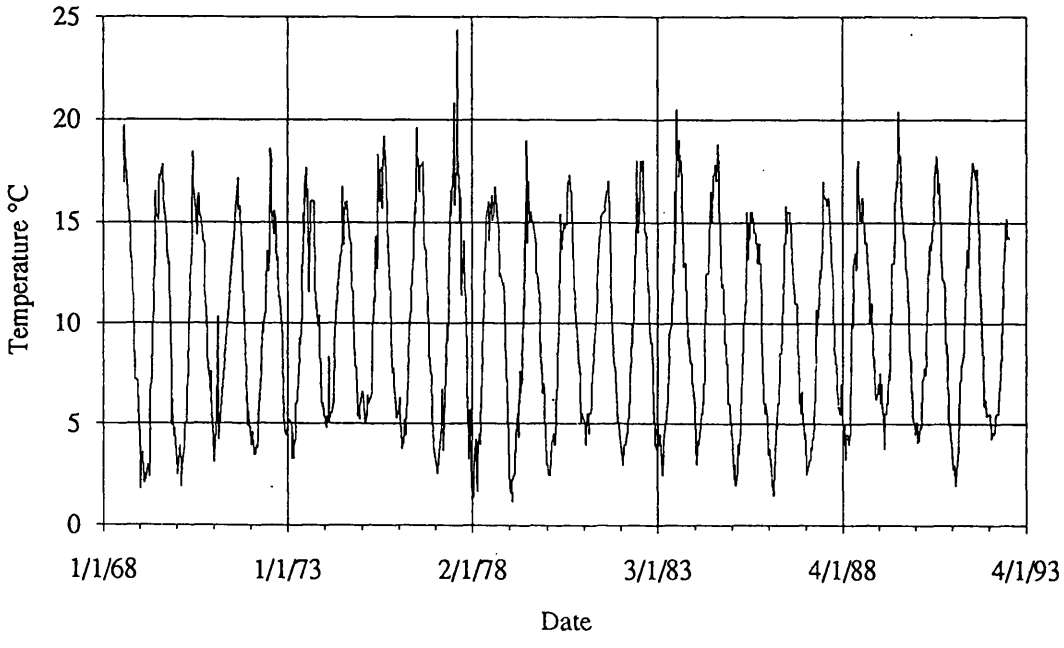

Figure 5.3 Weekly surface water temperature for Lough Neagh from 1968 - 1992

differences are relatively small. As an example of inter-annual variations in lake temperature Fig. 5.3 is the surface temperature cycle of Lough Neagh between 1968 and 1992 and this clearly shows several degrees variation in both the semi-amplitude and the mean temperature (A_1 and A_0 in Straskraba's model respectively) over this time period. It is interesting to note that there is no provision in Straskraba's model for this inter-annual variation.

As discussed in chapter 3, it has been found that the mean June surface temperature of Lake Windermere, England, which is almost a measure of (A_1 + A_0) in Straskraba's model, has a ≈10 year periodicity of magnitude 2°C (George 1989), which is not detectable in the corresponding air temperature record. The fact that the periodicity is more detectable in water temperatures has interesting implications, and careful consideration needs to be made of this result. Three possible explanations for this are: firstly, both the lake and the air temperature contain the periodicity but the characteristics of the lake are such that the periodicity is made more detectable. For example, as the water temperature is strongly dependant on the air temperature, the lake could be filtering out some of the noise in the air temperature record due to its natural variability. Secondly, the periodicity is in the air temperature but not in the sampled air temperature. This will depend on the nature of the sampling used to make up the mean June air temperature. Thirdly the periodicity is not in the air temperature but in another meteorological parameters to which the lake is sensitive, or in another way the unseen periodicity in the air temperature is reinforced with a similar periodicity in the other meteorological parameters.

George (1989) suggests that the lake has in effect "integrated the weather signal to reveal a pattern that was not very obvious in the raw meteorological signal". To understand whether a lake is an integrator one needs to consider how quickly a lake can respond to fluctuations in the meteorology and in particular air temperature, i.e. its response time or time constant. Edinger et al. (1968) shows that a lake can approximately respond as a first order linear system. The time constant of a linear first order system can be defined as the time taken for the system to change by 63% of an imposed change, i.e. if a 1° change in air temperature would cause a 1° change in the water and it took 1 week for the lake to change by 0.63° then the time constant of the lake would be 1 week. To show this more explicitly it is possible to integrate equation (3.2)

$$\Phi_{net} = \rho c_p h \frac{\partial T_w}{\partial t} = -K(T_e - T_w) \qquad (3.2)$$

to give

$$T_w = T_e - (T_e - T_0)e^{\frac{-Kt}{\rho c_p h}} \qquad (5.1)$$

where

t is time,
ρ is density of water,
h is mixed depth,
c_p is the specific heat of water.

This form of equation is typical of a low pass filter, which has well understood characteristics, where depending on the frequency of the input signal a degree of attenuation and phase shift is produced in the output signal relative to the input signal. The relationships between the phase shift and attenuation for this equation are plotted in Fig. 5.4. As one can see, for frequencies higher than the inverse of the time constant (in this case $-k/\rho hc_p$) there is considerable attenuation and approaching a 90° phase shift. The characteristic of a lake to frequencies with a 90° phase shift is similar to that of an integrator. However for frequencies near the time constant and below, the phase shift decreases and the integrating characteristics are lost. For frequencies considerably lower than the time constant the low pass characteristics are dominant with little attenuation and phase shift.

Therefore the lake can only act like an integrator for frequencies shorter than the time constant. As stated earlier the time constant is determined by the depth mixed by the wind and the heat exchange coefficient and, as will be shown in a later section, a 10m lake has a time constant of ~10 days, so it is unlikely that monthly means of lake temperature can be considered as an integral of the air temperature, although this will partly depend on how the monthly mean is generated. Therefore it is probably inaccurate to term a lake as an integrator of weather on time scales of a month but more appropriate for shorter periods.

When comparing air temperatures and water temperatures one should consider what they represent. Lake temperatures are determined by the net heat content of the lake which is the result of previous heat fluxes through the surface of the lake. The temperature of a parcel of air is similarly the net heat content of that air parcel. The differences are that the air parcel is mobile whereas the lake is fixed in location. For regions such as the UK the air temperature can be strongly influenced by conditions elsewhere (particularly the Atlantic) and so the actual air temperature can be influenced by conditions other than those locally. This is one of the reasons that air temperatures records have high variability. Therefore a daily air temperature reading beside a lake could contain less

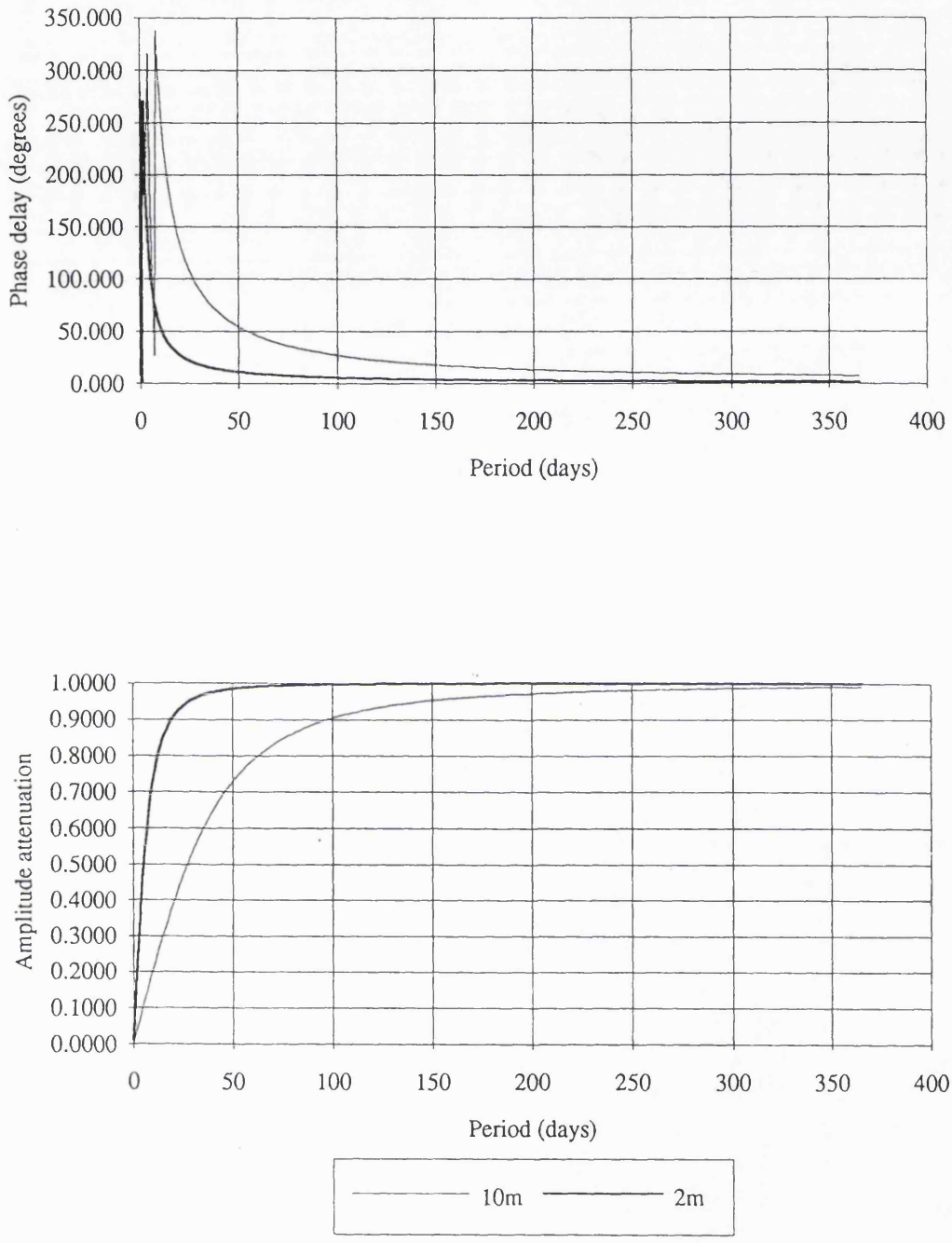

Figure 5.4 Phase delay (top) and attenuation (bottom) due to filtering of input signal Te, by lakes of 2m and 10m mixed layer depth.

information on the conditions of the region since the previous reading, compared to the information a daily water temperature would have. It is this high level of noise and reduced local information that might be preventing a periodicity being detected in the air temperature record.

A further consequence of the nature of air temperatures concerns the calculations of mean air temperatures. A single daily measurement will probably have a bias compared to 24 hour mean and would also be a poor representation of the whole 24 hours. If diurnal temperature cycle is constant then there should be no problem. However if this is not the case, for example warming of only the night time temperatures, then a single day sample will not reflect the night air temperature change. However for lake temperatures as they have longer than 24 hour time constants a single measurement would reflect some of this change. Obviously as the sampling interval is increased the lake measurement will become less representative. Another way of looking at this concept is to consider constant air and water temperatures except that there is a short spike in the air temperature. This will cause a spike in the water temperature but will be attenuated and will decay slowly. If there is regular sampling of both, and if the air temperature sample misses the spike, it will not be recorded yet due to the slow decay in the water temperature the event will have some record of its occurrence. If, however, the air temperature sample occurred during the spike the average of the air temperatures would be considerably biased, yet due to the attenuation by the lake the water bias is reduced. The importance of these effects are governed by the degree of non-symmetry of the air temperature, the time constant of the air and the lake, and the sampling frequencies. It is for reasons such as these that the sampled air temperature records might not contain the periodicities seen in the water temperatures, even though the whole air temperature record might contain them.

With the available data it is not possible to discern the true reason for the lack of periodicities in the air temperature record. In reality all the reasons described above could play their role, that is to say the filtering/integrating characteristics of lakes, the nature of air vs. water temperatures (e.g. mobility of the air), the sampling of the temperatures and the different meteorological parameters other than air temperature influencing the lake. Although it has been shown that air temperature variations dominate in determining the annual cycle in water temperatures, with regard to the smaller variations in that cycle from year to year (e.g. those detected by George), all parameters could cause significant effects. The importance of the meteorological parameters other than the air temperature in providing the periodicity, or reinforcing with a periodicity of their own, is impossible to tell without detailed data sets of all the

parameters. The individual strengths of these parameters influence is investigated through modelling in a later section.

Therefore, as regards to the structure of the annual cycle, it is suggested that it is the combination of the effect of each of the meteorological parameters (air temperature, cloud, humidity and wind) and the filtering characteristics of the lake response to these parameters, which is enabling a periodicity to be detected in the water temperature record which is not seen in the air temperatures.

5.4 Lake surface temperature and Climate

To progress with the idea that a lake responds to meteorological parameters other than just air temperature it is instructive to develop the ideas introduced earlier, of Edinger et al. (1986). The basic principle is that the lake is an energy reservoir and energy is exchanged with the environment by the various heat exchange processes through the surface water as described in chapter 3. The energy content is the mean temperature of the lake multiplied by the heat capacity of water. The rate of heat loss or gain will change as the meteorology changes through the seasons and this will be reflected in the heat storage of the lake and its temperature. As stated by Edinger et al. (1968) there will be a temperature, for a given set of meteorological conditions, where there will be no net heat transfer across the water surface, called the equilibrium temperature T_e. The surface water temperature, T_w, will always be changing towards T_e. As the meteorological conditions change through the day and the seasons, so will T_e. T_e is completely independent of the physical characteristics of the lake and is determined solely by the meteorological conditions and the heat exchange equations. T_w will always be changing towards T_e, yet because of the heat capacity of the lake and finite heat fluxes, it will lag behind. For more rapid fluctuations in T_e, T_w will respond with an increased lag and a reduced amplitude.

Therefore it is through these variables, T_e and T_w, that we can understand how lakes respond to climate. The climate signal is contained in T_e as it is determined by the meteorological conditions, T_w is the lake's response to this signal. To put it another way T_w is a "filtered" version of the climate signal T_e. Obviously T_e responds to daily weather conditions but just as climate is a measure of the expected weather and its variability so is the climatology of T_e. Thus a change in climate will have a given effect on T_e which will be represented in some way in T_w. The question of how lakes respond to climate now has two parts. Firstly how will change in meteorological climate change

the climatology of T_e, and secondly how does a lake respond to T_e in the form of T_w, and will this response alter with climate change?

5.4.1 Derivation of the equilibrium temperature, Te

To investigate the first question it is instructive to look at the formulation of T_e in detail. Unlike the formulation of Edinger et al. (1968) I will try to make as few approximations as possible so as to get as close, as the current understanding of the heat exchange equations will allow, to the correct nature of Te. Following Edinger et al. (1968), we have the net heat flux per day to be:

$$\Phi_{Net} = \Phi_{Sol} + \Phi_{Long\_in} - \Phi_{Long\_out} - \Phi_{Evap} - \Phi_{Cond} \tag{5.2}$$

putting $\Phi_{Net} = 0$

one gets:

$$0 = \Phi_{Sol} + \Phi_{Long\_in} - \Phi_{Long\_out_{Te}} - \Phi_{Evap_{Te}} - \Phi_{Cond_{Te}} \tag{5.3}$$

Unfortunately equation 5.3 is not solvable analytically for T_e but together with the equations in chapter 4, it shows that T_e primarily depends on air temperature, cloud amount, relative humidity and wind. Unfortunately T_e does not have a simple relationship with the meteorological variables and therefore it is unclear as to how to easily relate changes in T_e climatology to changes in the meteorological climatology, although it is this relationship which has suggested that T_e may have a higher sensitivity to climate change or a more detectable response than with air temperatures. This complicated response may hinder the acceptance of T_e as a useful climatic indicator by the climate research community as T_e will not provide evidence of, say air temperature change directly to which this community is more accustomed and which is easier to interpret. T_e however provides a general measure of climate, combining the effects of air temperature, wind, cloud and humidity, and could therefore be considered as a useful combined measure of the climate in the region of the lake, rather than looking at just an individual component such as air temperature.

There are however some problems with the formulation of T_e that should be assessed. If one considers lakes that are iso-thermal and continually mixed then the idea of a temperature which the net gain in energy for the lake is zero is quite simple. Yet on short time scales and looking at the energy exchange processes in detail this can only be an approximation of reality. For all the heat exchange processes, except for the absorption

of solar radiation, the rate of heat exchange is determined by the temperatures in the boundary layers of the air and water, which are only 0.4cm and 0.1cm respectively (Ragotzkie 1987). The absorption of solar radiation however is governed by the optical depth which can be several metres. Therefore for the concept of T_e to work there must be a region of water where the energy absorbed from the solar radiation is strongly coupled to the water surface boundary layer so as to be able to establish an equilibrium condition. Wind will generally ensure that this surface layer is well mixed but there could be occasions under extremely calm conditions when this is not the case. This would mean that the solar radiation term in the equation (5.3) is too large (due to some of the radiation passing through the water layer coupled to the boundary layer) and the calculated T_e too big. Fortunately these extremely calm conditions do not generally persist and if they are found to be a problem one could limit these studies to the night when there will have been more time for the solar radiation of the day to mix with the surface layers and the increased mixing due to cooling at the surface and the resulting convection.

The effect of stratification on T_e should also be considered. While the lake is in general circulation, obviously the temperature of the whole lake volume is changing towards T_e. When the lake has stratified there is very little energy exchange between the epilimnion and the hypolimnion (Ragotzkie 1987). This means that the body of water that is responding to changes in meteorology and hence T_e is the epilimnion, as determined by the thermocline depth. As long as this is deep enough, so that the solar penetration of solar radiation into the hypolimnion is small, then the equation for T_e is valid. This is generally found to be the case as the temperature of the hypolimnion, once formed generally does not change significantly throughout the summer (Hutchinson 1975), indicating that little radiation is entering the hypolimnion. One should therefore define a depth where T_e is applicable as the temperature of the water which is thermally coupled with the atmosphere. For stratified lakes this would be the water above the thermocline and for lakes in general circulation the mean depth.

5.4.2 Relationship between T_e and water temperature, T_w

The second question in understanding the response of lakes to climate concerns the relationship between T_e and T_w, the surface temperature of the water. As discussed earlier lakes can behave like a low pass filter to T_e. More specifically, if we subtract equations (5.3) - (5.2), we get:

$$\Phi_{Net} = \Phi_{Long\_out_{Te}} - \Phi_{Long\_out_{Tw}} + \Phi_{Evap_{Te}} - \Phi_{Evap_{Tw}} + \Phi_{Cond_{Te}} - \Phi_{Cond_{Tw}} \qquad (5.4)$$

Substituting using the heat exchange equations in chapter 4. we get:

$$\Phi_{Net} = \varepsilon_w \sigma\left(T_e^4 - T_w^4\right) + \left[\lambda\left(T_{ev} - T_{av}\right)^{1/3} + 0.0627u_2\right]\left(e_{se} - e_a + 0.61\times10^{-3} p\left(T_e - T_a\right)\right) - \left[\lambda\left(T_{wv} - T_{av}\right)^{1/3} + 0.0627u_2\right]\left(e_{sw} - e_a + 0.61\times10^{-3} p\left(T_w - T_a\right)\right) \quad (5.5)$$

where

Φ_{net} is the net flux into the lake
ε_w is the emissivity of the water
σ is the Stefan - Boltzmann constant
u_2 is the wind speed at 2m
e_{sx}, e_a are the saturated vapour pressure at temperature x and atmospheric vapour pressure respectivly
p is the atmospheric pressure
$\lambda = 0.027$ for $T_{wv} \geq T_{av}$
$\lambda = 0.0$ for $T_{wv} \leq T_{av}$

$$T_{xv} = \frac{T_x}{1 - \left(\frac{0.378 e_x}{p}\right)}$$

and if there is no convection i.e. λ=0 then this simplifies to:

$$\Phi_{Net} = \varepsilon_w \sigma\left(T_e^4 - T_w^4\right) + 0.0627u_2\left(e_{se} - e_{sw} + 0.61\times10^{-3} p\left(T_e - T_w\right)\right) \quad (5.6)$$

It is this equation which will determine the response of T_W to T_e or in other words equation (5.5) will determine the filtering characteristics of the lake for T_e. We can expect that the general form of this filter will be a low pass filter as in the Edinger case but that it will probably not behave like a first order linear filter due to the higher order terms. The time constant will be determined by two aspects, the amount of water involved and the rate at which heat can be lost or gained through the surface when $T_W \neq T_e$, i.e. a heat exchange coefficient.

Consider first the amount of water involved, defining this as the water which is thermally coupled with the heat exchange processes at the surface as discussed in an earlier section. Obviously for a given heat flux a smaller mass of water will respond more rapidly than a larger mass. If a lake is stratified this mass will be different from the whole lake mass, as in the general circulation case. The stratification depth can change from year to year depending on the wind during spring and early summer and the rate of heating (see chapter 3). Therefore the filtering performed by a particular lake or the characteristics of the filter can vary through the seasons and from year to year.

5.4.3 The heat exchange coefficient, K

The second aspect which will determine the filtering response of a lake is the nature and magnitude of the rate of heat loss due to a given water temperature/equilibrium temperature difference. Even though equation (5.5) is not linear it is still useful to consider it in the form given by Edinger et al. (1968) of:

$$\Phi_{Net} = -K(T_e - T_w) \tag{3.2}$$

where K is the heat exchange coefficient. Although K will depend on Te and Tw this equation is useful in understanding the response of the lake to (Te-Tw) differences. A large K will mean that the lake will respond quickly to any changes in Te and will pass higher frequencies and a small K the opposite. The combination of K and the water depth will determine the time constant of the lake. Note that K contains meteorological terms and therefore is not independent of climatic change and will affect the filtering characteristics of the lake.

Using the HS model the effects of this filtering and its inherent time delay in the heating and cooling can be investigated. The results are shown in Fig. 5.5 which is a plot of the difference (Te-Tw) through the year using the LN and UK meteorologies. The difference has been calculated for lakes of several different depths. As would be expected the deeper the lake the greater the temperature difference. Note also that the temperature differences are generally smaller for the Lough Neagh case and this is due to LN meteorology determining a larger heat exchange coefficient. Implicit in this is that the annual cycle for Lough Neagh will contain more of the shorter term fluctuations in Te. It is also interesting to note that the meteorological fluctuations produce several days in the year when Tw = Te.

It is possible to solve equation (5.6) numerically for solutions of K using the heat exchange equations in the HS model. Results using the Lough Neagh monthly meteorology are presented in Fig. 5.6. The values of K are found to be a little higher than those reported in the literature (Edinger et al. 1968), however Lough Neagh has a very high mean annual wind speed which has a large effect on K. There is considerable variation with season, as would be expected, as the meteorology of winter is considerably different to that of summer.

As stated earlier K also depends on T_e and T_w, i.e. the coefficient of heat exchange will vary depending on the magnitude and sign of (T_e-T_w). Therefore if there is a sudden

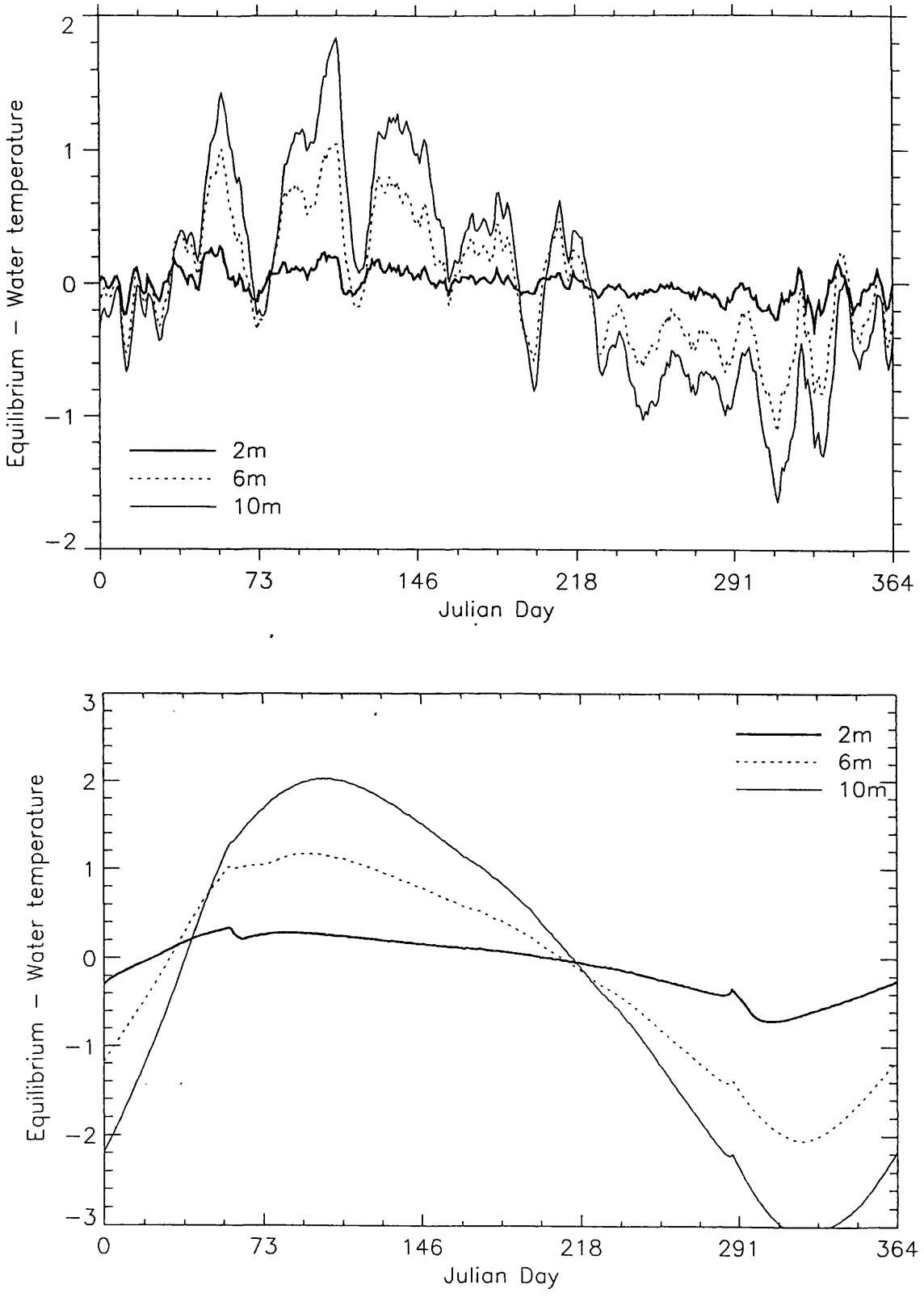

Figure 5.5 Top figure the difference (Te-Tw) for lakes of depth 2, 6 and 10m using LN meteorology. Bottom as above but for UK meteorology.

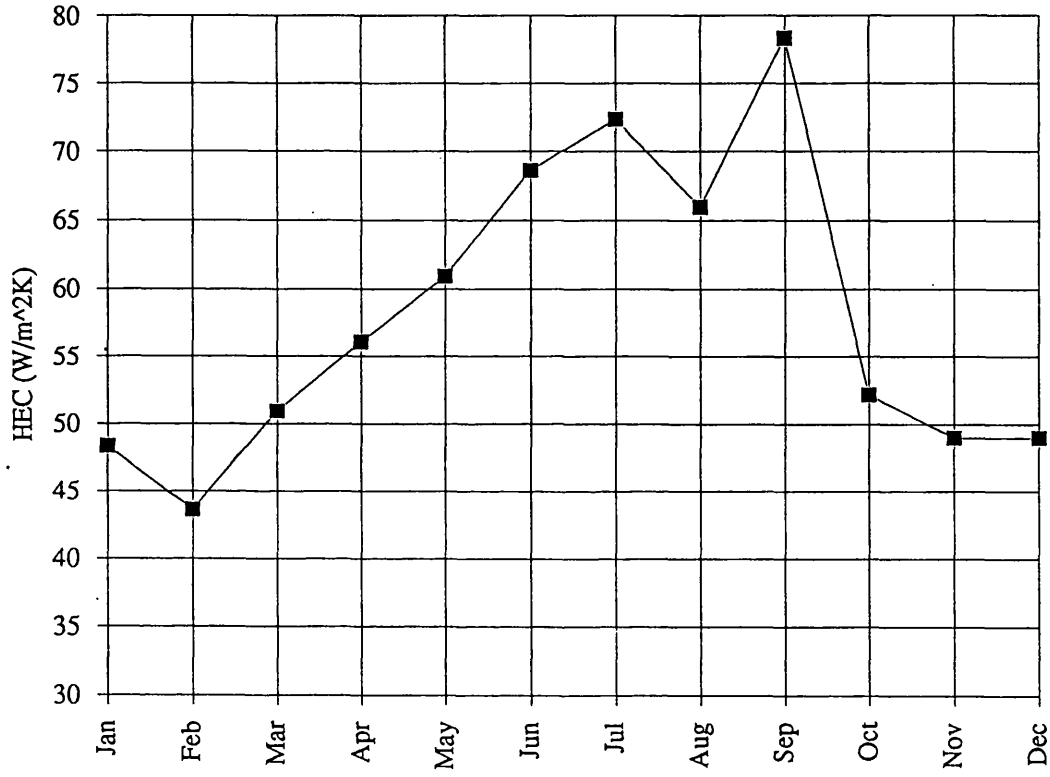

Figure 5.6 Calculated heat exchange coefficient (K) for Lough Neagh using LN meteorology for each month.

change in T_e, the forcing of T_w towards T_e will be different. Fig. 5.7 displays this dependence of K on T_e and T_w for the Lough Neagh meteorology. This was determined by calculating K for every other month for various values of Tw offset from T_e. It is interesting to note that the response to (T_e - T_w) is not symmetrical about zero. This is attributed to the quartic longwave radiation term and the vapour pressure increasing non-linearly. The shape of the curves are similar for each month. Since, however, the temperature difference (T_e-T_w) is usually small (Fig 5.5), K is relatively constant.

5.4.4 The time constant of a lake

The HS model can also be used to calculate the time constant of lakes for various depths and meteorology. This was done by allowing the temperature of a model lake to reach equilibrium and then increment the water temperature by a fixed amount and then measure the rate of decay back to the equilibrium temperature. This was done for several different depths and the results are plotted in Fig. 5.8. The temperatures have been normalised and decays for linear first order systems are also plotted for comparison. One can see from these plots that the lake does behave in a way which is quite similar to a first order linear system. This is a little surprising when one considers the heat exchange equation, since it contains water temperature terms to the fourth power. However, this is probably due to the difference (T_e-T_w) being too small for the higher order terms to have significant effect. Considering the fluxes affected by this step, as in Fig. 5.9, one sees that the fluxes which dominate are the evaporation and conduction terms. One can therefore deduce that the fluxes which are most responsible for driving the lake temperature towards Te are the evaporation and conduction components. One can also see that the time constants for lakes, where the depth of water which is thermally coupled to the boundary layer is less than 10m, are considerably shorter than a month or the length of the seasons.

The length of the time constant is important when trying to understand how a lake is responding to the weather and how we can use it to monitor climate. If the lake had a time constant of order of a month then it would be difficult determine monthly or seasonal means for Te as the lake would not be behaving as a low pass filter with regard to these time scales. If this were the case T_w records could only be used for monitoring the inter-annual variations of the annual means. The fact that 10m lakes have a time constant of approximately six days for LN meteorology means that such lakes would be passing through the interesting monthly/seasonal signal but would still be providing some filtering of the high frequencies in the meteorology. There are diurnal and day-to-day fluctuations within the meteorological signal which in climate terms can be considered noise and so with such a time constant there would be a considerable

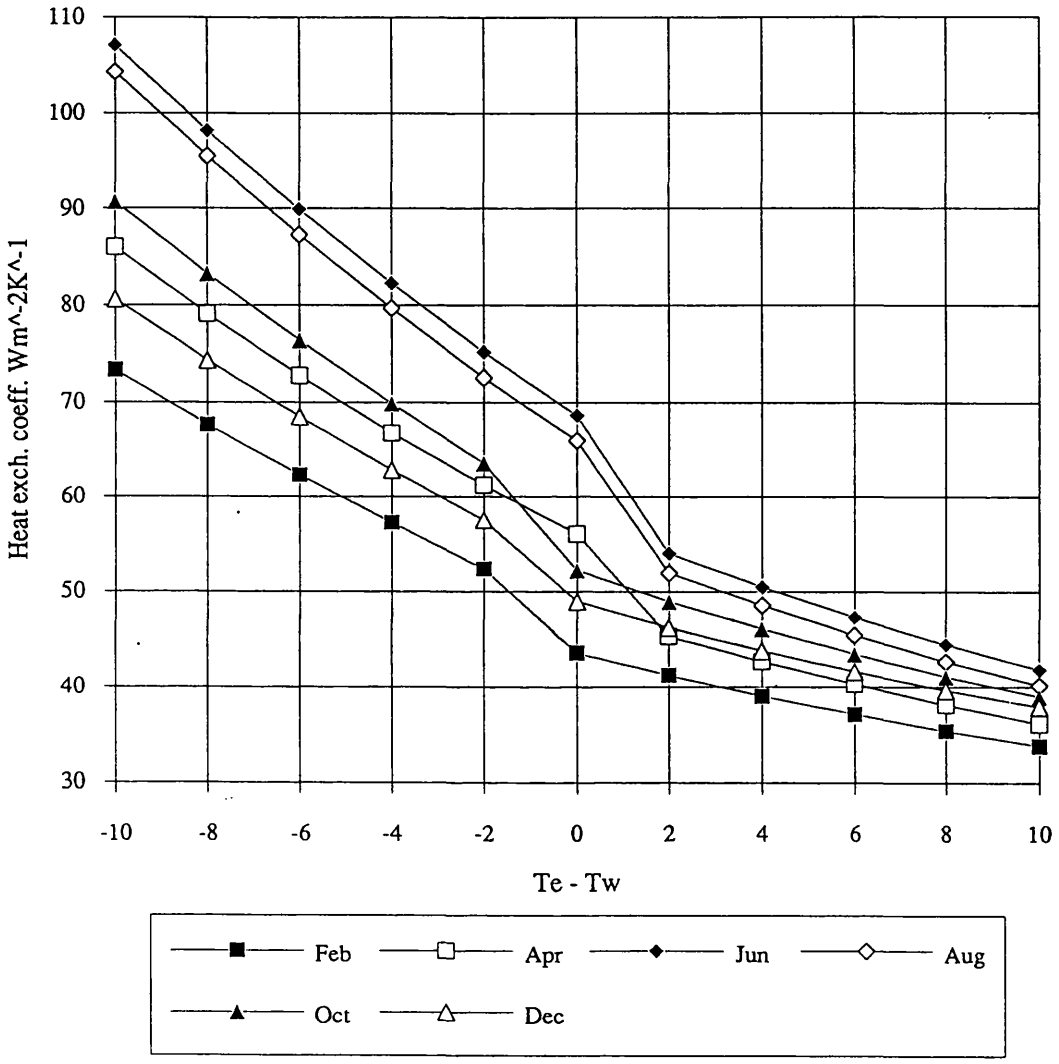

Figure 5.7 Variation of K with differences in (Te-Tw) for every other month.

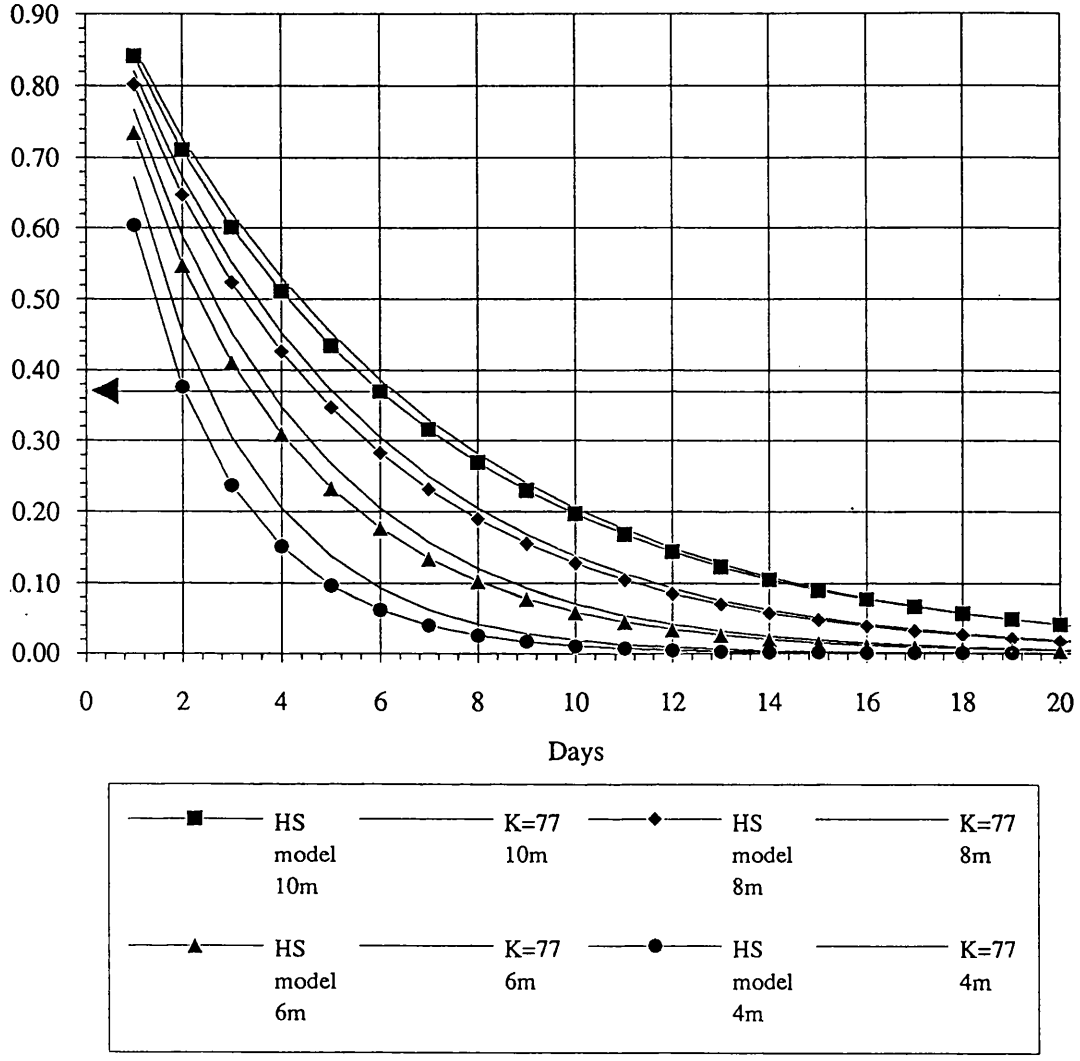

Figure 5.8 Lake temperature decay back to Te after an increase of 5°C. Calculated for lakes of depth 4,6..10m. Corresponding decays for 1st order system using K=77 and appropriate depths are also plotted for comparison. Each decay has been normalised.

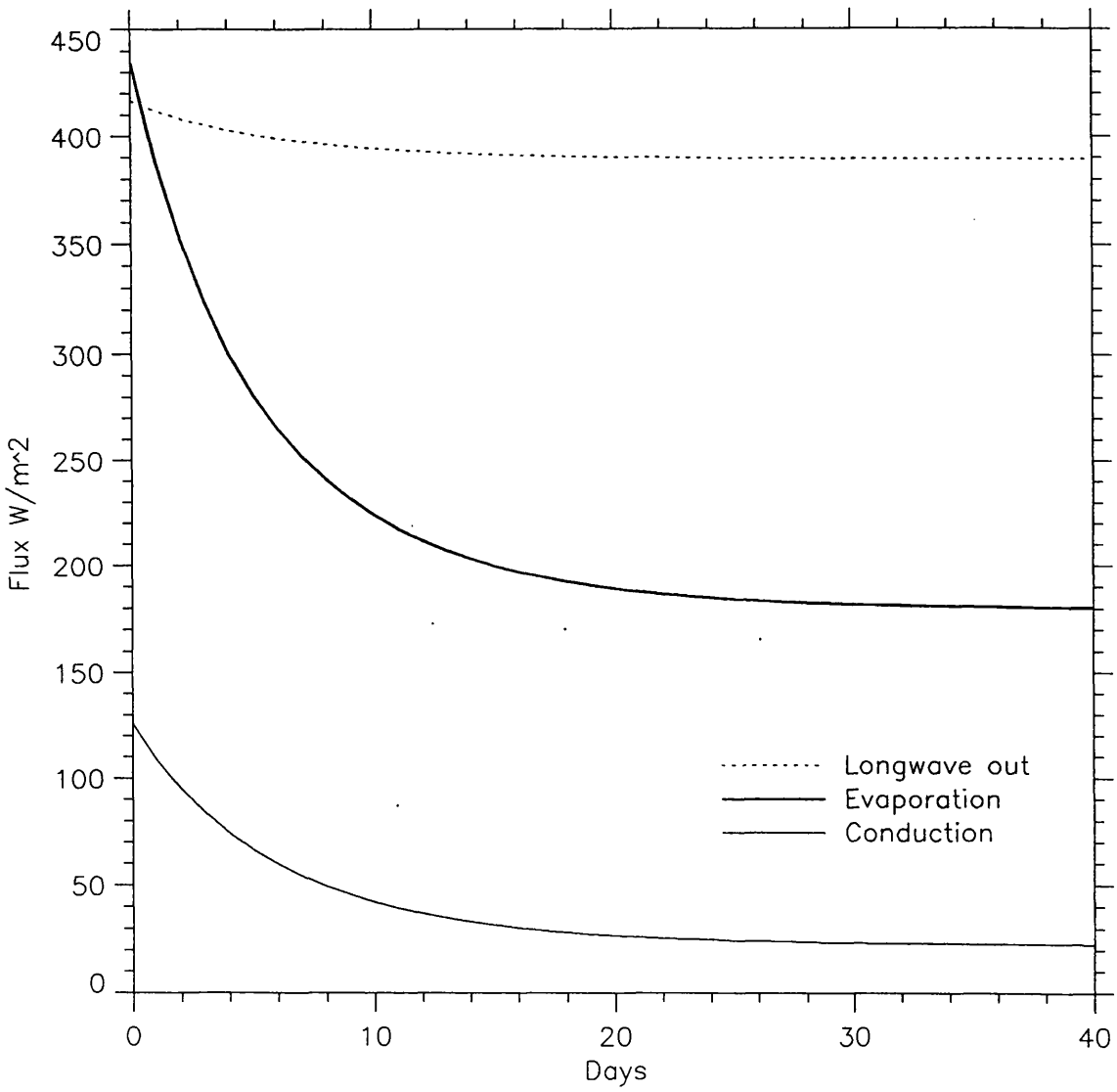

Figure 5.9 Fluxes associated with the step increase in temperature described in Figure 5.8.

attenuation of these components. Therefore the lake is acting as a geophysical filter to the weather signal, reducing the high frequencies of periods < 6 days, in this case, yet preserving the longer term (> 6 days) component.

The temperature decay with time, for Lough Neagh with a mean depth of 8.9m, is plotted in Fig. 5.10 together with the decay of a first order linear system which follows that of Lough Neagh, which have been derived from a 5° temperature step and July meteorology. The time constant of this linear system is just over 5 days. The effect of K on the time constant is also shown. Notice that quite a large change in K is needed to produce a significantly different time constant. The K for the decay which is most similar to that for Lough Neagh is 85 W/m^2K whereas the time constants for K=65 and 105 are only 4.1 and 6.7 days respectively compared to that for Lough Neagh of 5 days.

5.4.5 Regional lake temperature response

Having established equation (5.5) and the characteristics of how lakes respond to Te, it is interesting to consider how two lakes in the same region, which are close enough to experience the same climate and hence Te, will respond in relation to each other. If we have two lakes A and B and they are in a phase of the year where the water is cooler than the air and so there is no convection i.e. as for equation (5.6), then we have

$$\Phi_A = \varepsilon_w \sigma\left(T_e^4 - T_{Aw}^4\right) + 0.0627 u_2 \left(e_{se} - e_{sAw} + 0.61\times10^{-3} p\left(T_e - T_{Aw}\right)\right) \tag{5.8}$$

$$\Phi_B = \varepsilon_w \sigma\left(T_e^4 - T_{Bw}^4\right) + 0.0627 u_2 \left(e_{se} - e_{sBw} + 0.61\times10^{-3} p\left(T_e - T_{Bw}\right)\right) \tag{5.9}$$

Subtracting (5.8 - 5.9), gives

$$\Phi_A - \Phi_B = \varepsilon_w \sigma\left(T_B^4 - T_A^4\right) + 0.0627 u_2 \left(e_{sb} - e_{sA} + 0.61\times10^{-3} p\left(T_B - T_A\right)\right) \tag{5.10}$$

and rearranging for wind speed,

$$u_2 = \frac{\Phi_A - \Phi_B - \varepsilon_w \sigma\left(T_B^4 - T_A^4\right)}{0.0627\left(e_{sb} - e_{sA} + 0.61\times10^{-3} p\left(T_B - T_A\right)\right)} \tag{5.11}$$

So from two lakes which have the same Te we can estimate the wind speed if we know the heat fluxes for the lakes and their temperature. Once we have calculated the wind speed we can substitute back into (5.8) and calculate Te. To do this one needs the net heat fluxes into the lake (Φ_A and Φ_B). This could be calculated from the temperature records of the lakes and an estimate of the volume of the water corresponding to these

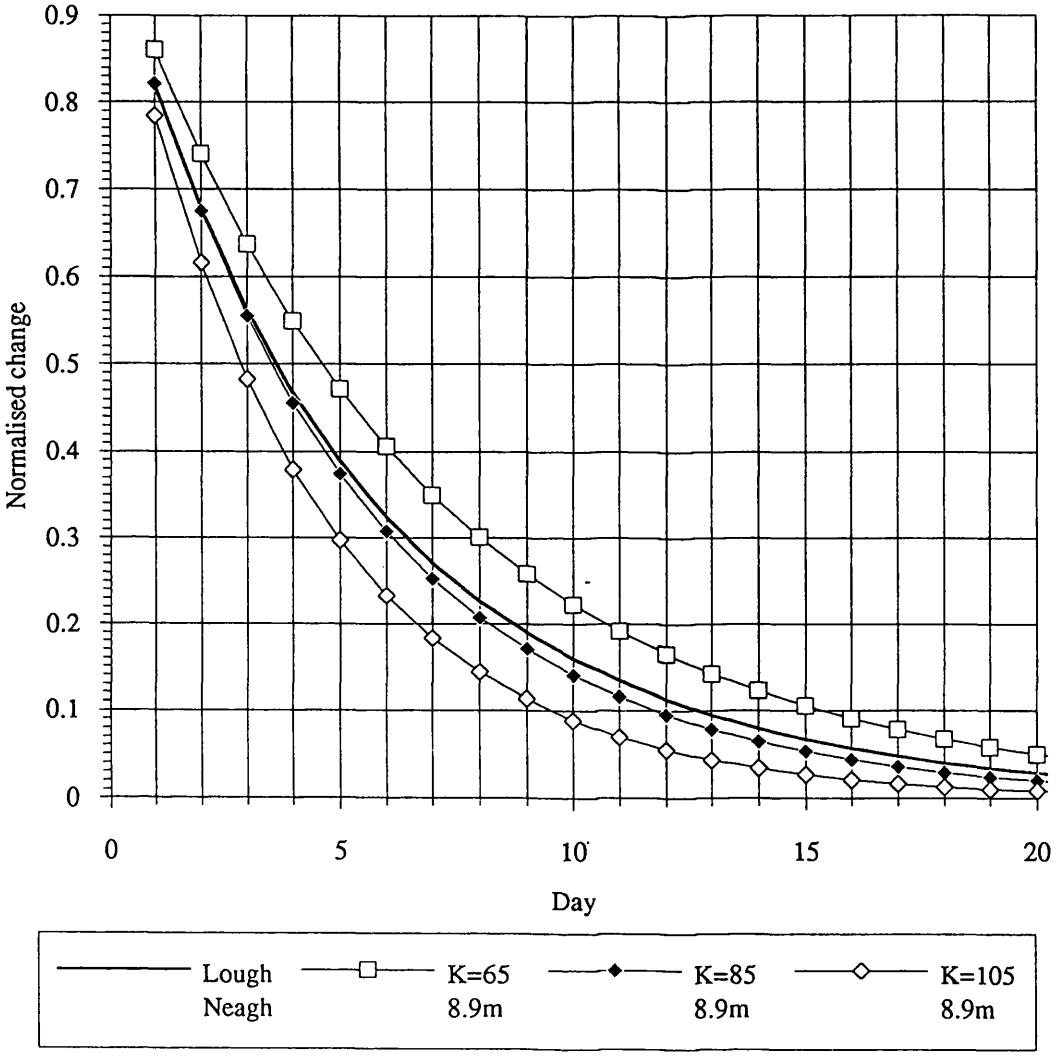

Figure 5.10 Normalised temperature decay back to Te after a 5° increase for a lake of depth of 8.9m, the mean depth of Lough Neagh. Plotted for comparison are the first order liner system decays for depth 8.9m but with K values of 65, 85, 105 W/m^2K. The decay with K=85 was found to be the closest to that of Lough Neagh.

temperatures. The lakes temperature would have to be measured over a time interval and then from the temperature difference the mean heat flux for that interval can be calculated. For the volume of water, this can be considered as being the epilimnion if the lake is stratified and, as discussed in chapter 3, this can be estimated from the fetch. Obviously this algebraic solution has only been possible due to the form of the heat exchange equations and they are only an approximation of reality, yet it is encouraging that such information can potentially be derived from lake temperatures.

Another way of looking at two lakes which experience the same climate is through equation (3.2). If these two lakes have a similar heat exchange coefficient, which one might expect, then one can rearrange for Te, e.g.

$$\Phi_A = -K(T_e - T_{Aw})$$

$$\Phi_B = -K(T_e - T_{Bw})$$

dividing,

$$\frac{\Phi_A}{\Phi_B} = \frac{(T_e - T_{Aw})}{(T_e - T_{Bw})}$$

to give,

$$T_e = \frac{\Phi_A T_{Bw} - \Phi_B T_{Aw}}{\Phi_A - \Phi_B} \qquad (5.12)$$

To test the assumption that K can be considered constant for two lakes the HS model was used to calculate the heat exchange coefficient for two lakes of differing depth, 2m and 10m. The meteorology used was the daily means for Lough Neagh. The results of this are plotted in Fig. 5.11. In general the heat exchange coefficients were very similar, however, there are considerable differences for particular parts of the year. These correspond to times when one of the lakes is experiencing convective heat removal while the other is not. This difference occurs because of the different time constants of the two lakes. So in spring the 2m lake heats up faster than the 10m lake and therefore reaches a temperature where there will be convective removal first. Similarly for the autumn case, the 2m lake will cool faster and therefore will stop convective removal first. The very large spikes for K in these regions are due to an artefact in the model. The transition between non-convection and convection is not particularly smooth as can be seen in Fig. 5.12 which shows the convective evaporative flux term for these two model lakes, and this produces the spikes in the K values.

To summarise, the net heat fluxes for lakes are such to change the water temperature towards an equilibrium temperature, where the net heat flux into the lake would be zero.

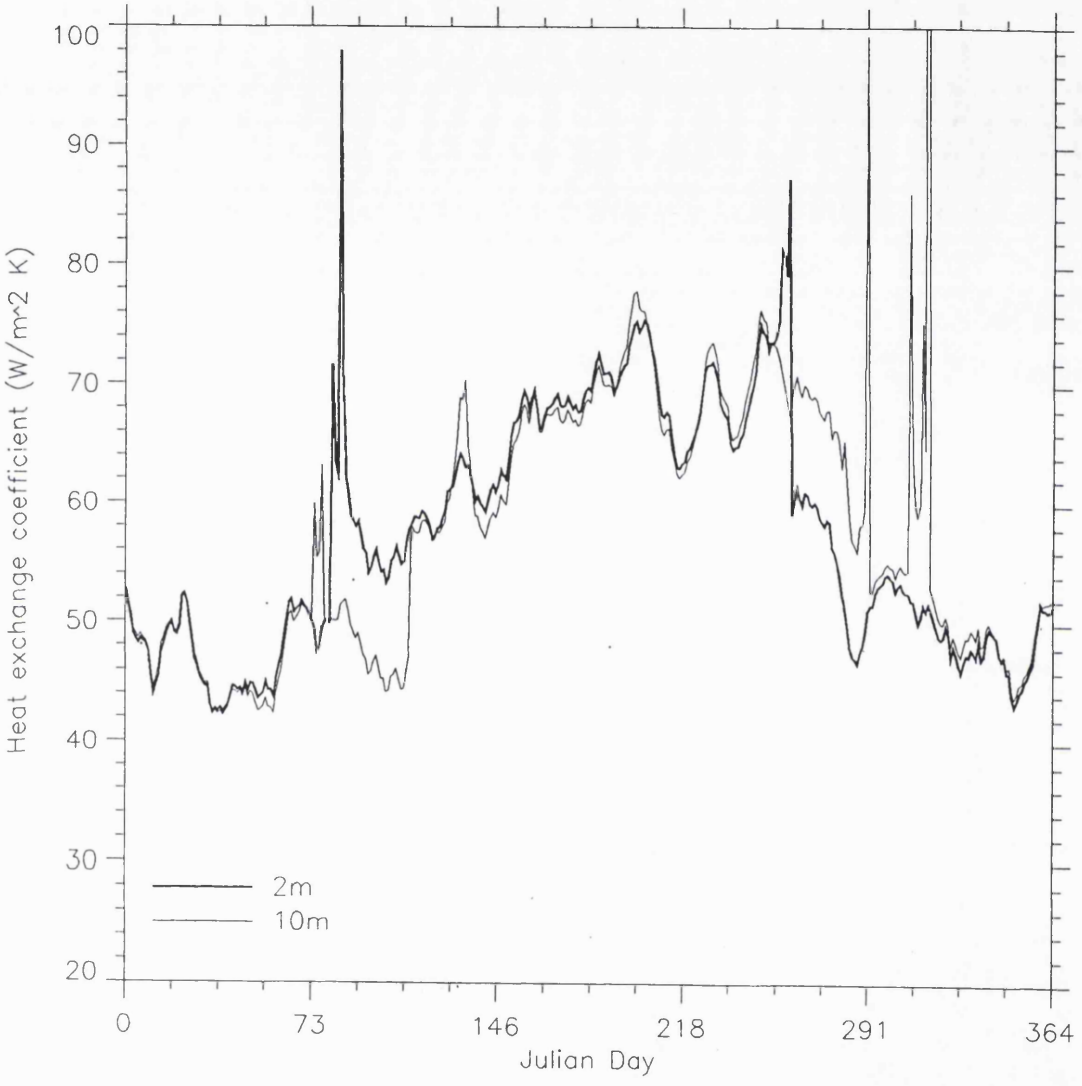

Figure 5.11 Modelled K for two lakes of 2m and 10m throughout the year using LN meteorology.

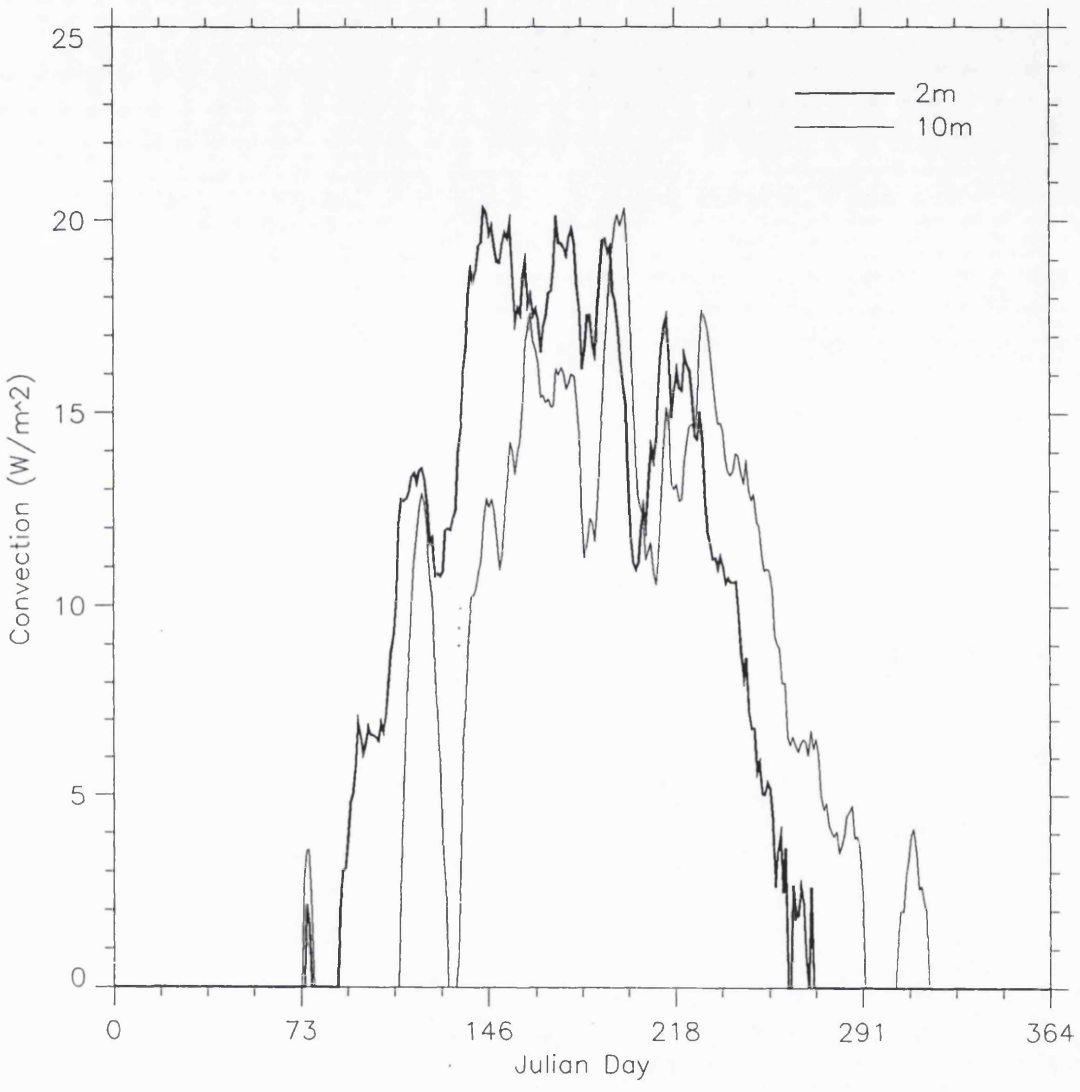

Figure 5.12 Modelled convective evaporative flux for the two lakes in Figure 5.11. The spikes are artefacts of the model in the progression from non-convection to convection. Note delay in the 10m lake compared with the 2m lake.

This temperature is determined by the meteorological parameters subjected by the lake. Due to the heat capacity of the water, the water temperature evolution will be a low pass filtered version of the equilibrium temperature evolution, for time scales which are longer than the time constant of the lake. The level of this low pass filtering is determined by the volume of the water thermally coupled to the atmosphere and the heat exchange coefficient which is in turn determined by the meteorology over the lake and the nature of the heat exchange processes. Lakes of different depth which experience the same meteorology are found for the majority of the year to have similar heat exchange coefficients. If there is more than one lake, for which this is true, it is possible to invert the water temperature records to acquire the equilibrium temperature.

These results are very encouraging for the use of lakes as proxy monitors of climate as T_e is derived exclusively from meteorological parameters and independent of lake type, and could potentially be monitored by remote sensing methods. These results suggest several areas which are worthy of more investigation. The first is to validate this relationship between lakes which are subjected to the same climate. The second is to establish over how large an area one can consider the climate to be constant, or over what distance is the above relation valid. Unfortunately it has not been possible to obtain a data set which will validate the above hypothesises. Whether these parameters can be measured through remote sensing methods is the subject of later chapters in this thesis.

5.5 The effect of climate on T_e and T_w

Through numerical modelling of equation 5.4, using an adapted version of the HS model described in chapter 4, it is possible to determine the significance and way in which the components of meteorology affect T_e and K. This is important to understand if changes in T_e are to be related to climate change and how climate change will affect the response of lake surface temperatures to T_e. We also need to know which meteorological parameter T_e is most sensitive to, and what a particular change in one parameter will produce in T_e. We also need to know the nature of change for each parameter and how they may combine to affect T_e, i.e. whether they will reinforce each other or whether they might cancel out. It is also important to consider how change in climate will affect the heat exchange coefficient and hence the behaviour of the filtering performed by the lake as this will determine how the relationship between T_w and T_e might change.

5.5.1 The effect of climate on T_e

To investigate these questions the HS model was used with mean monthly weather conditions from Lough Neagh. For the months June and December, T_e was calculated

for the measured meteorology and then for meteorology where one parameter was varied systematically. This was repeated for all the meteorological parameters. From this the response of T_e to specific changes in meteorology can be established. The results of this simulation are shown in Fig. 5.13a) - d) which is the absolute values of T_e and the meteorological parameters and Fig. 5.14a) - d) are the difference plots. The first point of note is that the effect of changing a parameter does not necessarily produce a similar change in magnitude, or of sign, for June and December. For example changes in wind or cloud have the opposite effect in June as in December and of different magnitude. Whereas for air temperature virtually the same change in T_e occurs in December as in June for a given air temperature change ($\approx 1°$ per $1°$ change). Another feature which is interesting for the wind and the cloud, is that during December they have very little effect on T_e. The explanation for the cloud is that during the winter the solar flux term is so small that a change in the cloud cover has very little effect. In fact we see a slight increase and this is due to the downwelling flux increasing with cloud. For the wind this is due to the conduction and evaporation fluxes being approximately equal and opposite in sign as can be seen from the equilibrium heat flux components in Fig. 5.15, so an increase in wind will just increase their magnitude and not change their sign, keeping them equally balanced.

The way in which these different changes might combine depends entirely on how they will change, as a change in one might cancel out a change in another. The winter situation is the simplest given that cloud and wind changes have little effect, so the response is just determined by the air temperature and the humidity. The summer situation is more complicated with all the components producing an effect. In assessing what will be the net result it is necessary to know what are realistic changes in the parameters. Here however I will just compare how much "change" is needed to produce a degree increase in T_e. For June therefore an air temperature change of + 1.2°C is needed, relative humidity needs to increase by +12%, the fraction of the day covered by cloud needs to decrease by 0.3 and wind speed needs to decrease by 1.3 m/s, to produce an increase of 1°C in T_e. One can estimate, however, the effects that different patterns of weather will have. For example, if the frequency of high pressure systems increases for the summer months then this will increase average air temperatures, decrease cloud, decrease relative humidity and reduce wind. The type of effect this would have on T_e for each respectively are, increase, increase, decrease and increase, so it would not be unreasonable to expect an increase in T_e for this scenario. Conversely if for the winter there is a greater frequency of low pressure systems then this will bring higher winds, more cloud, higher relative humidity and higher air temperatures relative to the winter high pressure systems. This will increase T_e due to an increase from the air and relative

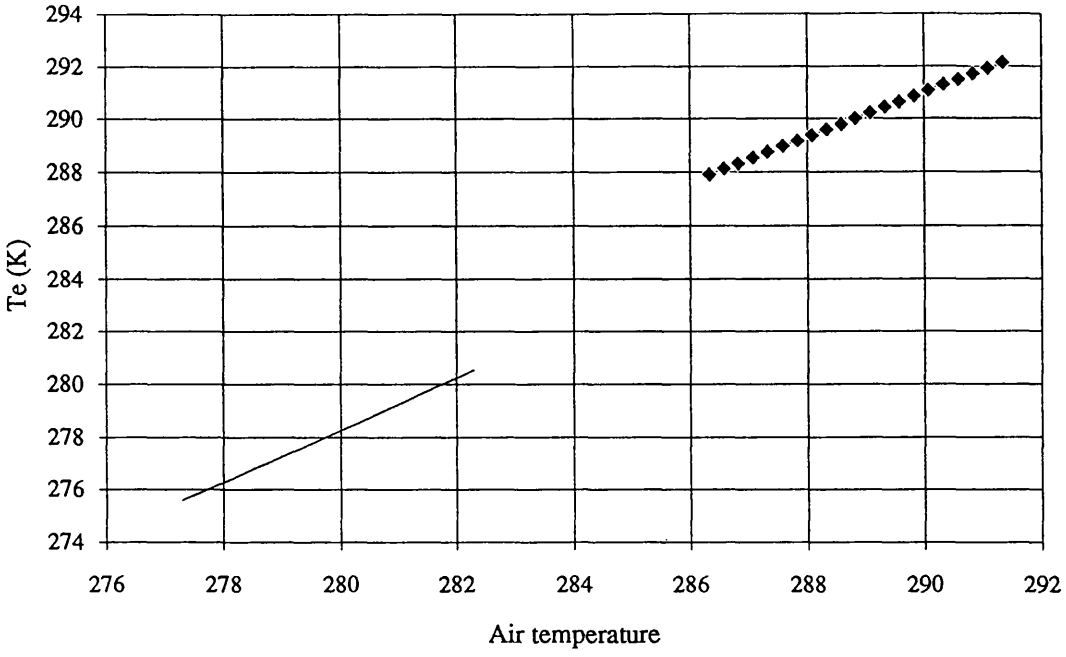
294
292
290
288
286
284
282
280
278
276
274
Te (K)
276
278
280
282
284
286
288
290
292
Air temperature

a)

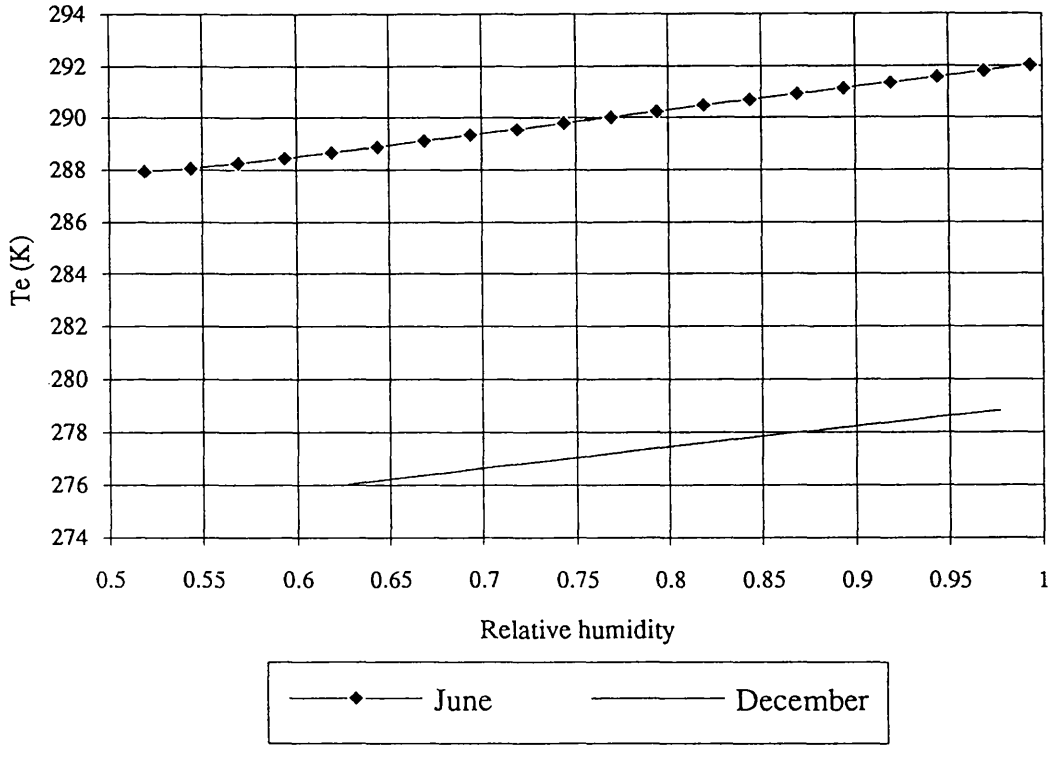
294
292
290
288
286
284
282
280
278
276
274
Te (K)
0.5
0.55
0.6
0.65
0.7
0.75
0.8
0.85
0.9
0.95
1
Relative humidity
June
December

b)

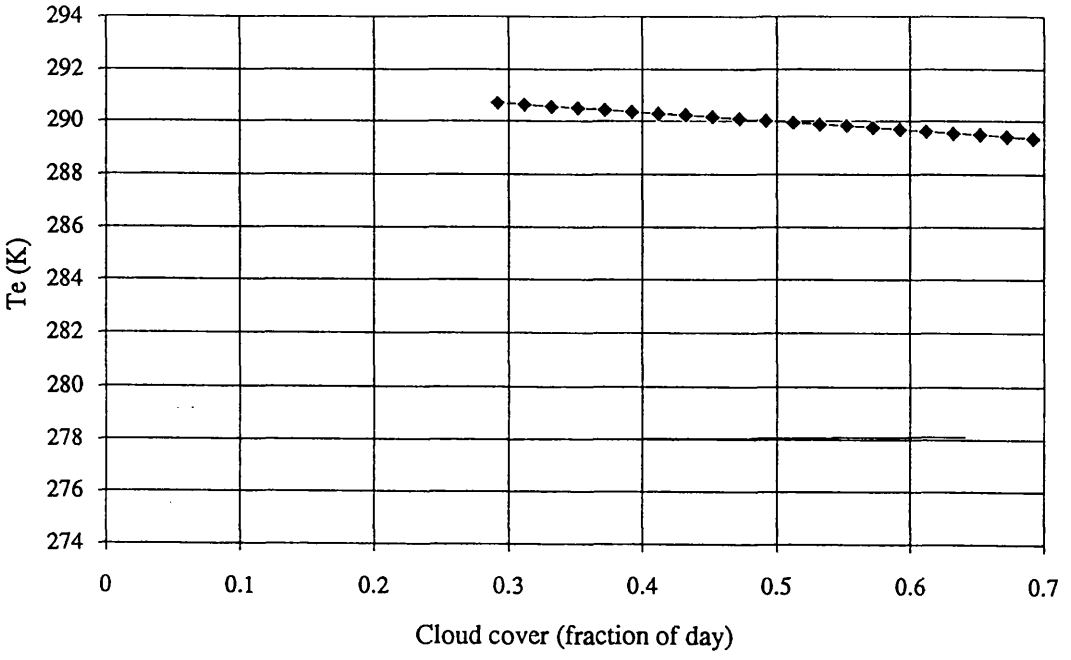

c)

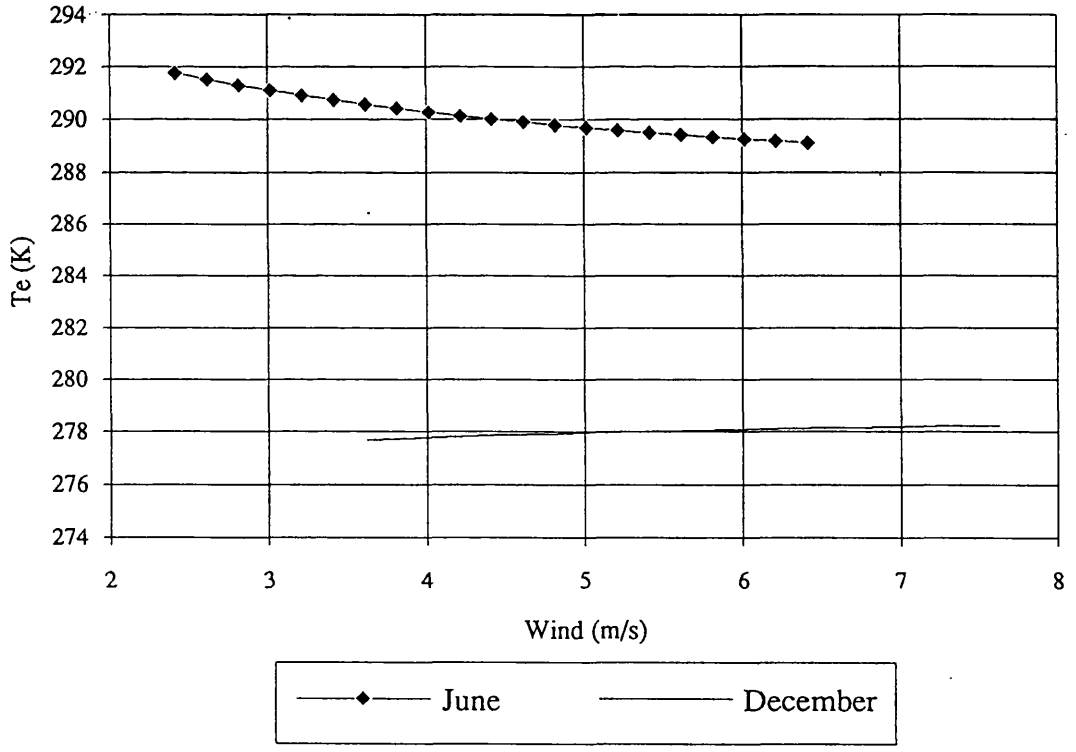

d)

Figure 5.13a)-d) Modelled response of Te to changes in meteorology, for a) air temperature, b) relative humidity, c) cloud cover, d) wind speed. Only effects for June and December are plotted for clarity.

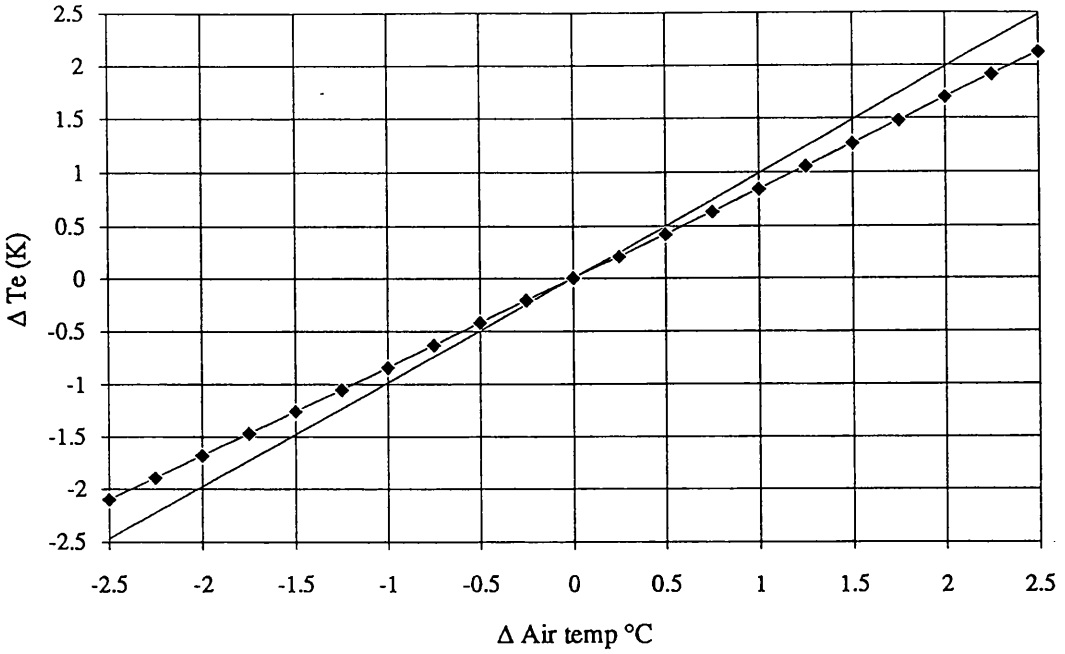
2.5
2
1.5
1
0.5
0
-0.5
-1
-1.5
-2
-2.5
Δ Te (K)
-2.5 -2 -1.5 -1 -0.5 0 0.5 1 1.5 2 2.5
Δ Air temp °C

a)

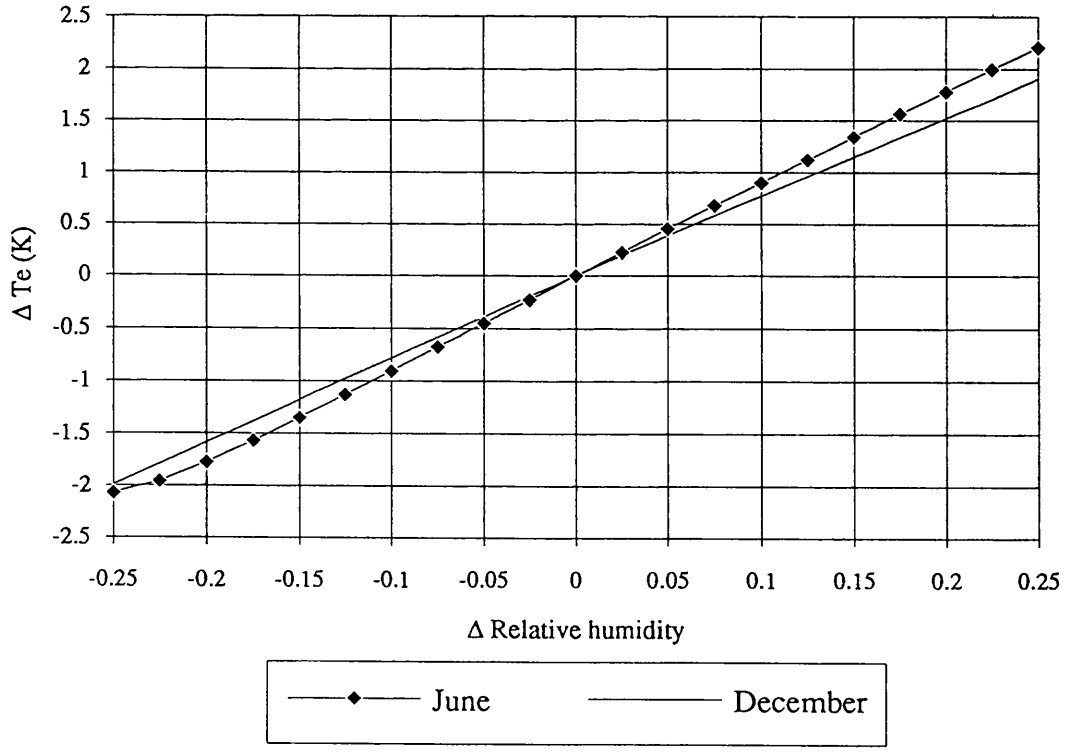
2.5
2
1.5
1
0.5
0
-0.5
-1
-1.5
-2
-2.5
Δ Te (K)
-0.25 -0.2 -0.15 -0.1 -0.05 0 0.05 0.1 0.15 0.2 0.25
Δ Relative humidity
June
December

b)

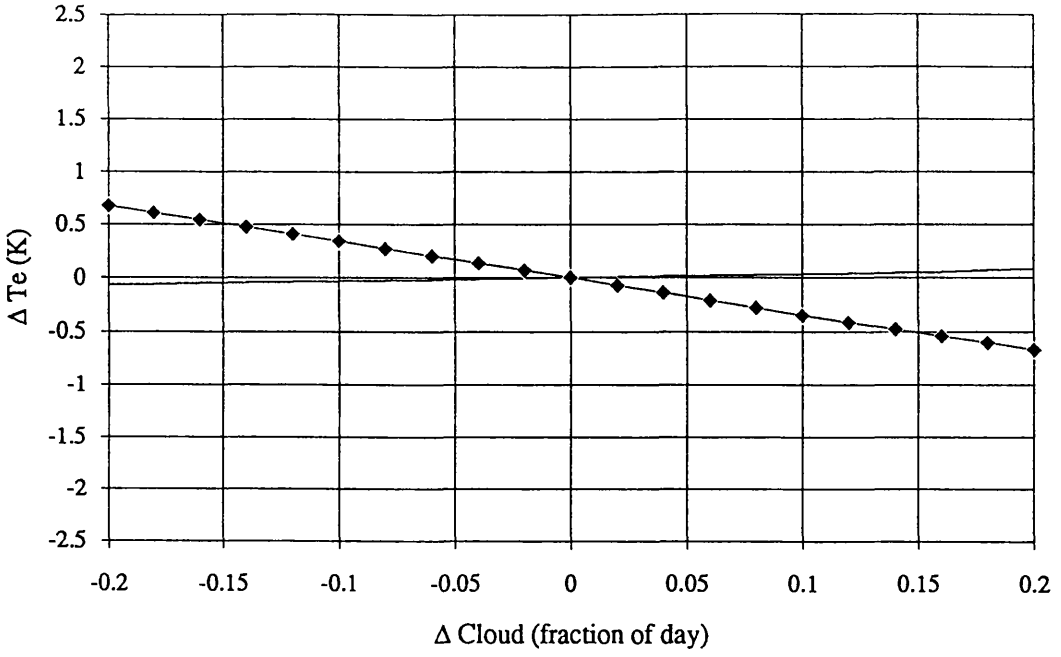

c)

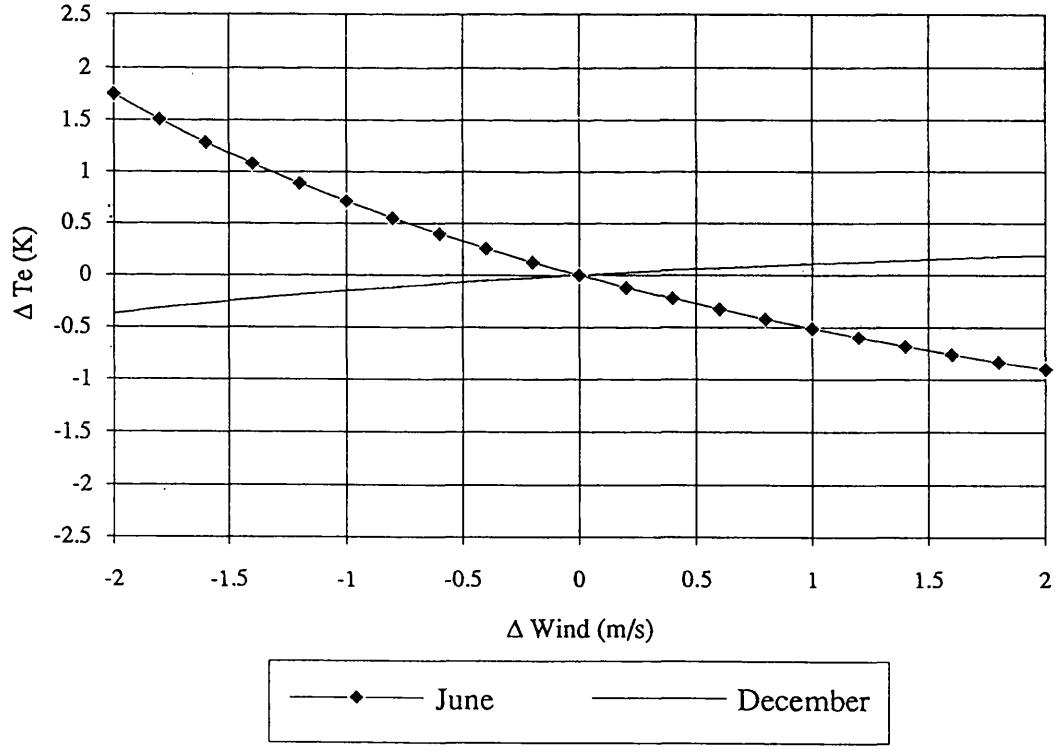

d)

Figure 5.14a)-d) Differences in Te plotted against differences in meteorology for a) air temperature, b) relative humidity, c) cloud cover, d) wind speed. Only effects for June and December are plotted for clarity.

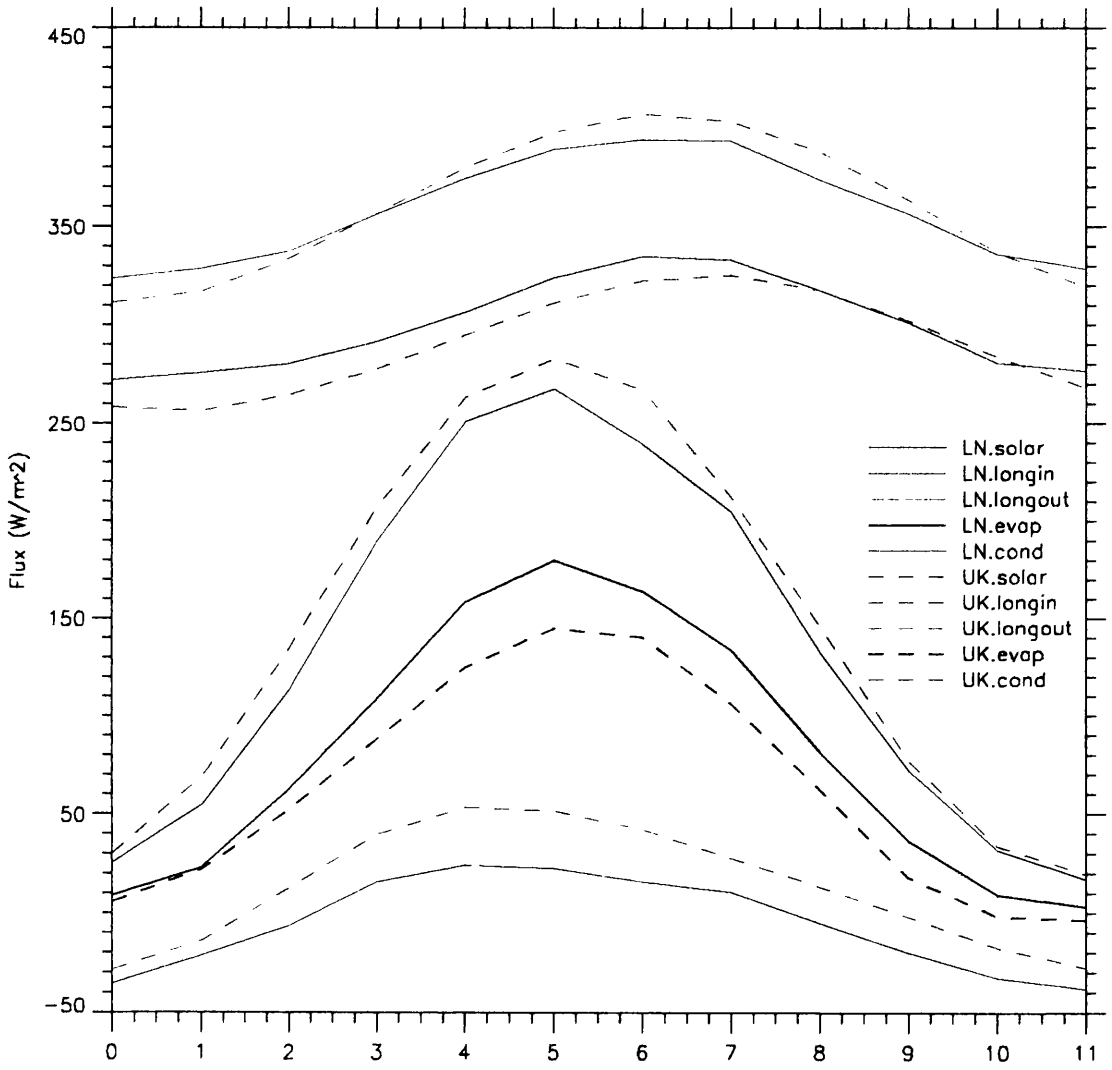

Figure 5.15 Heat exchange fluxes calculated at the temperature Te for each month and for the LN and UK meteorologies.

humidity but little effect from the cloud or wind. These calculations assume each parameter is independent and does not take into account the effect that changing one parameter will have on the effect of another.

5.5.2 The effect of climate on K and the time constant of a lake

The HS model was used to investigate the dependence of K on meteorology in a similar way as for T_e. K was calculated for the temperature, T_e, by a modified HS model for June and December while varying one of the meteorological parameters. As each new value of a parameter establishes a different T_e, a new T_e needed to be calculated every time the meteorology was changed. This was done for each of the meteorological parameters in turn. The results of this simulation are displayed in Figs. 5.16a)-d) with difference plots Figs. 5.17a) - d). One can see that for most cases a change in the meteorology causes little change in K and therefore one would expect a similar small effect on the time constant. The exceptions to this are the humidity in June and the wind speed. The main meteorological parameter affecting the heat exchange coefficient is the wind speed, with a ±1m/s change causing approximately ±10 W/m^2K. The effect of changing humidity becomes non-linear in June when the relative humidity falls by twenty percent of it current value. The conclusions which can be drawn from these results is that unless there are large changes in the wind speed or a large decrease in the humidity then K will not change sufficiently to significantly change the time constants of lakes since at least 20 W/m^2K was found to be needed to change the time constant by one day (see Fig. 5.10). However to determine exactly what the change in the heat exchange coefficient will produce one needs to combine all the expected changes in the meteorology which can only be done with GCM modelled data.

A future change in the wind and air temperature climatology will also produce a change in the thermocline depth and so change the mixed layer and therefore the time constant of this layer. This could result in an error when attempting to determine the change in T_e. This could potentially be minimised by using the appropriate weather forecasts, during the monitoring, to estimate the wind field and hence to model the expected thermocline depth more accurately. The effect of inaccurate thermocline depth on the determination of T_e needs further investigation but is beyond the scope of this thesis.

5.7 Chapter summary

In this chapter we have looked at the physical basis of how lakes respond to the annual weather cycle and from this how lakes can be used in the proxy monitoring of climate. This started with a critical investigation into published studies of how lakes temperatures

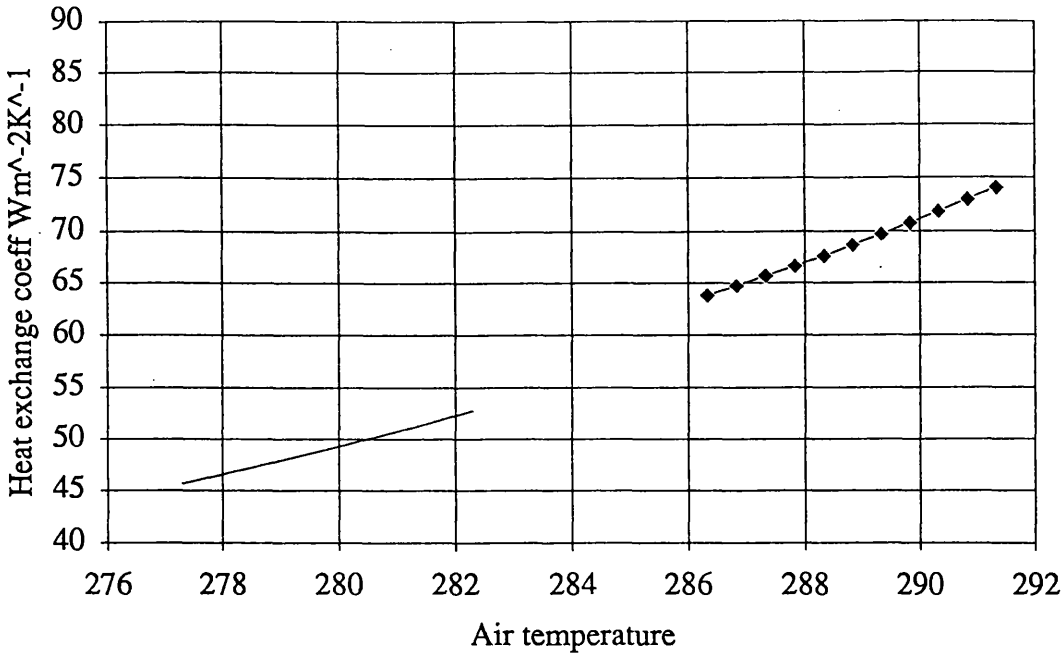
Heat exchange coeff Wm^-2K^-1
90
85
80
75
70
65
60
55
50
45
40
276
278
280
282
284
286
288
290
292
Air temperature

a)

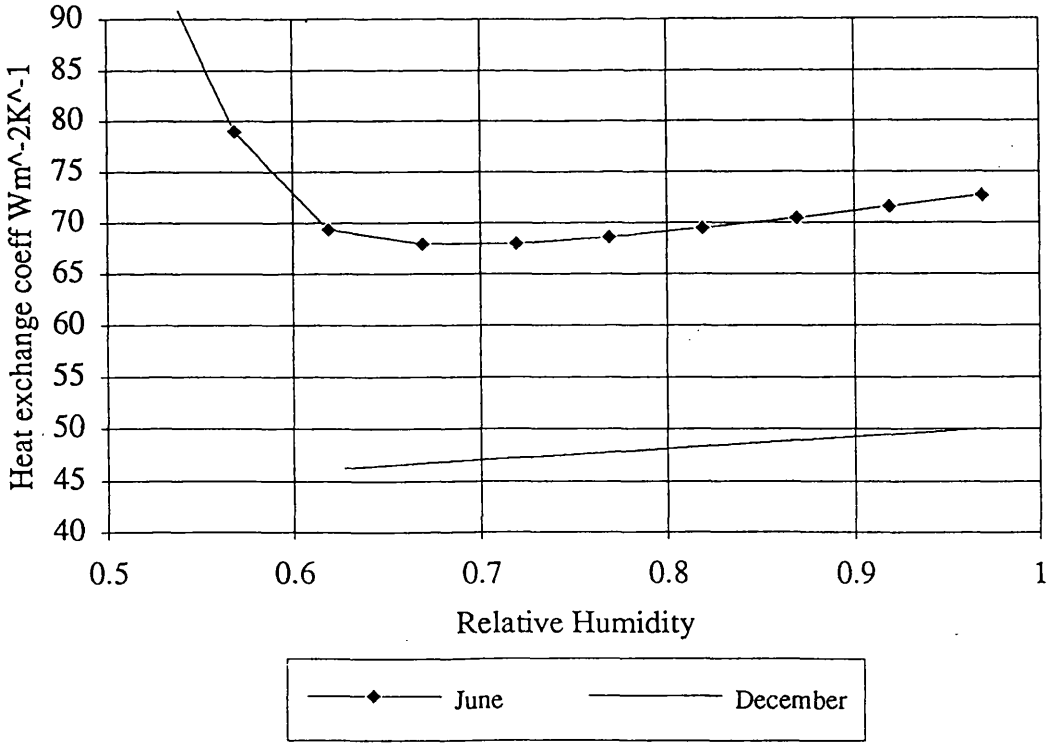
Heat exchange coeff Wm^-2K^-1
90
85
80
75
70
65
60
55
50
45
40
0.5
0.6
0.7
0.8
0.9
1
Relative Humidity
June
December

b)

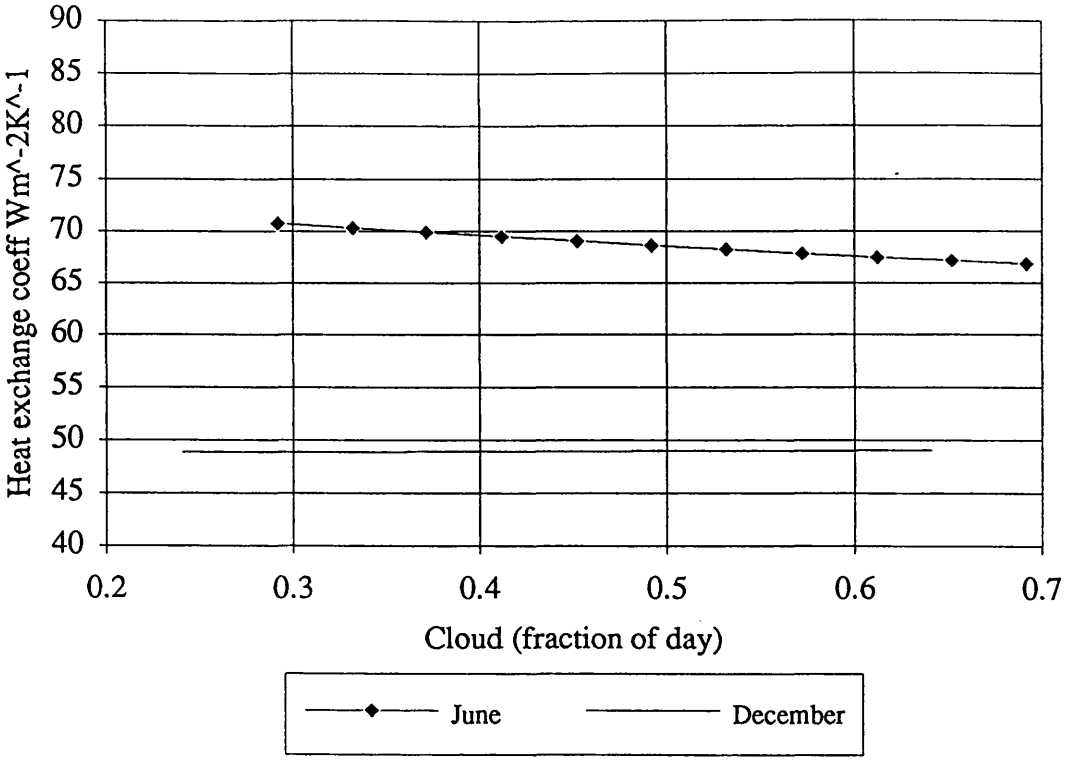

c)

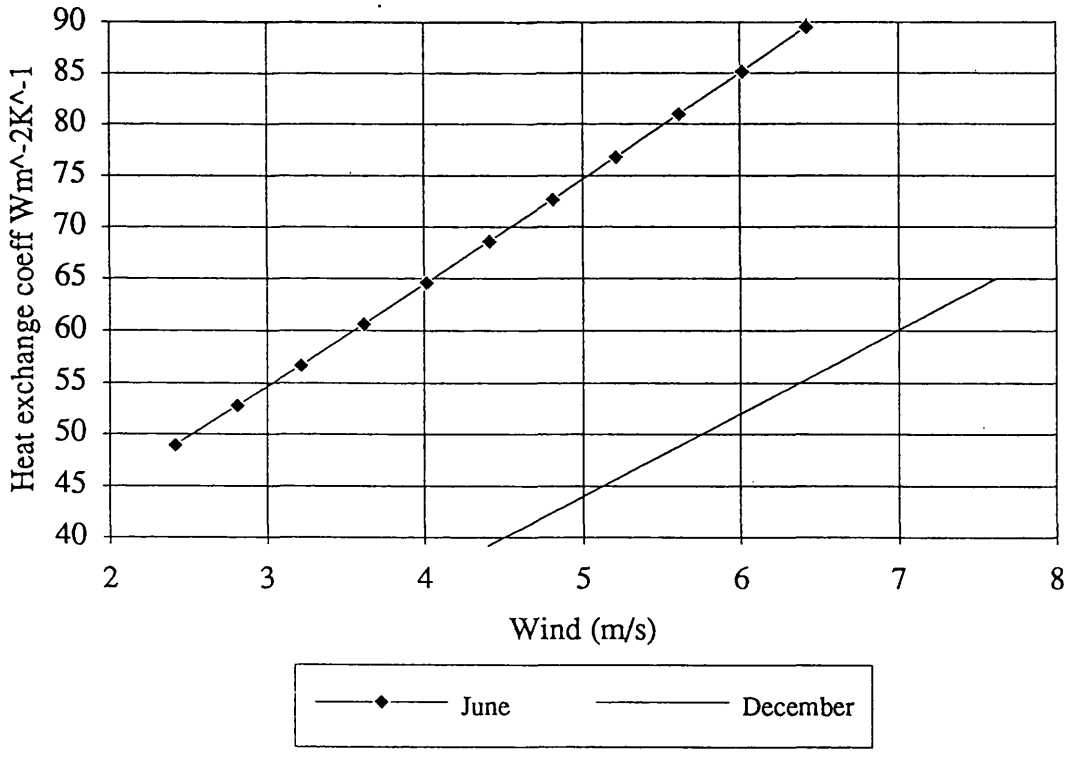

d)

Figure 5.16a)-d) Modelled response of K to changes in meteorology, for a) air temperature, b) relative humidity, c) cloud cover, d) wind speed. Only effects for June and December are plotted for clarity.

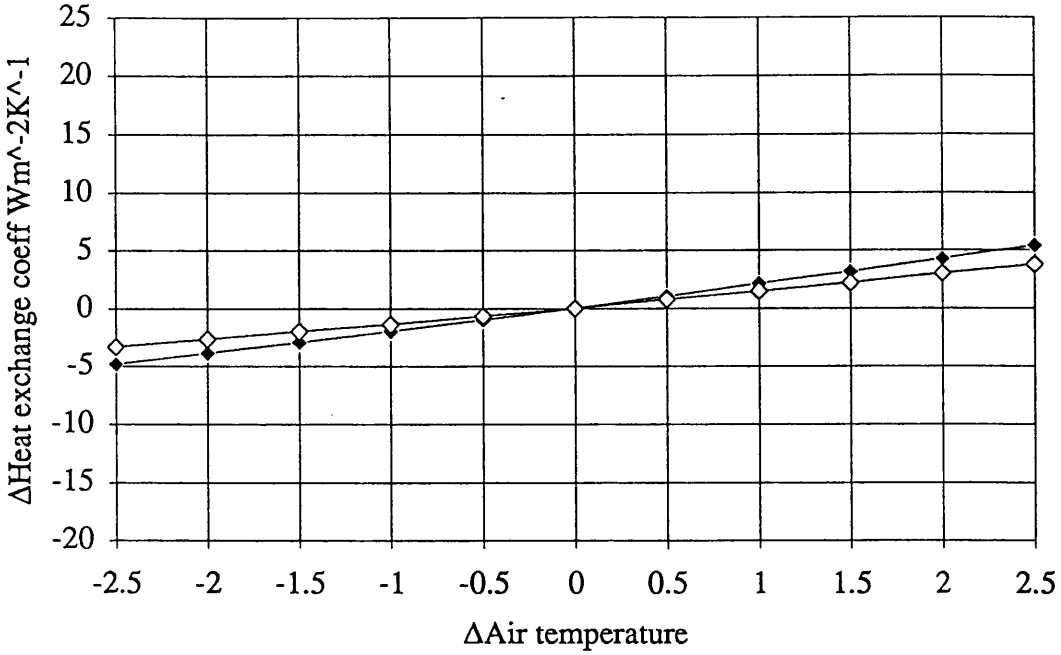
ΔHeat exchange coeff Wm^-2K^-1
25
20
15
10
5
0
-5
-10
-15
-20
-2.5
-2
-1.5
-1
-0.5
0
0.5
1
1.5
2
2.5
ΔAir temperature

a)

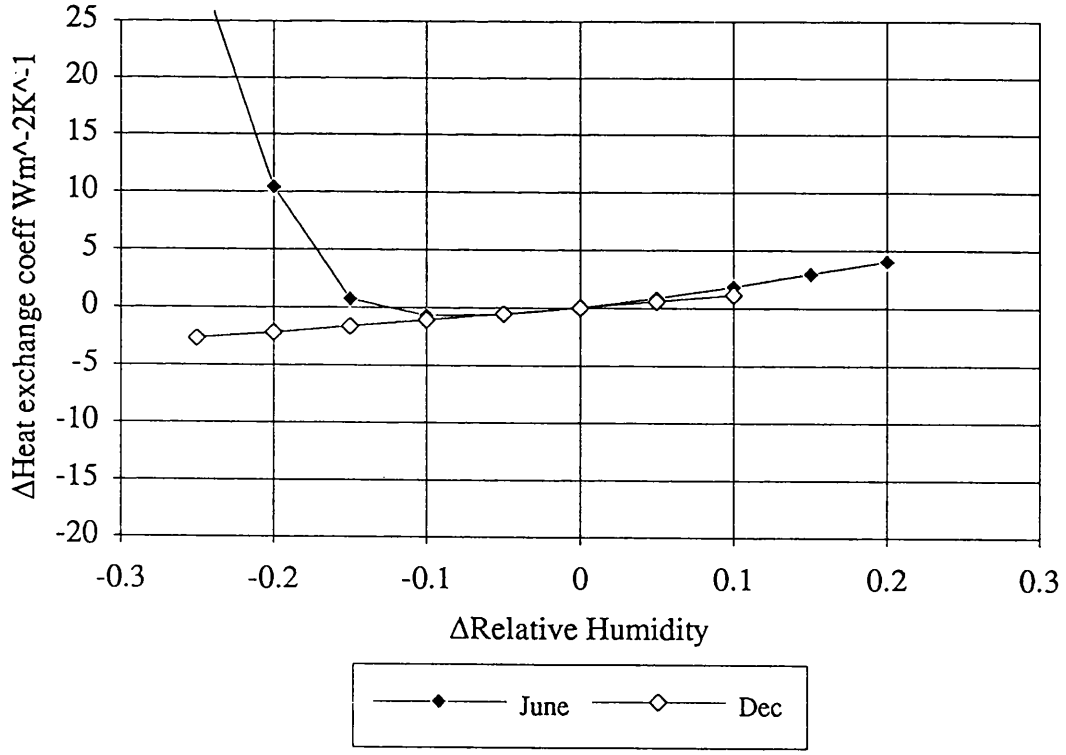
ΔHeat exchange coeff Wm^-2K^-1
25
20
15
10
5
0
-5
-10
-15
-20
-0.3
-0.2
-0.1
0
0.1
0.2
0.3
ΔRelative Humidity
June
Dec

b)

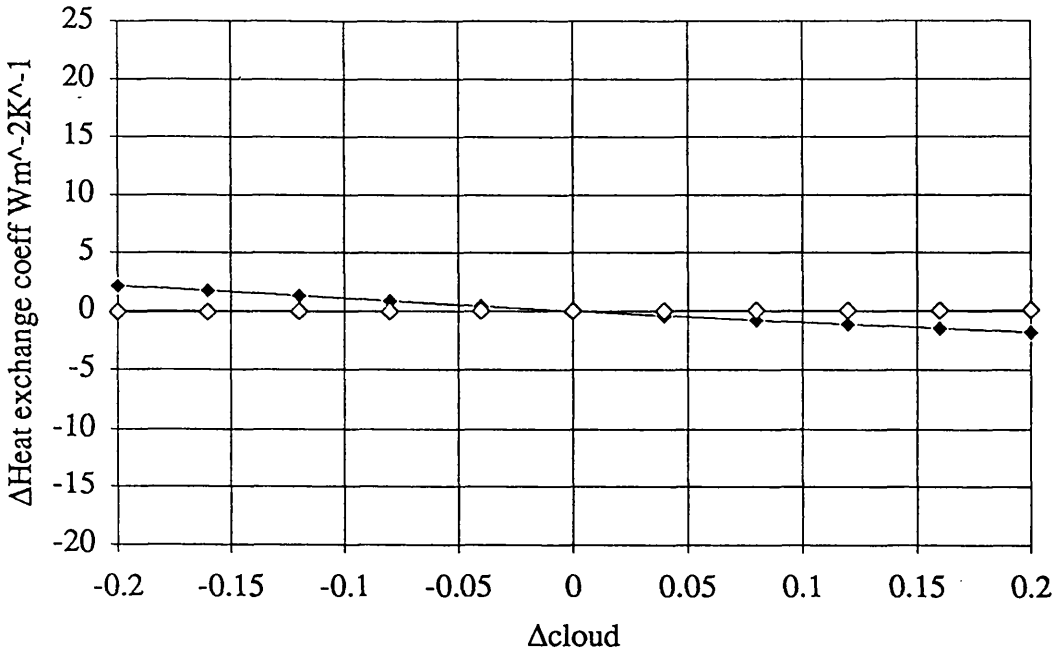

c)

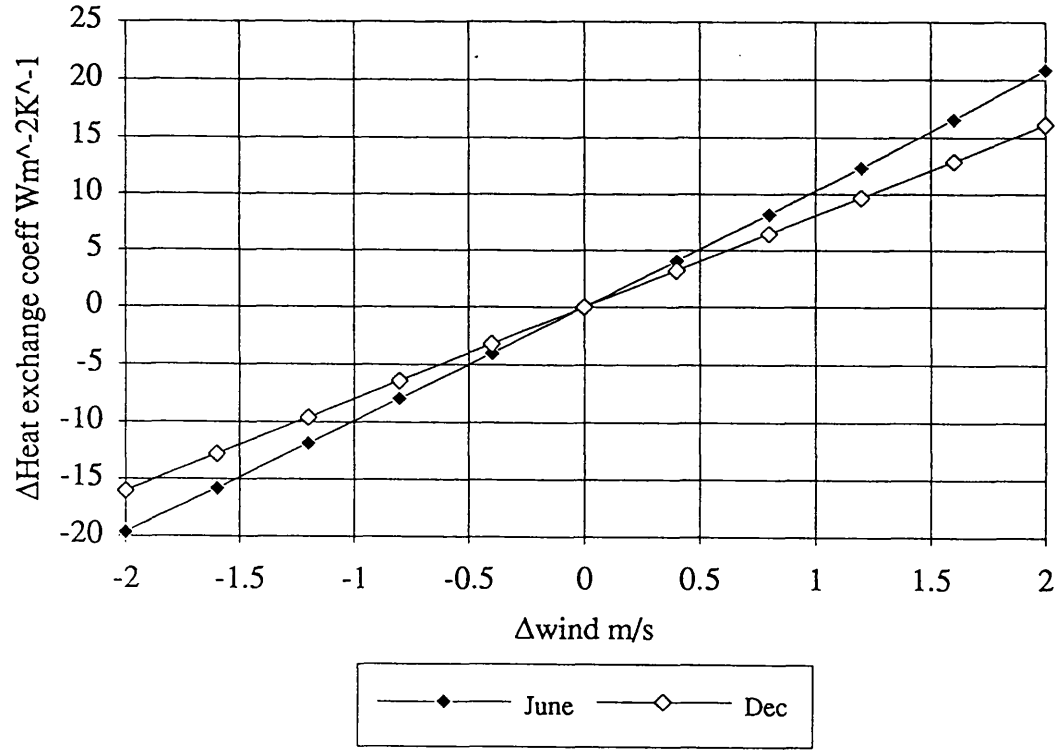

d)

Figure 5.17a)-d) Differences in K plotted against differences in meteorology for a) air temperature, b) relative humidity, c) cloud cover, d) wind speed. Only effects for June and December are plotted for clarity.

are related to climate. It was found that the model proposed by Sraskraba (1980) based on the correlation of lake sinusoidal annual temperature to a similar sinusoid of the solar insolation, is too restrictive when trying to establish what change in water temperature might occur due to climate change. The findings of George (1989) and their implications, where periodicities were found in lake temperature records which were not found in air temperature records, were discussed in detail. Possible reasons for these results were discussed and in particular how lakes can behave as low pass filters to the meteorological forcing of their temperatures. The possibility of lakes responding to meteorology other than air temperatures was also discussed. From these ideas (the HS model and the equation describing lake thermal behaviour proposed by Edinger et al. (1968)) the filtering characteristics of lakes were investigated, together with the effect and influence of the individual meteorological parameters, air temperature, wind, relative humidity and cloud. From this study, the equilibrium temperature T_e was proposed as the geophysical variable suitable as a proxy climate indicator. The equilibrium temperature has the characteristic that it is sensitive to all the meteorological parameters mentioned and so is a combined measure of the climate experienced by the lake. Although this in some ways an advantage it does render it a complex climate variable which does not lend itself to easy interpretation. Due to the unavailability of predicted meteorology from GCM's it was decided to qualitatively consider the combined effect of each of the meteorological parameters on T_e for two scenarios, the first was an increased frequency of winter low pressure systems and the second an increase in the frequency of summer high pressure systems. In both these scenarios it was suggested that there would be an increase in the equilibrium temperature. The chapter ends with an investigation into how climatic change might alter the filtering characteristics of a lake and it was suggested the effect of changing the heat exchange coefficient would be small and that the greatest effect on the time constant might arise from changing the mixed layer depth.

Chapter 6.

Retrieval of lake surface temperature from Satellites: - A validation field campaign.

6.1 Introduction

In the previous chapters a case has been made that lake surface temperature records have the potential to detect and monitor regional and global climatic change. The results of modelling Lough Neagh temperatures has indicated that the June surface temperature would change by ~1.0° for a 1.2° change in air temperature. It would have been instructive to try and model the water temperature change from a predicted climate, incorporating an increased level of CO_2, but as stated earlier this has not been possible due to delays in the distribution of data from the Hadley Centre. The following two chapters are concerned with the problems associated with the remote sensing of the surface temperature of lakes. The question addressed by this chapter is, to what accuracy can one measure lake temperature? From this one can get an indication of the air temperature change that might be able to be detected through the lake temperature. The next chapter looks at the feasibility of monitoring a lake's surface temperature through an annual cycle. The two studies also take place in different climatic regions, the first is in Malawi and consequently is a tropical/continental climate whereas the second is in Northern Ireland and therefore is a temperate/maritime climate.

This chapter reports the findings of a field campaign which was designed to indicate the level of accuracy possible for retrieving lake surface temperatures with satellite radiometers. As this study is only for one particular lake the application of the results to lakes in other regions would need to be made with caution. However, as this is in a tropical region, one could argue that this is probably the most difficult atmospheric correction situation as has been found for tropical sea surface temperature retrievals (Llewellyn-Jones et al. 1984), and therefore this could be considered a "worst case" scenario. The instrument used in this study is AVHRR/2 flown on the NOAA TIROS-N polar orbiting platforms. The campaign was incorporated into a current programme run by the Overseas Development Administration (ODA) and the Natural Resources Institute (NRi), who are supporting the UK/Southern African Development Community (UK/SADC) Pelagic Fish Resource Assessment Project on Lake Malawi. The field

campaign took place during a routine fish sampling cruise of the UK/SADC research vessel, the Usipa, from 10.11.92 - 20.11.92.

The field campaign consisted of two experiments which ran concurrently. The first was the measurement, at the surface, of the temperature of the emitting surface, i.e. the skin temperature, at the time of a satellite overflight. During these overflights the atmospheric profiles of temperature and water content were measured. This experiment was designed to allow the validation of the atmospheric correction and hence the surface temperature retrieved by the satellite. The second experiment was to monitor the skin-bulk temperature difference, or the skin effect, and was carried out during the time not used by the first experiment. It was hoped that the continuous monitoring at all times of day and under the extremes in conditions encountered during the cruise would characterise the skin effect so as to allow an estimate of the skin effect sufficient to enable the conversion of the satellite derived skin temperature to bulk temperature with a reasonable estimate of the uncertainty, if only for similar conditions and season.

6.2 The Validation Dataset

6.2.1 Satellite data

The AVHRR images of Lake Malawi were collected by a local receiving station developed by Bradford University installed at Senga bay by NRi. This system has been developed as a low cost, low maintenance system which uses a manually steered horn and is built around an IBM type PC. Chris Sear of NRi operated the receiving station during the cruise. Twelve images were collected during the cruise and five were found to have cloud free pixels near to where the Usipa was at the time of the pass, of which three were night time images.

6.2.2 In Situ data

In situ radiometric temperatures were taken with a two channel radiometer developed by CSIRO Australia as described in chapter 2. The channels are situated at the same frequencies as for AVHRR, that is to say 11 and 12μm. The internal calibration targets are used in a similar way to the calibration of AVHRR except the cold target temperature is at the ambient temperature of the instrument and not absolute zero of space. The hot calibration target is heated to ~10° above the cold target. The radiometer was run in two modes, the first for satellite overflights, the second for monitoring the skin effect. For the satellite overflight mode a calibration run was implemented manually, where each calibration target was viewed in turn, approximately 20 minutes before and after the overhead time. The radiometer and other instruments were sampled every 3 seconds. For the second mode, when monitoring the skin effect, the instruments were sampled every

20 seconds. This second mode used an automatic calibration cycle, which was a feature of the instrument, where the calibration targets were cycled into the field of view for 90 seconds in turn, inter-spaced with 90 seconds of external view, i.e. cold cal - view - hot cal - view - cold cal etc.

A further calibration was performed for each mode with a stirred bucket as described in chapter 2. This occurred 15 minutes before and after a satellite overpass in the case of the first mode and as regularly as possible for the other mode. This turned out to be approximately every two hours during the day with maximum intervals during the night of about eight hours. The temperature of the water in the bucket was monitored by a platinum resistance thermometer (PRT) with specially designed support electronics which allow temperatures to be measured to ±0.02°C under all realistic temperature regimes for the electronics and the connecting cable. The water intake for the pump which supplied water to the bucket was located as close to the lake surface as possible so as to make the calibration point temperature as near as possible to the target temperature. This was to reduce errors caused by any uncertainty in the slope of the calibration curve derived from the internal calibration targets and non-linearity in the detector response when extrapolating between the bucket temperature and the target temperature.

The correction to be applied to the radiance (as described in chapter 2) was taken as the mean of the difference in radiance between the calculated bucket radiance (from the bucket PRT) and the measured radiance for the two bucket calibration points either side of the overpass. The measured radiance is the radiance derived using the internal calibration targets. The resultant error in the corrected radiance (σ) with respect to the true radiance was calculated as the standard deviation of the residuals between the calculated radiance of the bucket (from the bucket PRT) and the corrected radiance measured with the radiometer, the equations for which are:

$$I_{corrected\_radiometer} = I_{radiometer} + I_{correction}$$

where

$$I_{correction} = \left(\overline{\left(I_{bucket} - I_{radiometer}\right)}_{prepass} + \overline{\left(I_{bucket} - I_{radiometer}\right)}_{postpass} \right) / 2$$

$$\sigma^2 = \sum_{i=1}^{n} \left(I_{bucket} - \left(I_{radiometer} + I_{correction} \right) \right)_i^2 / (n-1)$$

n is the number of points in the calibration
$I_{radiometer}$ is the radiance derived by the radiometer using internal calibration
I_{bucket} is the radiance derived from the bucket PRT

For all passes σ was found to be less than 0.1°C when converted to an effective temperature error.

The water temperature of the lake (other than the radiometric temperature) was measured in two ways. The first was by a mercury thermometer which had been integrated into a sampling device which consisted of a 4" diameter plastic tube with drainage holes to allow water into the tube but also to retain the correct amount of water to immerse the thermometer up to the desired level. This device could be lowered over the side to sample the top 5 cm of the water surface. The sampling was generally performed over the side of the vessel but before the water had been disturbed by the wake. From a cross calibration between the mercury thermometer and the PRT in the stirred bucket it was found that the mercury thermometer was reading 0.36° C high. To confirm this to be true and not due to a change in the calibration coefficients of the PRT the two thermometers were put into a bucket of melting ice which confirmed the mercury thermometer to be in error. This was also confirmed after the cruise against a certified reversing thermometer. The mercury thermometer had a precision of 0.05°C although this was often difficult to read especially if there was any swell. So, taking the detected error as being a constant bias then a reasonable estimate of the accuracy of the mercury thermometer based readings is 0.1°C.

The second method of measuring the water temperature was via the PRT in the stirred bucket and the water which was pumped from the surface. This allowed constant monitoring of the water temperature with no operator intervention. There were however several problems with this method, the first being that due to the physical set-up of the vessel the only place for the intake hose was in water which had been disturbed by the wake. It was therefore possible that the water taken in by the hose contained water mixed up from deeper layers which may be at a different temperature. To assess this possibility water temperatures measured with the mercury thermometer previously discussed, were taken from the opening of the hose and that further forward in undisturbed water. The difference in temperature for these two points, on a relatively calm day where this problem would potentially be greatest, was less than 0.1°C.

A further problem was the potential for heating of the water between the hose intake and the PRT. This could come from two sources, the heat generated from the pump and the heating of the hose between inlet to pump and pump to PRT. This second source obviously is greatest during the day when there is strong sunlight. To ascertain the magnitude of this heating the difference between the side sampled and the PRT sampled temperature was calculated and is shown in Fig. 6.1a) against date and 6.1b) against time of day. The sampling is not particularly biased to any particular time of day but rather randomly distributed. It is seen from Fig. 6.1a) that there can be large changes in the differences between the two temperatures in very short periods of time. It is difficult to find a satisfactory physical explanation of a mechanism for such a rapid change in the heating particularly for the night time cases, since the power of the pump is constant and the deck only heats up and cools slowly. If these changes do correspond to real heating changes then the sparsity of the temperature comparisons will not allow accurate removal of these biases. If, however, the short term fluctuations are due to some random sampling errors then the PRT temperatures can be corrected by a constant bias equal to the mean difference between the side and the bucket temperatures. From Fig. 6.1b) we can see that there is no pronounced diurnal effect with the second largest heating period occurring at 23:00. Note that there were no readings during the 4/10th period of the day. The lack of a diurnal variation is consistent with the hypothesis that the majority of the heating is coming from the pump. Therefore taking the heating to be constant the mean temperature difference between the side and the bucket measured temperature was found to be 0.34°C with a standard deviation of 0.1°C which is of similar magnitude of the uncertainty in the skin temperature derivation.

The meteorological parameters measured were air temperature humidity and wind. Due to the short time available to set up equipment before sailing, ideal positions for the meteorological instruments could not be found. The anemometer was situated at ~5.5m above the surface but could potentially have suffered funnelling or shielding effects due to the vessel's superstructure. Similarly it was not possible to position the air temperature/ relative humidity detector sufficiently away from the vessel to ensure that there was no heating of the air by the boat which had been heated by the sun, although this would only have a large effect during still sunny periods. Due to the vessel's design of having the engine exhaust at the back at water level no influence of the air temperature reading was taken to occur from the engine exhausts.

In addition to these regularly measured meteorological parameters, eight balloon radiosondes were launched to coincide with satellite overflights. These were launched ~15 minutes before the overhead time and generally reached ~50 mb within 1.5 hours.

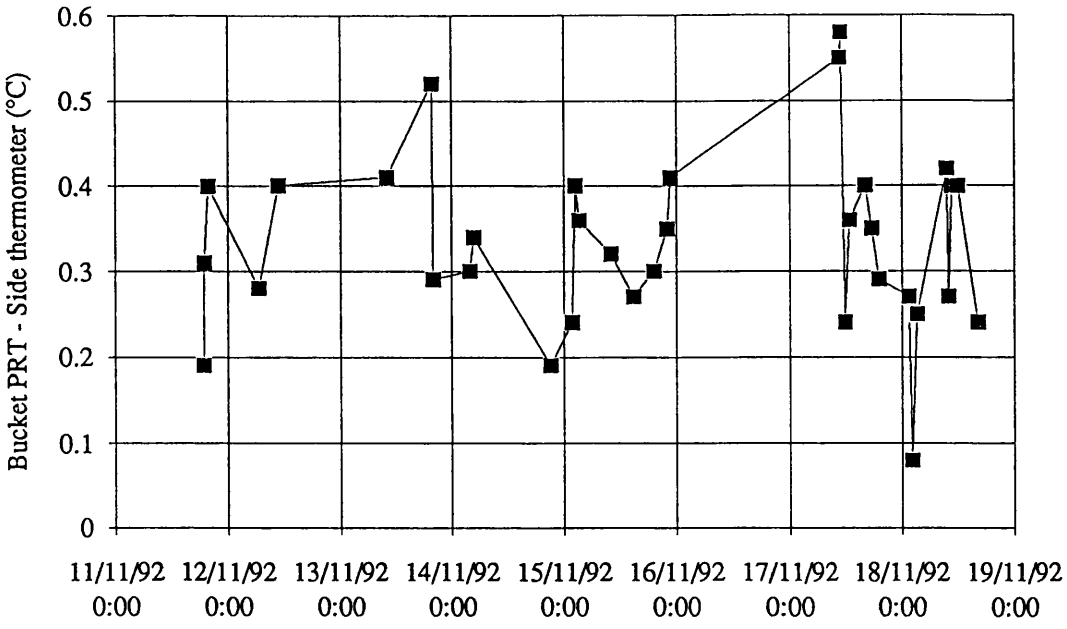

a)

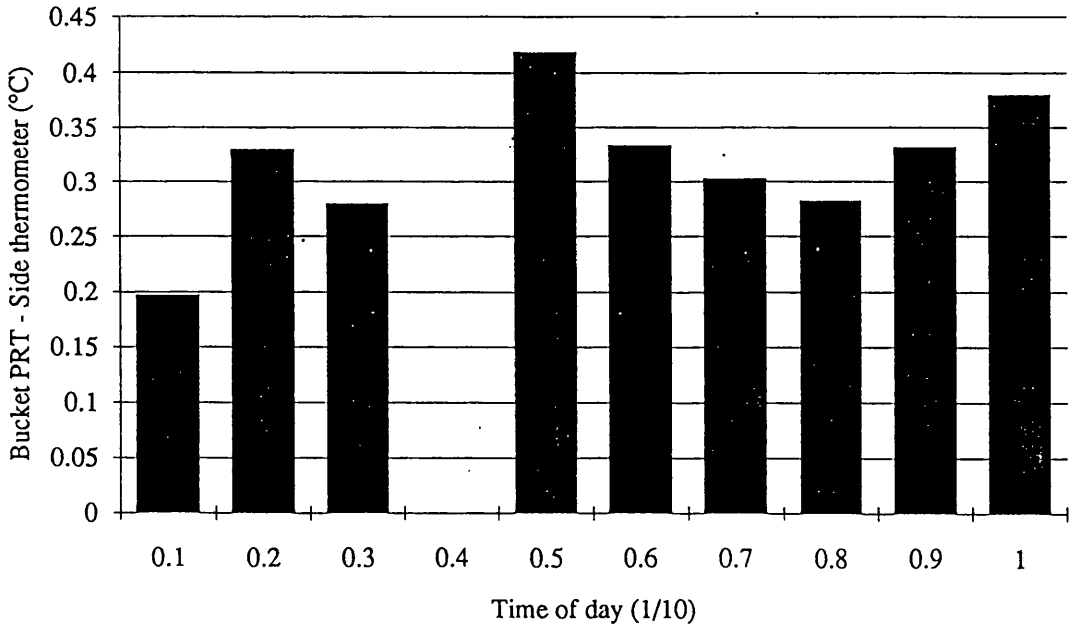

b)

Figure 6.1a) Temperature difference between the bucket PRT and the mercury thermometer temperature of water sampled over the side, for all samples throughout the cruise.

Figure 6.1b) Mean temperature difference between bucket PRT and side thermometer for every 1/10 day, indicating that the difference is not primarily due to solar/deck heating of the water during the passage from the intake to the bucket.

Some problems were encountered with reception of the sonde. This could have been due to antenna shadowing caused by the vessel's masts and rigging, the radiosonde battery overheating or atmospheric effects.

6.3 Analysis

6.3.1 Radiosonde

The radiosonde data was used in a line-by-line atmospheric transmission program specifically designed for thermal atmospheric correction of satellite images, developed by Albin Zavody at the Rutherford-Appelton Laboratory as described in chapter 2. The program has been modified at MSSL, substituting the emissivity of fresh water instead of that for sea water from Masuda et al. (1988). The model calculates the radiance and hence brightness temperatures at various wavelengths which would be detected by the satellite for a given atmospheric profile of water vapour and temperature, and surface temperature. These brightness temperatures are then regressed against the corresponding surface temperature that was used by the model to generate the atmospheric correction coefficients as discussed in chapter 2. Since the in situ measurements were not made at the sub-satellite point, brightness temperatures are calculated for various angles of incidence, and hence atmospheric path length across the swath. Coefficients were derived for the triple window (channels 3.7,11 & 12 μm) and split-window (channels 11 & 12 μm) method for each of the incidence angles. Errors in the regression were also calculated and incorporated with the NEΔT for each channel and the corresponding coefficient to determine the theoretical uncertainty for a single pixel retrieval.

Considerable pre-processing of the radiosondes was required before they could be used in the transmission program due to the reception problems discussed earlier which caused erroneous values. A considerable number of these corrupted values were stripped out with a simple program eliminating jumps above a specified threshold. However, final data checking needed to be carried out manually.

6.3.2 Image analysis

The images were stored in a format particular to the Bradford system consisting of the raw telemetry from the satellite but excluding 256 pixels from either edge of the image. The images were calibrated as described in chapter 2 and incorporated non-linear corrections following Steyn-Ross and Steyn-Ross (1992). The images were then resampled along the scan lines so that the panoramic effect of the scanning geometry of AVHRR was removed and so that the pixels are always 1km wide along the scan. Resampling of this nature is considered to be beneficial because it allows simple bi-linear warping of a map image to the AVHRR image without the need for large numbers of tie

points. This resampling is not considered to particularly degrade the signal since the instrument itself is continually integrating along the scan line and is sampled at a fixed time interval. Resampling across scan lines would not be considered acceptable because this is considerably different from the way that the detector samples. It is for the same reason that for the purposes of geolocation a map is warped to the image and not the image to the map. Positions of the Usipa, at the time of overflight, were indicated on the map image and it was therefore a simple procedure to extract the pixel values to an accuracy of ± 1 pixel when there were enough clear features to select as tie points. The retrieved temperature was produced by interpolating, with respect to air mass, between retrieved temperatures derived for air masses either side of the required air mass. Errors were calculated from the noise associated with each brightness temperature, the corresponding coefficient and the error in the atmospheric regression model, e.g. for the split window:

$$\sigma_T^2 = \sigma_{regression}^2 + a_1.\sigma_{T4}^2 + a_2.\sigma_{T5}^2$$

Cloud screening was initially by eye and then through the differences in the thermal pixel values. If the differences in these pixel values was greater than 0.25°C above the maximum predicted for clear sky from the radiosonde measurements with the atmospheric transmission model, then the pixels were considered cloudy, similar to a test described by Saunders and Kriebel (1988). Finally, if the image was during the night, and the difference between the retrieved temperatures from the 3.7, 11 & 12μm method and the 11 & 12μm method was larger than 2σ, it was deemed cloudy.

6.4 Results

The results from the atmospheric transmission calculation are summarised by Fig. 6.2a). This is a plot of the correction (T0-T11) needed to be applied to the 11μm brightness temperature against the difference in brightness temperature between the 11 and 12 μm channels (T11-T12), as described in chapter 2. The crosses are the results from a set of atmospheres assembled by NOAA to represent the range found in global ocean atmospheres and the straight line is a linear fit through them, representing a global split window algorithm of the form:

$$T0 - T11 = m(T11 - T12) + c$$

The circles are the results from the radiosondes sampled over Lake Malawi. It can be seen that the Lake Malawi atmospheres for a given correction have a larger T11-T12

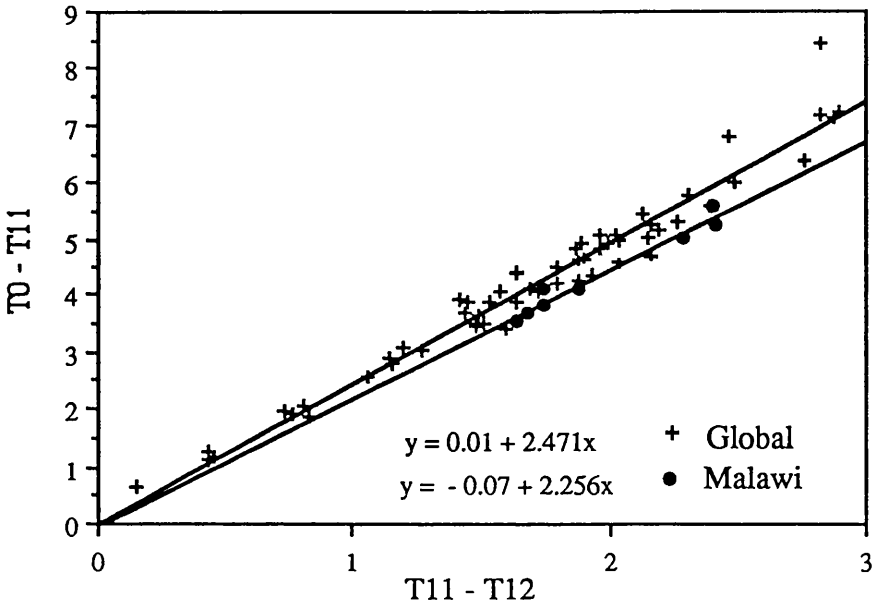

a)

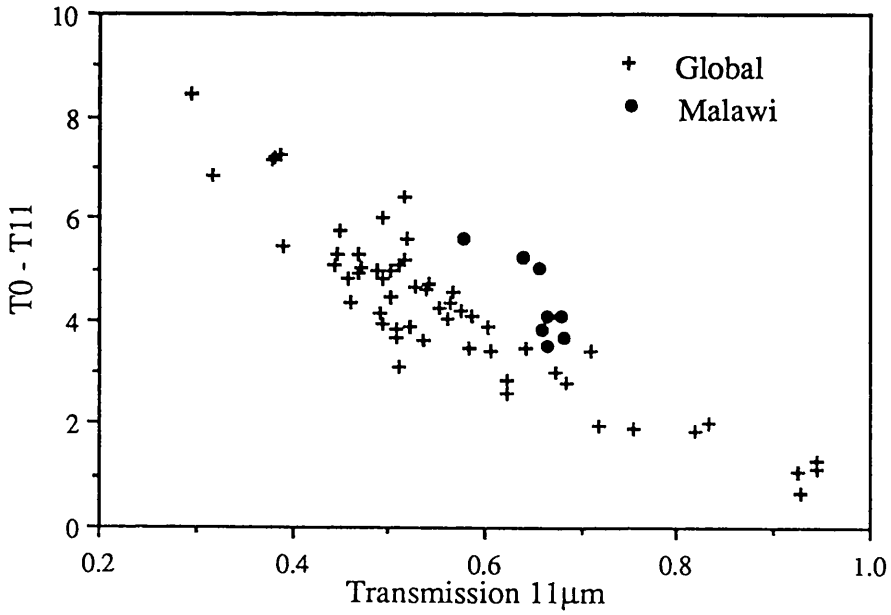

b)

Figure 6.2a) Modelled correction (T0-T11) vs. 11μm & 12μm brightness temperature difference for 56 global radiosondes and 8 radiosondes taken over Lake Malawi. The lines represent linear regression through the two datasets

b) Modelled correction (T0-T11) vs. 11μm transmission showing that for a given transmission the Malawi atmospheres need greater correction and hence have water vapour biased to higher levels.

difference. To understand the reason for this difference it is instructive to look at a plot of transmittance against T0-T11, as in Fig. 6.2b). Since transmittance is principally determined by the quantity of water vapour in the atmosphere (assuming all other absorbers are well mixed and have constant concentrations for all atmospheres) one can deduce that atmospheres with the same transmittance have similar total water vapour content. The variation in T0-T11 for atmospheres with the same transmittance is therefore primarily due to the distribution of that water vapour through the air column and hence its temperature. For example, if an atmosphere had a high transmittance (i.e. low net amount of water vapour) but had a high correction we can infer that the water vapour is situated high up in the atmosphere. One can conclude this as there is the same amount of absorption but less emission from the water vapour compared to an atmosphere where the water vapour is lower down, and therefore the atmosphere with the water vapour higher up has a lower brightness temperature values.

To see if Lake Malawi atmospheres have their water vapour biased higher up than atmospheres found over the ocean, atmospheres were selected from the ocean data set which have the same transmittance as the Lake Malawi atmospheres for the maximum and minimum transmittance values sampled by the Malawi radiosondes. Fig. 6.3 & 6.4 are plots of the water content against pressure for these two extremes respectively. These figures clearly show that the Lake Malawi atmospheres have relatively less water in the lower regions than the higher regions compared to the ocean atmospheres. A possible explanation for this different water vapour distribution is that there is stronger convection over land than ocean. The land has a lower heat capacity than the ocean and thus will be hotter for a given amount of solar insolation and therefore has the potential for stronger convection. It should be noted that these radiosondes were taken at the end of the dry season and Malawi had been experiencing quite a severe drought and therefore there was little water to evaporate. In the middle or end of the wet season there will more water available and the radiometric properties of the atmosphere might be quite different. The effect of the lake should be considered as this is a source of water vapour. The lake is quite narrow (50 km at the widest point) and was during the cruise generally cooler than the land and therefore would inhibit convection. The sharp rise in water vapour content shown in Fig. 6.4 for the very surface layers is suggested to be due to evaporation from the lake.

Lake Malawi is situated at ~650m above sea level which corresponds to about 960 mb and so one would expect this to be a factor in the difference between the global and Malawi atmospheres. To investigate this one could extrapolate down to sea level for the Malawi radiosondes and perform the transmission modelling again but as can be seen

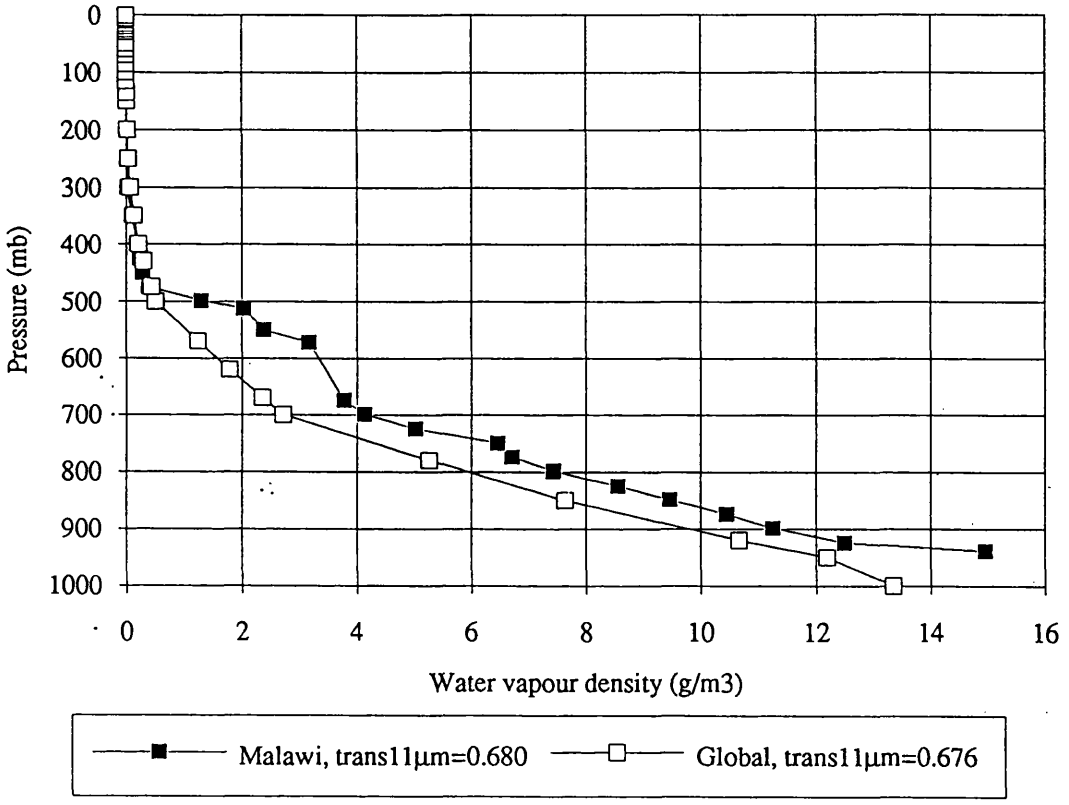

Figure 6.3 Atmospheric water vapour profile for an ocean atmosphere and an atmosphere sampled over Lake Malawi with the same transmission. The Malawi atmosphere has the largest transmission from those sampled.

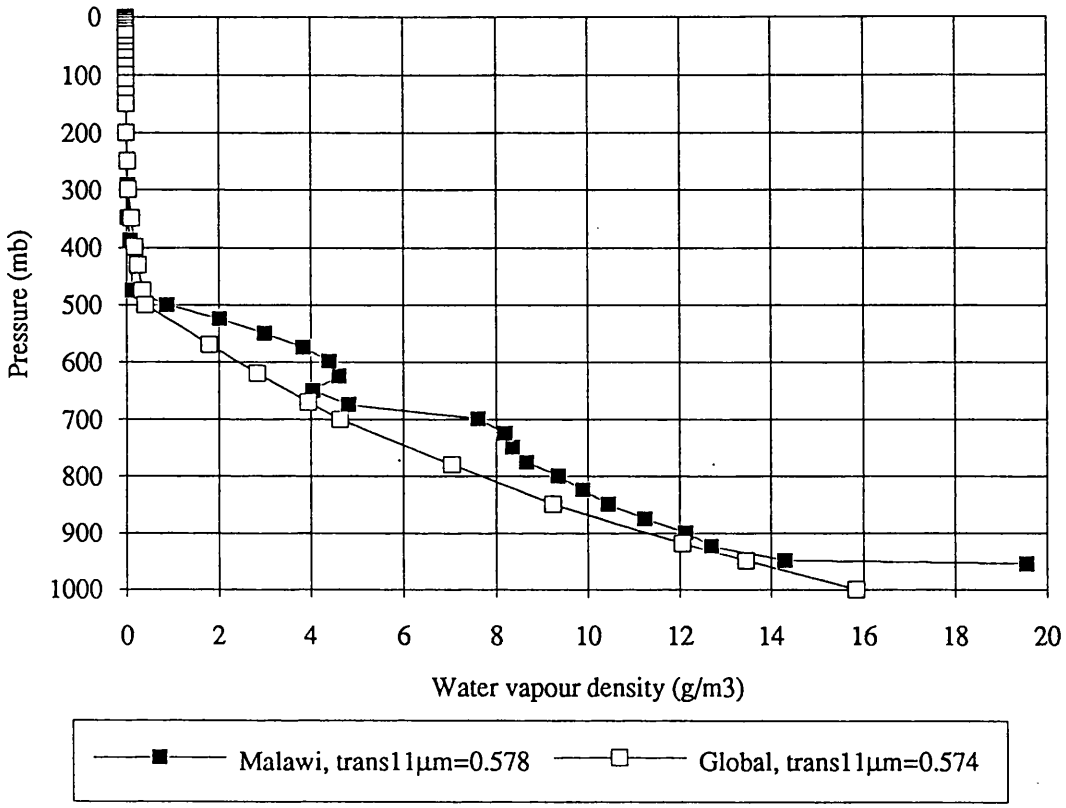

Figure 6.4 Atmospheric water vapour profile for an ocean atmosphere and an atmosphere sampled over Lake Malawi with the same transmission. The Malawi atmosphere has the smallest transmission from those sampled.

from Figs 6.3 and 6.4 the water vapour content increases rapidly towards the surface and extrapolation would produce impossibly high values. The other option is to remove the lower layers from the global radiosondes to the 960 mb level. This was the option chosen with the results of the transmission modelling in Figs 6.5 a) and b) which are the equivalent plots to Figs. 6.2 a) and b). From Fig. 6.5a) one can see that removing the bottom layer of the global radiosondes brings the regression line closer to the Malawi radiosondes but they are still significantly different. From Fig. 6.5b) we see that the Malawi atmospheres still have a high correction for a given transmittance. Together Figs 6.5 a) and b) indicate that the primary difference is due to the different distribution of water vapour in the atmospheric column with the "missing" lower layers being a second order effect.

As can be seen from Fig. 6.2a), although the Malawian atmospheres are different from the global atmospheres, they still show a linear trend. If the assumption is made that these are a representative sample and a linear regression is performed, correction coefficients can be derived for the satellite images of the lake. Obviously with so few points some uncertainty in the validity of the regression is unavoidable. The coefficients for NOAA9, 11 and 12 are given in Table 6.1. Coefficients have been calculated for the triple window and the split window and for 5 view angles corresponding to increments of 0.25 of an air mass starting at unit air mass. These coefficients are derived for the calculation of the "skin temperature", that is to say physical temperature of the emitting surface of the water. Fresh water emissivities have been taken into account.

The results of the comparison of the in situ measured skin temperatures and the satellite derived temperatures are summarised in Table 6.2. There are four images where there are both skin and bulk temperatures and a fifth where there is only bulk temperature. Both the triple and split window retrieved temperatures have been calculated. Fig. 6.6a) & b) are the results of the comparison between the satellite retrieved temperature and the skin temperature and the bulk temperature respectively. There is one skin temperature where the satellite does not agree within 1σ (standard deviation) of the in situ temperature but is within 2σ. The probability in a normally distributed population of a single random sample lying between one and two sigma is 0.26, therefore one might expect in a sample of 4 to have one point outside 1σ. However for this particular image the position of the boat at the time of the overflight was beneath a small cloud. The retrieved temperatures quoted here for this point came from a pixel 5km from the boat skin temperature. This could account for the disagreement due to horizontal temperature variations. Another explanation is that, by the boat under the cloud, the skin effect would be reduced. This is due to there being more downwelling radiation under the cloud and therefore a smaller

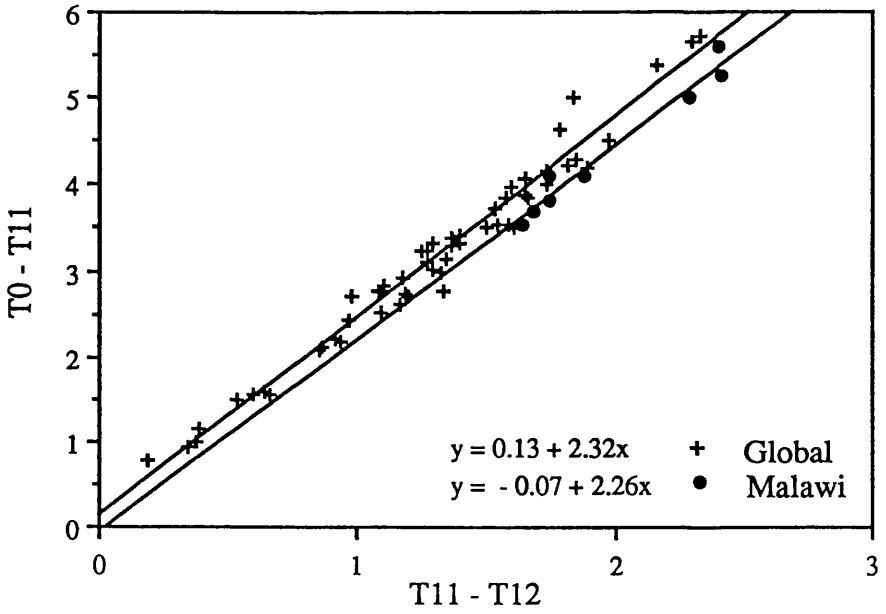

a)

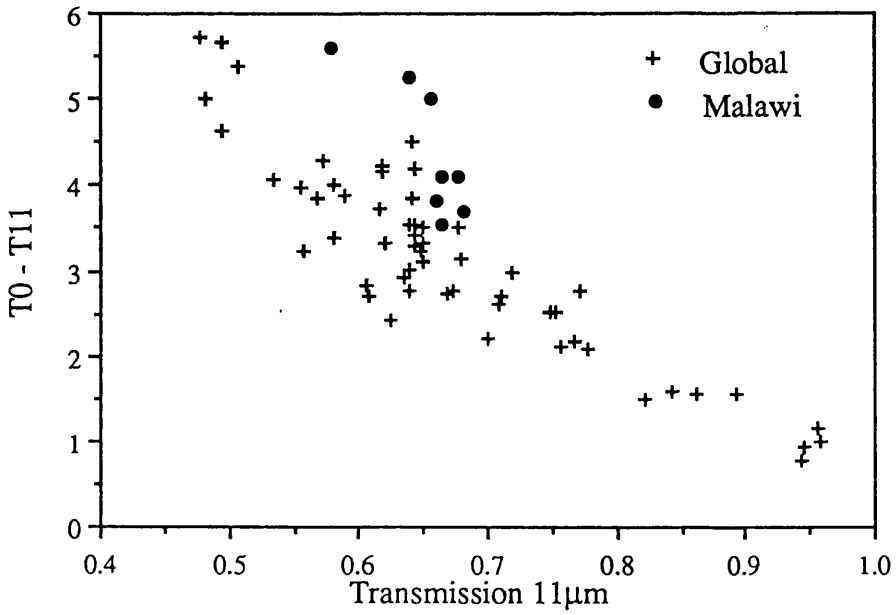

b)

Figure 6.5a) & b) Equivalent plots for Fig. 6.2a) & b) except that pressure levels 1000 - 950 mb removed from the Global radiosondes.

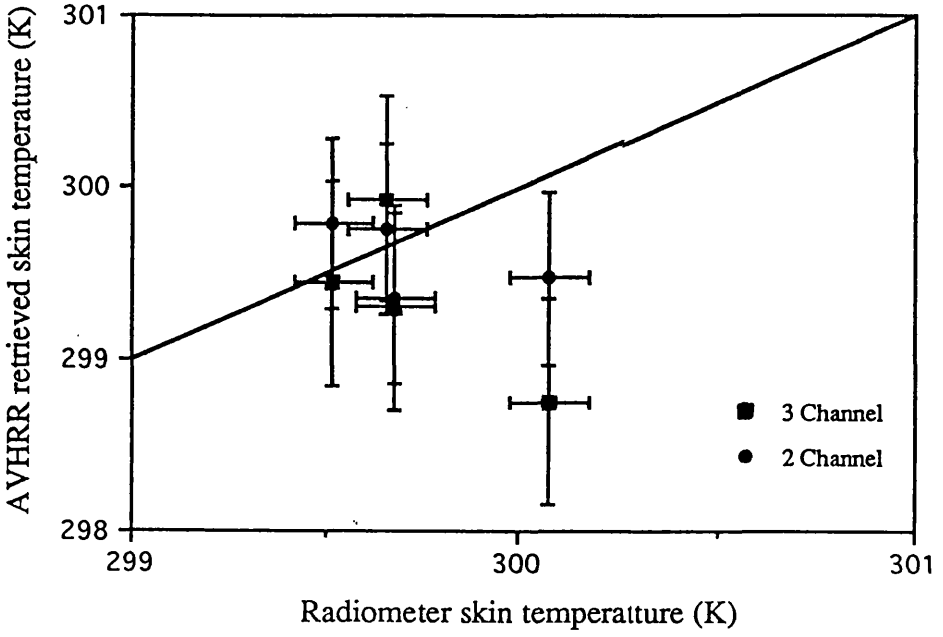

a)

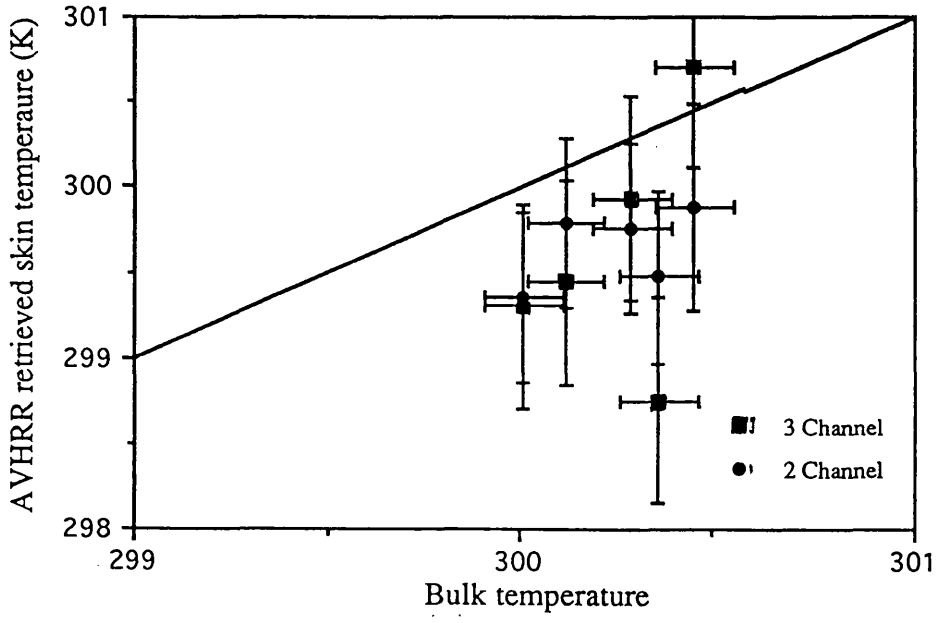

b)

Figure 6.6a) Comparison between satellite retrieved skin temperature and surface radiometer skin temperature.

b) Comparison between satellite retriieved skin temperature and surface bulk temperature (5cm).

View Angle	a0	a1	a2	a3	Regression Error
AVHRR NOAA-11	Triple Window				
0	-17.4283	0.9089	0.9261	-0.7713	0.07
37	-22.6102	0.9818	0.8223	-0.7214	0.08
48	-27.9666	1.0475	0.7338	-0.6787	0.10
55	-33.6258	1.1021	0.6723	-0.6505	0.12
60	-39.5881	1.1486	0.6309	-0.6331	0.14
AVHRR NOAA-11	Split Window				
0	2.8128	3.1166	-2.1258		0.13
37	4.8993	3.2508	-2.2670		0.18
48	7.6784	3.3731	-2.3983		0.23
55	9.6984	3.4779	-2.5090		0.27
60	10.0779	3.5764	-2.6076		0.32
AVHRR NOAA-12	Triple Window				
0	-18.6321	1.0318	0.5104	-0.4737	0.06
37	-24.2109	1.0931	0.4180	-0.4222	0.08
48	-29.8732	1.1466	0.3447	-0.3813	0.09
55	-35.7744	1.1942	0.2863	-0.3482	0.11
60	-42.0063	1.2382	0.2394	-0.3217	0.13
AVHRR NOAA-12	Split Window				
0	9.5406	3.0871	-2.1199		0.15
37	13.2920	3.2147	-2.2602		0.20
48	17.9880	3.3248	-2.3860		0.25
55	21.7619	3.4164	-2.4895		0.30
60	24.3493	3.4960	-2.5767		0.35
AVHRR NOAA-9	Triple Window				
0	-17.5602	0.8838	1.0231	-0.8429	0.07
37	-22.7366	0.9579	0.9189	-0.7939	0.08
48	-28.0639	1.0249	0.8296	-0.7518	0.10
55	-33.7461	1.0803	0.7694	-0.7256	0.12
60	-39.7269	1.1264	0.7313	-0.7111	0.14
AVHRR NOAA-9	Split Window				
0	1.2078	3.1721	-2.1757		0.13
37	2.8337	3.3117	-2.3206		0.17
48	5.2474	3.4384	-2.4550		0.22
55	6.7831	3.5500	-2.5709		0.27
60	6.6823	3.6534	-2.6727		0.31

Table 6.1 Correction coefficients derived from radiosondes over Lake Malawi for split and triple window for AVHRRs on NOAA - 9, 11 and 12. a0 is the intercept term, a1, a2 & a3 are coefficients for 3.7μm, 11μm & 12μm respectively for the triple window algorithm and a1 & a2 are coefficients for 11μm & 12μm respectively for the split window algorithm.

Image date	Time GMT	3.7μm	11μm	12μm	In Situ radiometer	In Situ Bulk	Triple window	Split window
10/11/92	0:31	296.97	294.65	292.57	-	300.45 ± 0.1	300.71 ± 0.6	299.88 ± 0.6
13/11/92	17:50	296.76	295.16	293.26	299.66 ± 0.1	300.35 ± 0.1	299.93 ± 0.6	299.76 ± 0.5
14/11/92	1:25	296.08	294.70	292.55	299.52 ± 0.1	300.21 ± 0.1	299.44 ± 0.6	299.79 ± 0.5
14/11/92	17:28	295.89	294.85	292.64	300.08 ± 0.1	300.69 ± 0.1	298.75 ± 0.6	299.47 ± 0.5
15/11/92	1:10	296.33	294.49	292.30	299.68 ± 0.1	300.34 ± 0.1	299.30 ± 0.6	299.35 ± 0.5

	Split window °C	Triple window °C
Satellite skin temp. - In situ skin temp.	-0.14 ± 0.2 SD = 0.4	-0.38 ± 0.3 SD = 0.7
Satellite skin temp. - In situ bulk temp.	-0.5 ± 0.06 SD = 0.1	-0.53±0.3 SD = 0.6

Table 6.2 Results of comparison between retrieved satellite temperature (split and triple window) and in situ radiometric temperature and bulk temperature (5cm).

Since this thesis was first drafted there has been other work published concerning the retrieval of surface water temperatures of lake Malawi with AVHRR (Wooster et al., 1994). In this work a retrieval algorithm was produced from the regression of in situ measured water temperatures at 1m depth with the brightness temperatures measured for coincident NOAA-11 AVHRR images. The data was collected between March and October 1992 and contained 59 points. This study indicates that the atmospheric correction is stable over this extended period, that is to say that a single correction algorithm performed well over the study period. However, when Wooster et al., 1994 coefficients are used with the data in this thesis, biases compared with in situ bulk temperatures are found of $1.28 \pm 0.1°$ and $0.35 \pm 0.1°$ for the split and triple window respectively. Reasons for these biases are unclear but it could be due to the data in this thesis being collected in November, the beginning of the wet season, whereas the period covered by Wooster et al. (1994) is only between March and October.

net heat flux out of the surface. This would produce a smaller skin effect and a higher skin temperature than under clear sky conditions, 5 km away, which is in accord with the discrepancy.

The mean difference (satellite derived temperature - radiometric in situ temperature) and the standard error in the mean is -0.14 ± 0.2 °C for the split window algorithm and -0.38 ± 0.3 °C for the triple window algorithm, with standard deviations of 0.4° and 0.7° respectively. Comparison of satellite temperatures with the bulk temperatures yielded -0.50 ± 0.06 °C for the split window and -0.53±0.3 °C for the triple window, with standard deviations of 0.1° and 0.6° respectively. There are four points, for both algorithms for the radiometer comparisons and five for the bulk comparisons. As there is considerable noise on the 3.7μm channel of the AVHRR which is the probable reason for the larger error and bias, it will not be included in further discussions. The results for the split window algorithm are consistent with zero bias between the retrieved temperature and the measured in situ skin temperature within the error of ± 0.2°. Furthermore a significant (5σ) skin effect of 0.5°was measured for the split window algorithm consistent with a skin effect produced from a net loss of heat through the surface.

Although there are relatively few points the results indicate that it is possible to retrieve a single pixel surface skin temperature to ± 0.2° (1 standard deviation) for the split window correction method. This result compares favourably with that found by Minnett (1991) where errors of the range 0.35-1.0°C are quoted. There are several potential reasons for this improvement, such as the sample is too small to have a true representation of the errors and the good agreement is by chance. Secondly as all the samples are taken within a two week period potentially only a small range in atmospheric conditions were encountered. Furthermore as the atmospheric correction coefficients were generated from contemporaneous radiosondes the correction is "tuned" to the data and therefore one might expect good agreement. In terms of monitoring the temperature of a lake throughout the year the uncertainty could be even smaller, for example if one is considering mean monthly temperatures it should be possible to get more than one pass. This assumes that the atmospheric correction coefficients are suitable for the whole year and, as discussed later, it may be necessary to produce "seasonal" coefficients. The error in the atmospheric regression could be reduced further for both algorithms with more radiosondes. The error for the three channel algorithm could also be substantially reduced if there was less noise in the 3.7 μm channel of AVHRR.

The results of the experiment to measure the range and characteristics of the skin effect are depicted in Figs. 6.7 and 6.8. Data used in these plots were not collected during

satellite overpasses but gathered whilst using the second mode of sampling described earlier. Fig. 6.7 shows the measured skin effect against time and date through the cruise and Fig. 6.8 is a histogram of these values. The mean value is 0.248 ± 0.004°C for 1932 samples and with a standard deviation of 0.18°. Figure 6.7 indicates that there can be fluctuations of the skin effect over very short time scales but figure 6.8 shows that the majority of the values are contained within ± 0.2° of the mean.

To see if there were any diurnal variations, this data set was binned up into 1/20ths of a day and the result is plotted in Fig. 6.9a); also included in b)-e) are the corresponding binned meteorological parameters and the water temperature. The error bars plotted are the standard error of the binned parameter. One sees from Figure 6.9a) that the binned data indicates that the mean skin effect is nearer ~ 0.3 ° with a diurnal variation of ~ ± 0.15°. The reason for this difference (from the histogram value) is in the number of samples in each bin. From Fig. 6.10 we see that the sampling is strongly biased towards the 0.25-0.45 portion of the day which is during a smaller skin effect period. Therefore the histogram and mean value is being biased by the non-uniform sampling and the binned values probably provide a better estimate of the skin effect. There are points which lie away from a smooth diurnal cycle, particularly in the latter part of the day, which does not seem to correspond to a difference in the meteorological variables. A possible reason for these outliers could also be due to the sampling. If Fig 6.7 is studied carefully then it can be seen that the majority of the samples for the 0.9 and 0.95 periods were taken on one day and therefore these outliers could be due to anomalous weather on that day. If the outliers at 0.7, 0.9 and 0.95/day are excluded the mean of the binned values for the skin effect is -0.3 ± 0.08.

One can see that the diurnal variations in the skin effect grossly correspond to similar variations in the meteorological parameters. The drop in the skin effect to ~-0.45° just after midday corresponds to a similar drop in the relative humidity and rise in the air temperature. This drop in relative humidity will allow a greater evaporative flux from the water surface which would in turn produce a larger skin effect which is what we see. Opposed to this will be the increase in air temperature which will tend to reduce the skin effect, however, as shown in earlier chapters evaporative fluxes are considerably larger than conductive fluxes and therefore it seems that the increased evaporation dominates.

If these values are compared with the skin effect from the AVHRR results one finds that they do not seem to agree particularly well. The satellite-bulk difference was found to be -0.5° compared to -0.3° for the binned data. However a bias 0.14° was found between the AVHRR and the radiometer temperatures. If this is taken to be real and not due to

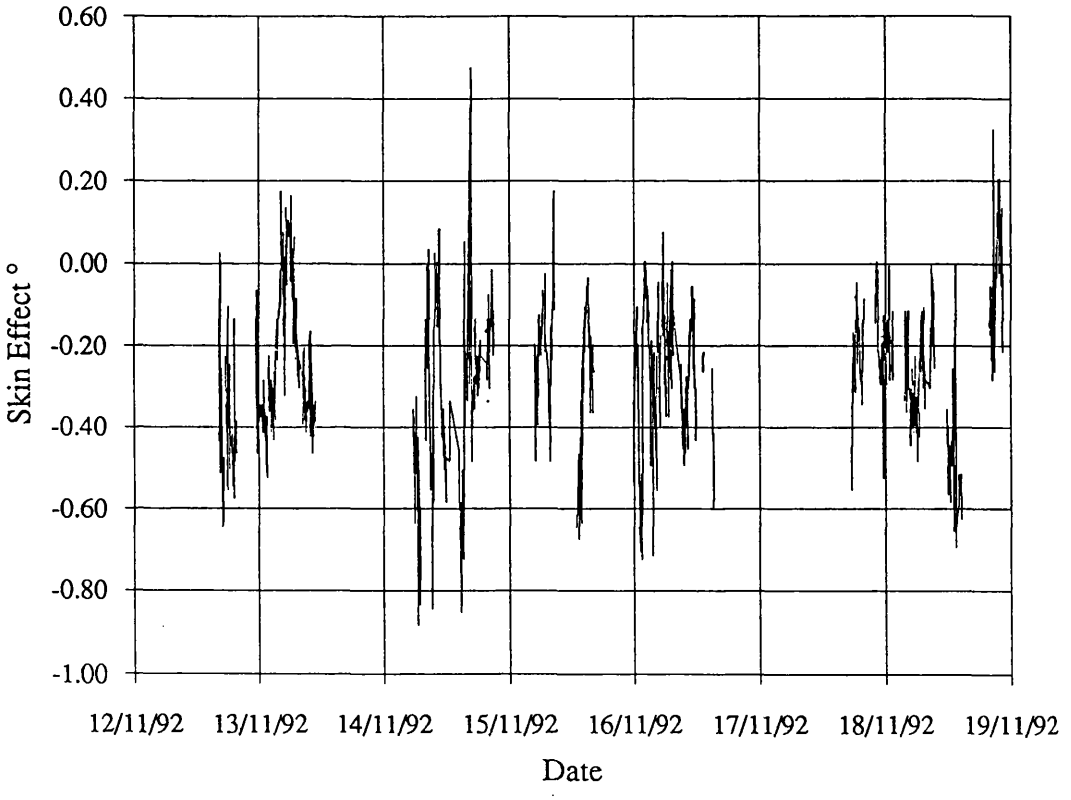

Figure 6.7 Measured skin effect through duration of cruise

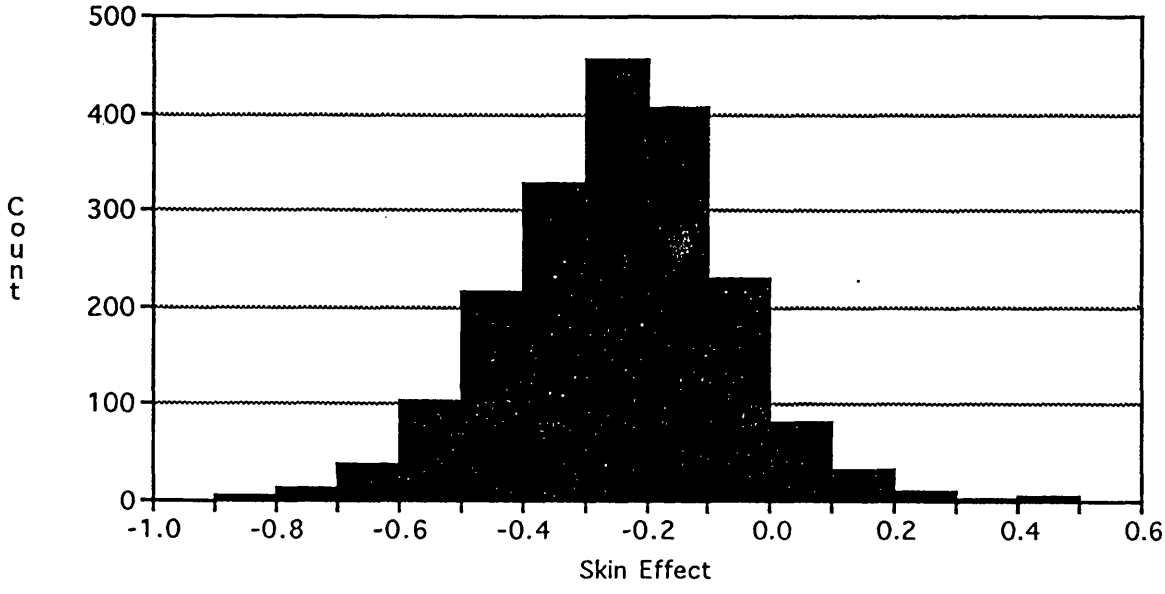

Figure 6.8 Histogram of skin effect measured during cruise.

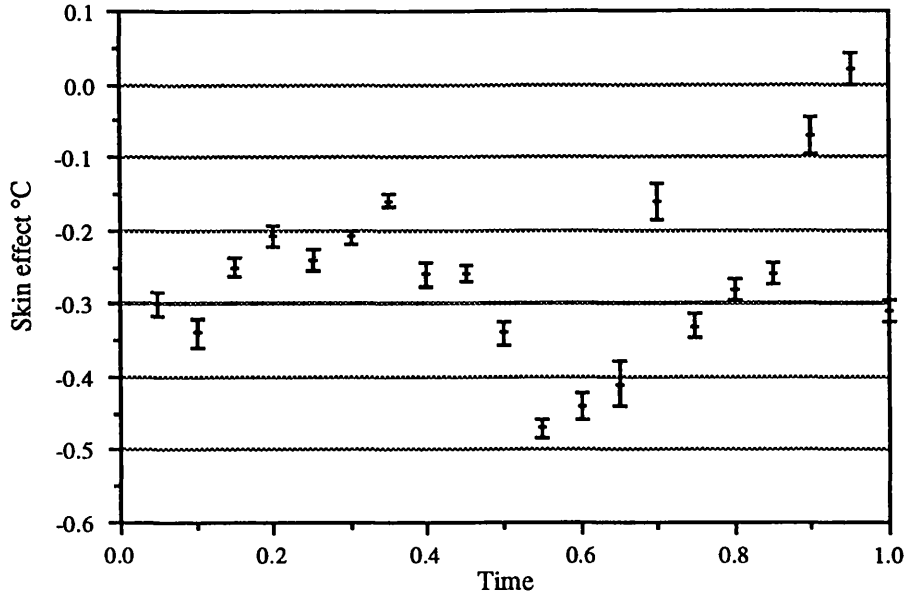
Skin effect °C
0.1
0.0
-0.1
-0.2
-0.3
-0.4
-0.5
-0.6
0.0
0.2
0.4
0.6
0.8
1.0
Time

a)

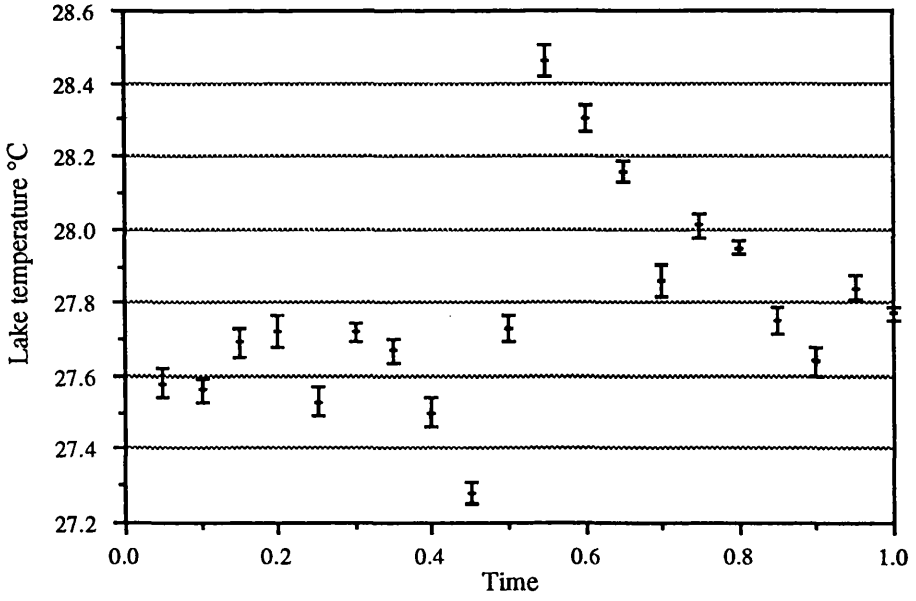
Lake temperature °C
28.6
28.4
28.2
28.0
27.8
27.6
27.4
27.2
0.0
0.2
0.4
0.6
0.8
1.0
Time

b)

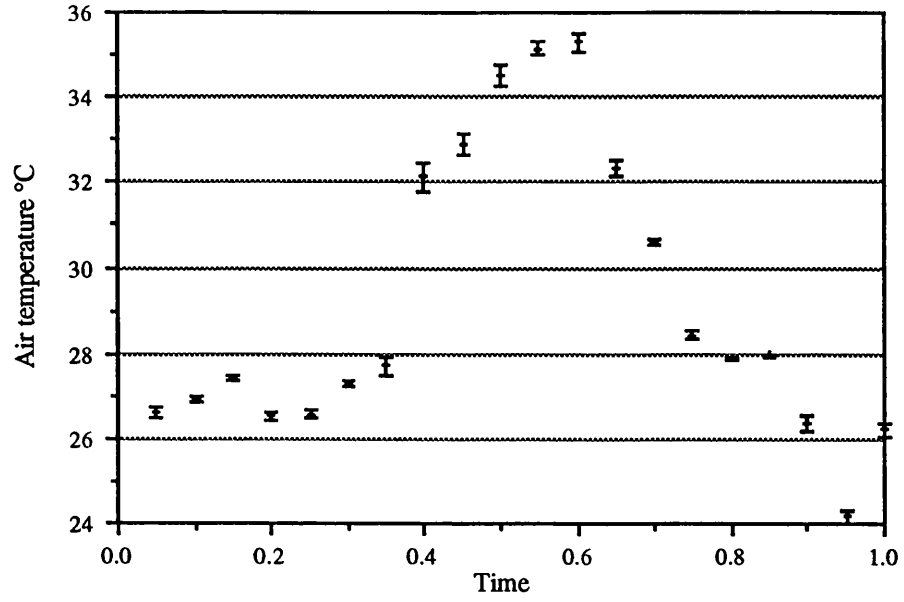
Air temperature °C
36
34
32
30
28
26
24
0.0
0.2
0.4
0.6
0.8
1.0
Time

c)

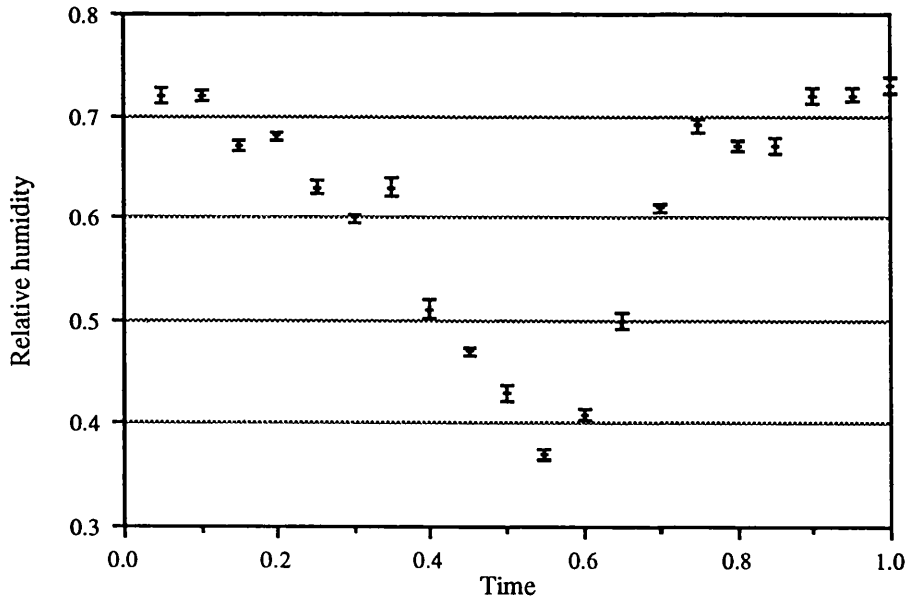
Relative humidity
0.8
0.7
0.6
0.5
0.4
0.3
0.0
0.2
0.4
0.6
0.8
1.0
Time

d)

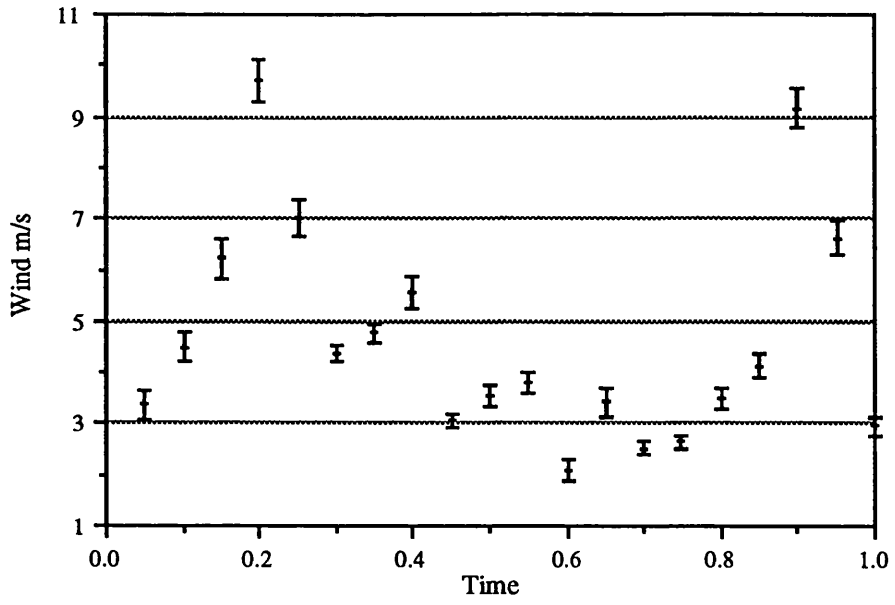

e)

Fig 6.9 a) - e)

a) Measured skin effect averaged into 1/20th day binns for entire cruse
b) As for a) but for lake temperature.
c) As for a) but for air temperature.
d) As for a) but for relative humidity.
e) As for a) but for wind.

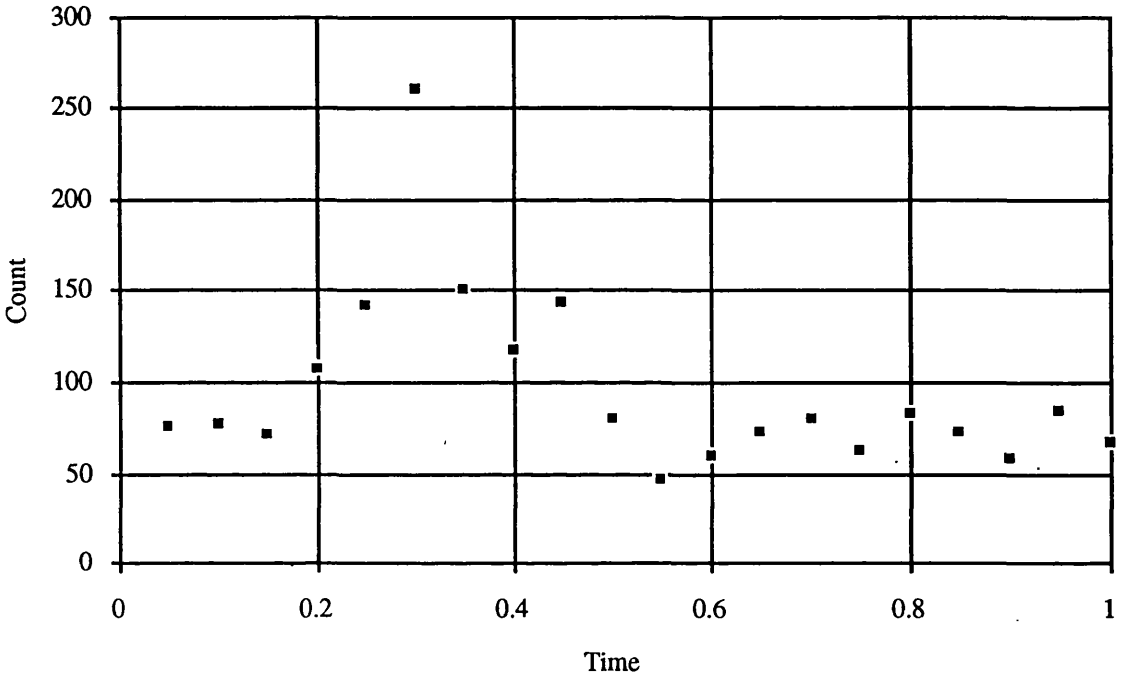

Fig 6.10 Number of readings for each binn in Figs 6.9 a) to e).

random error then it can either be due to the radiometer reading too high, or the AVHRR retrieved temperatures being too small. If it is the first case the binned skin effect value should be corrected similarly where it becomes -0.44°, the same as the measured satellite-bulk difference (0.5°), to within error. If it is the second case then the measured satellite-bulk difference needs to be corrected and it becomes -0.36° which now agrees with the binned value, to within error. Form the data sets it is not possible to determine which is correct and again the low number of samples by the satellite limits the significance of these corrections.

6.5 Discussion & Conclusions

The biasing of the water vapour to higher levels in the measured atmospheres is an interesting result as it has implications on the use of the split window correction method. The split window correction assumes that the atmosphere is "thin", that is to say, a linear approximation can be made to the absorption that the radiation undergoes as it passes through an atmosphere with respect to the amount of absorber. However, this method has been used with tropical atmospheres which have a very high water vapour content and could not be classed as "thin" and yet still produce reasonable results (Llewellyn-Jones, Minnett et al. 1984). The reason that this is so is that the split window method actually requires the change in transmittance in one of the channels to be linearly related to the change in transmittance in the other. If not the surface temperature cannot be accurately derived from a linear combination of brightness temperatures. In the case of tropical ocean atmospheres the annual variability of the density structure for the water vapour roughly satisfies this condition and so the split window can be used with some success. In the case of continental atmospheres, as we have here with Malawi, there is greater potential for the "transmittance linearity condition" to break down. This is due to there being a wet season and a dry season where there could be a large change in the actual quantity of water vapour in the atmosphere. Furthermore if there is also a change in either the amount or strength of convection, so changing the water vapour distribution, there could be a large change in the coefficients needed. Further work is necessary to investigate the possibility of these effects which would involve collecting a representative sample of the atmospheres occurring over Lake Malawi throughout the year and checking them with the atmospheric transmission model to test the stability of the split window coefficients through the seasons. This would also allow a better regression to be performed thereby obtaining correction coefficients with lower uncertainty and hence improved retrieved temperatures.

Further results from this study include:

- Temperatures derived by AVHRR have been found to agree to within 0.14 ± 0.2 °C with in situ radiometric temperatures for the split window correction method when using coefficients derived from local radiosondes. The single pixel retrieval accuracy is limited currently by the error in the regression (caused by the small number of radiosondes) between the modelled brightness temperatures and the surface temperatures and the significance of this result is compromised due to the small number of overflight/in situ comparisons. Nevertheless, even with this limited data set a zero bias has been indicated within a 1σ error of 0.2°C.

- A skin effect of -0.5 °C was detected with the satellite data when compared with the measured in situ bulk temperature to 5σ significance.

- The skin effect was monitored with a ground based radiometer under a variety of conditions and was found to have a mean value of ~-0.32°C and a small quasi-sinusoidal diurnal variation of ~0.15° with a period of ~12 hours. The largest skin effect occurred between 13:00 and 14:00 which corresponded to a minimum in the relative humidity.

In general these are encouraging results which indicate that the retrieval of lake surface temperatures from satellite for the purposes of monitoring climate should be feasible. The nature of the skin effect which was measured suggests that the conversion from skin temperatures to bulk temperatures can be achieved with some accuracy and that the major error source would be the retrieval of the skin temperature. The extension of these results and the assumption that they apply for the whole year should be made with caution as these measurements have only been made during a short two week period.

There are a number of questions which still need to be addressed which are listed below together with recommendations for future work to resolve them.

- This field campaign has indicated that single pixel surface skin temperatures can potentially be retrieved to an accuracy of 0.2°C (1σ) yet the significance of this result is poor due to the low number of data points. Therefore further validation is still needed to certify this result.

- The radiosondes used here were all launched within a two week period and therefore might not have sampled the full range of atmospheres which occur and so use with data from different times of the year

might be inappropriate. Therefore a representative sample of the atmospheres over the lake need to be acquired and assessed.

- Similarly the skin effect was only measured for a short period and therefore needs to be confirmed that this is representative for all conditions encountered over the lake.

- Lake Malawi is a tropical/continental lake and therefore the accuracy of retrieved lake temperatures for other climatic situations needs to be investigated.

Chapter 7.

Monitoring the annual temperature cycle of a lake with remote sensing: - a validation study.

7.1 Introduction

In the last chapter it was shown for Lake Malawi that the surface skin temperature of the lake could be measured with AVHRR to an accuracy of 0.2°C (1σ) but the significance of this result was compromised by the small number of validation points available. That validation study was only conducted over a two week period and therefore there is some uncertainty as to whether this result is representative for other seasons. If lakes are to be used as climatic indicators it will be necessary to know whether it is possible to monitor lake temperature cycles throughout the year and also for various climatic regions. This question breaks down into two parts, what is the retrieval accuracy throughout the year, and can the lakes be sampled regularly enough, with current satellites, to be able to determine the annual temperature cycle? This second point is quite subtle as it depends on how the lake is responding to weather changes and how important the shorter term fluctuations are when one wants to make a "mean measurement". If we restrict ourselves to seasonal changes then we can neglect many of the shorter term fluctuations as the lake can be considered on these time scales to be in equilibrium with the environment (cf. chapter 5). It is common practice to divide the year so that the seasons are three months in length, with winter starting at the beginning of December. It will be for these periods that this chapter will be assessing the possibility and problems involved in measuring the mean lake temperature and variance and whether the satellites currently available provide the accuracy and sampling to achieve this.

This chapter addresses these questions by performing a validation study on Lough Neagh in Northern Ireland, which is a northern maritime climate, using both AVHRR and ATSR to derive the annual surface temperature cycle. This lake was chosen due to the availability of comprehensive in situ data and that AVHRR data covering this region is archived at the University of Dundee. As discussed in chapter 2 the satellites on which these instruments are deployed have different repeat patterns and the instruments different accuracies. The period of the study covered 1.9.88 to 20.9.89 for AVHRR and 1.9.91 to 4.8.92 for ATSR.

7.2 The validation data set

7.2.1 In situ data

The in situ data were provided by Dr. C. E. Gibson and Dr. R. V. Smith of the Freshwater Biological Development Unit, Department of Agriculture for Northern Ireland, and consists of two data sets. The first, which shall be called the "weekly" data, is taken from a set of ongoing weekly measurements made of the surface temperature near the centre of the lough. This measurement is taken on Monday mornings, weather permitting, at approximately 10:00 am by boat at a depth of ≈ 20 cm. If this is not possible, for example due to bad weather, the next available opportunity is taken. The second data set is a high temporal resolution surface temperature measurement, to be called the "hourly" data, made from a floating platform ~ 5km from the shore in the NE corner during the summer period 14.6.89 to 22.8.89. These positions are shown on the map in Fig. 7.1. The sampling was initially at 0.5 hourly intervals but then increased to 1.5 hours. The surface temperature was measured from a plastic arm extending from the side of the platform at a depth of 5 cm. Both sets of measurements have been calibrated in the laboratory against a mercury thermometer to an accuracy of 0.1 °C. The absolute accuracy of the calibration thermometer is not known.

A comparison of the two in situ data sets for the coinciding period is shown in Fig. 7.2. The agreement is generally good apart from the "weekly" point on 19.6.89. Although the lake is generally well mixed horizontally this difference could be due to a cold upwelling of water at the weekly site. Otherwise the "weekly" reading could be taken as being in error. Notice that the lough can sometimes experience very large diurnal variations in surface temperature. This is due to the unusually high turbidity of the lough, containing considerable amounts of dissolved and suspended organic matter. The unity optical depth has been measured to be ~ 40 cm (Gibson, pers. comm. 1990), so 63% of the incident sunlight will be absorbed by this depth causing rapid surface heating in sunny weather. It is also possible to see "fair weather spikes" where surface temperatures are unusually high for a period of several days during stable fine weather conditions. The selection of scenes for the period outside that covered by the "hourly" data was therefore limited to night scenes to avoid the diurnal variation as much as possible. It should be noted that there is a potential for the selection of scenes to be biased towards these "fair weather" periods due to these having predominantly clear skies.

Radiosondes were also acquired which had been launched by the Met Office from an airfield approximately 25km from the east shore (see Fig. 7.1). Six of these radiosondes are during the period when the "hourly" surface temperatures were taken; the rest during the "weekly" data. The dates of the radiosondes were chosen to coincide with the clear

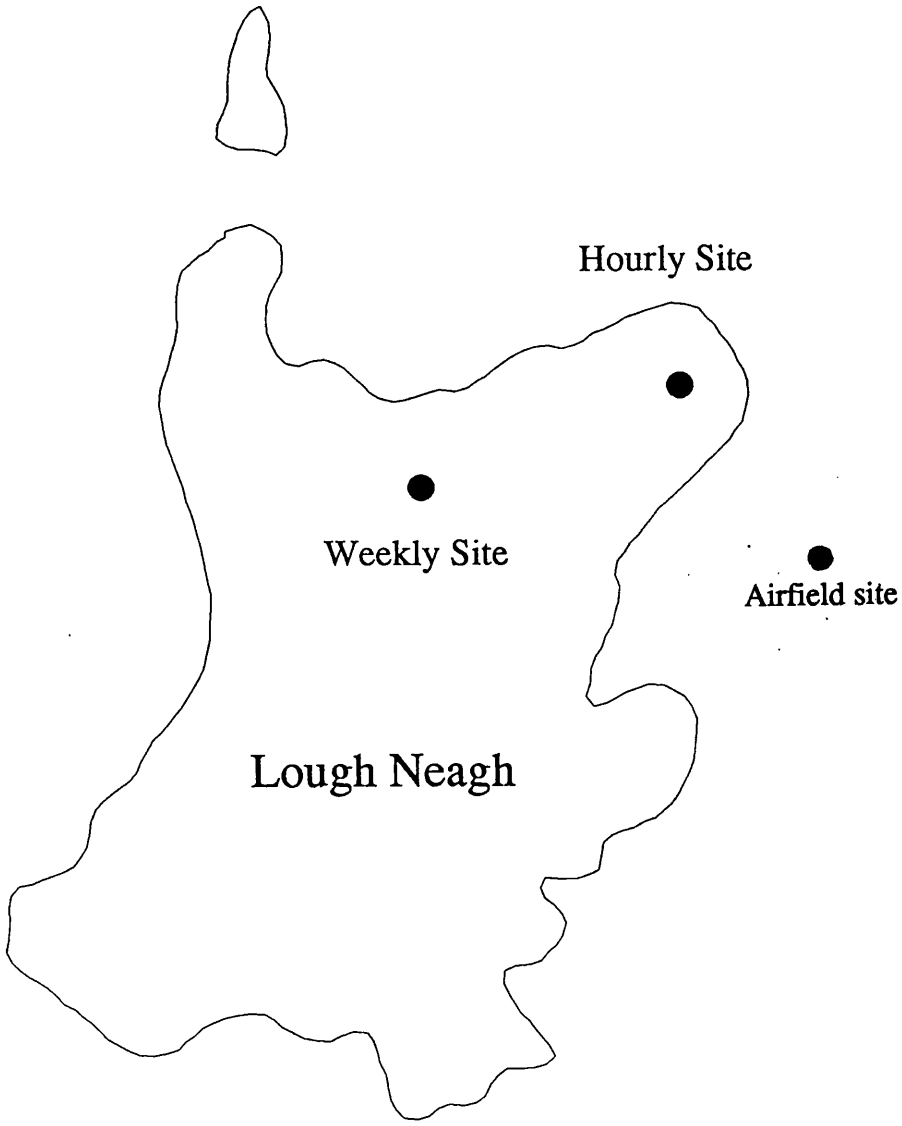

Figure 7.1 Map indicating the sampling positions of the "hourly" and "weekly" in situ data.

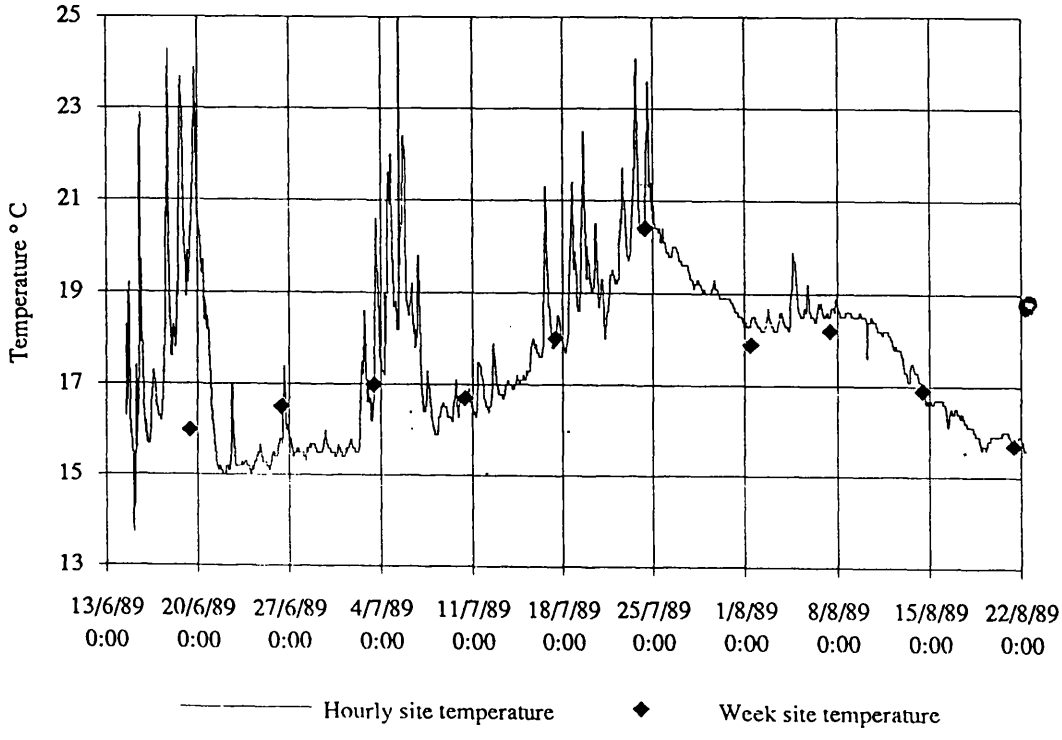

Figure 7.2 Comparison of contemporaneous "hourly" and "weekly" in situ data. Note general good agreement except for "weekly" point on 19/6/89 which is taken to be in error.

AVHRR scenes but the radiosondes were all launched at 00:00 and therefore are 2~3 hours before the satellite overpass.

7.2.2 Satellite Data

AVHRR data covering Europe is collected and archived by the University of Dundee Satellite Station. Quick-looks of the collected scenes are produced in the form of photographic prints where most of the panoramic effect of the scan geometry of AVHRR has been removed. Copies of the quick-look archive are distributed around the country and the one used for this study is held at the Imperial College Remote Sensing Library. The purpose of the quick-looks is to perform a preliminary cloud clearing procedure before actually ordering the scenes thereby reducing the data volume of the request. Unfortunately the dynamic range of the images in brightness terms is greater than that available from the photographic paper and therefore there are occasions when the contrast over the lough was very poor, resulting in reduced effectiveness of the quick look archive. As will be discussed later, after rigorous declouding 74 cloud free AVHRR scenes were collected. This should be compared with the repeat frequency of the instrument which is at least twice per day. There are, as mentioned in chapter 2, currently two of these instruments orbiting at any one time with a 12 hour separation and therefore for the 385 days of this validation period there would have been 1460 overflights of which 730 would be night time images. So we can see that there is ~ 10% success rate over the year. This is not quite accurate as at the beginning of the period NOAA 10 was in orbit which did not have the split window AVHRR and therefore reduced the number of images to select from. Countering this some daytime images were selected during the period for which there is "hourly" data. Therefore the figure of 10% success rate is only a rough estimate but is a useful guideline for estimating the cloud free statistics for Lough Neagh.

ATSR data has been selected out of MSSL's archive of this data which has been provided by and is a subset of the Rutherford Appleton Laboratory archive. The MSSL archive can be searched on latitude, longitude and date and provides a list of images which can then be retrieved off DAT cartridges. The success rate found for this instrument with its different repeat characteristics was found to be similar to that for AVHRR with 13 out of 124 images found to have both the forward and the nadir cloud free giving a success rate of again ~10%. This is as one might expect as the satellites are regularly sampling a quasi-random event and so the probability for a single sample being cloud free is constant.

7.3 Analysis

The radiosondes were processed in a similar way as for those over Lake Malawi, reported in chapter 6, to calculate correction coefficients for both AVHRR and ATSR. It has come to light in the past few years that there is considerable uncertainty in the value of the water vapour continuum absorption which accounts for much of the absorption in the AVHRR/ATSR channels. It has been suggested that the uncertainty is as large as 30% (Kilsby et al. 1992). To see what was most appropriate for Lough Neagh, brightness temperatures were calculated for the continuum value as given by Edwards (1987) and for 30% higher. Since each radiosonde preceded an AVHRR overflight by a few hours it was possible to compare the calculated brightness temperatures with those actually measured to see which continuum value produces the most realistic values. The surface temperature was incorporated into the brightness temperature calculation by interpolating between the two adjacent in situ samples. The results of this comparison are shown in Fig. 7.3 with the modelled and measured 11 & 12 μm (T11-T12) differences plotted against each other. One can see that the higher continuum value as proposed by Kilsby et al. (1992) produces the more realistic brightness temperature differences and is therefore favoured in our conclusions. The lower continuum results will be included for comparison. Even with the higher continuum there are considerable differences between the measured and calculated T11-T12. It is suggested that this could be attributed to errors in the interpolated surface temperature as it is possible for the surface water temperature to change considerably within a week, the in situ sampling interval.

To determine the correction coefficients we used three atmospheric scenarios. The first used 60 North Atlantic radiosondes supplied by NOAA, and the second the 19 radiosondes from near the lough. In both these cases the surface temperature was taken as the bottom of the atmosphere temperature (a common assumption in oceanic situations). The third scenario used the same 19 Lough Neagh radiosondes but used the interpolated in situ temperatures as the surface temperature. This was to investigate the fact that, unlike the oceanic case, the atmosphere above the lough has not necessarily been in contact with the water surface for a long enough period for the two temperatures to equilibrate. Therefore there could be a large temperature discontinuity between the bottom of the atmosphere and the surface of the lough. In fact it was found that for these data the water was between 0 to 8 °C warmer than the atmospheric base. The results of the three cases for AVHRR are plotted as atmospheric correction vs. (T11-T12) in Fig. 7.4, with the least squares fitted lines for each three giving the correction coefficients. It can be seen that the correction coefficients are very similar for all the scenarios, including the case where the model takes into account the temperature difference between the

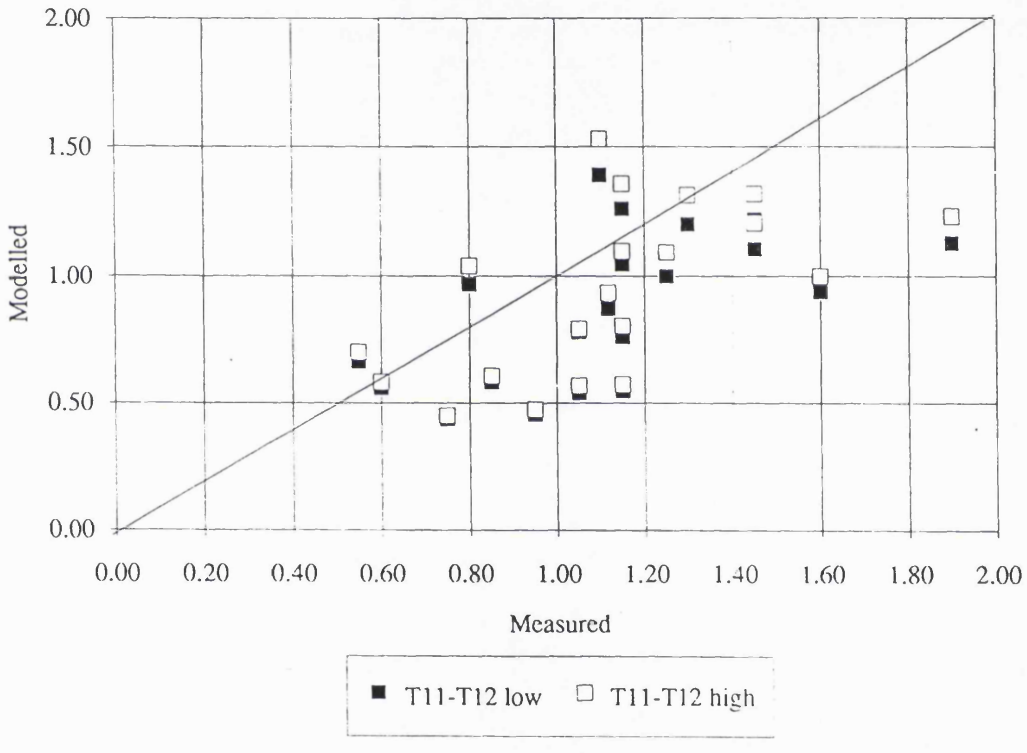

Figure 7.3 Comparison between modelled and measured 11 & 12 μm brightness temperature differences for both high (open boxes) and low (closed boxes) water vapour continuum absorption values.

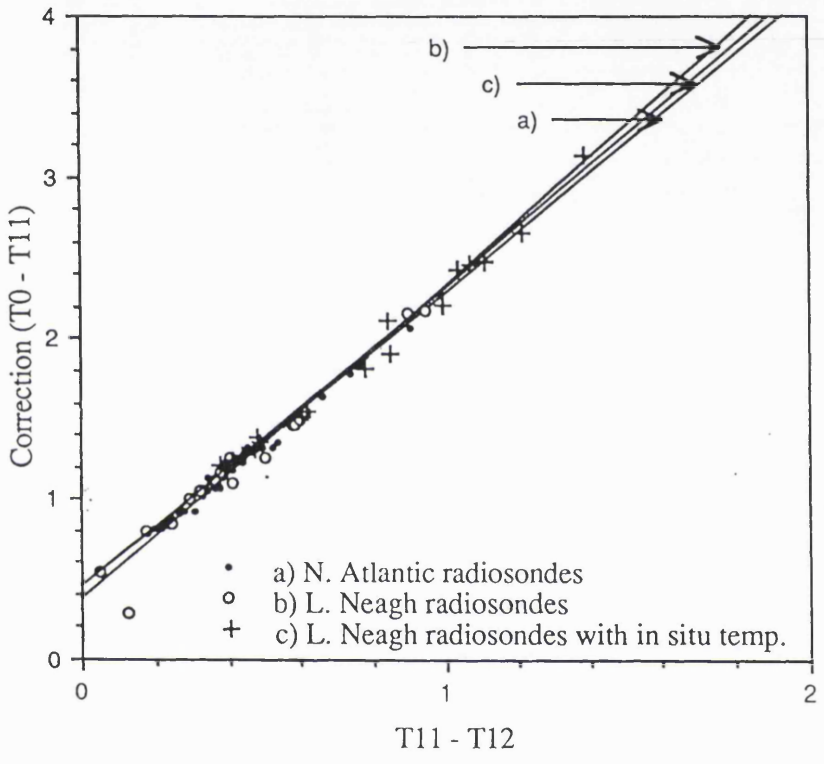

Figure 7.4 Results of modelling the atmospheric correction required for the 11 μm brightness temperature with respect to the 11-12μm difference. Three scenarios are used a) 60 North Atlantic radiosondes, b) 19 radiosondes collected over Lough Neagh with the ground temperature taken to equal the bottom of the atmosphere temperature and c) same as b) but with ground temperature interpolated from in situ temperature. Regression lines are plotted for all three cases.

bottom of the atmosphere and the lough. Therefore since the algorithm seems to be particularly robust and unaffected by the temperature discontinuity, and since the North Atlantic radiosondes produce very similar results, the coefficients derived from the NOAA radiosonde set are used for this analysis. This is because they are independent and more numerous, producing a more accurate regression. The similarity between the North Atlantic radiosondes and those taken over the lough is not particularly surprising as N. Ireland is on the edge of the Atlantic and the prevailing wind for this region is south-westerly.

Split window coefficients for AVHRR were calculated in a similar way as for the Malawi radiosondes in chapter 6, but due to the different scanning geometry and approach of ATSR, different viewing angles are needed. Furthermore with the forward look, correction algorithms are not restricted to the split window but can be any combination of the three channels and two views. Since the 3.7μm channel of ATSR failed in May 1992 and the AVHRR 3.7μm suffers from interference it was decided to concentrate on the 11 & 12μm algorithms, for which the following coefficients were calculated:

- 11 & 12 μm nadir only (AVHRR & ATSR)
- 11 & 12 μm forward only (ATSR)
- 11 & 12 μm nadir and forward (ATSR)
- 11 μm only, nadir & forward (ATSR)
- 12 μm only, nadir & forward (ATSR)

Site specific atmospheric correction coefficients were required and also the use of freshwater emissivities, so the ATSR SST products generated by RAL were not suitable, and an atmospheric correction procedure for ATSR needed to be devised. The scanning geometry of ATSR is complicated, as was shown in chapter 2, and as can be seen from Fig. 7.5a) the rate of change in incidence angle from centre to edge is non-linear and different for the forward image and the nadir image. However, it is found that due to the geometric arrangement of ATSR, the change in air mass from centre to edge for the nadir and forward images is linear in nature, Fig 7.5b). It was therefore decided that coefficients would be generated for the centre and the edge pixels and then intermediate coefficients for the 255 pixels in-between would be linearly interpolated with respect to air mass (cf. RAL correction procedure Závody (1994)). This has the advantage that to generate a whole SST image, the 255 coefficient table only needs to be calculated once and so is computationally efficient. Another advantage of this system is in the low number of sets of coefficients which are required. For the five algorithms above only ten sets of coefficients are needed whereas if the RAL procedure was used then 25 sets would be required.

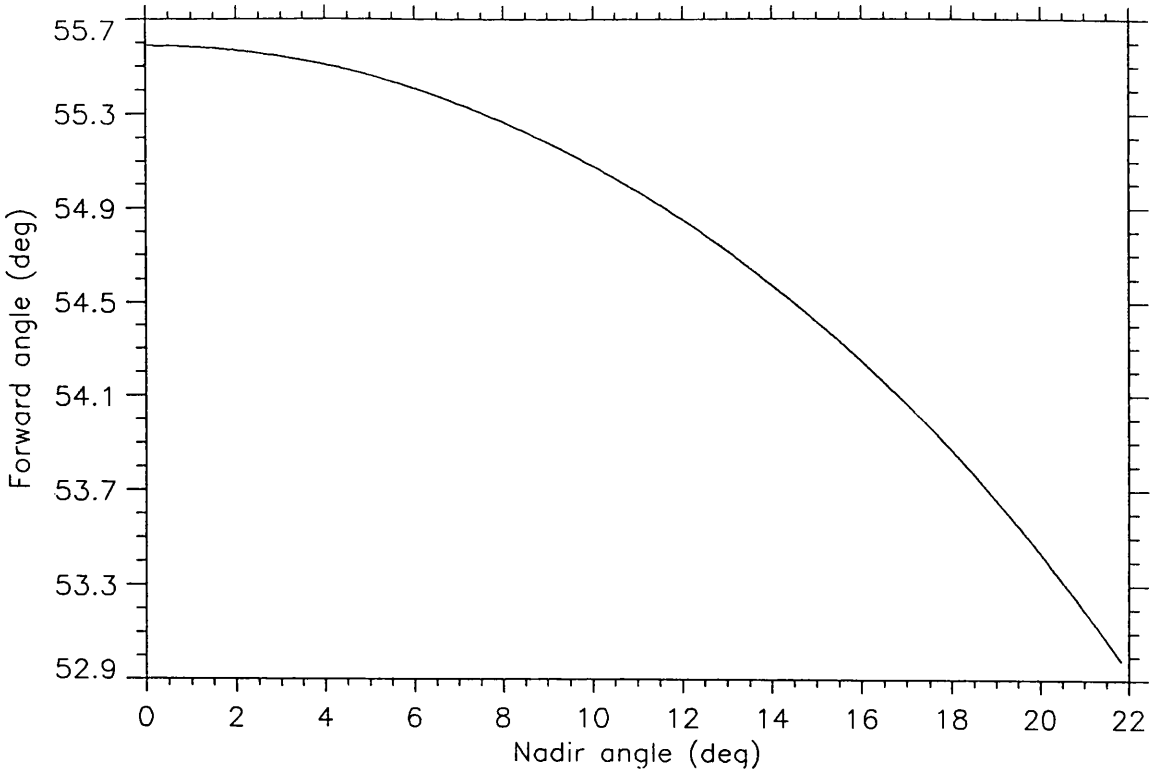

a)

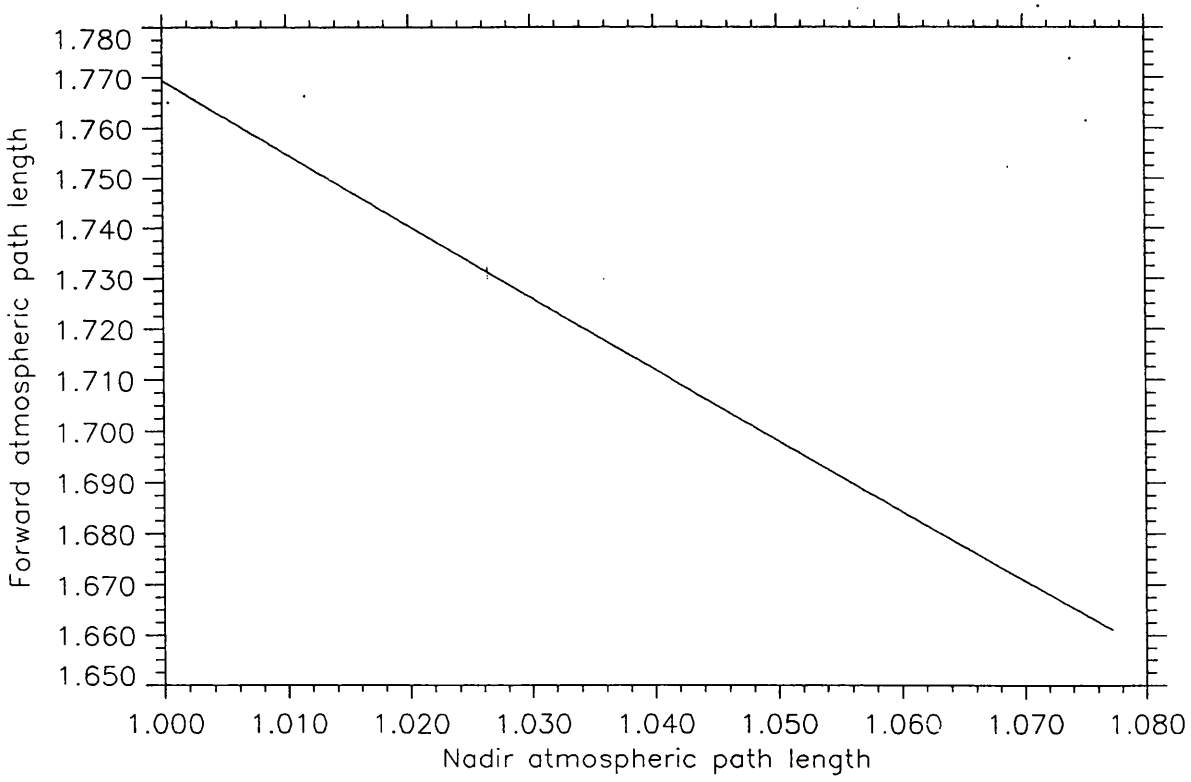

b)

Figure 7.5a) Change in look angle for forward vs. nadir images from centre to edge of each image.

b) Equivalent to a) except for atmospheric path length.

The selection of cloud free scenes was initially made for the AVHRR images with an implementation of the APOLLO cloud clearing algorithms (Saunders and Kriebel 1988) and then a final decision taken by a visual inspection of the images. For the ATSR images cloud screening was purely visual. Image navigation of AVHRR was also by eye and estimated to be within one pixel due to the availability of reference points on the shore. This was necessary even for the ATSR images which are processed by RAL and contain geolocation information, but it was found that considerable errors were present, not only in the geolocation but also in the collocation of the forward and nadir images. Lough Neagh is a well mixed lake and generally experiences very low surface temperature gradients (Gibson 1990) which therefore lowers the required accuracy for pixel location. In addition to this the sampling site for the "weekly" data was not fixed but was determined by visual reckoning of shore features.

The r.m.s. error in the retrieved temperature of a single pixel was calculated by propagating the detector noise, calibration error in the case of AVHRR, and the algorithm error through the algorithm. This assumes that the calibration error of AVHRR is random which is perhaps unrealistic as it will be similar across one scene, but this approach assumes that this error is not correlated between scenes and therefore can be treated as random when considering a series of images. The detector noise for AVHRR was taken as 0.12 °C (NOAA 1986) for both channels and the calibration error of 0.2 °C (Brown et al. 1985). More recently the accuracy of the absolute calibration of AVHRR has been reviewed and this estimate of the calibration error could be an underestimate (Weinreb et al. 1990). The calibration error of ATSR is very small when compared with the error in the algorithm regression and is therefore ignored. The channel noise for ATSR is 0.03° for the 11μm and 0.08° for the 12μm. This difference is due to restrictions in the telemetry system for ERS-1. Although the digitisation noise for the 12μm is at the 0.03° level there is not enough bandwidth to transmit all the data bits and therefore a "difference" mode is employed where the difference between the 11 and 12μm channels is transmitted and the 12μm image reconstructed on the ground. This results in an increase in the detector noise which has been found to be in the region of 0.08°. The atmospheric correction algorithm error was calculated from the regression analysis implemented on the brightness temperatures produced by the RAL transmission model. This produced a nadir single pixel retrieved r.m.s temperature error of 0.45 °C for AVHRR (inclusive of 0.2° calibration error). The error for the equivalent algorithm for ATSR is 0.15 °C. This represents the lowest standard deviation (SD) value that we might expect. However there may also be other errors in the in situ comparison such as the temporal non-coincidence of the in situ data for the "weekly" data set or the

variability of the skin effect which have not been incorporated and therefore one might expect greater scatter than predicted here.

7.4 Results

7.4.1 AVHRR comparison with in situ

The mean differences between the in situ and the retrieved satellite temperatures are presented in Table 7.1. Results are given for the correction coefficients derived from the two levels of continuum absorption as discussed earlier. The data have been divided up as follows:

a) Non-summer night scenes.
b) A subset of a) with in situ data ≤ 8 hours after overpass.
c) Summer night scenes (2:23 - 4:04), covering the period with hourly in situ data.
d) Summer day scenes (12:13 - 14:05), covering the period with hourly in situ data.

The "weekly" data set do not include any scenes during the period where there is "hourly" data. The "weekly" retrieved temperatures are plotted in Fig. 7.6 with the 'within 8 hours' points highlighted and the in situ data. The "hourly" retrieved temperatures are plotted in Figs. 7.7a), b) and c) (note the different time scales).

It is encouraging that all the biases are ≤ 0.5 °C and the SD's are all ≤ 0.7 °C. Nevertheless the biases and the SD's are greater than expected by instrumental and atmospheric correction errors alone and so warrant further discussion. The following discussion and figures will only be concerned with the "high" continuum results due to the modelled brightness temperatures being more realistic as discussed earlier.

Considering first the "weekly" non-summer data, it can be seen from Fig. 7.6 that the "weekly" retrieved temperatures follow the in situ annual temperature cycle closely, but from Table 7.1 the retrieved satellite temperatures are on average 0.3 °C too high. The "within 8 hours scenes" also show a similar bias indicating that this difference is not due to the satellite overpass being on a different day than the in situ sampling. However, a possible reason for this bias is that the weekly in situ data was sampled at 10:00 whereas the majority of the satellite overpass times were between 02:00 and 03:00. It is suggested that the lough will generally cool down between the satellite overhead time and the in situ sampling time, making the in situ measurements lower than the satellite temperatures. This is due to there being predominantly cooling processes, evaporation,

Data Set	High Continuum	Low Continuum
a) Weekly (non-summer)	0.32 ± 0.07 SD = 0.5	0.36 ± 0.08 SD = 0.5
b) Within 8 hrs. (non-summer)	0.29 ± 0.1 SD = 0.3	0.40 ± 0.1 SD = 0.4
c) Hourly night (summer)	–0.52 ± 0.2 SD = 0.6	–0.44 ± 0.2 SD = 0.6
d) Hourly day (summer)	0.10 ± 0.2 SD = 0.7	0.16 ± 0.2 SD = 0.7

Table 7.1 Mean temperature difference for AVHRR (Satellite - in situ) for the four data sets (see text for details). The standard deviation (SD) of the differences is also given. All values in °C.

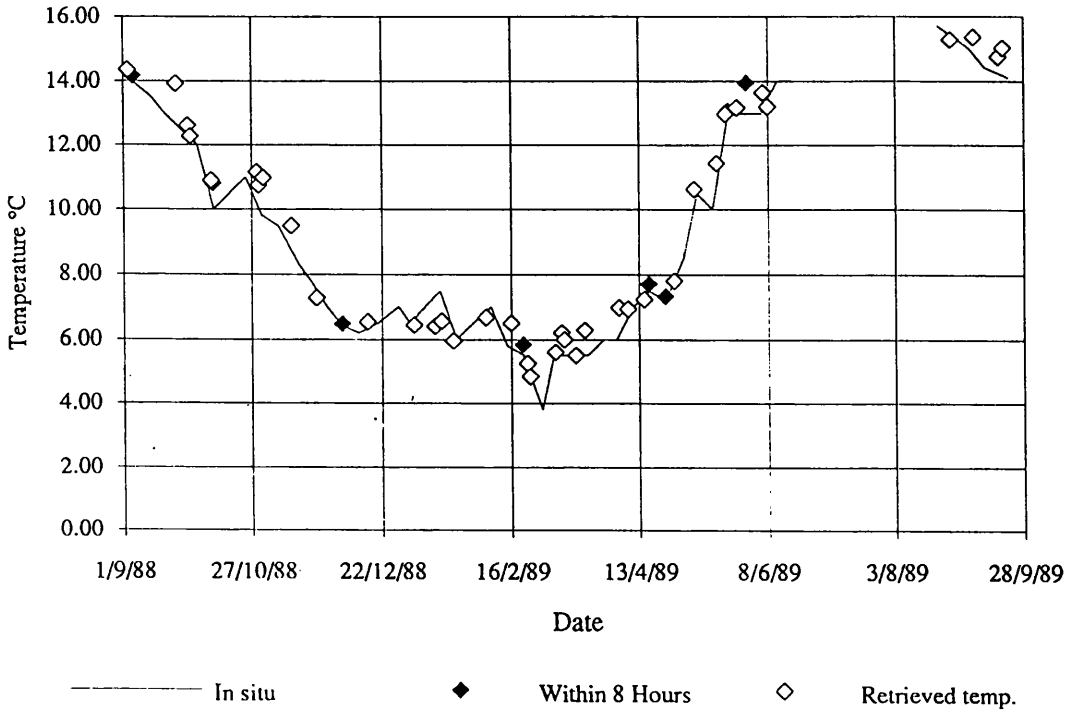

Figure 7.6 Retrieved AVHRR temperatures compared with in situ Lough Neagh temperatures for the "weekly" data set. Satellite passes which were within 8 hours of the in situ sampling time are highlighted.

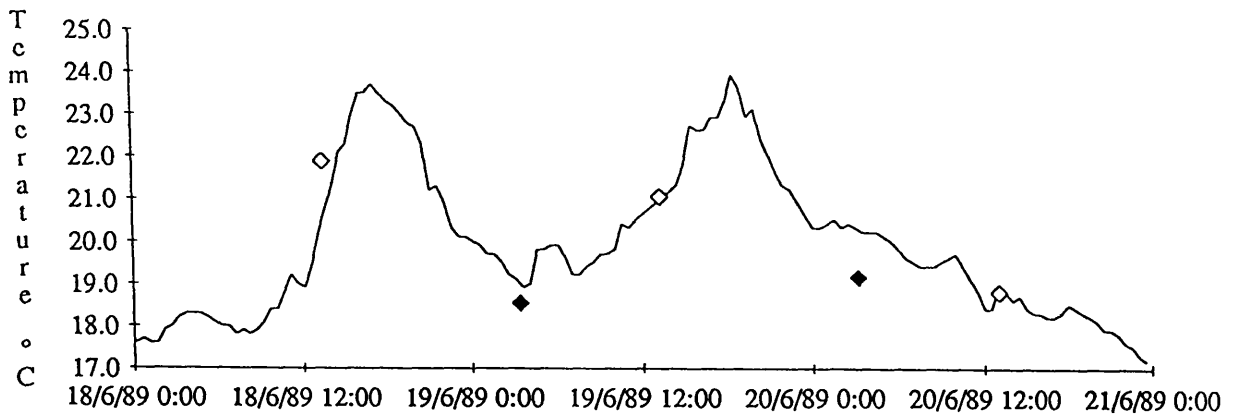

a)

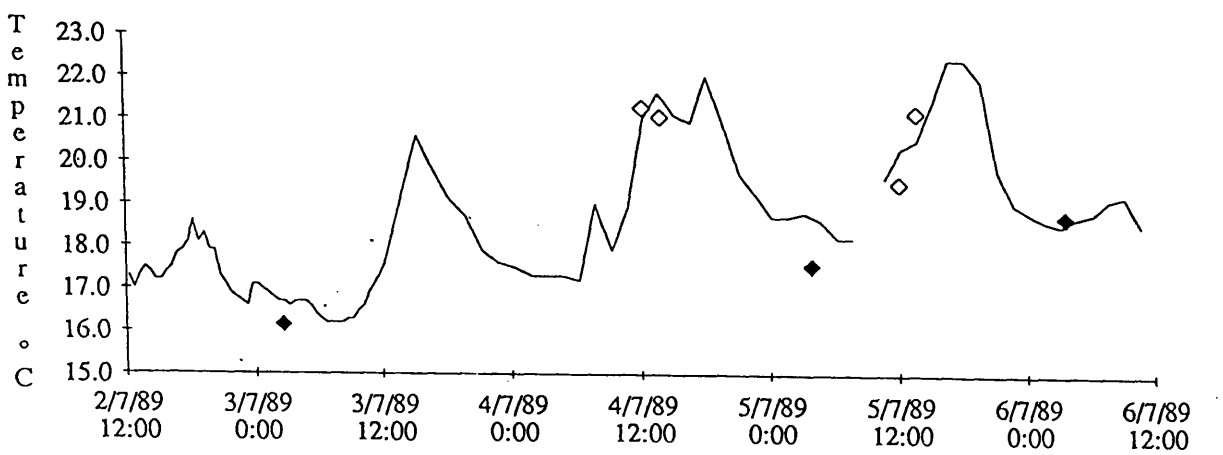

b)

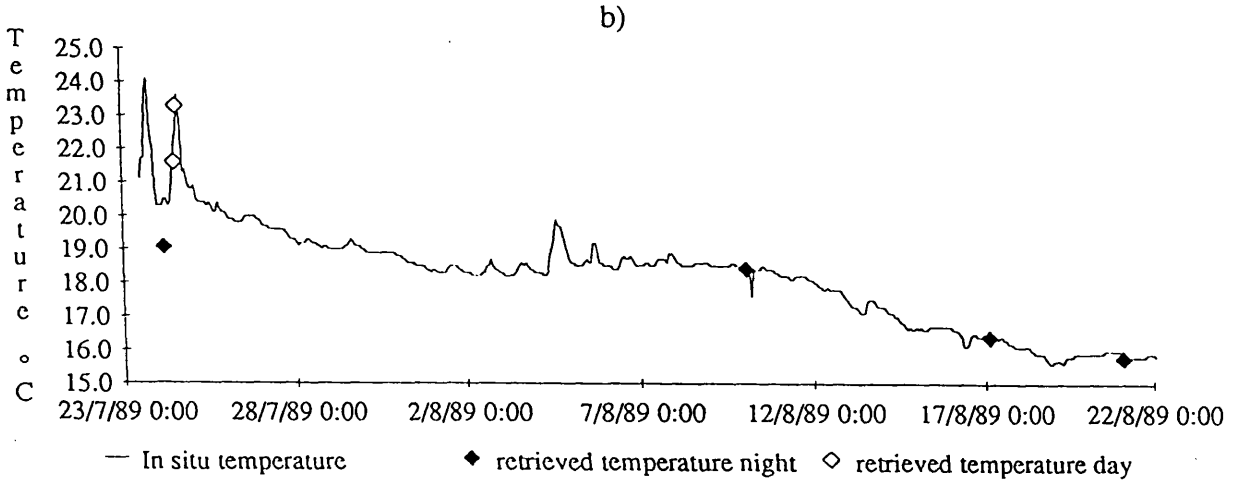

c)

Figure 7.7a), b) and c) Retrieved AVHRR temperatures compared with in situ Lough Neagh temperatures for the "hourly" data set. Night satellite passes are highlighted.

conduction and radiative cooling, during the period from 02:00 to 10:00 which is before strong solar heating.

Another possible reason for the bias is that the atmospheric correction is in error for the non-summer scenes. There is certainly cause for concern here, since in Fig. 7.3 there are non-summer radiosondes for which the atmospheric transmission model has not correctly calculated the T11-T12 difference. However, the demonstrated robustness of the algorithm to the varying of the continuum absorption and the ground temperature, argues against this possibility. The biases could also be accounted for by an error in the calibration of the thermal channels. It has been reported that the reference black body used to calibrate the instrument, pre launch, had an uncertainty of 0.35° K (Weinreb et al. 1990). Evidence against these two possibilities comes from the fact that the summer data demonstrated no such bias. There could also be errors in the calibration of the mercury thermometer used in the in situ measurement as was found in the Malawi field campaign.

However, with these data sets it is impossible to determine which is the real cause for this small bias. The scatter of the retrieved temperatures for the "weekly" data is slightly higher than the expected error calculated earlier. This can be attributed to the non temporal coincidence of the weekly data with the satellite overpass, which in extreme cases was up to 3.5 days apart. This explanation is supported by the subset which are within 8 hours of the overpass having a scatter at about the level predicted.

One would expect that the retrieved temperatures should have negative bias due to the skin effect yet this is not the case. There is no easy explanation for this except that perhaps the above effects are large enough to reverse the skin effect bias. Alternatively it could be that the skin effect is very small due to the meteorological conditions during the "weekly" data.

With such a large change in the continuum one might expect the differences in the retrieved temperatures to be much larger. However if we look at the derivation of the coefficients in chapter 2. they offer an explanation. If we assume that a change in the absorption properties of an absorber is equivalent to a change in the amount of absorber then increasing the continuum value will be equivalent to adding more water vapour. So if we increase the coefficients k1 & k2 by 30% the ratio k1/k1-k2 will stay the same and similarly for -k2/k1-k2. Therefore in the thin atmosphere approximation, changing the continuum value will have very little effect on the coefficients. There will be an effect, however, regarding the "thinness" of the atmosphere. Increasing the continuum will make the atmosphere less thin and therefore for an atmosphere where the thin atmosphere

approximation is already poor, the increased continuum will make the approximation less realistic.

For the "hourly" summer night time scenes there is no problem with the temporal coincidence of the in situ data, but the satellite retrieved temperatures are significantly lower than the in situ values. From Figs. 7.7a), b) and c) it can be seen that this bias tends to be greater for nights which follow a large diurnal spike, and this is consistent with a negative skin effect. After the strong heating during the day and a cold clear atmosphere at night there will be a large heat flux out of the lake (i.e. cooling) and this will produce a negative skin effect i.e. the skin temperature cooler than the bulk surface temperature. If we further select only days where the lough cools by ≥ 2 °C from the daytime maximum, we find that the bias becomes -0.75 ± 0.2. This is a significant result (3.75 sigma) and there is strong indication that in the main it is due to a large negative skin effect experienced by the Lough for these specific, rather extreme conditions. Further more if the bias detected in the weekly data is also present in this data (i.e. if bias due to the correction algorithm or satellite calibration) then this detected skin effect is yet larger.

The "hourly" day time scenes produce no statistically significant bias but do have a larger scatter than expected from instrumental and atmospheric correction errors alone. Again if the bias in the weekly data is present in these results it would indicate that there is a day time skin effect of ~-0.2 °C (skin cooler than bulk). The large scatter might also be accounted for by the skin effect. The skin effect over the sea during the day has generally been found to be negative, though smaller than the extreme cases above, but under the right meteorological conditions it can be positive (Schluessel et al. 1990). These conditions are early afternoon on calm warm sunny days, and this certainly occurred during some of the "hourly" day time scenes where a positive bias is observed. However the skin effect does respond very quickly to changes in meteorological conditions ($\approx$ 10 seconds (Robinson 1985)) and therefore it is not unreasonable to expect both negative and positive skin effects in the "hourly" daytime data set and hence producing a higher than expected scatter. The lower scatter in the "weekly" data suggests that the skin effect is less variable in the non-summer months where the rates of heating and cooling are lower than the summer period.

To access the accuracy to which the seasonal averages could be determined, the night summer scenes were included with the "weekly" scenes and the data set divided into Dec-Jan-Feb, Mar-Apr-May etc. and the means and statistics calculated. To ensure a uniform data set the "weekly" in situ temperatures were used with the summer images as

for the non-summer images. The results of this are presented in Table 7.2 and from them one can see that the biases between the in situ and retrieved temperatures seem to change with the seasons. For the winter and summer quarters the differences are within the expected error of zero bias with respect to the in situ data. However, for the spring and the autumn the differences are quite marked with the spring 3σ and the autumn 5σ from a zero bias. The explanation of this seasonal change in retrieved temperature error is difficult to explain, however, it should be noted that for the seasons where the bias is small the lake is at the maximum or minimum of its temperature cycle (summer & winter respectively) whereas for the other two seasons the lake is changing from minimum to maximum (spring) or vica versa (autumn). Explanation of the biases could be provided if during these seasons where the lake is changing temperature the lake undergoes large diurnal cycles. One might expect this as during the spring the lake is being strongly heated during the day and cooled at night. For the autumn the lake is experiencing a general cooling and so again one might expect the average 03:00 temperature to be warmer than the 10:00 temperature.. An alternative potential cause for the seasonal biases could be due to the atmospheric correction being in error with the meteorological conditions associated with these seasons. It is not possible, however, with the available data to ascertain the true cause of these biases.

7.4.2 ATSR comparison with in situ data

No "hourly" data was collected for the period of available ATSR data and therefore only comparisons can be made with the "weekly" data together with its inherent non-coincident problems. The results of the comparison between interpolated in situ temperatures and retrieved temperatures, for the five different correction algorithms, are presented in Table 7.3 with the corresponding plot of temperature vs. date in Fig 7.8. Correction coefficients for these data were derived from the same atmospheric scenario as used for the AVHRR study to allow comparison. This scenario constituted using North Atlantic radiosondes with the bottom of the atmosphere temperature taken as the surface temperature.

The first point of note is that for the equivalent algorithm used in the AVHRR study there is no bias between the in situ temperatures and retrieved temperatures as found with AVHRR. One might have expected the retrieved temperatures to be cooler on average with respect to the in situ temperatures due to the skin effect. This particular data set does not demonstrate this explicitly but if we limit the possible values of the true mean to one sigma from this result, this allows the skin effect to be -0.1°C (skin cooler than bulk) which is small when compared to published values for the ocean (Schluessel et al. 1990).

Season	Retrieved - In Situ	Standard error	No. of points
Dec - Feb	-0.07	± 0.12	16
Mar - May	0.39	± 0.10	14
Jun - Aug	0.09	± 0.21	12
Sep - Nov	0.59	± 0.11	15

Table 7.2 Mean temperature difference for AVHRR (Satellite - in situ) for the four seasons using weekly sampled in situ data (see text for details). All values in °C.

Algorithm	Retrieved - In Situ °C
1 look nadir: 11 & 12 μm	0.01 ± 0.1 SD = 0.40
1 look forward: 11 & 12 μm	-0.20 ± 0.1 SD = 0.40
2 looks: 11 & 12 μm	0.37 ± 0.2 SD = 0.59
2 looks: 11 μm	0.28 ± 0.1 SD = 0.52
2 looks: 12 μm	0.19 ± 0.2 SD = 0.66

Table 7.3 Mean temperature difference for ATSR (Satellite - in situ) for the five algorithms sets (see text for details). The standard deviation (SD) of the differences is also given. All values in °C.

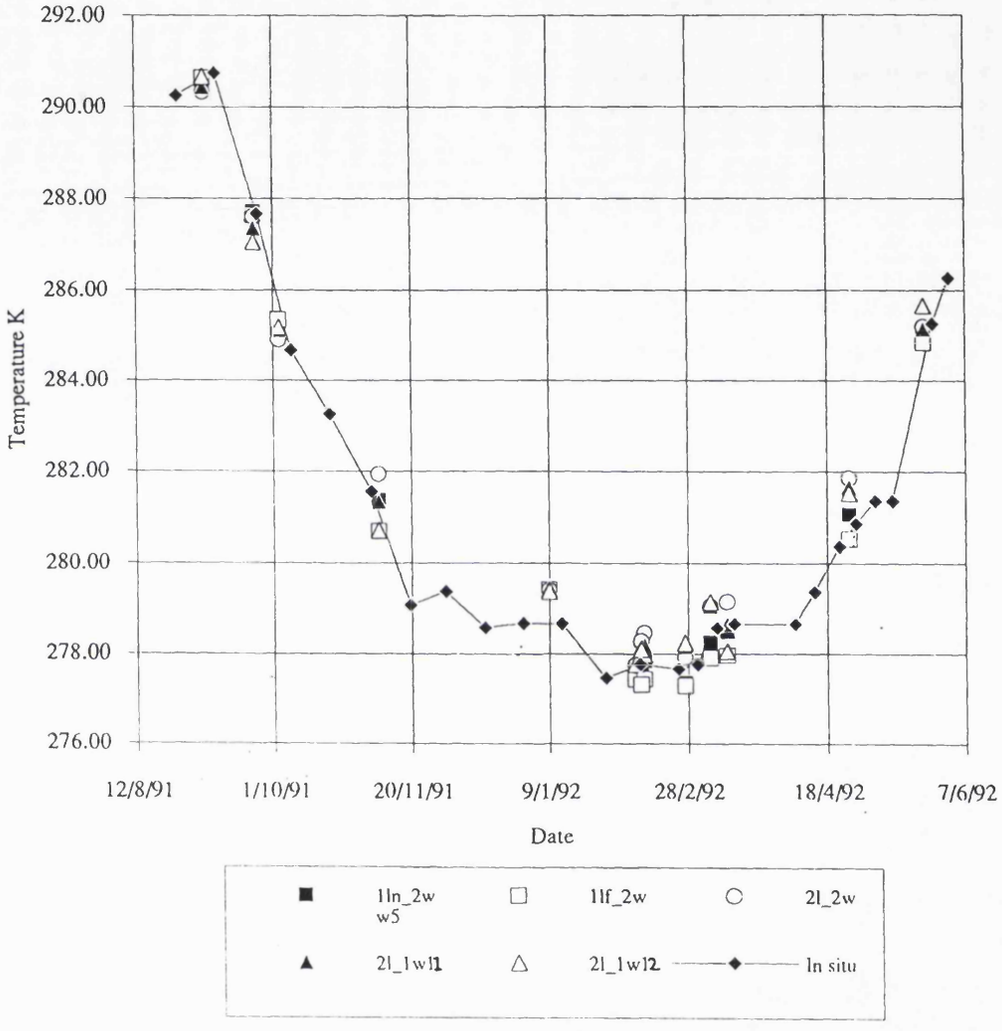

Figure 7.8 Retrieved ATSR temperatures compared with weekly in situ temperatures. Retrievals from 5 different algorithms:

11n_2w corresponds to split window using nadir image,

11f_2w corresponds to split window using forward image,

21_2w corresponds to using 11 & 12μm for both nadir and forward images,

21_1w11 corresponds to using nadir & forward images, 11μm only

21_1w12 corresponds to using nadir & forward images, 12μm only

The potential cooling effect mentioned during the discussion of the AVHRR results would also apply here as the ATSR overflights occur at ~22:00 and one might expect cooling between 22:00 and 10:00.

The second point of note and one which is rather surprising is that the different algorithms are in considerable disagreement. This is surprising as it has been shown (McMillin 1975) that a measurement made through a different air mass can be considered equivalent to one made at a different wavelength with different absorption. This is how the four channels are currently used in the derivation of coefficients for atmospheric correction, not only of this work, but also for the production of the RAL ATSR's SST product. Each of the four brightness temperatures (11, 12μm, forward and nadir) are modelled through the RAL transmission program and a multiple regression performed to produce correction coefficients. These results indicate that either there is a problem with the assumption of the equal nature of the nadir and forward looks, or that the modelling of the different views is in error. The literature reports numerous validation exercises for AVHRR and there is a fair body of evidence that the "single look" type algorithms perform well (Barton (1983), Llewellyn-Jones et al. (1984), McClain et al. (1983) for example) which indicates that the problem probably lies with the treatment of the forward look.

It is instructive to look at the coefficients to try and determine the cause of the algorithm differences. To provide a baseline to work from it is assumed that the split window nadir look produces a correct result; that is to say that the physics used to predict the brightness temperatures at nadir is realistic, that the predicted nadir brightness temperatures can be considered correct and the split window nadir produces correct retrieved temperatures. Considering first the twin look single window algorithms we see that they are over correcting, more so for the 11μm than the 12μm. The form of these two algorithms is;

$$T_{retrieved} = a_0 + a_1 T_{nadir} + a_2 T_{forward}$$

where a_2 is negative and $a_1 + a_2 \approx 1$. This implies that, as the algorithm is over correcting and assuming the modelled nadir brightness temperatures are correct, the forward modelled brightness temperatures are too large. This would lead to a less negative a_2 in the regression and therefore when used with real brightness temperatures the algorithm would over correct.

Such an over estimation of the modelled forward temperatures should be consistent with the split window forward only algorithm under correction. To test this it is useful to

consider a plot of the correction needed to be applied to the 11μm channel forward vs. the 11-12μm forward difference, as described in chapter 2, e.g. Fig 7.9. If the 11μm is over estimated then the value of (T0-T11) will decrease as indicated on the y-axis. The value of T11-T12 will slightly increase, suggested by the result of the single wavelength two look results where the over correction is slightly greater for the 11μm algorithm. This is indicated on the x-axis. The result of this would be to produce correction coefficients (represented by the lower regression line) that would produce retrieved temperatures that are too small. Although in this data set this effect is small (forward-only split window retrieved temperatures are lower relative to nadir-only split window) this has been found to predominate in oceanic ATSR images (Harris, pers. comm. 1993).

The effect that overestimation of brightness temperatures for the forward look has on the twin look split window is difficult to determine due to the complicated nature of the algorithm. It is perhaps sufficient to say, given the results of the single look one window algorithms and the forward only split window algorithm, assuming the nadir split window algorithm is correct, that use of any algorithm which contains the forward look should be made with caution until the causes of these discrepancies are found.

It is suggested that there are two areas where the source of the discrepancies between the algorithms could lie. These are the radiative properties of the atmosphere and the source of the surface radiation. This is not proposed as an exhaustive list. The first of these is thought unlikely as the nadir only split window method has been found to be successful for AVHRR. Furthermore as the difference in calculating the absorption and emission at different angles is purely a case of different path lengths it is unlikely that the problem lies in this area. It is therefore suggested that these errors arise at the water surface and that a possible cause is the treatment of the water emissivity in the transmission model.

Very little has been published on the effect of emissivities on retrieved surface water temperatures. The atmospheric transmission model used in this study takes into account the change in emissivity with incidence angle. The emissivity of water is also known to vary with wind speed (Masuda et al. 1988), but as can be seen in Fig. 7.10, the effect is very small when considering small angles of incidence. However at larger angles, particularly at 55°, the angle of ATSR's forward look, the effect of wind speed increases to a substantial level. It could be the small variation at small incidence angles that has led investigators away from considering the importance of wind speed in the retrieval of surface water temperatures but for ATSR and the high incidence angle of the forward look it is necessary to take it into account. Therefore, to investigate the effect of different emissivities due to wind speed in ATSR derived surface water temperatures,

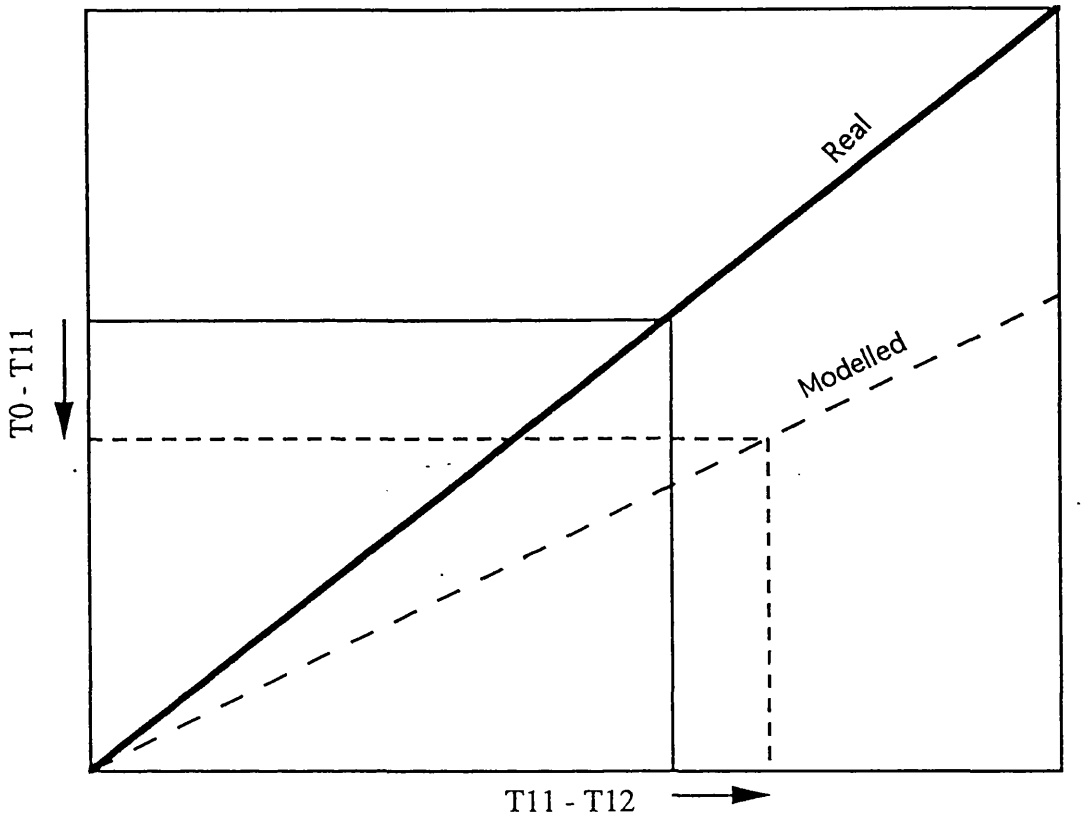

Figure 7.9 The effect of underestimating the emissivity of water at large incidence angles on the T_0-T_{11} vs. T_{11}-T_{12} relationship, leading to under correction of split window forward look only SST's.

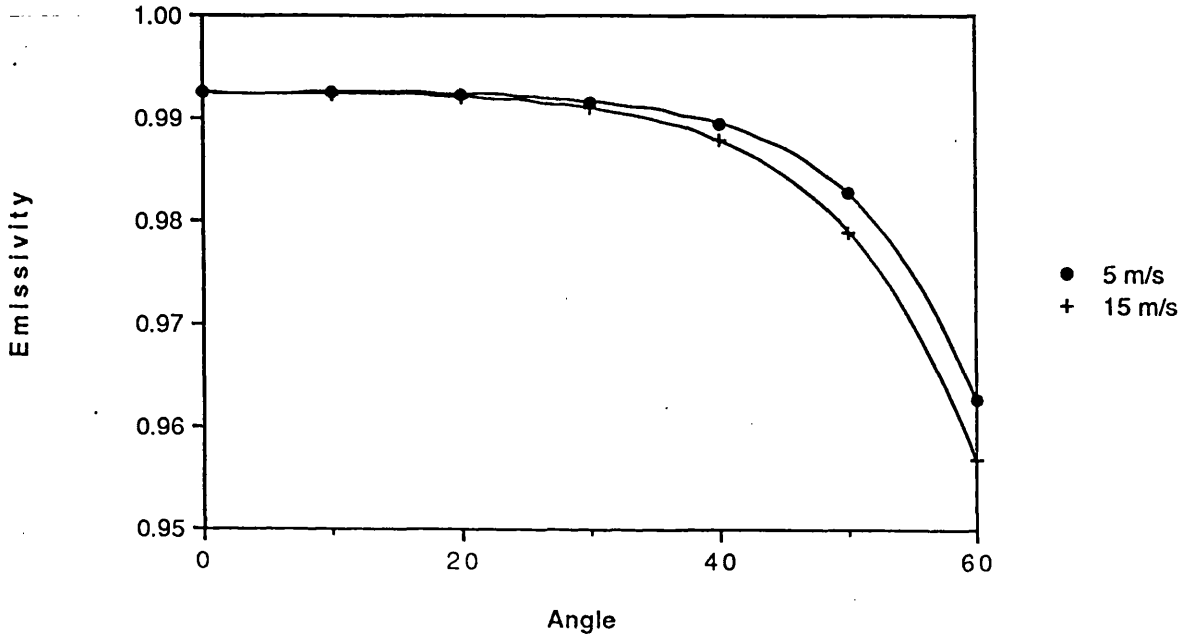

Figure 7.10 The effect of wind roughening of the sea surface on emissivity with respect to view angle, for 5 & 15 m/s wind speed (Masuda et al. 1988). Note that maximum difference in emissivity is approached at ~55°, the forward look view angle of ATSR.

the transmission model was modified to calculate brightness temperatures for water emissivities calculated at 15m/s wind speed. These can then be compared with the previously calculated brightness temperatures which were derived with water emissivities at 5m/s, the approximate annual average wind speed in N. Ireland. Correction coefficients were calculated and retrieved temperatures obtained for the same ATSR images as previously, and the results of the comparison with in situ temperatures are in Table 7.4 and the differences between the retrieved temperatures for the two wind speeds in Table 7.5.

One can see that there is a distinct reduction in the biases between the in situ data and the retrieved temperatures for the 15m/s wind speed emissivities and that there are considerable differences between the two scenarios for any algorithm which involves a forward view. One can draw two conclusions from these results. The first is that this result highlights the importance of incorporating the wind speed when calculating surface temperatures with the forward look of ATSR. This effect has recently been investigated by Harris et al. (1994) in which they calculated the potential biases in global SST's due to the zonal nature of the earth's winds. Their results are presented in Fig 7.11 which is a global map of SST error derived from the ERS-1 altimeter wind speed product for 1-3 August 1991. The errors are quite considerable when compared with the design goal of ATSR for SST retrievals of an accuracy of $\pm$ 0.3°C. Fortunately for ATSR there is also the altimeter and scatterometer on board ERS-1 and therefore it would be possible to obtain contemporaneous wind speeds, albeit only along the satellite ground track and one edge of the ATSR image where the scatterometer overlaps, which would allow correction for this wind effect.

The second conclusion that can be drawn from these results is that, as 15 m/s average wind speed is considerably different from the measured average (of ~ 5 m/s), this would indicate that the values used for the emissivity at 5 m/s are in error and that they should be nearer the values at 15 m/s, and the 15 m/s emissivities are in error as well.

When the two retrieval temperature sets are compared with the in situ data, Fig 7.12a) & b), we notice that the spread between the different algorithms is reduced for some of the images in the 15m/s case but for some points it is increased. This can be attributed to the noise which is on each of the brightness temperatures. As the error on each brightness temperatures is random, the effect of these random biases when passed through the correction algorithm will also be random yet magnified as the coefficients are generally

Algorithm	Retrieved - In Situ °C
1 look nadir: 11 & 12 μm	-0.01 ± 0.1 SD = 0.40
1 look forward: 11 & 12 μm	-0.03 ± 0.1 SD = 0.41
2 looks: 11 & 12 μm	0.06 ± 0.2 SD = 0.56
2 looks: 11 μm	0.07 ± 0.1 SD = 0.51
2 looks: 12 μm	0.13 ± 0.2 SD = 0.68

Table 7.4 Mean temperature difference for ATSR (Satellite - in situ) for the five different algorithms (see text for details) using water emissivities corresponding to 15m/s wind speed. The standard deviation (SD) of the differences is also given. All values in °C.

Algorithm	Retrieved e5m/s - Retrieved e15m/s °C
1 look nadir: 11 & 12 μm	0.02 ± 0.003 SD = 0.01
1 look forward: 11 & 12 μm	-0.17 ± 0.01 SD = 0.03
2 looks: 11 & 12 μm	0.31 ± 0.02 SD = 0.06
2 looks: 11 μm	0.21 ± 0.02 SD = 0.06
2 looks: 12 μm	0.05 ± 0.03 SD = 0.10

Table 7.5 Differences in retrieved temperatures from coefficients derived from water emissivities corresponding to 5m/s and 15m/s wind speeds. All values in °C.

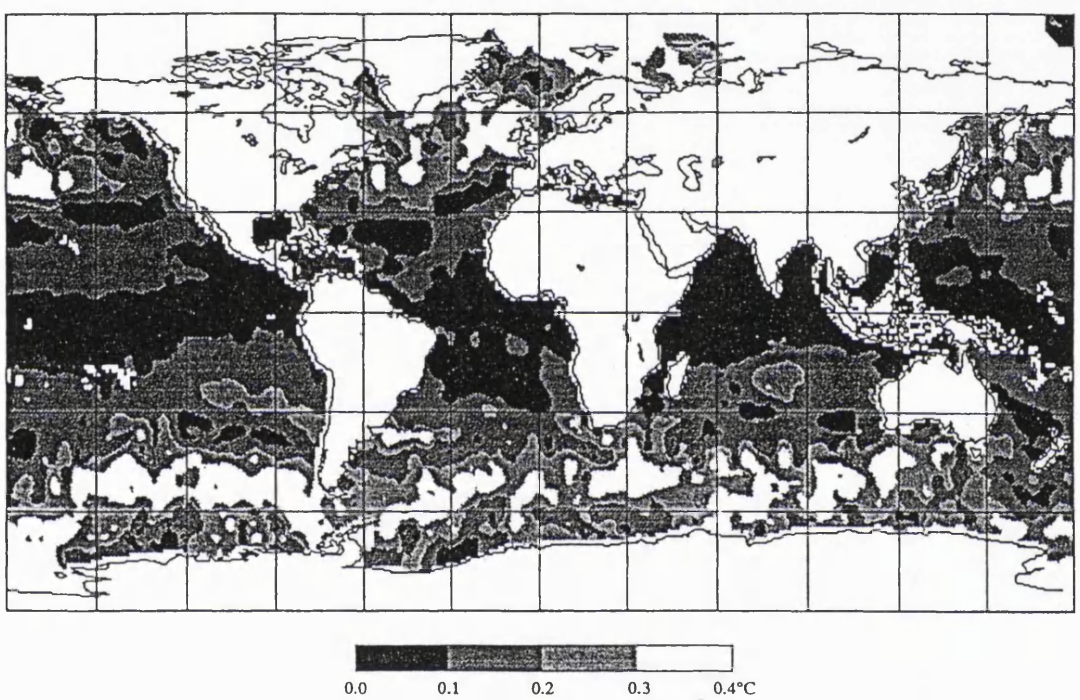

Figure 7.11 Calculated SST error due to wind/emissivity effects on the forward look of ATSR, from Harris et al. (1994).

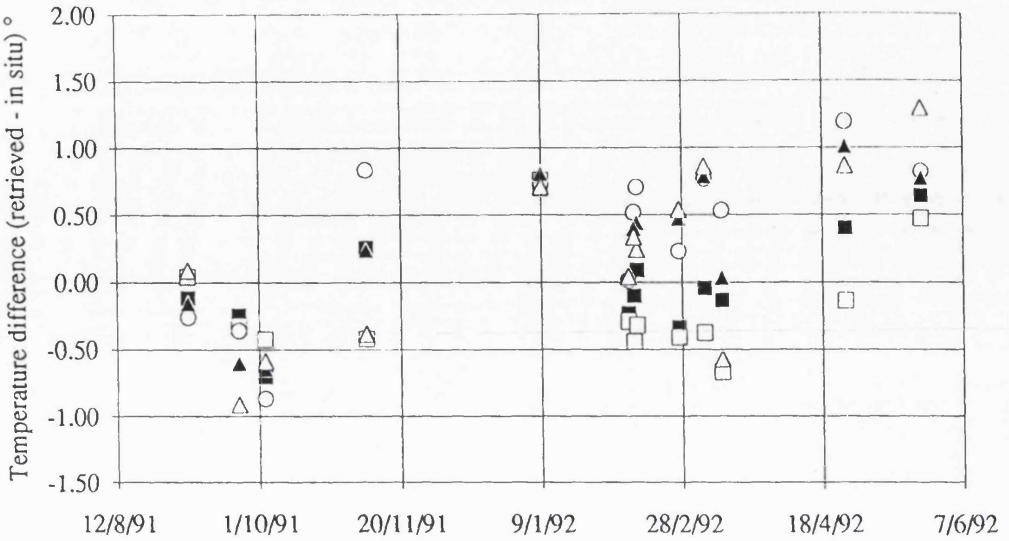

a)

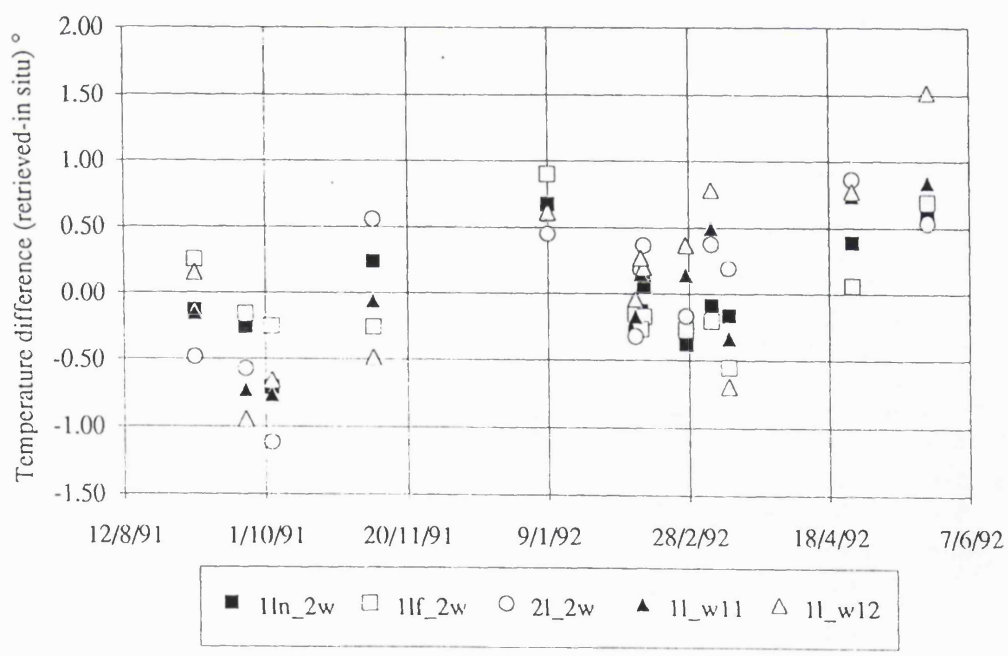

b)

Figure 7.12a) Retrieved-in situ temperature differences for ATSR of Lough Neagh using emissivities corresponding to 5 m/s wind speed and b) 15 m/s wind speed. Explanation of symbols can be found in Fig. 7.8.

greater than one and combine more than one brightness temperature. Therefore, there will be different biases between two algorithms for different images, for both 5 & 15 m/s retrieved temperatures. The important result is in the mean bias which, as demonstrated, is smaller for the 15 m/s case.

As for the AVHRR study the quarterly mean temperatures were calculated and are presented in Table 7.6. The lower repeat frequency of ERS-1 means that there are fewer samples per quarter and furthermore at the time of this study a full year of ATSR data was not available and so a value for June-July-August could not be calculated. Although the uncertainties in the mean quarterly differences are larger due to the smaller number of points there is some indication that the largest bias is in the spring as was found with the AVHRR data.

7.5 Conclusions and Recommendations

This validation study set out to discover whether current satellite-borne infrared radiometers could measure annual lake temperature cycles for the purpose of monitoring climate change. This was perceived to contain two questions, firstly would it be possible to acquire high enough temporal resolution for temperature retrievals due to the problem of cloud and secondly how accurate would the retrieved temperatures be. To answer these questions this case study involving AVHRR and ATSR images of Lough Neagh and in situ temperatures was performed.

The finding of this study for these questions is summarised as follows:

- For both satellites it was found that ~10% of all overflights are cloud free. This allows very regular monitoring by AVHRR, even if restricted to night scenes, to approximately 70 images per year. On the other hand with the repeat frequency of ATSR being effectively 3 days this only provides ~1 per month, which is at the limit of temporal resolution if the annual temperature cycle of the Lough is to be reconstructed but should provide sufficient coverage to determine the quarterly average temperatures.

- For the majority of the year, excluding the summer months, the surface temperature was retrieved by AVHRR with a bias of 0.32 ± 0.07°C on average (retrieved temperature greater than in situ), with the uncertainty of a single retrieval of 0.5° (1σ), for 46 images spanning 1.9.88 to 28.9.89. Summer night scenes were found to have a bias of -0.52 ± 0.2°C (satellite temperature less than in situ), and an

Season	Retrieved - In Situ	Standard error	No. of points
Dec - Feb	0.11	±0.18	5
Mar - May	0.31	±0.19	4
Jun - Aug			0
Sep - Nov	-0.11	±0.19	4

Table 7.6 Mean temperature difference for ATSR (Satellite - in situ) for the four seasons (see text for details). All values in °C.

uncertainty of a single retrieval of 0.6° (1σ), for 9 images. The source of the non-summer bias is unclear but it is suggested that it might be due to: i) general cooling of the Lough between 03:00 and 10:00 (the times of the satellite overflight and the in situ measurement respectively), ii) Satellite calibration error, iii) in situ calibration error. The summer bias is suggested to be predominantly due to the skin effect cooling the surface relative to the bulk. For the equivalent algorithm with ATSR the result was -0.01 ± 0.1°C for a data set spanning 1.9.91 to 4.8.92, and an uncertainty of a single retrieval of 0.4° (1σ) for 13 images.

- When the summer scenes of AVHRR were filtered to contain only images which followed a night of >2° cooling the retrieved bias was found to be -0.75 ± 0.2°C and this was considered to be a statistically significant measurement which is suggested to be predominantly caused by a skin effect due to a large heat flux out of the lake.

- When mean quarterly temperatures are calculated from the AVHRR data it is found that the summer and winter quarters are retrieved with no statistical bias from the in situ temperatures but with the spring and autumn quarters the retrieved temperatures are significantly too large. Possible cause of this effect was attributed to the fact that in the spring and autumn the lake is rapidly changing temperature and therefore one might expect there to be a large diurnal cycle which would possibly produce such an effect. A similar result was found for ATSR although less pronounced.

- Correction algorithms for different combinations of the available ATSR channels and views were found to give significantly different retrieved temperatures with the error seeming to lie with the use of the forward view radiances. A possible cause of this was suggested to be an incorrect value for the water emissivities in the forward view used in the RAL atmospheric transmission program which provided the brightness temperatures required to produce correction coefficients. The effects of such an error on the correction algorithms is discussed.

- The importance of accounting for the change in emissivity due to wind speed was demonstrated and the associated error which can be attributed to its omission was determined, in this case, to be ~0.3°C over correction if the lough was experiencing a 15 m/s wind and correction coefficients derived for 5 m/s were used.

These findings suggest many new areas of research, some which are quite specific to the use of lake temperature as climatic indicators, and others which are more general in nature. With regard to lake temperatures, this study used a lake where the atmospheres are dominated by the North Atlantic. To be able to use lake retrieved temperatures globally further case studies need to be performed to ensure the atmospheric correction procedures are valid for other climatic regimes. Such an important climatic region to consider would be a temperate continental.

In a more general context the effect of wind speeds on surface water temperature retrieval and the suggestion that there might be an error in the values of the emissivity have far reaching implications especially in the field of global sea surface temperature retrieval and climate research. The importance and effect of these discoveries need to be investigated further. This applies particularly to ERS-1 with its synergistic ability to measure wind speed and hence the potential to develop wind speed corrected sea surface temperatures.

Chapter 8.

Concluding remarks and recommendations.

8.1 Summary of work presented

This thesis starts with an introduction to the principal aims for the work presented which are whether lake surface temperatures can provide a useful proxy climatic indicator and if so whether remote sensing techniques can provide a routine monitoring of these temperatures. The origins of these aims are from the generally observed thermal behaviour of lakes over the globe and the characteristics of remote sensing which make it an ideal tool for the global monitoring of climate related variables.

To provide a knowledge base from which to develop a research strategy, a review of the remote sensing techniques currently available for the retrieval of surface water temperatures and the nature of lakes thermal behaviour with respect to climate was undertaken. The review of remote sensing techniques is presented in chapter 2 and begins with a discussion of the nature of thermal radiation followed by a review of how that radiation can be measured. Three examples of infrared radiometers together with their characteristics are discussed, two designed for use in space (AVHRR & ATSR) and the last for ground-based use (CSIRO). Calibration of such radiometers is highlighted particularly with the CSIRO instrument where external cross calibration is needed. This takes the form of a "stirred bucket", the nature and use of which is discussed. The effect of the atmosphere on space-based measurements of surface radiation is addressed including atmospheric absorption and radiation transfer. This leads on to the techniques of atmospheric correction for such data. The chapter ends with a description of the skin effect which has important consequences for the retrieval of surface water temperatures.

The review of lakes' thermal behaviour with respect to climate is presented in chapter 3 and can be broken down into two sections. The first concerns the thermal behaviour of lakes through the annual cycle together with descriptions of the heat exchange mechanisms which drive the annual cycle and environmental factors which alter the temperature cycle from lake to lake. The second part reviews the modelling of lake temperature and work published concerning the link between lake temperatures and the climate. The chapter ends by highlighting the general areas of research required to assess the suitability of lake temperatures for proxy climate monitoring.

To investigate the thermal behaviour of lakes with respect to climate change it was decided to develop a lake thermal model which could be used as a tool for this purpose. The model is a one dimensional heat budget model which is a synthesis of the heat exchange equations reviewed in chapter 3 and was validated using a comprehensive in situ and meteorological data set for Lough Neagh, Northern Ireland. The results of the lough climatology, derived from this meteorological data, are compared with a representation of the climatology of the UK as a whole.

The first of the research goals pursued in this thesis was to establish whether lake surface temperatures could be used to provide a proxy climatic indicator. It was found that the approach of Sraskraba (1980) describing the global variation of lake temperatures was not appropriate when trying to consider climate change. The approach of Edinger et al. (1968) was found to be more flexible and from this the equilibrium temperature T_e, the temperature to which a lake would naturally tend, was isolated as the best geophysical parameter from which to construct a proxy climatic indicator. The equilibrium temperature was shown to be independent of the lake's physical characteristics and only dependent on the meteorological parameters of air temperature, cloud cover, relative humidity and wind. It was also demonstrated that the lake acts as a low pass filter to the equilibrium temperature. The nature of this low pass filter was investigated and it was shown that it can be approximated to a linear first order system and that a lake's mixed layer depth is instrumental in determining the cut-off frequency of the filter. When using the meteorology for Lough Neagh it was found that the time constant for a 10m deep lake is six days and therefore such a lake can be considered to be filtering out the diurnal and short term "noise" in the equilibrium temperature but passing frequency components on longer time scales such as a month or the seasons, which are typical time periods for which average temperatures are computed. The rate at which a lake can exchange energy with the environment can be characterised by the parameter K, the heat exchange coefficient. It was found that Lough Neagh had an average coefficient of 58 W/m^2K and a range of 43 to 78. It was also found that a large change in K was needed to change the time constant significantly, with the K values of 65 and 105 W/m^2K having time constants of 4.1 and 6.7 days respectively. The response of lakes with different depths but within the same region and hence the same equilibrium temperature was investigated. It was found that if one could estimate the mixed layer depth it would be possible to invert two temperature series to retrieve the equilibrium temperature.

To determine the change that might occur to the equilibrium temperature due to increased levels of atmospheric CO_2 it was originally proposed to generate these temperatures from predicted meteorology from the Hadley Centre's global circulation model but

unfortunately this was not possible as there have been delays in the distribution of these data. Instead the effect of changing each meteorological parameter individually on the equilibrium temperature was investigated and it was found that to increase it for June by 1°C required an increase in air temperature of 1.2°, or an increase in relative humidity of 12%, or a decrease in the wind speed of 1.3 m/s or a decrease in the fraction of the day covered by cloud by 0.3. The net effect of an increase in the occurrence of summer high pressure systems and winter low pressure systems was qualitatively discussed with the conclusion that for both cases one might expect an increase in the equilibrium temperature. Potential changes in the lake's response was modelled by calculating the heat exchange coefficient for similar changes in meteorology. It was found that little change occurred to K and therefore little change in the filtering characteristics can be expected. However, it was noted that a change in the spring meteorology which would change the depth of the thermocline could change the time constant of a lake considerably.

To address the remote sensing of lake temperatures two case studies were performed; the first consisting of a field trip to Lake Malawi (chapter 6) and the second a measurement of the annual temperature cycle of Lough Neagh (chapter 7). For Lake Malawi, in situ radiometric temperatures were collected during satellite overpasses as well as meteorological measurements and sub-surface water temperatures. Radiosondes were also launched during satellite overflights and it was found that water vapour was biased to higher levels in the atmosphere over the lake when compared with oceanic tropical radiosondes. This necessitated the production of site specific coefficients from the local radiosondes. Using such coefficients, AVHRR retrieved temperatures were found to agree with in situ radiometric temperatures to 0.14±0.2 K (retrieved - in situ) for four samples. The skin effect was also measured during the campaign and was found to have a value of ~-0.32 K with a small diurnal variation of 0.15 K, the maximum occurring between 13:00 & 14:00. The accuracy of the retrieval error, however, is compromised by the small number of satellite/in situ comparisons, and the applicability of these results to other times of the year is unknown.

The case study on Lough Neagh was performed to assess the feasibility of monitoring the temperature of a lake throughout the year as this is, ultimately, what is trying to be achieved. This entailed not only determining the accuracy to which the annual cycle can be determined but also whether the lake can be sampled regularly enough, due to cloud cover, to provide useful information. The case study used satellite data from both AVHRR and ATSR but which covered different years. For both satellites it was found that for the Lough Neagh region one could expect ~90% of the passes to be contaminated

by cloud. For AVHRR this still allowed regular sampling of ~70 night images per year but for ATSR this only allowed one scene per month on average. For the majority of the year, excluding summer months, the surface temperature was retrieved by AVHRR with a bias of 0.32±0.07 K (retrieved temperature greater than in situ value) and a single pixel retrieval error of 0.5 K. Possible reasons for this bias were suggested to be a) a cooling of the lough between the satellite overflight time (03:00) and the in situ sampling time (10:00), b) satellite calibration error and c) in situ calibration error. Summer night scenes were found to have a bias of -0.52±0.2 K compared to high temporal resolution in situ data. If these summer scenes were restricted to nights which followed > 2K cooling from the daytime maximum, the retrieved temperature was found to have bias of -0.75±0.2 K (satellite cooler than in situ). This was suggested to be predominantly due to the skin effect caused by the large heat flux out of the lake. When the retrieved temperatures were divided into seasonal quarters the retrieved biases were found only to occur during the spring and the autumn. Possible explanation of this phenomenon was suggested that as the lake is rapidly changing temperature during these seasons one might expect there to be a large diurnal cycle which would emphasise the cooling between 03:00 and 10:00. This result also argues against the reasons b) & c) stated above to explain the bias.

For the ATSR images it was found that the equivalent algorithm to that used for the AVHRR study produced no statistical bias from the in situ temperatures. It was found, however that algorithms that used different combinations of the available channels of ATSR produced significantly different results. It was suggested that the cause of this was due to an error in the emissivities used at the angle of the forward look. It was also noted that wind speed could have a significant effect on retrieved temperatures by changing the effective emissivity for the forward look, so that if the lough was experiencing a wind of 15 m/s, use of coefficients derived using emissivities for 5 m/s would introduce an error of 0.3 K. The effect that this might have on global SSTs was noted.

8.2 Discussion of results with respect to initial aims

The question as to whether lake surface temperatures could be useful in climate research, particularly in the capacity of a proxy indicator, has several aspects. Obviously the first is whether lakes actually respond to climate changes and as argued in chapter 1 this is clearly so, which immediately leads on to the question of how they respond. Published work on this matter was found to mainly consist of empirical correlations which by their nature are limited in providing detailed understanding of how lakes might respond to climate change. This thesis took a different approach, that of modelling the physical heat

exchanges undergone by the lake, and has concluded that the equilibrium temperature T_e (the temperature that all lakes experiencing the same climate would tend to is the geophysical parameter that should be used for climate research and as a proxy indicator. In other words T_e is effectively the climatic signal that the lake is responding to. The advantages of T_e are that it is independent of the physical characteristics of any particular lake. Size, depth, opacity or shape have no influence on T_e. This allows the use of this single parameter over all the earth's land surface. Another characteristic of T_e is that it is sensitive to air temperature, relative humidity, wind and cloud cover. This means that it is a general measure of a region's climate, a combined measure of these four meteorological parameters. This could be considered an advantage as it is a more complete measure of a region's climate than, say, air temperature alone. However, this combined response could also be considered a disadvantage as it is difficult to know how to relate a change in T_e to a change in the meteorology.

Another aspect of the use of lakes as climatic indicators, if T_e is selected as the geophysical parameter to be used, is the link between T_e and lake temperature. What is the relationship between the lake temperature and T_e? It is shown that the lake behaves as a low pass filter which and can be approximated to that of a linear first order system. Therefore one can say that the lake surface temperature is a low pass filtered version of the equilibrium temperature, which is the climate signal. The nature of this filter has been investigated and has been shown to be strongly linked with the mixed depth of a lake and less strongly determined by the meteorological parameters. Therefore, if wind speed characteristics change, the nature of the filtering would also change. However, it is pointed out that it might be possible to invert the temperature records of two or more lakes to extract T_e and therefore eliminate the effects of the change in filter characteristics. A simple method for such an inversion is presented.

The final aspect of the use of lakes as climatic indicators is the size of signal that might be expected and its noise characteristics. In this thesis only partial investigation of these items has been possible due to problems in acquiring GCM output from the Hadley Centre as previously mentioned. Instead, the sensitivity of T_e to the individual meteorological parameters was investigated. From the two postulated scenarios one can see that the effect of the individual meteorological parameters can often combine constructively to increase the change in T_e. If this is so in reality then it is encouraging for the use of lake temperatures as indicators as the larger the signal the more likely it is to be detected sooner. The meteorological parameters were assumed to be independent which of course they are not and so estimating actual signal that might occur cannot be done with confidence until modelled with the GCM data. The noise characteristics have

not yet been investigated. Projected changes in the air temperature have been suggested to be of the order of 0.3K per decade (Houghton et al. 1990), so if this was the sole change in the meteorology for Lough Neagh then the signal would be similar to this for December and slightly less for June.

Concerning the remote sensing of lake temperatures, the first case study has indicated that with a representative sample of atmospheres it is possible to retrieve the skin temperature for a ten day period of Lake Malawi to 0.2 K with AVHRR. This is significantly greater accuracy than previously reported (Robinson (1985), McClain (1989), Minnett (1991)) but this could be a feature of the small sample number. Although it is not possible to extrapolate temporally or geographically and assume that this accuracy can be achieved globally or for different seasons for Malawi, it is still encouraging. One should note that this accuracy does not represent the limit of change in Te that can be detected as many retrieved temperatures will be used to generate the whole annual cycle and so one might expect to determine the seasonal temperatures with greater accuracy.

The results of the case study on Lough Neagh are also encouraging. They show that the annual cycle of the lough can be measured with AVHRR with its frequent coverage but with ATSR the coverage is marginal. However there were some areas of concern which will be addressed in the recommendations for future work, such as the bias between the retrieved AVHRR temperatures and the in situ data, the seasonal variation of this bias and the differences found between different ATSR algorithms.

To summarise the work of this thesis, it has shown that there is great potential in the use of lake temperatures as a proxy climate indicator and the use of remote sensing to monitor these temperatures. The equilibrium temperature can be seen as a combined measure of the climate of a region and it has been indicated that if more than one lake is monitored in a region it might be possible to extract this parameter. Thus we have a parameter which is independent of any particular lake, which is distributed globally over the land surface and for which it seems likely that it will be able to be measured by remote sensing. However, this thesis has raised a number of questions which need further investigation.

8.3 Proposed future work

The obvious next step in this research is the prediction of expected changes in T_e from GCM data. This would not only help in establishing the level of accuracy required from

remote sensing but would also establish how the different meteorological parameters combine (whether constructively or destructively) and so whether T_e is a more sensitive climatic indicator than say air temperature (cf. the chapter 5 discussion of the results of George (1989)). The natural noise characteristics of T_e also needs to be established. These, together with the expected signal, would define the signal to noise ratio which would help in establishing how long such T_es would need to be monitored before one might expect a signal to be detected.

These are the two main areas of new research which are needed in the establishing of lake surface temperatures as a valid and useful climate proxy indicator. However, there are also a number of other areas which require further investigation, particularly:

- The retrieval of surface temperatures in this thesis have been of the skin temperature and not of what is normally considered the surface temperature (approximately the top few cm). Therefore the effect of retrieving the skin temperature on the determining of T_e needs to be investigated. The relationship between the skin temperature and the surface temperature could potentially change and so could obscure or falsely indicate changes in T_e.

- The values of T_e have been calculated from the HS model which has been validated with data from Lough Neagh. This model needs to be tested for other regions and modified if necessary before similar calculations can be made and globally applied.

- The inversion technique of converting two or more water temperature records into T_e values needs to be tested and modified if necessary. The extent to which it can be assumed that T_e is constant will also need to be established. The proposed method requires the mixed layer depth to be estimated. It would be an obvious advantage if an inversion technique could be developed which did not require this.

- The validity and applicability of the accuracy achieved between retrieved temperatures and measured in situ temperatures during the field campaign on Lake Malawi needs to be tested for different seasons and climatic regions. As regions with a tropical continental climate and a temperate maritime climate have been investigated with Lake

Malawi and Lough Neagh, an important climatic region still to be investigated would be temperate continental.

- The seasonal biases between the retrieved satellite temperatures and the in situ data for Lough Neagh need to be investigated further and the proposed explanation of non-temporal coincidence tested.

- The final area where further work is suggested is the investigation of the source of differences between different algorithms of ATSR. This has implications for other climatic research disciplines, particularly that of sea surface temperature. Such an investigation is already in progress as MSSL with initial theoretical algorithm errors due to wind speed having been calculated on a global basis (Harris et al. 1994).

The proposed research outlined above, if successful, would confirm the usefulness of lake surface temperatures in climatic research and the detection of climatic change. The satellite data which has already been archived for more than a decade could provide a unique record of global lake temperatures and provide a valuable contribution to climatic research, and the continued monitoring of these temperatures could be a valuable tool in the early detection of climate change.

References.

Anderson, J. C. (1987). On the Use of Lake Ice Conditions to Monitor Climatic Change. Canadian Climate Centre.

Barton, I. J. (1983). "Dual channel satellite measurements of sea surface temperature." Quarterly Journal of the Royal Meteorological Society **109**: 365-378.

Birkett, C. M. (1994). "The creation of a new global lakes database and its application to a remote sensing program to study climatically sensitive lakes." *in prep.*

Brown, O. B., J. W. Brown, et al. (1985). "Calibration of advanced very high resolution radiometer infrared observations." Journal of Geophysical Research **90**(c6): 11667 - 11677.

Brown, S. J., I. M. Mason, et al. (1991). "Lake surface temperatures from space for climate research." paper presented at 5th AVHRR data users meeting, Tromsø, Eumetsat, 211-216.

Budyko, M. I., G. S. Golitsyn, et al. (1988). Global Climate Catastrophes. New York, Springer Verlag.

Cox, C. and W. Munk (1955). "Some problems in optical oceanography." Journal of Marine Research **14**: 63-78.

Delderfield, J., D. T. Llewellyn-Jones, et al. (1986). "The Along Track Scanning Radiometer (ATSR) for ERS-1." paper presented at Instrumentation for optical remote sensing from space.

Deschamps, P. Y. and T. Phulpin (1980). "Atmospheric correction of infrared measurements of sea surface temperature using channels at 3.7 11 and 12 μm." Boundary Layer Meteorology **18**: 131-143.

Edinger, J. E., D. W. Duttwieler, et al. (1968). "The response of water temperatures to meteorological conditions." Water Resources Research **4**: 1137-1143.

Edwards, D. P. (1987). "Atmospheric transmittance and radiance calculations using line-by-line computer models." paper presented at SPIE, pp. 94-116

Eifler, W. (1992). "Modelling the skin-bulk temperature difference near the sea-atmosphere interface for remote sensing applications." paper presented at International Space Year, Munich, pp. 335-340

Eifler, W. (1993). "A hypothesis on momentum and heat transfer near the sea-atmosphere interface and a related simple model." Journal of Marine systems **4**: 133-153.

Ewing, G. and E. D. McAlister (1960). "On the Thermal boundary-layer of the ocean." Science **131**: 1374.

Folland, C. K., T. R. Karl, et al. (1990). Observed climate variations and change. Climate Change - The IPCC Scientific Assessment Eds. J. T. Houghton, G. J. Jenkins and J. J. Ephraums. Cambridge, Cambridge University Press. 195-238.

George, G. D. (1989). "The thermal characteristics of lakes as a measure of climate change." paper presented at Conference on climate and water, Helsinki, The Academy of Finland, pp. 402-412

Gibson, C. E. (1990). Personal Communication.

Gorham, E. and F. M. Boyce (1989). "Influence of Lake Surface Area and Depth Upon Thermal Stratification and the Depth of the Summer Thermocline." Journal of Great Lakes Research **15**(2): 233-245.

Grassl, H. (1976). "The Dependence of the Measured Cool Skin of the Ocean on Wind Stress and Total Heat Flux." Boundary-Layer Meteorology **10**: 465-474.

Halbfass, W. (1923) "Grundzüge einer vergleichenden Seenkunde", pp. 354, Borntraeger, Berlin.

Harries, J. E. (1990). Earthwatch. Chichester, Ellis Horwood.

Harris, A. R. (1991). "Satellite Infrared Radiometry of Surface Parameters for Climate Research." PhD thesis, University College London.

Harris, A. R., S. J. Brown, et al. (1994). "The effect of wind speed on sea surface temperature retrieval from space." Geophysical Research Letters *in press*:.

Harris, A. R. and I. M. Mason (1992). "An extension to the split-window technique giving improved atmospheric correction and total water vapour." International Journal of Remote Sensing **13**(5): 881-892.

Henderson-Sellers, B. (1984). Engineering Limnology. London, Pitman.

Henderson-Sellers, B. (1986). "Calculating the surface energy balance for Lake and Reservoir modelling - a review." Review of Geophysics **24**(3): 625-649.

Hepplewhite, C. L. (1989). "Remote observation of the sea surface and atmosphere. The oceanic skin effect." International Journal of Remote Sensing **10**(4&5): 801-810.

Houghton, J. T., Ed. (1984). The Global Climate. Cambridge, Cambridge University Press.

Houghton, J. T. (1987). The Physics of Atmospheres. Cambridge, Cambridge University Press.

Houghton, J. T., G. J. Jenkins, et al., Eds. (1990). Climate Change - The IPCC Scientific Assessment. Cambridge, Cambridge University Press.

Houghton, J.T. and P. Morel, (1984) The World Climate Research Programme, in *The Global Climate,* edited by J.T. Houghton, pp. 1-12., Cambridge University Press, Cambridge.

Hutchinson, G. E. (1975). A Treatise on Limnology. New York, Wiley.

ITT (1989). AVHRR/2 Publicity material.

Kilsby, C. G., D. P. Edwards, et al. (1992). "Water vapour continuum absorption in the tropics; aircraft measurements and model comparisons." Quarterly Journal of the Royal Meteorological Society **118**: 715-748.

Leith, C. E. (1984). Global Climate Research. in *The Global Climate* Ed. J. T. Houghton. Cambridge University Press.

Llewellyn-Jones, D. T., P. J. Minnett, et al. (1984). "Satellite Multichannel Infrared measurements of sea surface temperature of the N.E. Atlantic Ocean using AVHRR/2." Quarterly Journal of the Royal Meteorological Society **110**: 613-631.

Mason, G., (1991) Test and calibration of the Along Track Scanning Radiometer, a satellite designed to measure sea surface temperature, PhD. thesis University of Oxford.

Mason, I. M., M. A. J. Guzkowska, et al. (1994). "The response of lake levels and areas to climate change." Climatic Change **27**: 161-197.

Mason, I. M., P. Sheather, et al. (1990). "On-board calibration of infrared radiometers." paper presented at Royal Aeronautical Society conference on "Earth Observation Satellites - The Technology behind the Image", RAS.

Masuda, K., T. Takashima, et al. (1988). "Emissivity of Pure and Sea Waters for the Model Sea Surface in the Infrared Window Regions." Remote Sensing of Environment **24**: 313-329.

McClain, E. P. (1989). "Global Sea Surface Temperatures and Cloud Clearing for Aerosol Optical Depth Estimates." International Journal of Remote Sensing **10**: 763-770.

McClain, E. P., W. Pichel, et al. (1983). "Multichannel Improvements to Satellite Derived Global Sea Surface Temperatures." Advances in Space Research **2**: 43-47.

McClain, E. P., W. G. Pichel, et al. (1985). "Comparative performance of AVHRR-based multichannel sea surface temperatures." Journal of Geophysical Research **90**(C6): 11,587-11,601.

McCormic, M. J. (1990). "Potential Changes in Thermal Structure and Cycle of Lake Michigan Due to Global Warming." Transactions of the American Fisheries Society **119**: 183-194.

McMillin, L. M. (1975). "Estimation of sea surface temperature from two infrared window measurements with differential absorption." Journal of Geophysical Research **80**: 5113-5117.

Minnett, P. J. (1991). "Consequences of sea surface temperature variability on the validation and applications of satellite measurements." Journal of Geophysical Research **96**(NC10): 18,475-18,489.

Mutlow, C. T., D. T. Llewellin-Jones, et al. (1994). "Sea surface temperature measurement by the Along Track Scanning Radiometer (ATSR) on ESA's ERS-1 Satellite: Early results." *Submitted to J. Geophys. Res.*

NOAA (1986). NOAA Polar Orbiter Users Guide. NOAA.

Palecki, M. A. and R. G. Barry (1986). "Freeze-up and Break-up of Lakes as an Index of Temperature Changes during the Transition Seasons: A Case Study for Finland." Journal of Climate and Applied Meteorology **25**: 893-902.

Paulson, C. A. and J. J. Simpson (1981). "The temperature difference across the cool skin of the ocean." Journal of Geophysical Research **86**(C11): 11,044-11,054.

Ragotzkie, R. A. (1987). Heat Budget of Lakes. in *Lakes: Chemistry, Geology, Physics* Ed. A. Lerman. New York, Springer-Verlag. 1-19.

Robertson, D. M. (1989). "The Use of Lake Water Temperatures and Ice Cover as Climatic Indicators." PhD thesis University of Wisconsin-Madison.

Robertson, D. M., R. A. Ragotzkie, et al. (1992). "Lake Ice Records Used to Detect Historical and Future Climatic Changes." Climatic Change **21**: 407-427.

Robinson, I. S. (1985). Satellite Oceanography. Ellis Horwood Ltd.

Robinson, I.S., (1992) Marine Science Applications of Ocean Colour Remote Sensing, in *Space Oceanography,* edited by A.P. Cracknell, pp. 163-196., World Scientific Publishing Co., Singapore.

Robinson, I. S., N. C. Wells, et al. (1984). "The Sea Surface Thermal Boundary Layer and its Relevance to the Measurement of Sea Surface Temperature by air-borne and space-borne Radiometers." International Journal of Remote Sensing **5**: 19-45.

Ruosteenoja, K. (1986). "The Date of Break-up of Lake Ice as a Climate Index." Geophysica **22**(1-2): 89-99.

Saunders, P. M. (1967a). "Aerial measurements of sea surface temperature in the infrared." Journal of Geophysical Research **72**: 4109-4117.

Saunders, P. M. (1967b). "The temperature at the ocean-air interface." Journal of Atmospheric Sciences **24**: 269-273.

Saunders, P. M. (1973). "The skin temperature of the ocean, a review." Mém. Soc. r. Sci. de Liège **6**(Vi): 93-98.

Saunders, R. W. and K. T. Kriebel (1988). "An Improved Method for Detecting Clear Sky and Cloudy radiances from AVHRR data." International Journal of Remote Sensing **9**: 123-150.

Schindler, D. W., K. G. Beaty, et al. (1990). "Effects of Climatic Warming on Lakes of the Central Boreal Forest." Science **250**: 967-970.

Schluessel, P., W. J. Emery, et al. (1990). "On the bulk - skin temperature difference and its impact on satellite remote sensing of sea surface temperature." Journal of Geophysical Research **95**(c8): 13,341-13,356.

Schott, J.R. and A. Henderson-Sellers, (1984) Radiation, the atmosphere and satellite sensors, in *Satellite Sensing of a Cloudy Atmosphere,* edited by A. Henderson-Sellers, pp. 45-90., Taylor and Francis.

Skinner, W. R. (1986). The Break-up and Freeze-up of Lake and Sea Ice in Northern Canada. Canadian Climate Centre.

Sraskraba, M. (1980). The effects of physical variables on freshwater production: analyses based on models. in *The Functioning of Freshwater Ecosystems* Ed. E. D. L. a. R. H. McConnell. Cambridge, Cambridge University Press. 13-84.

Stewart, D. A. and C. E. Gibson (1987). "A model for the heat budget of Lough Neagh." Record of Agriculture Research **35**: 67-75.

Steyn-Ross, D. A. and M. L. Steyn-Ross (1992). "Radiance Calibration for Advanced Very High Resolution Radiometer Infrared Channels." Journal of Geophysical Research **97**(c4): 5551-5568.

Tramoni, F., R. G. Barry, et al. (1985). "Lake Ice Cover as a Temperature Index for Monitoring Climate Perturbations." Zeitschrift für Gletscherkunde und Glazialgeologie :

Weinreb, M. P., G. Hamilton, et al. (1990). "Nonlinearity Corrections in Calibration of Advanced Very High Resolution Radiometer Infrared Channels." Journal of Geophysical Research **95**(c5): 7381-7388.

Závody, A. M. (1982). Appendix J. The Along-Track Scanning Radiometer with Microwave Sounder. Response to the ERS-1 Announcement of Opportunity. Rutherford Appleton Laboratory.

Závody, A. M., M. R. Gorman, et al. (1994). "The ATSR processing scheme developed for the EODC." International Journal of Remote Sensing : In press.

Závody, A. M., C. T. Mutlow, et al. (1994). "A radiative transfer model for sea surface temperature retrieval for the along track scanning radiometer (ATSR)." *Submitted to J. Geophys. Res.*

Wooster, M. J., C. B. Sear, et al. (1994). "Tropical lake surface temperatures from locally received NOAA-11 AVHRR data - comparison with in situ measurements." International Journal of Remote Sensing **15**(1): 183-189.

Gosink, J. G. (1987). "Northern lake and reservoir modelling." Cold Regions Science and Technology **13**: 281-300.

Henderson-Sellers, B. (1984). "Development and application of "U.S.E.D.": a hydroclimate lake stratification model." Ecological Modelling **21**: 233-246.

Henderson-Sellers, B. (1986). "Calculating the surface energy balance for Lake and Reservoir modelling - a review." Review of Geophysics **24**(3): 625-649.

Imberger, J. and J. C. Patterson (1981). A dynamic reservoir simulation model - DYRESM: 5. Transport models for inland and coastal waters Ed. H. B. Fisher. New York, Academic press. 310-316.

Imberger, J. and J. C. Patterson (1990). "Physical Limnology." Advances in Applied Mechanics **27**: 303-475.

"CE-QUAL-R1: a numerical one-dimensional model of reservoir water quality: user's manual." (1982). *Instruction Report E-82-1* Environmental Laboratory, U. S. Army Engineer Waterways Experiment Station. CE, Vicksburg, Miss.

Rice, D. A., T. Tsay, et al. (1989). "Modelling thermal stratification in transparent Adriondack lake." Journal of Water Resources Planning and Management **115**(4): 440-456.